heat pump programme

IEA
OECD

Annex 14

Operating Agent:
Japan

Working Fluids and Transport Phenomena in Advanced Absorption Heat Pumps

Final Report: Volume 2

Working Fluids and Transport Phenomena in Advanced Absorption Heat Pumps

(Final report: Volume 2)

Annex 14

Edited by Takamoto Saito
University of Tokyo

August 1995
(first published in March 1990)

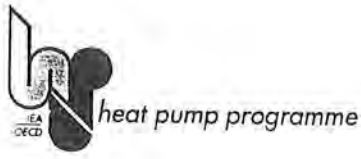

Report No. HPP-AN14-1

The IEA

The IEA was established in 1974 within the framework of the Organization for Economic Cooperation and Development (OECD) to implement an International Energy Programme. A basic aim of the IEA is to foster cooperation among the 22 IEA participating countries to increase energy security through energy conservation, development of alternative energy sources, new energy technology and research and development (R&D). This is achieved, in part, through a programme of energy technology and R&D collaboration, currently within the framework of over 40 Implementing Agreements.

The IEA Heat Pump Programme

The Implementing Agreement for a Programme of Research, Development, Demonstration and Promotion of Heat Pumping Technologies (IA) forms the legal basis for the IEA Heat Pump Programme. Signatories of the IA are either governments or organizations designated by their respective governments to conduct programmes in the field of energy conservation.

Under the IA collaborative tasks or 'Annexes' in the field of heat pumps are undertaken. These tasks are conducted on a cost-sharing and/or task-sharing basis by the participating countries. An Annex is in general coordinated by one country which acts as the Operating Agent (manager). Annexes have specific topics and workplans and operate for a specified period, usually several years. The objectives vary from information exchange to the development and implementation of technology. This report presents the results of one Annex. Coordination of activities and assistance to Operating Agents is provided by the Technical Support Services Unit, the administrative arm of the Programme. The Programme is governed by an Executive Committee, which monitors existing projects and identifies new areas where collaborative effort may be beneficial.

The IEA Heat Pump Centre

A central role within the IEA Heat Pump Programme is played by the IEA Heat Pump Centre (HPC), Annex 16. Consistent with the overall objective of the IA the HPC seeks to advance and disseminate knowledge about heat pumps, and promote their use wherever appropriate. Activities of the HPC include the production of a quarterly newsletter, the organization of workshops, an inquiry service, a promotion programme, and the performance of analyses. The HPC also publishes selected results from other Annexes, and this publication is one result of this activity.

For further information about the IEA Heat Pump Programme contact the Technical Support Services Unit (TSSU) and for inquiries on heat pump issues in general contact the IEA Heat Pump Centre at the following address:

IEA Heat Pump Centre / TSSU
P.O. Box 17
6130 AA Sittard
The Netherlands
Tel.: +31-46-595 236
Fax: +31-46-510 389

Published by

IEA Heat Pump Centre
Swentiboldstraat 21, 6137 AE Sittard
P.O. Box 17, 6130 AA Sittard
The Netherlands
Tel.: +31-46-595 236
Fax: +31-46-510 389

Legal Notice

Neither the IEA Heat Pump Centre nor any person acting on its behalf: (a) makes any warranty or representation, express or implied, with respect to the information contained in this report; or (b) assumes liabilities with respect to the use of, or damages resulting from the use of this information. Reference herein to any specific commercial product, process, or service by trade name, trademark, manufacturer, or otherwise, does not necessarily constitute or imply its endorsement, recommendation or favouring. The views and opinions of authors expressed herein do not necessarily state or reflect those of the IEA Heat Pump Centre, or any of its employees. The information herein is presented in the authors' own words.

Production

IEA Heat Pump Centre, Sittard, the Netherlands

First published in March 1990
Reprint of Heat Pump Technology Center of Tokyo, Japan, report

PREFACE

In the IEA Annex XIV Activities workshops, a number of experts on absorption heat pumps from several countries met to discuss the characteristics of refrigerants. I thought it would be useful if the workshop participants could share the latest information about absorption heat pumps in addition to the task report. Fortunately, my wish was granted. Ten topics were introduced at the Chicago workshop, and another ten were introduced in Stockholm. Because each of the presentations has significance for our activities, I am including all of them in the Volume II of the Annex XIV Final Report. I want to thank each of the contributors for their cooperation.

Takamoto Saito, Professor, Dr.
University of Tokyo

Table of Contents

The National Team of Sweden

The National Team of U.S.A.

Annex XIV
Principal Investigators

Belgium	J. Berghmans, Professor, Dr. Katholieke Universiteit Leuven Instituut Mechanica Celestijnenlaan 300A B-3030 Heverlee Belgium
Denmark	Hans Joergen Hoegaard Knudsen, Professor, Dr. Refrigeration Laboratory Technical University of Denmark DTH Bldg. 402B DK-2800 Lyngby Denmark
Germany	K. Stephan, Professor, Dr. Institut für Technische Thermodynamik Universität Stuttgart D-7000 Stuttgart 80 Federal Republic of Germany
Japan	Takamoto Saito, Professor, Dr. Faculty of Engineering University of Tokyo 3-1, Hongo 7-chome Bunkyo-ku, Tokyo 113 Japan
Sweden	Fredrik Setterwall, Professor, Dr. Department of Chemical Engineering The Royal Institute of Technology S-100 72 Stockholm Sweden
USA	Robert C. DeVault Energy Division Oak Ridge National Laboratory Oak Ridge, Tennessee 37831 U.S.A.

The National Team of Denmark

1. CURRENT SITUATION OF RESEARCH AND DEVELOPMENT OF ABSORPTION TECHNOLOGY IN DENMARK

H.J.H. Knudsen
Refrigeration Laboratory
Technical University of Denmark
Denmark

Solar refrigeration

The main interest in absorption technology in Denmark has been solar absorption refrigeration. As working media is used ammonia as refrigerant and calcium cloride as absorbent.

The work in this area has been going on the last 12 years, and at present plant for block ice production using solar absorption refrigeration is being erected in Gambia with economical surport from the danish government.

Absorption refrigeration systems

Mathematical models for static simulation of one stage absorption systems using ammonia and water as working pair have been developed.

The thermodynamic properties for the working pair are calculated with the correlation of Ziegler and Trepp. The Themophysical properties are calculated using polynomials developed at the Refrigeration Laboratory, Technical University of Denmark, based on the data given in: Plank Handbuch der Kältetechnik, Bind VII (Author Niebergall). Heat and mass transfer is calculated with help of data/correlations given in this work too. The programme has been made during three master projects.

Resorption heat pumps

A matematical model for the thermodynamic simulation of a resorption heat pump, using ammonia and water, has been worked out. The transport phenomena are taking in account by means of prescribed temperature differences in the different components. The programme has been used to evaluate the use of heat source of 60 ℃ in a district heating system working with a forward temperature of 80-85℃.

A theoretical investigation of heat pump with solid absorbent and a number of stages has been performed. A small test plant has been built, and the results from this plant has shown, that the heat capacities in this form of solid absorption heat pump is ruinous to the performance, and it is decided to close this project. A report is under preperation.

Absorption heat pumps

A test plant using ammonia and water as working pair has been built. The primarily results has shown, that the absorber used (falling film) is not well suited to the small flows used in this heat pump, estimated to have a capacity of 10 kW. A new absorber is planned to be built. At present the construction is not made, but the absorber will presumable be a bubble absorber. In a master project has the performance of a bubble absorber been investigated and it is believed, that this form of absorber will be suited in an ammonia, water-absorption plant with small capacity.

2. MULTI-STAGE SOLID ABSORPTION HEAT TRANSFORMERS FOR RECOVERY OF INDUSTRIAL WASTE HEAT

P. Worsøe-Schmidt and Kim Sørensen
Refrigeration Laboratory
The Technical University of Denmark
Denmark

SUMMARY

An overview of solid-absorption (resorption) heat pumps and heat transformer cycles of varying complexity are given. All cycles are derived from a basic intermittent cycle in which ammonia is alternately absorbed in and desorbed from two metal halides having their equilibrium curves at different temperature levels.

Equilibrium data for some 60 ammoniates have been extracted from the literature. Because most data are taken at low pressure (up to atmospheric pressure) equilibrium p,T - data have been measured at higher pressures for one of the promising reactions ($MnCl_2 \cdot 2NH_3 + 4NH_3 \rightleftharpoons MnCl_2 \cdot 6NH_3$). The specific volume of the ammoniates has been shown to be additive to a good approximation, and the very few data on the specific heat capacity indicate that treating it as additive also should give a conservative estimate of cycle performance.

The existing data on the kinetics of the reactions in question show that except for absorber dimensions which are considerably smaller than what can be used in a practical design the controlling process is thermal conduction rather than reaction kinetics. Reliable data for the thermal conductivity have been found only for the ammoniates of calcium chloride, but it seems reasonable to assume that they are representative as to the order to magnitude.

The feasibility of using solid-resorption cycles for upgrading industrial waste heat can be evaluated only on the basis of a reasonably cdetailed design. For this reason the main dimensions of a continuously operating heat pump for energy recovery form a drying process has been worked out. The design is based on a large number of elemental absorbers comprising a rotating drum in the manner of rotating heat regenerators.

A mathematical model consisting of the differential and algebraic equations that covers the heat transfer processes and the reaction processes has been developed and used for simulation of a few heat pump cycles. The equations are solved simultaneously by a programme complex called SPADE.

The results of the simulations are presented in terms of the coefficient of performance supplemented by temperature curves showing the cyclic variation of air, gas absorbent and equilibrium

temperatures. In comparison with what could be obtained if all processes proceeded reversibly the results are disappointing. Large irreversibility occur particularly at the low temperature end of the cycles where the impossibility of arranging for regenerative heat exchange is felt most. Based on a comparison with an ordinary rotary regenerator the conclusion is that solid absorption heat pumps (and heat absorbers) are too bulky and the investment in all probability too high for the proposition to be interesting.

OBJECTIVE

The aim of the project has been to investigate the feasibility of using solid-absorption heat pumps and heat transformers for upgrading industrial waste heat to temperatures at which it can be used for process purposes. In particular systems utilizing ammonia as the working substance and metal halides as absorbents seem to offer promising prospects.

INTRODUCTION

In many process industries waste heat is available at temperatures up to 80-90°C either in the form of hot water or, particularly in drying operations, as hot and humid air. For such heat to become useful for process purposes it must be upgraded to a higher temperature, preferably at least 120-180°C. With absorption heat pumps this upgrading can be accomplished with a smaller heat input at a high temperature whereas an absorption heat transformer can upgrade a correspondingly small part of the waste heat without the need for any input of high grade energy (apart from what is necessary for pumps and/or fans). The energy flow of these two cycles are illustrated in figure 1.

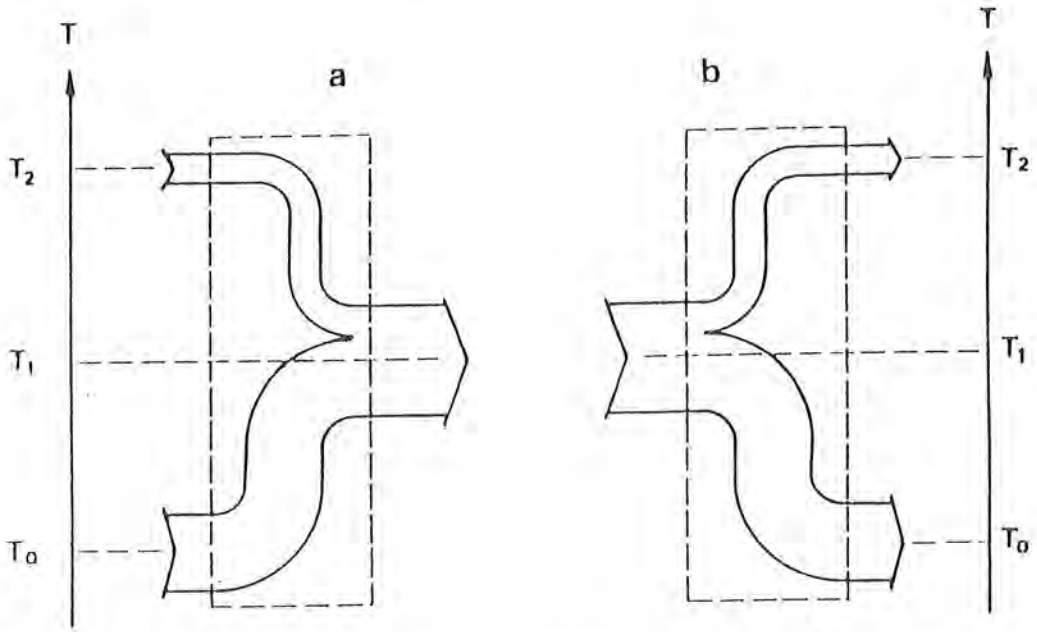

Figure 1. Energy flow in an absorption (resorption) heat pump (a) and heat transformer (b) cycle.

The only type of absorption heat pump which is presently used to any extent for this purpose is the lithium-water machine. However, the temperature lift that can be obtained is limited by crystallization of the salt at high concentrations. This together with rapidly increasing rates of corrosion at high temperatures limits the temperature to approximately 150°C.

For temperatures above this range solid-absorption cycles using ammonia as the working substance and metal halides as absorbents seem to offer a number of advantages:

- A large number of potential absorbents are available which makes it possible to operate at moderate pressures over a wide temperature range.

- Since the system is completely devoid of water corrosion problems should not arise even at high temperatures.

- The heat of reaction is large, up to three times the latent heat of vaporization which should make it possible to obtain reasonable high energy densities.

- Solid absorption systems are basically extremely simple and therefore potentially very reliable.

The drawbacks of a solid-absorption system arises partly from the immobility of the absorbent, partly from the kinetics of the reaction and the thermo-physical properties of the ammoniates:

- The basic cycles are intermittent. This necessitates special precautions in order to adapt these cycles to a continous process and effectively limits the application to heating and cooling of gas streams.

- For an intermittent cycle regenerative heat exchange between the hot and the cold absorbent is at best very different to establish and it can never attain a very high effectiveness. The COP of a solid-absorption cycle is therefore inherently lower than what could be obtained with a liquid absorbent.

- Gas-solid reactions proceed at low rates compared with gas-liquid mass transfer. For this reason significant departures from equilibrium are necessary in order to obtain sufficiently large reaction rates.

- Poor thermal conductivity of the ammoniates calls for small dimensions of the absorbers and large heat transfer areas.

The fact that the basic solid-absorption cycle is intermittent does not preclude continous heating and cooling of external streams, if the system is divided into a number of units each containing two absorbents between which ammonia can be exchanged, and these units successively exchange heat with the external streams continous heating and cooling can be obtained. This kind of operation lends itself in particular to heating and cooling of gas streams.

CONCLUSIONS

Numerical simulation of a heat pump cycle operating with a heat source temperature of 250°C and waste heat from a drying temperature at 90° shows that when the fan power is taken into account a coefficient of performance of less than 1.2 is obtained. The primary reasons for this rather poor result are:

- Due to the impossibility of incorporating regenerative heat exchange when absorbers are transferred from the hot to the cold zone too much of the thermal potential is lost. This is particularly true at the low temperature part of a heat pump; for a heat transformer the high temperature part would suffer most which would be even more detrimental to the performance.

- Even with absorber dimensions of the order of only 5 mm the poor thermal conductivity of the absorbents makes it necessary to operate the cycle at large temperature differences which cause a further reduction in the coefficient of performance.

Both causes arise from the basic physics of the cycle and, therefore, one cannot hope for significant improvements through better design. A comparison with conventional rotary regenerators shows that the power density that can be obtained for a solid-absorption heat pump is only about 20 percent of what is found for rotary regenerators.

Since the price of solid-absorption equipment is closely related to the power density it is apparent that the very modest coefficient of performance that can be obtained is not nearly enough to pay for the substantially higher cost of solid-absorption heat pumps or heat transformers. However promising the theoretical cycles appear, in a concrete design they do not stand up to the requirements in terms of pay-back time that must be met by industrial equipment.

1. SOLID-ABSORPTION HEAT PUMP AND HEAT TRANSFORMER TAXONOMY

The basic element in solid absorption (resorption) heat pumps and heat transformers consists of two absorbers charged with different absorbents between which the working substance can be exchanged. Each of the absorbers (one of which may be a condensor/evaporator) must be able to exchange heat alternatingly either with one of the external streams, or with other absorbers.

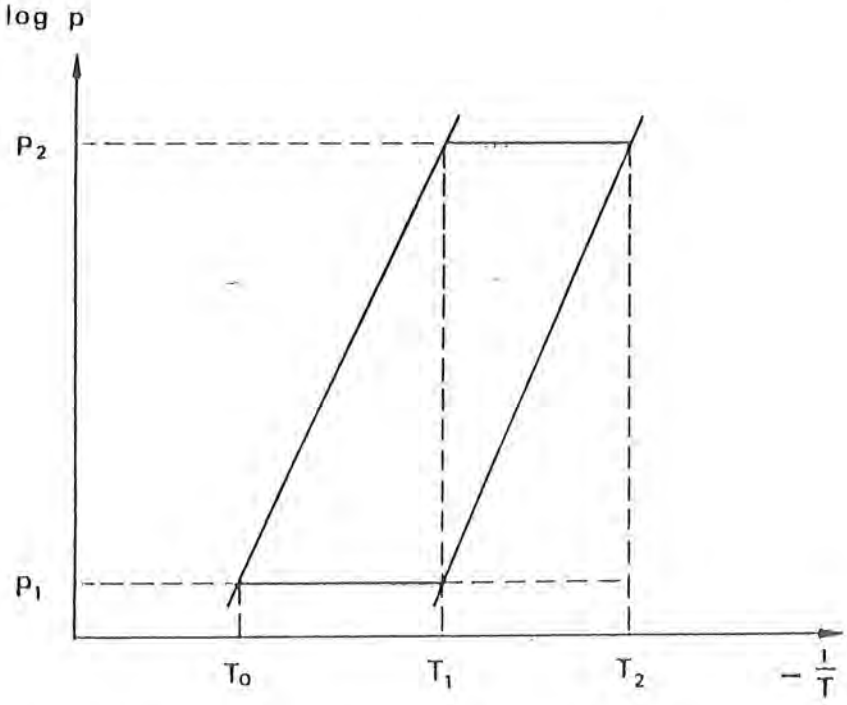

Figure 2. Simple heat pump or heat transformer cycle with only one set of absorbers (ref. figure 1.).

The basis process is conveniently depicted in a -1/T, log p-diagram (Figure 2) in which the equilibrium curves for the reactions between the working substance and the absorbents appear as nearly straight lines. The system operates alternatingly at the high and at the low pressure level, the pressure being uniform throughout the system at any one time. The temperature GAP that can be bridged by the system, that is, the difference in temperature each of the absorbents experience when the pressure level is changed is subject to limitations that are imposed by practical considerations. The upper limit is set by the strength of the components whereas the lower limit are more likely to be imposed by reaction kinetics. On the other hand, the temperature difference between the desorber and the absorber operating at the same pressure level is not limited. In complex systems with several stages this difference may comprise several standard temperature gaps, but when switching from one mode of

operation to the other the temperature change of each absorber/desorber is limited to one standard temperature gap.

The simplest solid-absorption heat pump or heat absorber consists of one absorber/desorber pair. In one mode it operates between and upper and an intermediate temperature level, in the other mode between the intermediate and the ambient temperature. The latter is for heat pump operation the temperature level of which waste heat is available. Figure 3 shows in symbolic form various combinations from the simple single-stage system to what could be called a three-stage-system spanning four standard temperature gaps. It is, however, more appropriate just to refer to the number of absorber/desorber pairs that constitute the system (not counting duplication of absorber/desorber pairs operating at the same temperature levels).

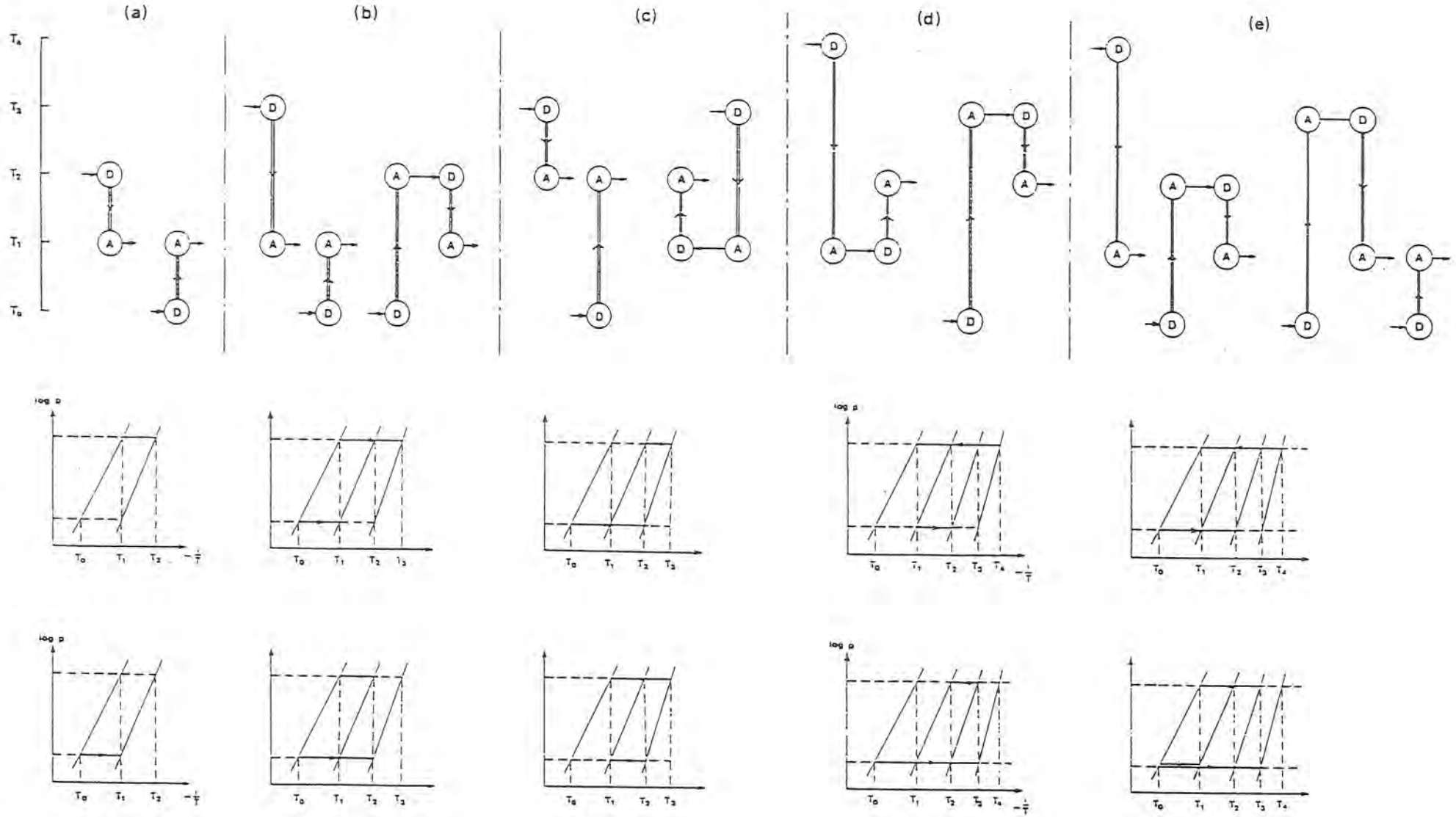

Figure 3. Heat pump configurations with one (a), two (b,c,d), and three (e) sets of absorbers. A designates absorber, D desorber. Vertical arrows indicate flow of ammonia horizontal arrows heat flow.
In each of the symbolic figures the coupling to the left refers to the upper row of the log p, -1/T-diagrams, the coupling to the right to the lower row.
Heat transformer configurations are obtained by switching A to D and vice versa and reversing all arrows both vertical and horizontal.

With the simple one-pair system a heat pump can upgrade waste heat through one temperature gap, using as the driving force heat at the next higher temperature level. It delivers two "units" *) of heat for one unit of waste heat and one unit of higher grade heat received. Working as a heat transformer the system delivers one unit of heat at the high temperature level for an input of two at the intermediate level. One unit must be rejected to the ambient.

With two absorber/desorber pairs one of which span two standard temperature gaps two different couplings are possible depending on whether the intermediate level is closer to the ambient or to the high level. In both cases a heat pump will deliver three units of heat at the intermediate level, in the former case, however, at the expense of one unit at the high level, whereas in the latter case two units of heat must be supplied at the high level. Correspondingly, a heat transformer will deliver one or two units of heat at the high level for an input of three units of the intermediate level.

By raising the top temperature by one standard gap one of two possible improvement can be obtained. In the heat pump mode either the high temperature input can be reduced from two units to one unit for heat delivery at the upper intermediate level, or four units in stead of three can be obtained at the lower intermediate level for an input of one unit at the high level.

More absorber/desorber pairs could be added, and heat could be supplied and delivered at more than one level. The present examples should suffice, however, to indicate the possibilities that exist for designing a heat pump or heat transformer system to any given set of circumstances.

It is tempting to take the ratio of the number of "heat units" delivered to the number of units supplied as a first approximation to the COP of the system. This would, however, be highly misleading. In the first place, even for a system that operates ideally, that is, with negligible temperature differences and no departure from equilibrium, curves towards the right in the -1/T, log p-diagram the ammonia is bound more strongly than in those closer to the saturation curve of ammonia and, therefore, the heat of reaction is considerably

---

*) As will be explained below a "Unit of heat" is not a fixed quantity. The amount of heat depends strongly on the temperature level and other conditions of operation.

larger. When to this is added the effects of departure from equilibrium of temperature differences in heat exchangers and of losses due to the cyclic heating and cooling of the absorbers, the actual COP comes out far below the ratio between "heat units".

2. THERMODYNAMIC PROPERTIES OF METAL HALIDE AMMONIATES.

Most metal halides form several stable complexes with ammonia according to the reaction scheme

$$M \cdot \alpha NH_3 + \beta NH_3 \rightleftharpoons M \cdot (\alpha+\beta) NH_3$$

where M stands for the metal halide.

We have here a system of three phases (two solid and one gaseous), three components and one reaction. According to the phase rule the system has only one degree of freedom so that at equilibrium the temperature is determined by the pressure or vice versa. Like the vapour pressure curve of a pure substance the equilibrium curve is to a good approximation a straight line when plotted in a -1/T, log p-diagram.

Equilibrium data for a large number of ammoniates was determined for purely scientific reasons from the late 19th century and up through the 1920's. Particularly the work by Biltz and his co-workers (summarized in ref.1) covers a large number of compounds. Later Hart and Partington (2) extended measurements of some compounds to higher pressures.

As examples of potential absorbents the halides of the alkaline earth metals and those of the iron group are taken. The former accommodate up to eight moles of ammonia (BaJ_2 even 10), the latter up to six moles. In figures 4 and 5 the equilibrium p,T-curves for the various transitions are shown.

Most of the data are extrapolated from pressures below atmosphere. Comparison with more recent investigations (2-8) as well as measurements carried out in the course of the present investigation (see appendix A) seems to indicate that although some data may need correction the overall picture is correct. What transpires is that in the temperature range up to 500°C enough potential absorbents are available for designing a variety of heat pumps and heat transformers.

The heat of reaction, which to the first approximation is proportional to the slope of the equilibrium curve, varies from about 2500 kJ/kg NH_3 (that is, almost twice the latent heat of vaporization) for the higher ammoniates of the alkaline earth halides to almost 6000 kJ/kg NH_3 for the monammines of nickel and cobolt.

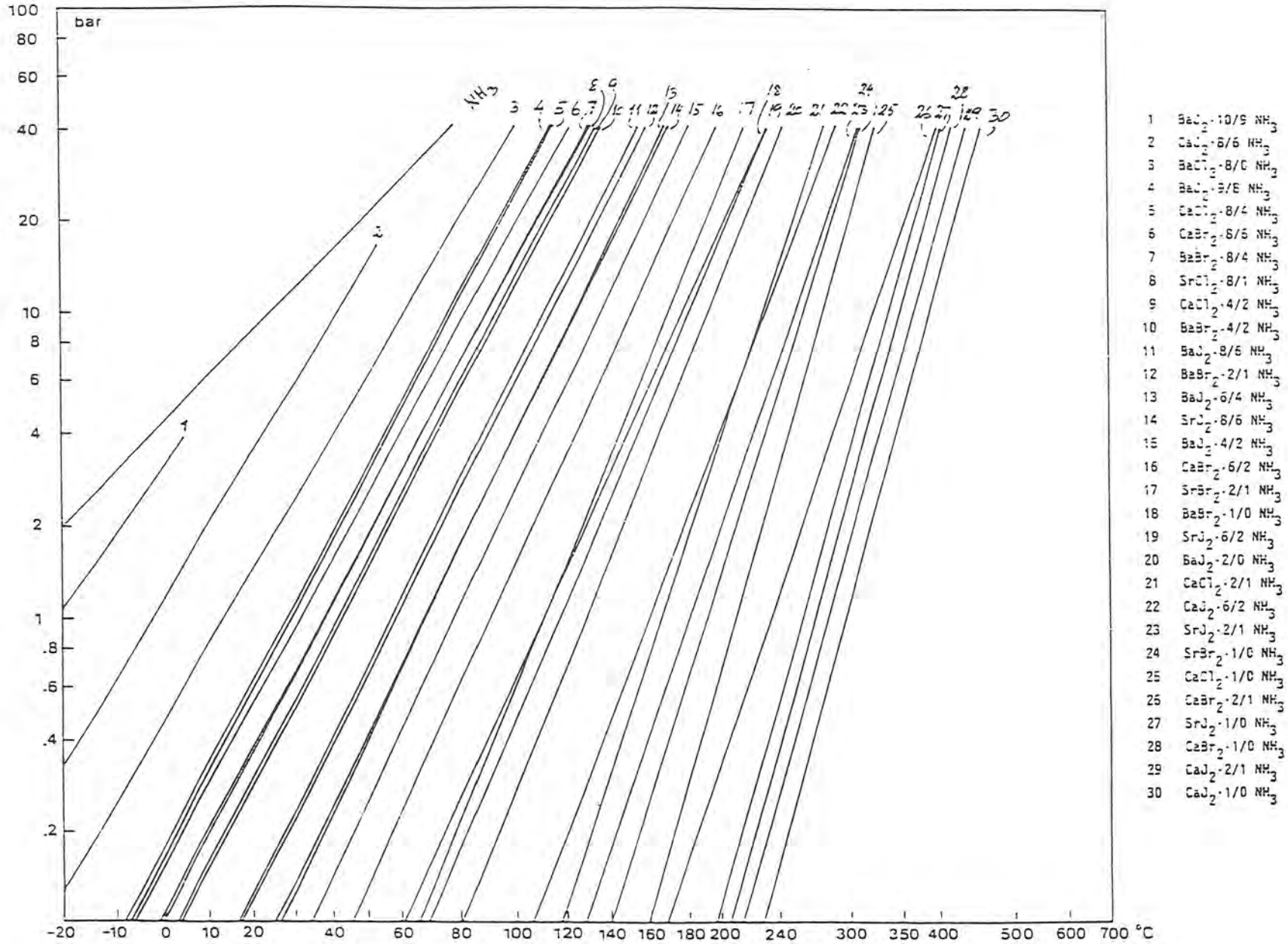

Figure 4 Equilibrium curves for the formation and dissociation of ammoniates of the alkaline earth halides.

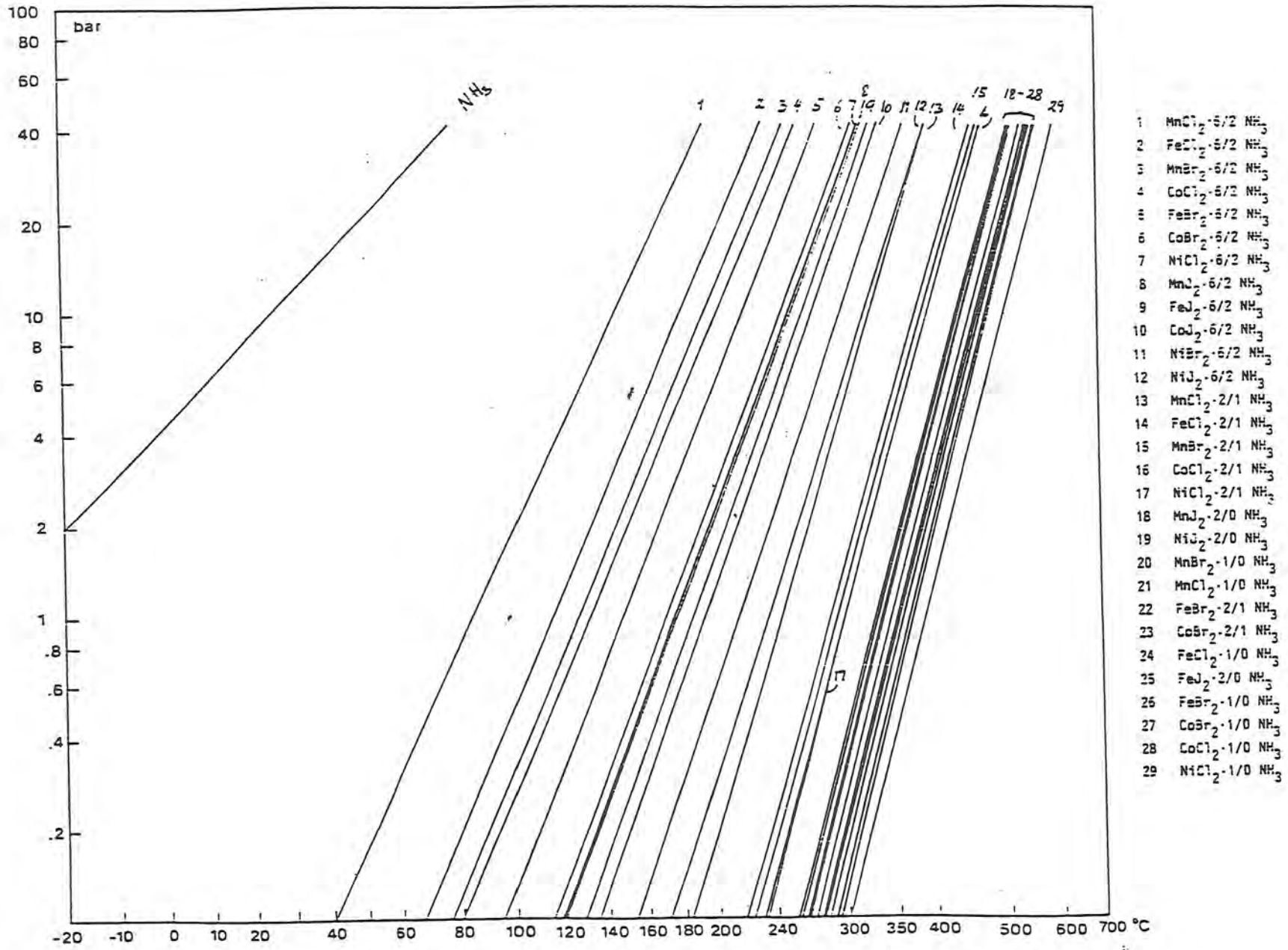

Figure 5 Equilibrium curves for the formation and dissociation of metal halides of the iron group.

Because of the high heats of reaction compared with the latent heat of vaporization, resorption cycles where the ammonia is driven off at a high temperature and is absorbed (resorbed) in a second absorbent have a higher COP than cycles where the ammonia is condensed as a pure liquid. A further benefit is that for a given temperature the resorption pressure is considerably lower than the saturation pressure of ammonia.

If in the simple resorption cycle as shown in Figure 2 a pressure ratio of 1:100 can be achieved, for example from 0.3 to 30 bar, the temperature gap that can be bridged (see the previous section) is 90-100°C at the low temperature end and 150-200°C at high temperatures. Correspondingly, the heat of reaction increases by a factor of approximately two.

For the evaluation of a resorption process knowledge of the specific heat capacity of the participating ammoniates is needed, particularly because the regenerative heat transfer between hot and cold absorbent in most cases can not be accomplished. From the literature only experimental data for the tetra and octo ammine of calcium chloride has been found (9). These data show a strong temperature dependence and whereas Kopp's law, that the molar specific heat is 6n cal/mol·K (n being the number of atoms), holds to a good approximation for many metal halides, the contribution from the ammonia is somewhat less and not completely additive. In lieu of better data, however, the use of Kopp's law would give a conservative estimate of the performance. Alternatively, the average specific heat of the NH_3-group as determined from the data of ref. 9 could be used additively.

3. THERMOPHYSICAL PROPERTIES OF METAL HALIDE AMMONIATES

Two properties are of capital importance in the design of ammonia absorbers with solid absorbents. One is the density of the ammoniate, the other the thermal conductivity. The importance of the former stems from the fact that the volume of the metal salts increases considerable when ammonia is absorbed. If sufficient room for expansion has not been provided the ammoniate may be compacted to a degree when it is virtually impervious to ammonia, and in extreme cases the absorber may burst.

The thermal conductivity is important because unless the dimensions of the absorber are extremely small the rate of reaction is primarily controlled by the rate of which the heat of reaction can be conducted to or from the containing wall.

The specific volume of several metal halide ammoniates are reported in the literature and can be found in standard handbooks. By comparing these data with the specific volume of the pure salts it appears that in most cases the molar volumes are additive to a good approximation. Table 1 gives the molar volume of the NH_3 group as found from such data. With $FeCl_2 \cdot 6NH_3$ an $CuCl_2 \cdot 2NH_3$ as the exceptions the volume is very close to 21 l/kmol.

To the volume of the ammoniate must be added sufficient pore volume to allow for the flow of ammonia vapour to and from the individual grains of absorbent. How large this pore volume should be depends on how long a way the vapour has to migrate, that is on the dimensions of the absorber and on whether flow channels are provided in the axial direction. Experience with $CaCl_2$ in absorbers for refrigeration systems in which the cross-sectional dimension is of the order of 10 mm and the axial dimension about 1 metre seams to indicate that with a pore volume of 100-150 l/kmol the flow of ammonia is not impeded. It should be held in mind, however, that for such systems the absorption/-desorption time is of the order of hours whereas in the case of heat pumps and heat transformers the cycling times must be of the order of minutes.

Data on the thermal conductivity of metal halide ammoniates are extremely scarce. The most reliable are probably those of Andreasen (8) who made measurements on di-, tetra- and octoammoniate of calcium chloride. If these data can be taken as representative the thermal conductivities of metal halide ammoniates lie in the range 0.10-0.25 W/mK with the high values for the higher ammoniates and denser packing. Since the thermal conductivity is of great

importance for the degree of departure from equilibrium and, hence, for the degree of irreversibility at which a heat pump or heat transformer operates, more accurate data are needed before a detailed design can be undertaken.

TABLE 1. Molar volume of ammonia in metal halide complexes.

Compound	Molar volume, l/kmol		
	Salt	Complex	Ammonia
$CoCl_2 \cdot 2NH_3$	38.7	α_1 78.2	19.8
		β_1 79.1	20.2
$CoCl_2 \cdot 6NH_3$	38.7	155.0	19.4
$CoBr_2 \cdot 6NH_3$	44.6	171.5	21.2
$CoI_2 \cdot 6NH_3$	55.0	198.0	23.8
$FeCl_2 \cdot 6NH_3$	40.1	118.7	13.1
$NiCl_2 \cdot 6NH_3$	36.6	157.9	20.2
$NiBr_2 \cdot 6NH_3$	42.9	174.6	22.0
$NiI_2 \cdot 6NH_3$	53.6	197.4	24.0
$CuCl_2 \cdot 2NH_3$	39.7	72.6	16.4
$CuCl_2 \cdot 6NH_3$ *	39.7	160.0	20.0
$CaCl_2 \cdot NH_3$ *	51.0	70.9	19.9
$CaCl_2 \cdot 2NH_3$ *	51.0	90.3	19.6
$CaCl_2 \cdot 4NH_3$ *	51.0	129.6	19.6
$CaCl_2 \cdot 8NH_3$ *	51.0	208.2	19.6
$BaCl_2 \cdot 8NH_3$ *	53.6	225.8	21.5

Ref. 10.

4. REACTION KINETICS OF ABSORPTION AND DESORPTION

Contrary to what is the case for condensation and evaporation of pure substances where the deviation from equilibrium at the interface is negligible even at high transferences, gas-solid reactions require significant departures from equilibrium conditions in order to proceed at finite rates. Not very much is known about the reaction kinetics and reliable experimental data are scarce.

The question of reaction kinetics is complicated by the fact that several physical processes contribute to the overall reaction rate. Depending on the packing density of the absorbent and the ammonia pressure, diffusion of the gas and/or thermal conduction may be the controlling processes rather than the kinetics of the reaction. This is amply demonstrated by the widely scattered results obtained by various researchers. Clausen and Worsøe-Schmidt (6) found differences of at least an order of magnitude between data obtained from small samples in a differential thermal analyzer (3,4) and measurements performed on bulk quantities (7,11,12). The former presumably represent most truthfully the actual kinetics of the reaction whereas the latter are heavily influenced by thermal and diffusion resistances in the absorbent. Andreasen (8) developed an indirect method by which he could ascertain the reaction rate from measurements on a cylindrical test absorber. For evaluation actual absorber designs this method could be very useful. For the numerical simulations described in a subsequent section a model developed by Andreasen was used,

$$\frac{d\mu}{dt} = A \exp\left(-\frac{E_a}{RT_a}\right)(T-T_a)^n$$

Here

- μ is the degree of reaction
- t is the time
- A is a constant
- E_a is the activation energy
- R is the universal gas constant
- T is the absorbent temperature
- T_a is the equilibrium temperature

For the exponent n values between 2 and 4 were found. Some of the compounds exhibit a behaviour of hysteresis as can be seen from Figure 6. If such data were to be correlated by the above expression a very large exponent would be needed.

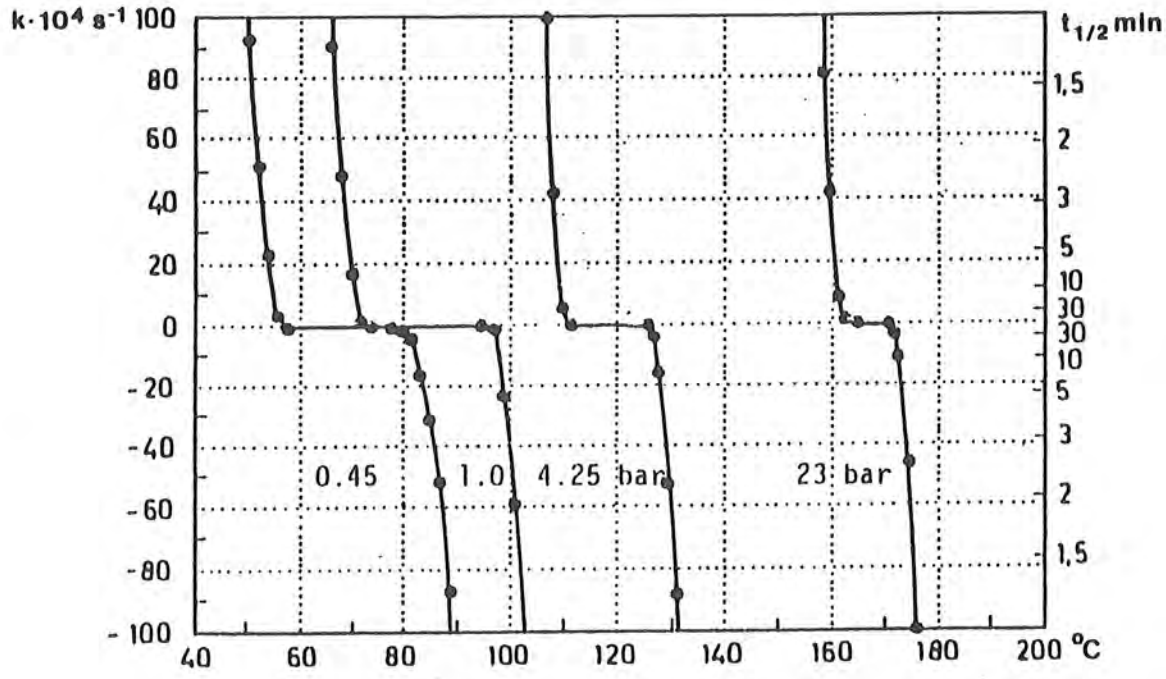

Figure 6. Rate constant and half-time for the reaction

$MnCl_2 \cdot 2NH_3 + 4NH_3 \rightleftharpoons MnCl_2 \cdot 6NH_3$ (from ref. 4)

5. PRELIMINARY DESIGN OF A SOLID-RESORPTION HEAT PUMP

The feasibility of the solid-resorption heat pump or heat transformer concept cannot be evaluated without reference to a reasonably concrete design. The reason is that the many departures from ideal (that is, fully reversible) operation which are imposed by practical considerations need to be evaluated. As in a typical example the design of an intermediate-temperature heat pump for energy recovery from a drying process has been worked out in some detail.

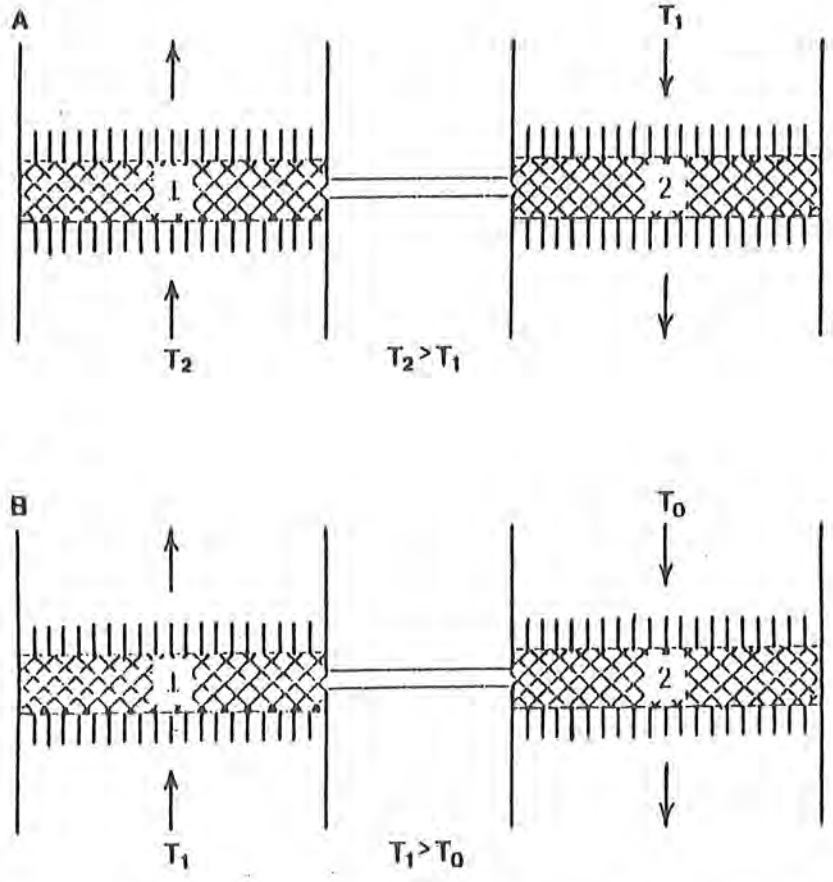

Figure 7. Basic element in solid-resorption heat pump, cf. Figure 3 (a).

In order to keep the design reasonably simple a configuration corresponding to figure 3(a) with just one set of absorber/ desorber was chosen as the first example. The basic element in the construction is an assembly of two absorbers charged with a "high-temperature" (HT) " and a "low temperature" (LT) absorbent, respectively, as shown in Figure 7. An extended outer surface provides a large transfer area for transferring heat to and from air streams. During a cycle the HT-absorber is alternatively in contact with the stream of exhaust air which provides the high temperature heat source, and with the already preheated fresh air to which heat is delivered. The LT-absorber is

alternatively taking up heat from the already somewhat cooled exhaust air and delivering heat to the fresh air. In order to attain continuous heating and cooling of the gas streams a large number of such absorber pairs are arranged in a drum which revolves (see Figure 8) at moderate speed.

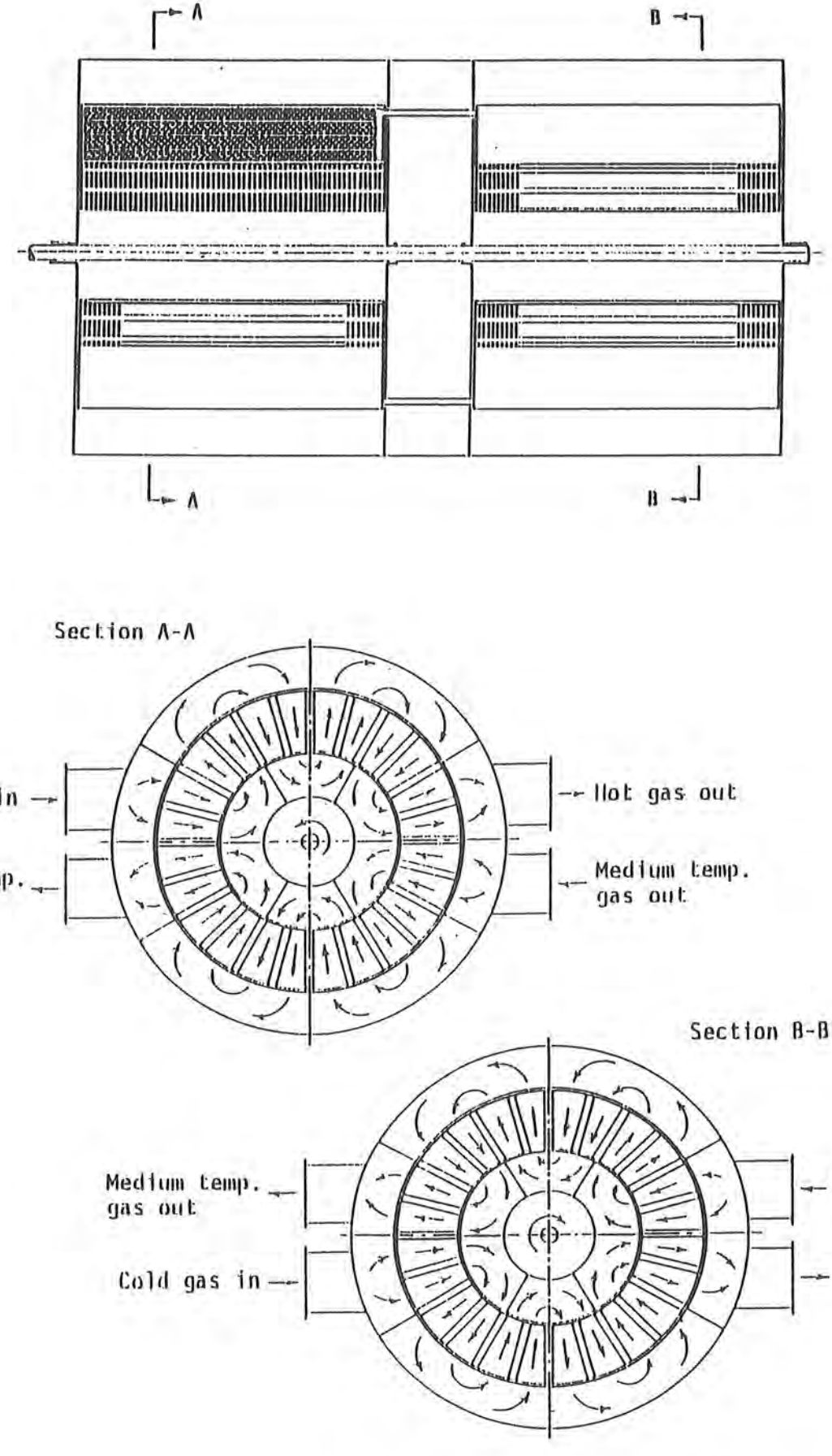

Figure 8. Schematic design of solid-resorption heat pump for continuous heating and cooling of gas streams. Inner and outer flow chambers are stationary while absorbers in drum-like structure rotate.

For a heat pump like the one described above to be an attractive investment the COP must be of a magnitude where the energy savings are sufficient to pay for extra investment above what a simple heat exchanger would require. Furthermore the space requirements should not be excessive in comparison with that of the primary process equipment. This means that on the one side departures from equilibrium should as small as possible while on the other side cycle times must be kept small, of the order of minutes. On the air side compact heat transfer surfaces are needed in order to keep the temperature differences small.

Due to the very low thermal conductivity of the ammoniates the rate of reaction in an absorber will usually be controlled by thermal conduction rather than by reaction kinetics (except when the reaction is near to completion). Rapid cycling, therefore, is obtained by keeping the conduction path small or by providing internal ribs of high conductivity. For the present purpose a simple design of the elemental absorbers which combined a small conductive path with a compact external surface could be obtained by using so-called skivefin tubes (13). These are extended aluminium profiles with a number of parallel rectangular passages. On the outside an extended surface has been provided by a shaping operation as shown in Figure 9. The cross-sectional areas of the passages are 15-25 mm^2 and profiles are available with from three to 16 passages (see Appendix B). the ratio of external to internal transfer area varies from 6 to 10 depending on the fin spacing. Due to the interruption of the fins reasonably high heat transfer coefficients are obtained on the outer surface for moderate air volocitics.

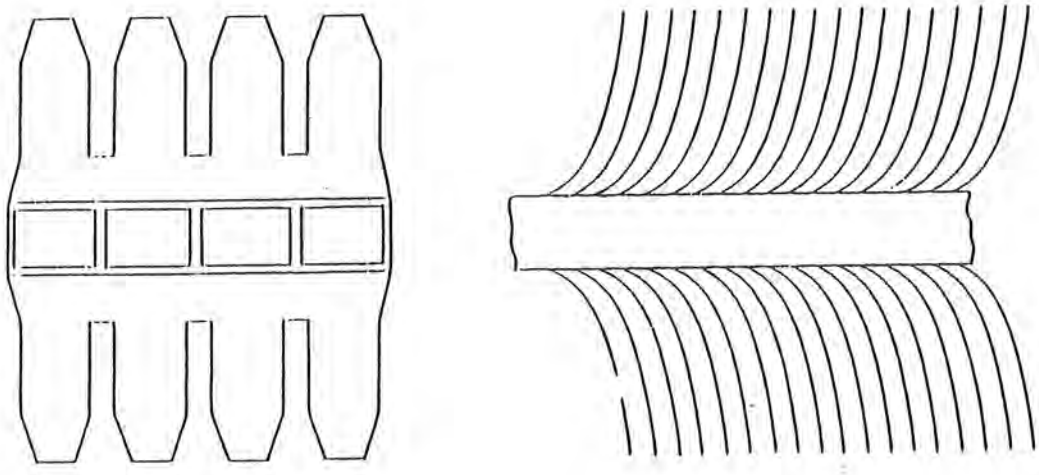

Figure 9. Skivefin profile

Absorber elements can be made from such profiles simply by removing the fin on a short length at the separation between the two absorbents providing a plug for separating the absorbents, load the absorbents and close the passages at both end by brazing or welding. If, say, 48 elements are placed axially as indicated in Figure 8 the air streams can be conducted in various ways with different numbers of flow passages in parallel and in series.

6. NUMERICAL SIMULATION OF ROTARY HEAT PUMP OPERATION.

Because the processes of absorption and desorption in solids are inherently transient and the thermodynamic states of a solid-absorption heat pump or heat transformer are determined by a balance of heat and mass transfer processes and reaction kinetics in two absorbers, process calculations must be performed dynamically, that is, they can be accomplished only by numerical simulation of the entire system.

A complete solution would require that the transient conduction equation with a source (or sink) term controlled by a rate-of-reaction equation was solved to the proper geometric simultaneously for the two absorbers together with energy-balance equations for each of the two external streams. This would necessitate simultaneous finite-difference or finite-element solutions in two spatial and the time dimension together with the reaction equations and with rather complex boundary conditions. Obviously, the computation time, even on a fast computer, would be prohibitively long. For this reason a lumped parameter approach was adopted so that the problem could be formulated in terms of a number of algebraic and ordinary differential equations.

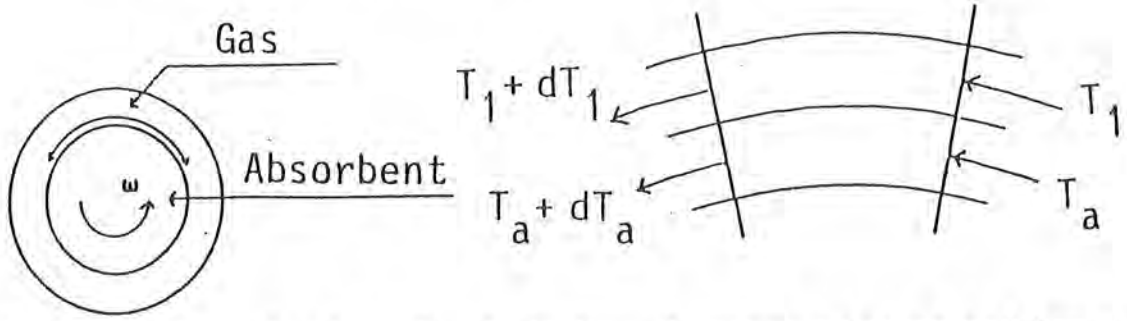

Figure 10. Control volume for derivation of energy balances and heat transfer rate equations.

The governing equations are formulated for the control volume shown in Figure 10. In the derivation it is assumed that there is through control volume a uniform tangential flow of absorbent as well as of gas. For each of the two absorbers that constitute a pair the following differential equations are derived:

- an energy balance for the absorbent flow combined with a rate equation for the heat transfer rate between absorbent and gas;
- an energy balance for the gas flow combined with the same heat transfer rate equation;

- a rate equation for rate of reaction;

These six equation are supplemented by two systems equations

- an overall ammonia balance simply stating that what is desorbed in one absorber is absorbed in the other;

- an equation linking the equilibrium temperatures of the two absorbers through the fact that the pressure is the same throughout the system at any particular moment.

These eight equations which are listed in appendix C are sufficient to determine the eight unknowns of the system:

- the temperature of the hot and the cold gas;

- the temperature of each of the absorbents

- the two equilibrium temperatures

- the degree of reaction in each absorber

The pressure in the system follows from either one of the equilibrium temperatures.

The thermal capacity of the containing walls are lumped with that of the absorbent. The latter depends strongly on the amount of ammonia absorbed. Whereas the salt contributes very little.

As independent variable is chosen the angle; time derivatives are expressed in that variable.

The equations are solved by means of a programme complex called SPADE (14) (Simulation Programme for Algebraic an Differential Equations) which solves simultaneously up to some twenty algebraic and first-order differential equations.

For the simulation of a complete cycle the equations must be solved twice, once at the high temperature and pressure level and once at the low. Since not all starting values are known before- hand the procedure must be repeated a number of times before a quasi-static solution is obtained. Some iteration will also be needed because in each computation one of the integrations will proceed against the gas flow which means that the temperature at the start (which is

the exit temperature) is not known. Details of the simulation programme can be found in ref. 15.

7. RESULTS OF THE NUMERICAL SIMULATIONS

As the first example was taken a simple heat pump cycle corresponding to the one depicted in Figure 3(a). The heat source is flue gas (or hot air) from a furnace at 250°C. Exhaust air is available at 90°C. The two absorbents were ammoniates of $ZnBr_2$ and $NiBr_2$, respectively. For the cycle the transient between the di- and the hexa-ammoniates were utilized. Equilibrium curves for the two reactions are shown in Figure 11.

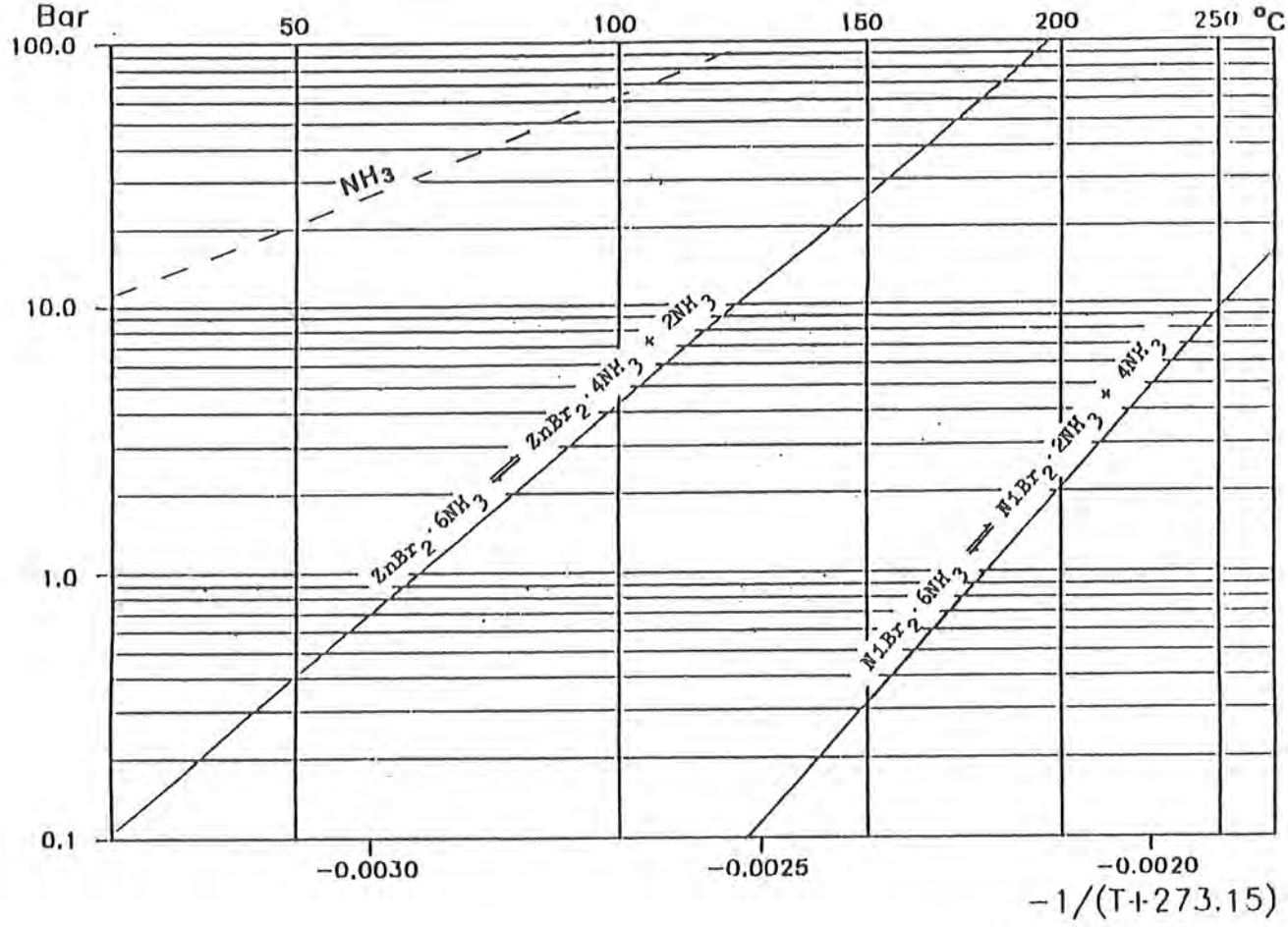

Figure 11. Equilibrium curves for the reactions used for simple resorption heat pump.

Since no kinetic data for these reactions were available the rate constant for the reaction between the tetra- and octo-ammoniate of $CaCl_2$ was used,

$$K = 2.331 \cdot 10^{-3} \exp(-1368/T_a)(T_a - T_e)^{2.0}$$

where T_a is the absorbent temperature
T_e is the equilibrium temperature

The rotating drum consisted of 48 absorber pairs made from skivefin tubes of type 1876 (see Appendix B) with 10 fins per inch placed radially. The air was guided past four elements in parallel which gave six passages for each air stream if the drum was divided equally between the two air streams. The thermal capacity rates were 200 W/K for all four air streams. With a length of the drum of 0.285 m the pressure drops for each 60° sector of the drum amounted to approximately 300 Pa.

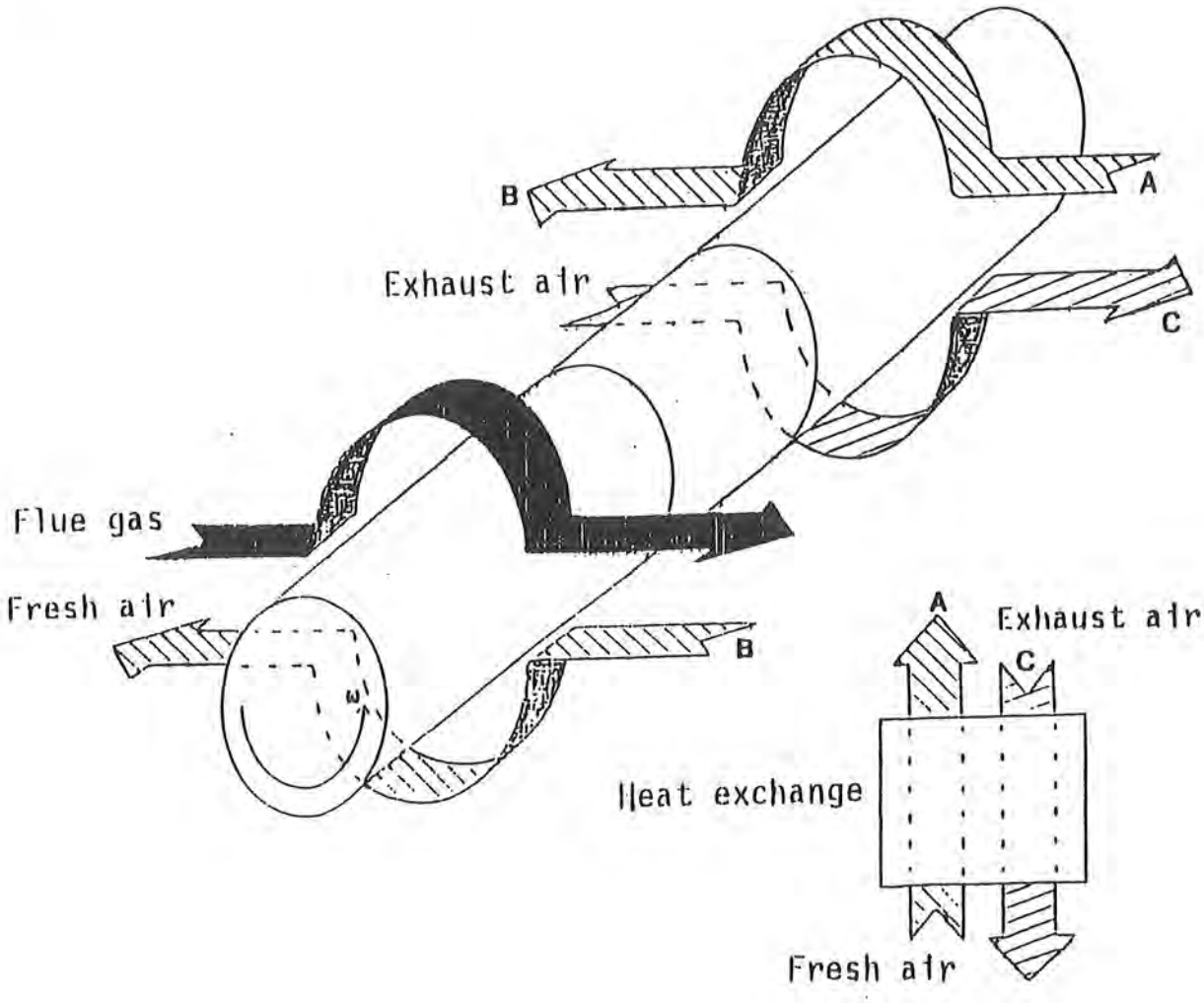

Figure 12. Schematic diagram of air and gas flows in simple resorption heat pump. Letters, indicate how air and gas flows are connected.

Figure 12 shows schematically the gas and air flows. The results of the simulation are plotted in Figure 13. Both from the temperature curves and, in particular, from curves showing the degree of reaction it is evident that the reactions have gone to an end after 120° of revolution. During the last 60° both halves of the drum are inactive.

An energy balance shows that the heat extracted from the flue gas amounts to

$$Q_{flue} = 9.8 \text{ kW}$$

and the heat transferred to the fresh air

$$Q_{fresh} = 13.2 \text{ kW}$$

This gives a coefficient of performance of

$$COP = 13.2/9.8 = 1.35$$

The total power consumption for circulating air and flue gas over the heat transfer surfaces is

$$W_{fan} = 2.1 \text{ kW}$$

Taking this into account the coefficient of performance drops to

$$COP_{tot} = 13.2/(9.8 + 2.1) = 1.17$$

In order to obtain a better utilization of the rotating drum the thermal capacity rates of flue gas, exhaust air and fresh air were all increased by 50 percent to 300 W/K and the time per revolution was decreased by 50 percent to 600 seconds. The results of these changes can be seen in Figure 13.

From the degree-of-reaction curves 7 now appears that the thermal load is well matched to the absorber size and the time of revolution. Because the capacity rates of the air and gas streams and of the "flow" of absorbent have been changed in the same proportion the coefficient of performance based on the amount of heat transferred is practically unchanged:

$$Q_{flue} = 13.4 \text{ kW}$$

$$Q_{fresh} = 18.2 \text{ kW}$$

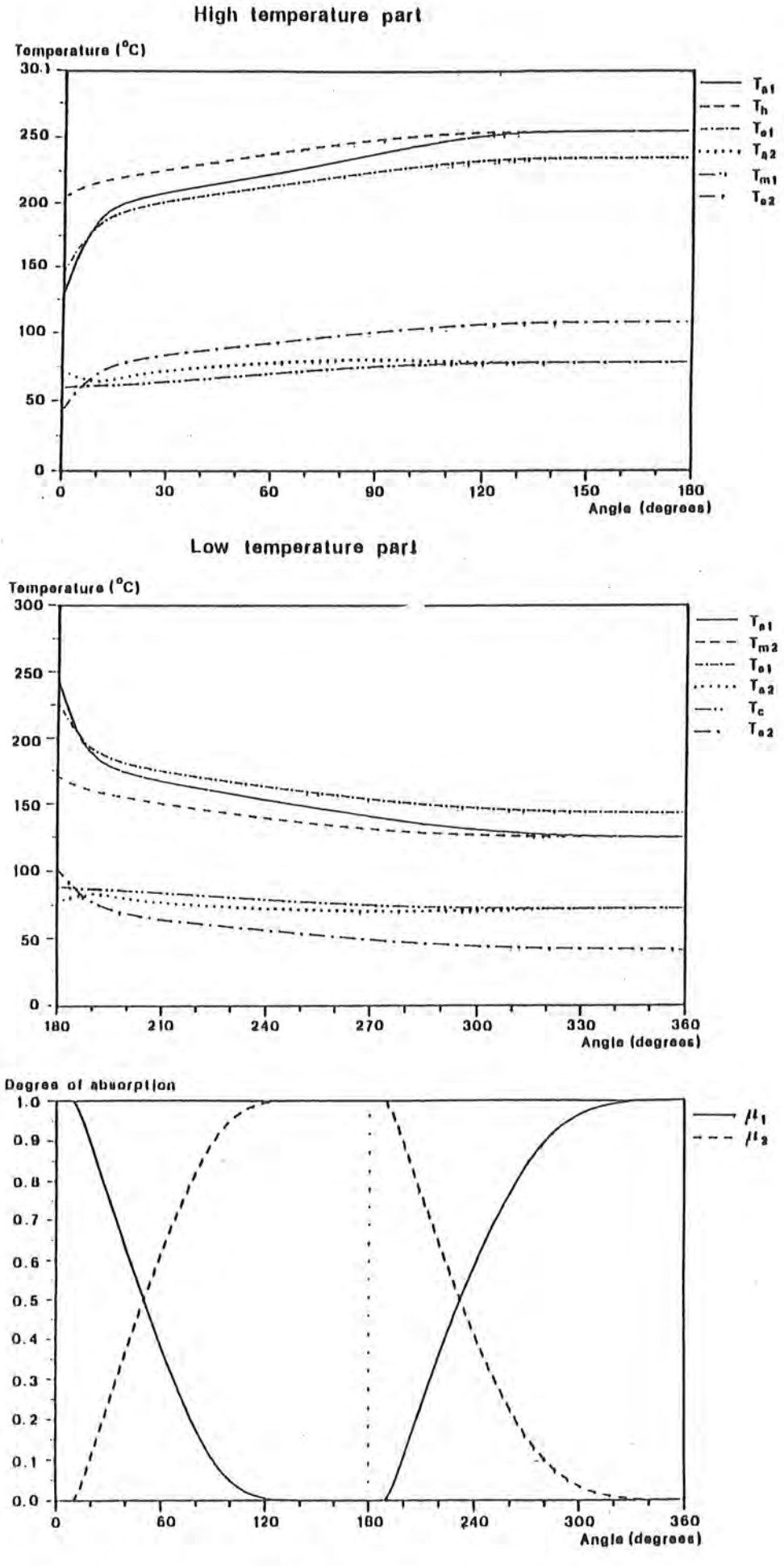

Figure 13. Results of heat pump simulation # 1.

For meaning of symbols see list of nomenclature in Appendix C.

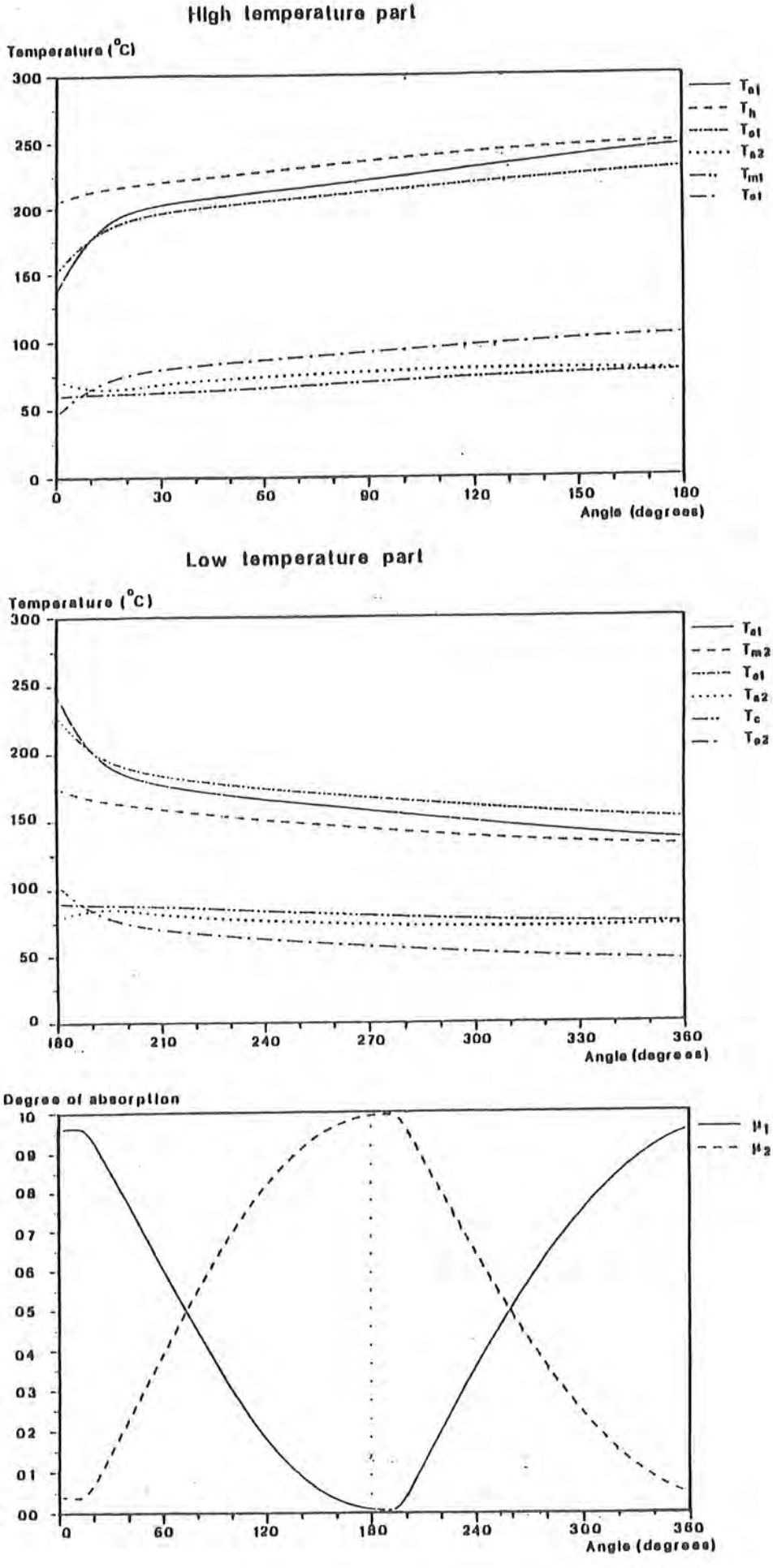

Figure 14. Results of heat pump simulation # 2.

For meaning of symbols see list of nomenclature in Appendix C.

$$COP = 18.2/13.4 = 1.36$$

The fan power, however, increases dramatically

$$W_{fan} = 5.6 \text{ W}$$

so that the total COP drops to

$$COP_{tot} = 18.2/(13.4 + 5.6) = 0.96$$

By increasing the length of the drum in proportion to the increase in air and gas flow the mass velocities would be the same as before. Since the fan power then would increase in the same proportion as the heat transfer the total COP would remain unchanged. With a temperature of the heat source of 250°C a total coefficient of performance of the order of 1.2 is clearly not satisfactory.

A different way of illustrating the processes is shown in Figure 14. Here both absorbent and air/gas temperatures from the second simulation are plotted together with the equilibrium temperatures in a ln p, -1/T- diagram. This presentation sheds some light on the (rather poor) results obtained, but the curves, in particular those for the air and gas temperatures, should be interpreted with some caution because vertical distances are not directly related to the time scale or to the angle of revolution. What comes out clearly are the large departures from equilibrium especially at the low temperature absorber. The reason is that the absorbent temperature must be below the equilibrium temperature when the latter is high and below when it is low. For the high temperature absorber the relation is the reverse and therefore the absorbent temperature is much closer to the equilibrium temperature. The difference is even more pronounced than what is immediately apparent because of the non-linear temperature scale.

The result of the large departures from equilibrium is that very little heating of the fresh air occurs in the low temperature absorber by cooling of the exhaust air. An ordinary heat exchanger in which the fresh air can be heated by the flue gas after it has passed the high temperature absorber is clearly needed.

FIGURE CAPTIONS

Figure 1. Energy flow in an absorption (resorption) heat pump (a) and heat transformer (b) cycle.

Figure 2. Simple heat pump or heat transformer cycle with only one set of absorbers (ref. figure 1.).

Figure 3. Heat pump configuration with one (a), two (b,c,d), and three (e) sets of absorbers. A designates absorber, D desorber. Vertical arrows indicate flow of ammonia horizontal arrows heat flow.

In each of the symbolic figures the coupling to the left refers to the upper row of the log p, -1/T-diagrams, the coupling to the right to the lower row.

Heat transformer configurations are obtained by switching A to D and vice versa and reversing all arrows both vertical and horizontal.

Figure 4. Equilibrium curves for the formation and dissociation of ammoniates of the alkaline earth halides.

Figure 5. Equilibrium curves for the formation and dissociation of metal halides of the iron group.

Figure 6. Rate constant and half-time for the reaction

$$MnCl_2 \cdot 2NH_3 + 4NH_3 \rightleftharpoons MnCl_2 \cdot 6NH_3$$ (from ref. 4)

Figure 7. Basic element in solid-resorption heat pump, cf. Figure 3 (a).

Figure 8. Schematic design of solid-resorption heat pump for continuous heating and cooling of gas streams. Inner and outer flow chambers are stationary while absorbers in drum-like structure rotate.

Figure 9. Skivefin profile.

Figure 10. Control volume for derivation of energy balances and heat transfer rate equations.

Figure 11. Equilibrium curves for the reactions used for simple resorption heat pump.

Figure 12. Schematic diagram of air and gas flows in simple resorption heat pump. Letters, indicate how air and gas flows are connected.

Figure 13. Results of heat pump simulation # 1. Number of absorber elements: 48. Type of elements: Skivefin 1876 (10 fins/in.) Division between hot and cold side: 180°/180°C. Length of rotating drum: 0.285m. Thermal capacity rate of air streams 200 J/K. Time per revolution: 900 s.

Figure 14. Results of heat pump simulation # 2. Design data as for simulation # 1 except Thermal capacity rate of air streams 300 J/K. Time per revolution 600 s.

Figure A. Data points and correlation for equilibrium temperature and pressure of the reaction $MnCl_2 \cdot 2/6\ NH_3$

REFERENCES

1. W. Biltz, Z.anorg. allg. Chem, 130 (1923) 93.

2. A.B. Hart and J.R. Partington, J. Chem, Soc 65 (1943) 104.

3. F.A. Jaeger, W.R. Hass and J.E. Andersson, Development of ammoniated salts thermochemical energy storage systems-Phase II. Final Rept. for the period July 1978- March 1979. U.S. Dept. of Energy (Contract No. 18-6825) June 1979.

4. M. Furner, Thermoanalytische Untersuchungen ausgewählter Komplexe von anorganischen Chloriden mit Ammoniak und Ammoniak Derivaten. Eidgenoss. Inst. für Reaktorforsch., Würenlingen (Schweiz). EIR-Berich 392, April 1980.

5. R.W. Carling, J. Chem. Thermodynamics 13 (1981) 503.

6. N.E. Clausen and P. Worsøe-Schmidt, Analysis of ammoniated metal salt suspensions for the use in solar refrigeration systems. Proc. IIR Comm. E1-E2, Meeting, Jerusalem (Israel 14-14 March, 1982, p. 177.

7. N.E. Clausen, Soldrevne køleanlæg-anvendelse af fast absorbent i suspension (Solar-driven refrigeration plants-Application of solid absorbent in suspension, in Danish). Ph.D. diss. Refrigeration Laboratory, The Technical University of Denmark, July 1984.

8. O. Andreasen, Absorption af ammoniak i metalsalte (Absorption of ammonia in metal salts, in Danish) Ph.D. diss. Refrigeration Laboratory, The Technical University of Denmark, May 1987.

9. S. Lourdudoss, T. Schuler and W. Raldow, Inorg. Chim. Acta 54 (1981) L31.

10. L.J. Gillespie and H.T. Genry, J. Am. Chem, Soc. 53 (1931) 3962.

11. W. Mehl, Z. Ges. Kälte-Ind. 41 (1934) 186

12. P. Worsøe-Schmidt and P. Bechtoft Nielsen, Design of a combined solar collector/absorber/desorber for a solid-absorption refrigerating system. ASME paper 78-HT-35 (1978).

13. R.G. Schmöle Metallwerke, Skyvefin-Wärmaustauschen. Catalogue 875.07 (8/1984).

14. P. Munter, Brugervejledning til simuleringsprogrammet SPADE (users manual for the simulation programme SPADE, in Danish). Rept. F52-79.0, Refrigeration Laboratory, The Technical University of Denmark, November 1979.

15. K. Sørensen, Resorptionsanlæg til komfortkøling/ varmepumper (Resorption plants for comfort cooling/heat pumps, in Danish). M.S. thesis, Refrigeration Laboratory, The Technical University of Denmark, July 1986.

16. W. Biltz and G.F. Hüttig, Z. anorg. allg. Chem, 109 (1919) 89.

17. F. Ephraim, Z.phys.Chem. 81 (1913) 518.

APPENDIX A. Equilibrium data for $MnCl_2 \cdot 2/6\ NH_3$

Measurements of the equilibrium temperature and pressure for the reaction

$$MnCl_2 \cdot NH_3 + 4NH_3 \rightleftharpoons MnCl_2 \cdot 6NH_3$$

were performed in an aluminium cell of 50 cm^3 volume placed in a thermostatic bath. The bath temperatue was measured with a Pt 100 thermometer with an accuracy of ± 0.1 K and the ammonia pressure with a pressure transducer with an accuracy of ± 0.0035 bar. The temperature range was 20 - 150°C corresponding to a pressure range of 1.1 - 13 bar.

The salt was first saturated with ammonia. Then sufficient ammonia was blown off to ensure that hexa- and diammoniate coexisted throughout the pressure and temperature range in which measurements were taken. The measurements proceeded first with descending temperatures, then with ascending temperatures in order to ascertain whether any hysteresis were present (cf. Figure 6). Inspection of the data in Table A below shows this not to be the case.

The data could be correlated by the following expression

$$\ln p = 16.36 - \frac{5886}{T}$$

with a correlation coefficient r = 0.9996

This is in exact agreement with the correlation obtained by Hart and Partington [2] and with the data of Biltz and Hüttig [16] at pressures below atmospheric pressure. Previous data by Ephriaim show some deviation from the former as can be seen on Figure A.

TABLE A. Equilibrium data for $MnCl_2 \cdot 2/6\ NH_3$

Temperature, K	Pressure, bar
427.0	13.10
421.8	10.96
416.5	9.337
411.0	7.917
406.0	6.424
400.8	5.508
395.6	4.643
390.4	3.553
385.2	2.918
380.0	2.410
374.8	1.854
369.7	1.547
364.5	1.364
359.3	1.107
374.9	1.878
374.9	1.896
406.0	6.446
406.0	6.458
406.1	6.461
406.0	6.363

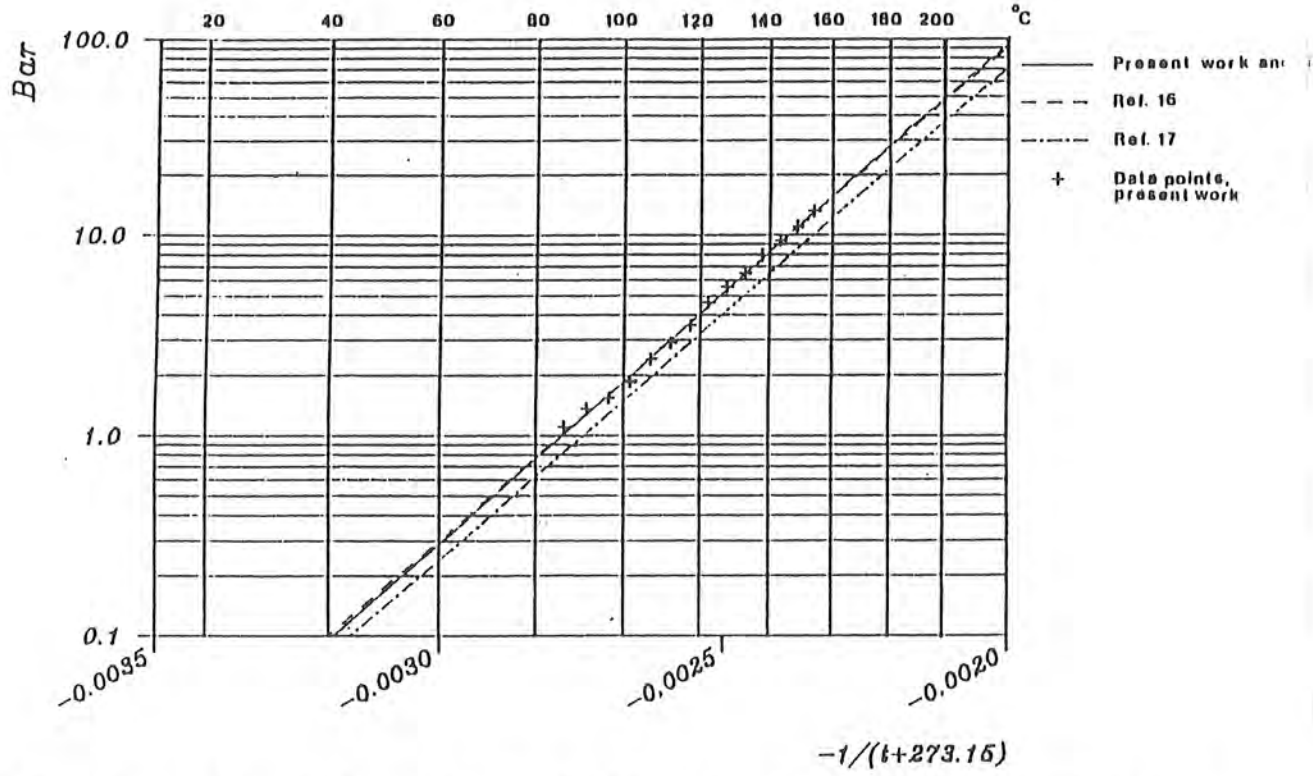

Fig. A. Data points and correlation for equilibrium temperature and pressure of the reaction $MnCl_2 \cdot 2/6\ NH_3$

APPENDIX B. Dimensions of SKYVEFIN tubes.

Skyvefin-Rohrtyp Nr.	Rippenzahl i 1/Zoll	Rippenmaß D mm	Rohrabmessungen d mm	Rohrabmessungen l mm	Rohrteilung s_q mm	Innenquerschnitt q_i cm²	Außenoberfläche A_a m²/m	Innenoberfläche A_i m²/m	Flächenverhältnis A_a/A_i –	ungefähres Gewicht G_{Al} kg/m
714	10	min. 24,5	4,7	18,35	24,5	0,42	0,32	0,047	6,8	0,25
mit	12	min. 24,5	4,7	18,35	24,5	0,42	0,37	0,047	7,9	0,25
3 Strömungs-	14	min. 24,5	4,7	18,35	24,5	0,42	0,42	0,047	8,9	0,25
kammern	16	min. 24,5	4,7	18,35	24,5	0,42	0,47	0,047	10,0	0,25
1087	10	min. 24,5	4,7	27,80	24,5	0,67	0,46	0,07	6,6	0,39
mit	12	min. 24,5	4,7	27,80	24,5	0,67	0,52	0,07	7,4	0,39
4 Strömungs-	14	min. 24,5	4,7	27,80	24,5	0,67	0,60	0,07	8,6	0,39
kammern	16	min. 24,5	4,7	27,80	24,5	0,67	0,68	0,07	9,7	0,39
1876	10	min. 24,5	4,7	47,65	24,5	1,15	0,80	0,12	6,6	0,67
mit	12	min. 24,5	4,7	47,65	24,5	1,15	0,90	0,12	7,5	0,67
7 Strömungs-	14	min. 24,5	4,7	47,65	24,5	1,15	1,00	0,12	8,3	0,67
kammern	16	min. 24,5	4,7	47,65	24,5	1,15	1,10	0,12	9,2	0,67
3625	10	min. 27,0	5,8	91,85	27,0	3,40	1,58	0,27	5,7	1,34
mit	12	min. 27,0	5,8	91,85	27,0	3,40	1,85	0,27	6,7	1,34
13 Strömungs-	14	min. 27,0	5,8	91,85	27,0	3,40	2,13	0,27	7,7	1,34
kammern	16	min. 27,0	5,8	91,85	27,0	3,40	2,41	0,27	8,7	1,34
4528	10	min. 27,0	5,8	112,60	27,0	4,15	1,95	0,33	5,9	1,60
mit	12	min. 27,0	5,8	112,60	27,0	4,15	2,29	0,33	6,9	1,60
16 Strömungs-	14	min. 27,0	5,8	112,60	27,0	4,15	2,63	0,33	8,0	1,60
kammern	16	min. 27,0	5,8	112,60	27,0	4,15	2,97	0,33	9,0	1,60

Andere Abmessungen auf Anfrage!

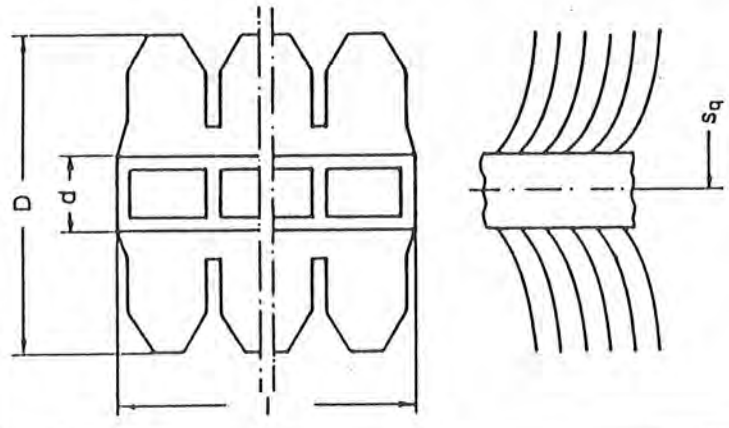

APPENDIX C. Mathematical model for numerical simulation of solid-absorption heat pump.

Nomenclature

A	heat transfer area
A_i	constant in equilibrium p,T-relation
A_j	constant in eq. C-1
B_i	constant in equilibrium p,T-relation
B_j	constant in eq. C-1
c	specific heat capacity
$\dot{C}$	thermal capacity rate
H_r	heat of reaction
$K_j(T_{ai}, T_{ei})$	reaction-rate-constant
$K(\mu_i)_{ai}$	thermal capacity rate of absorbent and its containment
m	mass (relating to hot or cold end of drum)
$M_{max,i}$	maximum amount of ammonia desorbed and reabsorbed
$Q_{max,i}$	maximum heat of reaction (cf.eq.C-3)
T	temperature
U	overall heat transfer coefficient

Greek letter symbols:

α	minimum number of moles of ammonia absorbed
β	number of moles of ammonia desorbed and reabsorbed
φ	angle of rotation
μ	degree of reaction
ω	angular velocity

Indices:

1	relating to high temperature absorber
2	relating to low temperature absorber
a,abs	absorber
al	aluminium
c	cold gas stream
e	equilibrium
h	hot gas stream
i = 1,2	relating to absorbers
j = 1,2	1-desorption ; 2-absorption
m1	intermediate temperature gas stream (upper)
m2	intermidiate temperature gas stream (lower)

In the equations below which constitute the mathematical model of the desorption/reabsorption process the following abbreviations are introduced.

Reaction rate constant:

$$K_j(T_{ai}, T_{ei}) = A_j \exp(-B_j/T_{ei}) (T_{ai}-T_{ei})^{n_j} \qquad j = 1,2 \qquad \text{(C-1)}$$

Thermal capacity of absorber:

$$K(\mu_i)_{ai} = m_{abs,i}(c_{abs,i} + (\alpha + \beta\mu_i)_i c_{NH3,i}) + m_{al,i} c_{al} \qquad i = 1,2 \qquad \text{(C-2)}$$

Total heat of reaction:

$$Q_{max,i} = M_{max,i}(H_r + c_{NH3}\Delta T) \qquad (C\text{-}3)$$

The absorber mass relates to either the hot or the cold part of the drum.

Desorption from absorbent 1, absorption in absorbent 2

$$\frac{dT_{a1}}{d\varphi} + \frac{UA(T_{a1}-T_h)}{\omega K(\mu_1)_{a1}} = \frac{Q_{max,1}}{K(\mu_1)_{a1}} \frac{d\mu_1}{d\varphi} \qquad (C\text{-}4)$$

$$\frac{dT_h}{d\varphi} + \frac{UA(T_{a1}-T_h)}{2\pi\dot{C}_h} = 0 \qquad (C\text{-}5)$$

$$\frac{d\mu_1}{d\varphi} + \frac{K_1(T_{a1},T_{e1})}{\omega}\mu_1 = 0 \qquad (C\text{-}6)$$

$$\frac{dT_{a2}}{d\varphi} + \frac{UA(T_{a2}-T_{m1})}{\omega K(\mu_2)_{a2}} = \frac{Q_{max,2}}{K(\mu_2)_{a2}} \frac{d\mu_2}{d\varphi} \qquad (C\text{-}7)$$

$$\frac{dT_{m1}}{d\varphi} - \frac{UA(T_{a2}-T_{m1})}{2\pi\dot{C}_{m1}} = 0 \qquad (C\text{-}8)$$

$$\frac{d\mu_2}{d\varphi} - \frac{K_2(T_{a2},T_{e2})}{\omega}(1-\mu_2) = 0 \qquad (C\text{-}9)$$

$$M_{max,1}\frac{d\mu_1}{d\varphi} + M_{max,2}\frac{d\mu_2}{d\varphi} = 0 \qquad (C\text{-}10)$$

$$A_1 - \frac{B_1}{T_{e1}} = A_2 - \frac{B_2}{T_{e2}} \qquad (C\text{-}11)$$

Desorption from absorbent 2, absorption in absorbent 1

$$\frac{dT_{a1}}{d\varphi} + \frac{UA(T_{a1}-T_{m2})}{\omega K(\mu_1)_{a1}} = \frac{Q_{max,1}}{K(\mu_1)_{a1}} \frac{d\mu_1}{d\varphi} \qquad (C\text{-}12)$$

$$\frac{dT_{m2}}{d\varphi} + \frac{UA(T_{a1}-T_{m2})}{2\pi\dot{C}_{m2}} = 0 \qquad (C\text{-}13)$$

$$\frac{d\mu_1}{d\varphi} - \frac{K_2(T_{a1},T_{e1})}{\omega}(1-\mu_1) = 0 \qquad (C\text{-}14)$$

$$\frac{dT_{a2}}{d\varphi} + \frac{UA(T_{a2}-T_c)}{\omega K(\mu_2)_{a2}} = \frac{Q_{max,2}}{K(\mu_2)_{a2}} \frac{d\mu_2}{d\varphi} \qquad (C\text{-}15)$$

$$\frac{dT_c}{d\varphi} - \frac{UA(T_{a2}-T_c)}{2\pi\dot{C}_c} = 0 \qquad (C\text{-}16)$$

$$\frac{d\mu_2}{d\varphi} - \frac{K_1(T_{a2}, T_{e2})}{\omega}\mu_2 = 0 \qquad \text{(C-17)}$$

$$M_{max,1}\frac{d\mu_1}{d\varphi} + M_{max,2}\frac{d\mu_2}{d\varphi} = 0 \qquad \text{(C-18)}$$

$$A_1 - \frac{B_1}{T_{e1}} = A_2 - \frac{B_2}{T_{e2}} \qquad \text{(C-19)}$$

In each set of equations the first two are the energy balances for the absorbent and for the gas (air), respectively. The third is the reaction rate equation. The following equation is an overall mass balance for ammonia and the last equation expresses that the pressure is equal in the two absorbers.

The National Team of F. R. Germany

3. WORKING FLUIDS AND TRANSPORT PHENOMENA IN ADVANCED HEAT PUMPS

K. Stephan R. Hengerer
Institut für Technische Thermodynamik
und Thermische Verfahrenstechnik
Universität Stuttgart
Federal Republic of Germany

1. Type of Problem

The intention of this international cooperation is to collect all literature in the field of absorption working fluids, to analyse the results obtained in the field and to publish them systematically.

The area of this task can be divided into the following three main parts. References concerning

a) Working fluids
b) Absorption cycles and
c) Transport phenomena

The Institute of Technische Thermodynamik and Thermische Verfahrenstechnik of the University of Stuttgart will deal with references published in German.

2. Work Schedule

The work schedule can be divided into four steps as shown in Figure 1.

	ITT University of Stuttgart
– Detailed definition of the main working areas – Literature survey – Evaluation of the literature – Exchange of the results	Work Schedule
	RH 0588

Figure 1: Work schedule

The different steps are described in more detail in the following.

2.1 Definition of the main working areas

In this first step we fixed the scope of our work and sub-

divided it into three main areas.

a) Working fluids
The working fluid of absorption cycles normally consists of a lower boiling component, the refrigerant, and of a higher boiling component, the absorbent. The topic "working fluids" summarizes all properties of the fluids important for the use in absorption cycles. Thereby both properties of the pure components and of the mixture must be mentioned. In figures 2.1 to 2.3 the properties important for the use in absorption cycles are listed. It is noteworthly that not only thermopysical properties but also economical and safety criterions such as price and toxicity are taken into account.

– thermal and chemical stability up to 200°C – melting point above the deepest process temperature – normal boiling point between the temperature in the evaporator and condenser – high heat of evaporation – flat gradient of vapor pressure curve – low specific heat capacity of the liquid – low viscosity – high thermal conductivity – small surface tension – non toxic – no decomposition of ozone by the refrigerant – low cost	ITT University of Stuttgart Required Properties of the Refrigerant RH 0688

Figure 2.1: List of requirements for a suitable refrigerant

– thermal and chemical stability up to 200°C – normal boiling point more than 200°C higher than the normal boiling point of the refrigerant – low specific heat capacity of the liquid – low viscosity – high thermal conductivity – non toxic – no decomposition of ozone by the absorbent – low cost	ITT University of Stuttgart Required Properties of the Absorbent RH 0788

Figure 2.2: List of requirements for a suitable absorbent

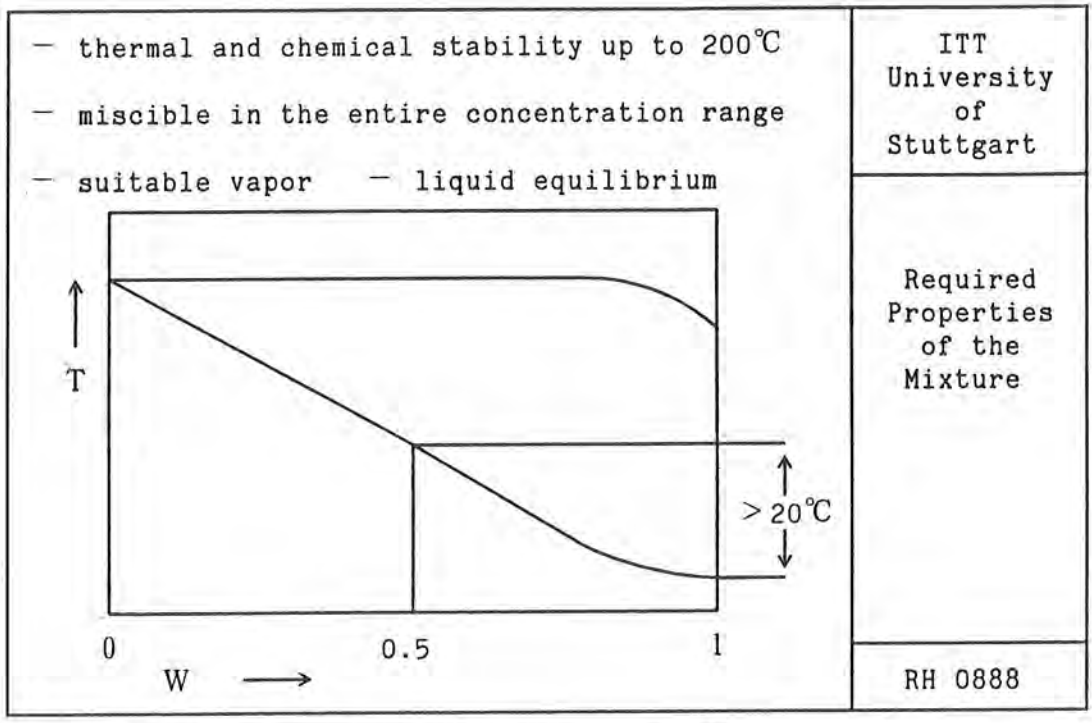

Figure 2.3: List of requirements for the mixture

b) Absorption Cycles
The three main types of absorption cycles

- absorption heat pump
- absorption cooling cycle
- absorption heat transformer

and their variations, such as two or more stage cycles, are part of this topic. Furthermore publications dealing with operation and control and calculation procedures of absorption cycles must be assigned to this topic.

c) Transport phenomena
This group contains all work concerning transport phenomena in one of the five main apparatus of an absorption cycle, namely

generator, evaporator, condenser, absorber and heat exchanger.

Publications about the design of this apparatus should also be included into this subtopic.

2.2 Literature survey

The literature survey is done at the computer center of the University of Stuttgart, which itself is linked to several data bases. Therefrom we receive informations about author, title of the paper, source and a short abstract of the publication.

Copies of the publications are obtained and collected for the use of those, who are interested in the field. Furthermore we evaluate the citation list of each publication.

2.3 Evaluation of the literature

In order to analyse the literature two data bases were installed on a personal computer. The structure of data administration is shown in Figure 3. The first data base contains all the bibliographic references of the collected publications. They are stored according to the name of the authors, the title, the source, the document type [journal, book, report or dissertation etc.], the language and the reference number as identifier of the publication within the files. In the second data base we have stored the index number and the scientific information. By means of the index number a coordination between the two data bases is given.

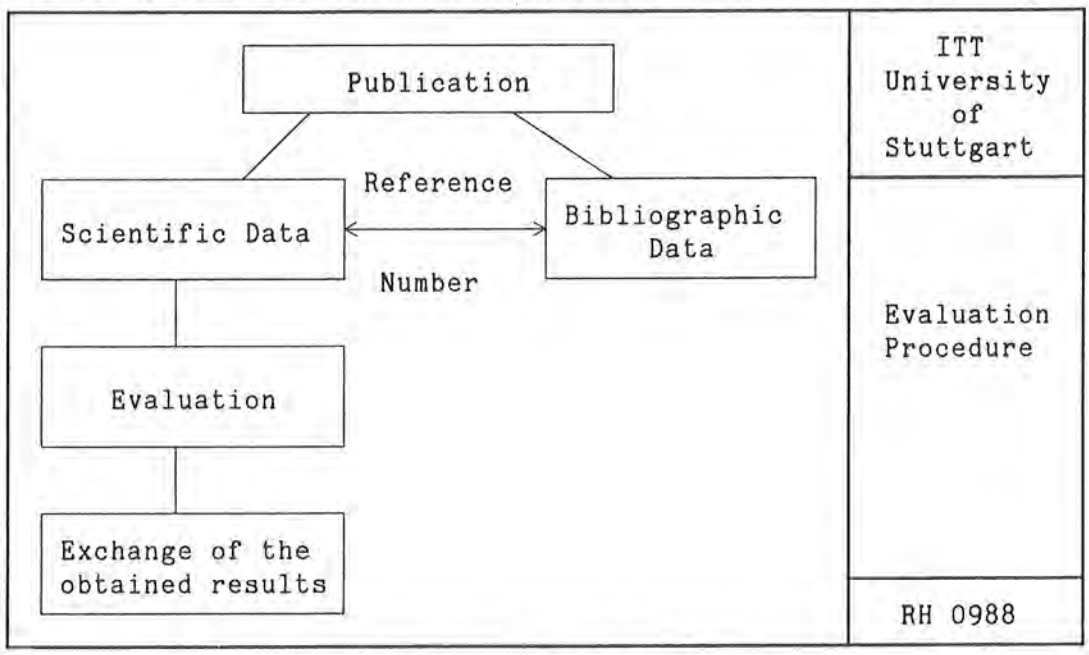

Figure 3: Structure of the data administration

The following scientific data are stored:

- Reference Number
  - Identification of the publication
- Refrigerant
  - Chemical abstracts name
  - Total formula
  - Abbreviation
- Absorbent
  - Chemical abstracts name
  - Total formula
  - Abbreviation
- Data Type

- Experimental
- Calculated

- Experimental Setup

- Experimental conditions
  - Pressure range
  - Temperature range
  - Concentration range

- Comments

Subgroup Working Fluid

- Physical Properties studied
  - according to Table 2.1 to 2.3

- Number of data

Subgroup Absorption Cycles

- Type of Cycle studied

- Number of stages

- Operation Experiences

- Control

Subgroup Transport Phenomena

- Apparatus studied

- Design

2.4 Exchange of the obtained literature

After evaluating the individual publications the questionaires of the Heat Pump Technology Center of Japan will be filled out and send to the operating agent.

3. Status

We have started with this work on behalf of the German Ministry of Research and Technology in April this year. For this reason we are still involved in the literature survey.

Searches in the data bases Energy, Dechema, Verfahrenstechnische Berichte were performed until today.

Thereby we have located 143 publications and we have obtained copies from most of them.

From this 143 publications

24 are included in list 2 received from the operation agent and

119 are new publications, not included in list 1.

They belong to the main areas as follows.

58 working fluids

78 absorption cycles

5 transport phenomena

* Two references could not be assigned to one of the main areas so that the sum is only 141.

Next a literature survey in the database friginter of the IIR in Paris will be done and the citation lists of the obtained literature will be studied so that we can hope that most of the publications available in our working area are located.

3A. Ternary Working Fluid TFE - H_2O — E 181

K. Stephan R. Hengerer
Institut für Technische Thermodynamik
und Thermische Verfahrenstechnik
Universität Stuttgart
Federal Republic of Germany

1. Introduction

The binary fluid TFE — E 181 has been investigated as working fluid for absorption cycles by several authors. Stephan and Seher measured the thermophysical properties of this mixture and developed computer programs in order to calculate the stationary process of various absorption cycles.

In comparison to other working fluids, e.g. ammonia - water or water - lithiumbromide, TFE — E 181 seems to be superior for the application in absorption heat transformers.

TFE — E 181 is completely miscible in the entire concentration range and it is thermally and chemically stable up to temperatures above 200°C. Because of the normal boiling point of TFE of 73.6°C the pressure in an absorption heat transformer will be only slightly above atmospheric pressure. This leads to lower investment costs, because the wall thickness of the apparatus is low and the design of the liquid pumps is less complicated. Furthermore TFE — E 181 is not corrosive and allows the use of common steel.

The only disadvantages of this working fluid are

- the low thermal conductivity of TFE
- and the comparatively low heat of vaporization of TFE.

Because of the low heat of vaporization large vapor streams have to be generated and therefore large apparatus and tube dimensions are required. Furthermore due to the small thermal conductivity the heat transfer coefficients are low and thus large evaporator and condenser sizes are necessary. These effects are partly but not totally compensated by the higher density of TFE compared to that of water or ammonia under the same pressure and temperature.

To avoid the disadvantages some authors proposed water as a refrigerant. Several binary working fluids using water as the refrigerant and various high boiling organic components such as E 181 have been studied. Vapor - liquid equilibrium data of these systems, however, have a bubble point line, as shown in Figure 1.

Such a shape is not suitable for absorption cycles because of the low absorption capacity. According to Niebergall the slope of the bubble point line should be at least 20 K, if the concentration is lowered from 1.0 to 0.5.

For this reason the ternary system TFE — H_2O — E 181 was selected for further investigation, because then it should be possible to combine the advantages of both binary subsystems and to avoid the mentioned disadvantages.

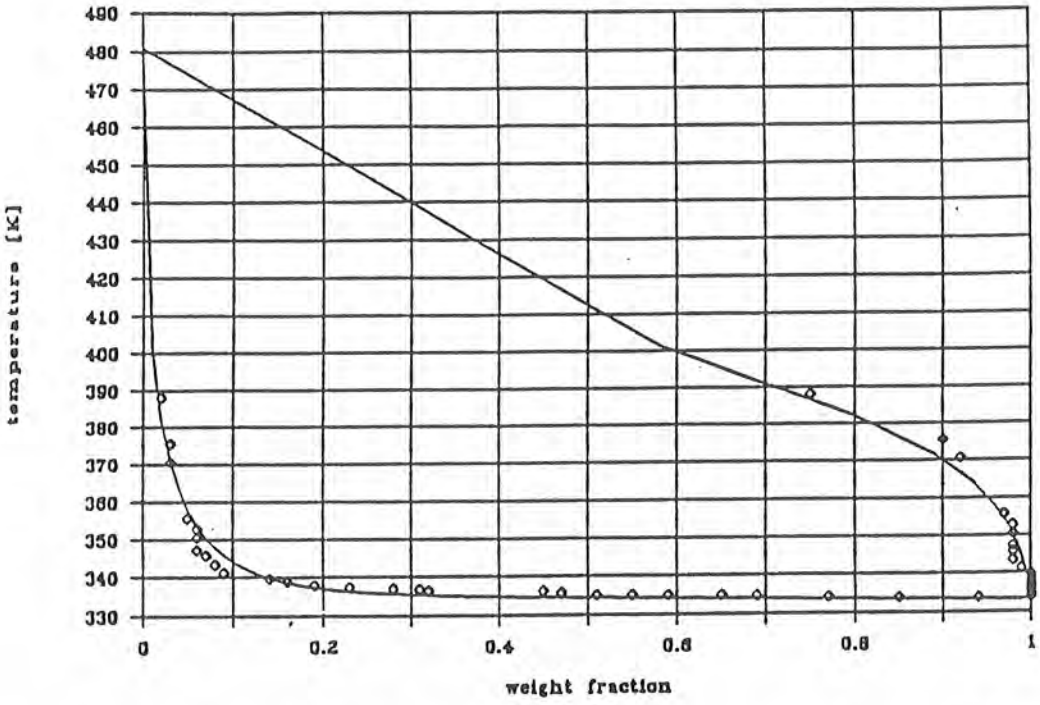

Figure 1: Vapor - Liquid Equilibrium of H_2O - E 181

2. Thermodynamic Properties of TFE – H_2O – E 181

The suitability of new working fluids, even ternary systems, can be assessed by means of computer programs for the calculation of the stationary process of an absorption heat transformer. One obtains information about

- pressure and concentration in the cycle
- heat and mass flows in the apparatus
- the characteristic numbers of the process, e.g. the coefficient of performance COP and transfer surface coefficient TSC.

The informations needed are:

- Vapor - Liquid Equilibrium
- Density
- Enthalpy

The influence of the additional component H_2O on the heat transfer in the apparatus can be assessed from the

- viscosity

and

- thermal conductivity of the mixture.

Before starting the measurements and calculations the thermal stability of TFE – H_2O – E 181 was tested.

2.1 Thermal and Chemical Stability

The stability of the mixture was tested over the whole concentration range up to temperatures of 250°C. The test substances were filled in a steel vessel and kept at constant temperature over a period of several weeks. During each run the pressure in the vessel was recorded continously and samples of the mixture were taken daily. The samples were analyzed in a gas chromatograph to detect even small effects of decomposition. Up to 250°C no decomposition could be observed by the GC analysis. Also the pressure in the vessel did not change, which is another indicator for thermal stability of the mixture.

2.2 Vapor - Liquid Equilibrium

One of the most important properties for the assessment of new working fluids is the vapor liquid equilibrium. From this information the pressure, concentration and mass flow in each apparatus can be calculated. Hence great efforts were undertaken to measure and calculate the VLE of the ternary system with great accuracy.

Both the VLE of the three binary subsystems

- TFE – H_2O
- TFE – E 181
- H_2O – E 181

and of the ternary system were measured. For measurements below atmospheric pressure a dynamic VLE - apparatus of Gillespie-typ, above atmospheric pressure an apparatus of static type developed at our institute was used. In order to calculate the VLE several methods were tested. Thereby the NRTL-method of Renon and Prausnitz turned out to be superior to other methods. The nine NRTL - Parameters required for a ternary system were determined by fitting the parameters to the experimental data by means of the least square error method. Figure 2 shows a comparison of calculated and measured data at 100°C and 0.96 bar.

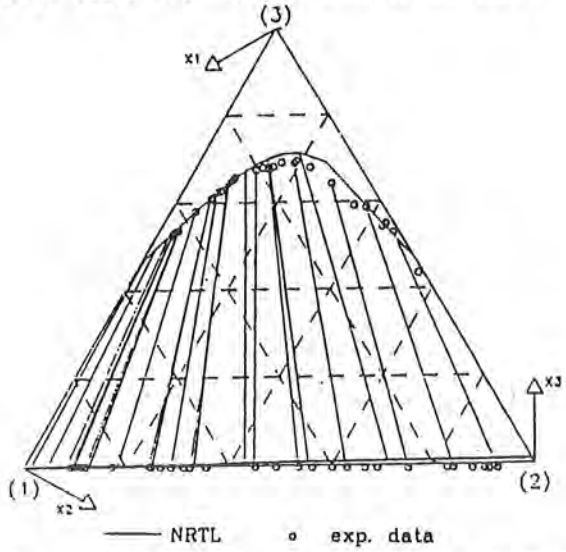

Figure 2: Vapor - Liquid Equilibrium of TFE – H_2O – E 181

2.3 Enthalpy

The enthalpy of the ternary system was calculated without considering the heat of mixing

$$h = x_1 * h_{01} + x_2 * h_{02} + x_3 * h_{03},$$

because the required data even those for the binary subsystems are unknown. This yields, since the heat of mixing according to a rough test turned out to be negative, in absorption heat transformers slightly too low COPs, as can be seen in Figure 3 for the binary system TFE – E 181.

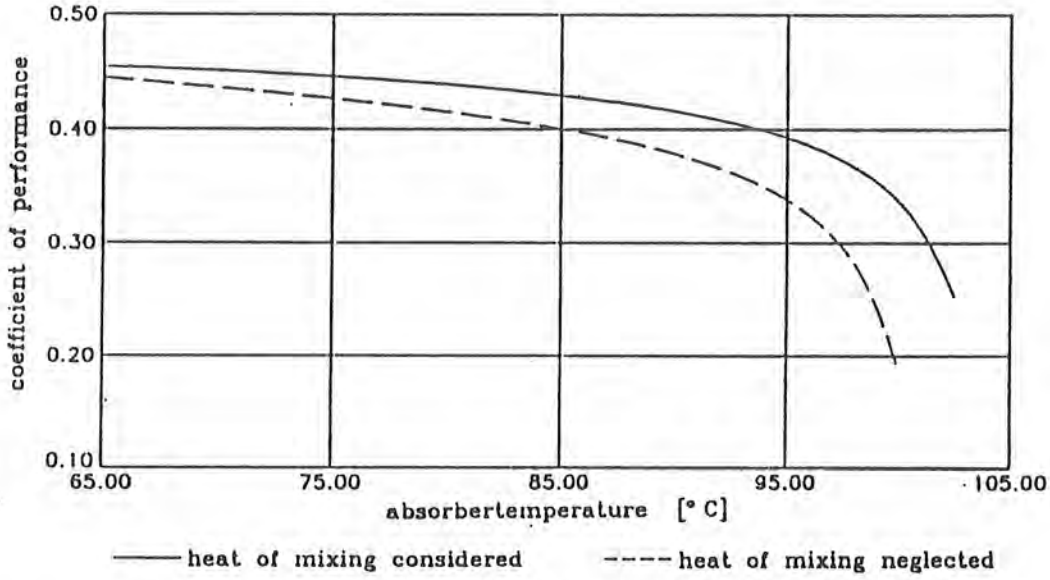

Figure 3: Influence of the Heat of Mixing on the COP

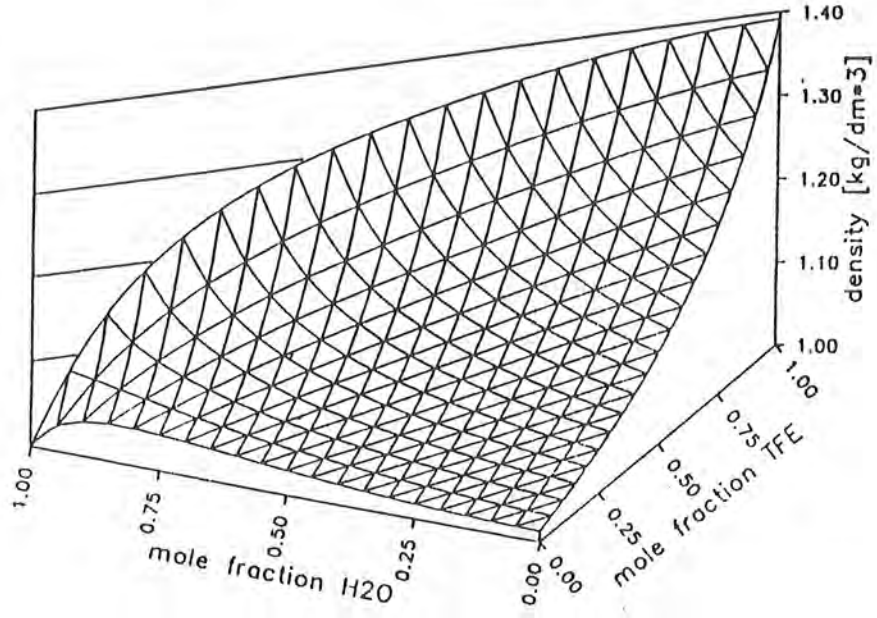

Figure 4: Density of TFE – H_2O – E 181

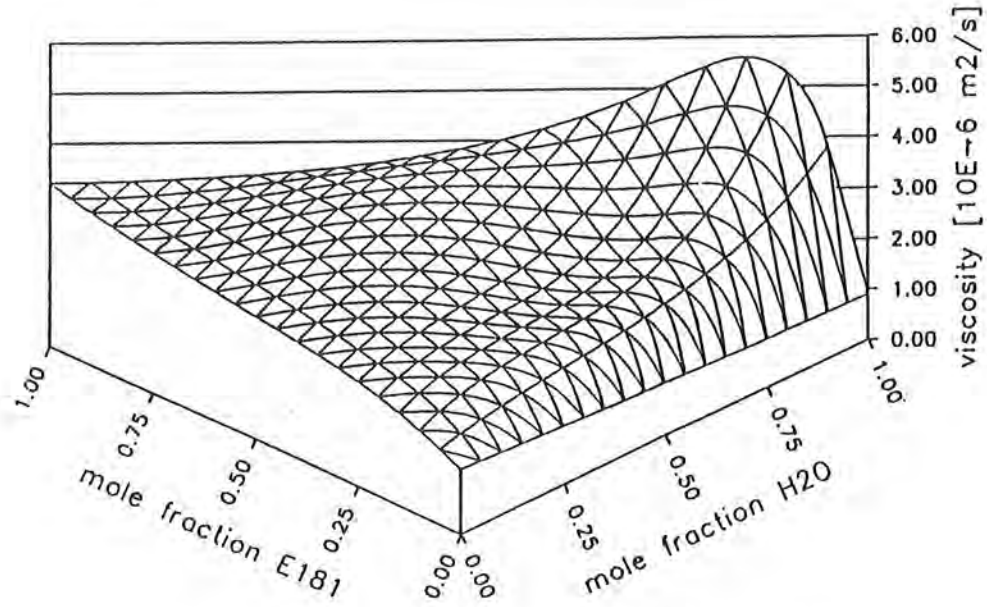

Figure 5: Viscosity of TFE – H_2O – E 181

2.4 Density and Viscosity

The liquid density and viscosity of the binary subsystems and the ternary mixture were measured at atmospheric pressure in the temperature range between 15°C and 90°C. Comparison with literature data for TFE – H_2O and H_2O – E 181 show good agreement. Figure 4 represents the density, Figure 5 the viscosity of TFE – H_2O – E 181 at 25°C. Thereby one has to consider that the base of these 3D-plots is a triangular, spread out by the three binary subsystems.

2.5 Thermal Conductivity

The purpose of the addition of H_2O aimed at an enhancement of the heat of vaporization and of the thermal conductivity in the evaporator and condenser. Because of the small amount of E 181 in the vapor its influence on the thermal conductivity can be neglected. Therefore only the thermal conductivity of TFE – H_2O was investigated. It was calculated by means of several methods. As can be seen from Figure 6, the method of Fillipov,

$$\lambda m = w_1 * \lambda_1 + w_2 * \lambda_2 - 0.72 * w_1 * w_2 * (\lambda_1 - \lambda_2)$$

yields the best results. The addition of only 10 weight percent water enhances the thermal conductivity for about 16.5% from 115 mW/K m to 134 mW/K m.

3. Results

With a computer program the stationary process of a single stage absorption heat transformer was calculated for the binary system TFE – E 181 and the ternary system TFE – H_2O – E181. For the latter system it was assumed that the vapor leaving the generator contains 10 weight percent H_2O. As can be seen in Figure 7, the

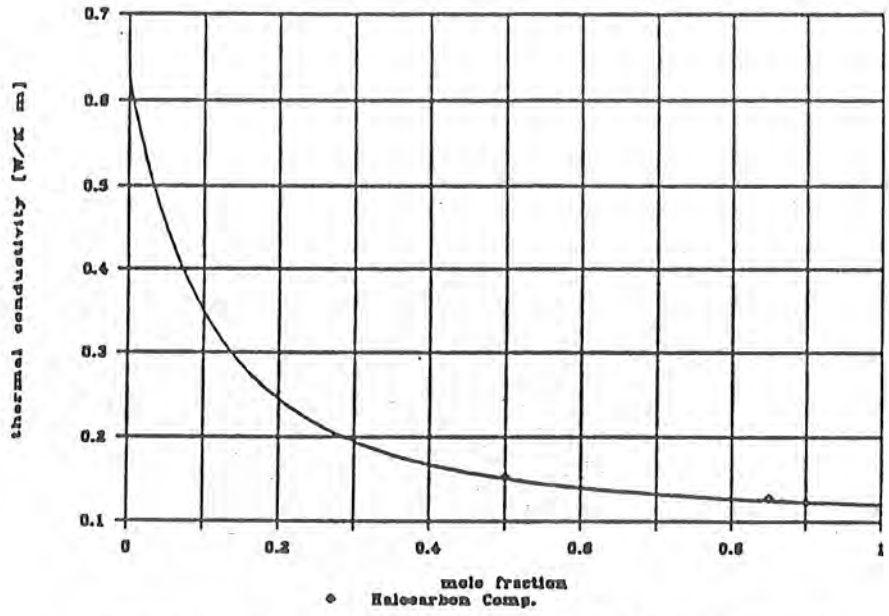

Figure 6: Thermal Conductivity of TFE – H_2O

COP using the ternary system is slightly lower than that of the binary TFE – E 181.

But one has to consider that the computer program does not account for economical aspects. The enhanced heat transfer in the apparatus leads to lower heat transfer surfaces and hence to lower costs for the apparatus. Furthermore the price for the working fluid is lowered by the addition of H_2O.

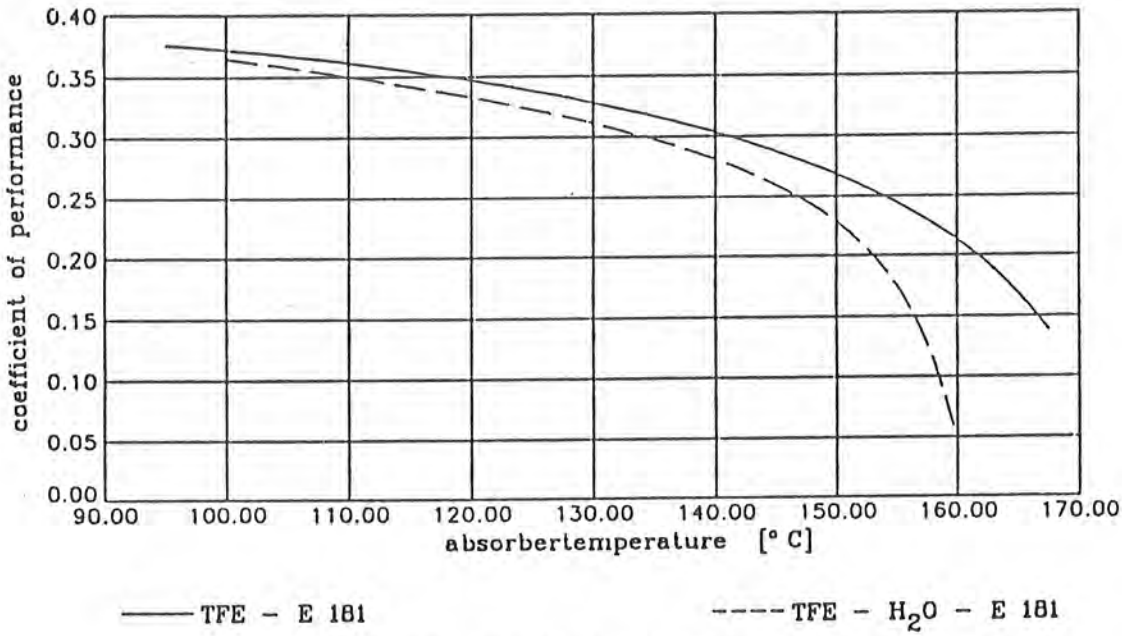

Figure 7: Calculation Results

4. Prospects

The ternary system TFE – H_2O – E 181 seems to be a promising alternative. Measurements of the heat of mixing of the ternary system are planned, which enable better predictions of the process. Also the enhancement of the heat transfer by the addition of H_2O shall be studied in detail. The theoretical results shall then be tested in a pilot plant, which is under construction.

The National Team of Japan

4. RESEARCH AND DEVELOPMENT ON WORKING FLUIDS

Atsushi Manago
Research Center, Osaka Gas Co., Ltd.
Osaka, Japan

1. Introduction

The history of absorption chillers originated in the first proposal of the concept of using a working fluid composed of ammonia refrigerant and water absorbent at the beginning of this century. In 1940s, absorption chillers using water as refrigerant and lithium bromide as absorbent were developed in the U.S.A.

In Japan, double-effect absorption chillers using such an H_2O-LiBr working fluid were developed in the 1960s. This type absorption chiller has since advanced dramatically, and is now the dominant type of the large-capacity air-conditioning heat source units. Currently, air-cooled units have been developed and are expected to be commercialized in the earliest future. Absorption heat pumps and heat transformers, which have drawn attention as a means to increase the amount of heat from various kinds of waste heat (heat pump) and to raise their temperatures (heat transformer), respectively, have also been under development. However, absorption heat pumps using an H_2O-LiBr working fluid face difficulties in practical use for air-conditioning, because of restrictions due to physical properties inherent in the working fluid. At present, emphasis is being placed on developing a new working fluid to replace H_2O-LiBr.

In the U.S.A., air-cooled chillers using an NH_3-H_2O working fluid were commercialized around 1970 and absorption heat pumps with this working fluid were developed as air conditioners in 1980. Nevertheless, this working fluid, which does not easily produce a double-effect cycle, leads to a low efficiency and is not expected to undergo further development. In addition, its toxicity and flammability, two characteristics of ammonia, prevent practical use of the NH_3-H_2O working fluid in Japan.

Under the circumstances, an enormous number of refrigerants and absorbents have already been investigated as possible alternatives to the H_2O-LiBr and NH_3-H_2O working fluids. According to Macriss et al., more than 450 documents on working fluids have been reported by about 200 organizations from many countries, primarily Japan, the U.S.A., West Germany, the U.K., France, and the U.S.S.R.[1)2)] Although several promising working fluids have been developed to the phase of prototype operation, none have been commercialized yet.

This report describes the conventional working fluids previously investigated and the prospective working fluids now under development for use in absorption chillers and heat pumps.

2. Requirements for Working Fluid

Requirements for the working fluid in absorption chillers and absorption heat pumps are discussed in many documents and books.[3)4)] Table 2-1 shows the major requirements for an absorption heat pump working fluid, which Bokelmann et al., to be mentioned later, take into consideration when selecting such a working fluid.[5)6)]

Table 2-1 Major Requirements for Working Fluid

Working Fluid	Requirements
Refrigerant	° Workability at low temperatures (∿ -20°C) ° Large latent heat for vaporization ° Low running pressure sufficient for a double effect cycle within the limits of legal regulations, safety, equipment size, and cost
Absorbent	° High degree of solubility ° Large boiling point difference between absorbent and refrigerant
Refrigerant-absorbent	° Small solution circulation ratio ° Small pump energy (Small pressure difference, high density) ° Small heat to be exchanged between solutions (small specific heat) ° Thermal and chemical stability ° No toxicity

The solution circulation ratio f, specific pump energy np, and specific heat to be exchanged between concentrated and dilute solutions n_L are defined as follows:

$$f = \frac{Xc}{Xc - Xd}$$

$$n_p = \frac{f \cdot \Delta P}{ro \cdot \rho}$$

$$n_L = \frac{(f-1) \cdot C \cdot \Delta t}{ro}$$

where

ro: Latent heat for vaporization of refrigerant at 0°C (kJ/kg)
Xc: Concentration of concentrated solution (wt%),
$\xi a = 100 - Xc$
Xd: Concentration of dilute solution (wt%),
$\xi r = 100 - Xd$
ΔP: Pressure difference between evaporator and condenser (bar = 0.1 MPa)
$\Delta \rho d$: Density of dilute solution (kg/m^3)
C: Specific heat of concentrated solution ($kJ/kg \cdot °C$)
Δt: Temperature difference between generator and absorber (°C)

3. Limitations of H_2O-LiBr and NH_3-H_2O Mixtures

3.1 H_2O-LiBr working fluid

H_2O-LiBr working fluid fails to meet all of the requirements shown in Table 2-1. For example, this working fluid, which uses water as the refrigerant, freezes at 0°C or below; therefore, the evaporator temperature cannot be reduced to 0°C or below. Also, it is difficult to use the working fluid in air heat-source absorption heat pumps, since the absorber temperature cannot be raised to 50°C or more which is necessary for heating, due to the solubility limit of LiBr. In the former case, adding a small quantity of LiBr to the refrigerant causes the freezing point to lower. In the latter case, however, virtually no problem-solving method has been found. As shown in Fig. 3-1, at a vaporization temperature of 0°C and an absorption temperature of 50°C, the concentration of lithium bromide aqueous solution is approximately 65 wt%; if the solution at that concentration is used as the dilute solution, no cycle cannot be established. In addition, this type of working fluid, which is corrosive, requires regular maintenance such as corrosion inhibitor concentration control.

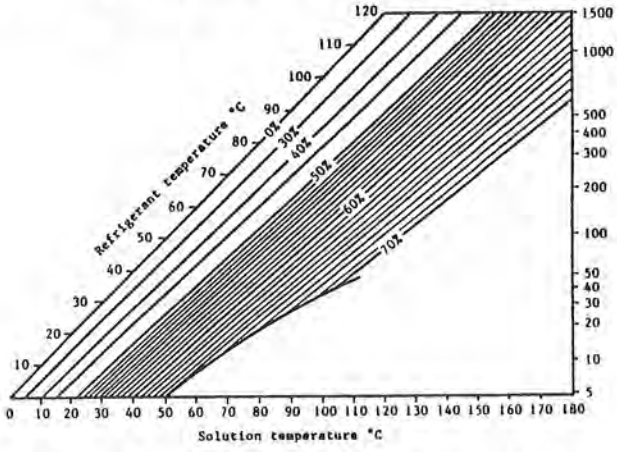

Fig. 3-1 Dühring Curve of Lithium Bromide Aqueous Solution

3.2 NH_3-H_2O type working fluid

NH_3-H_2O type working fluid also fails to meet all of the requirements mentioned above. In addition to the toxicity and flammability inherent in NH_3, the NH_3-H_2O working fluid requires a high running pressure, which prevents its double effect cycle. The specific heat of the solution is high. With a small difference (133°C) between the boiling points of the refrigerant and the absorbent, the type requires a rectifier, thereby expanding the entire equipment and resulting in high cost.

In the U.S.A., GAX (Generator Absorber Heat Exchange) cycle[7] and dual cycle[8] are being developed, taking advantage of the workability of NH_3 at 0°C or below, in order to improve the coefficient of performance (C.O.P.). The cycles, both designed for double effect, are shown in Figs. 3-2 and 3-3, respectively. The former uses NH_3-H_2O-LiBr as the working fluid, whereas the latter uses a combination of two independent cycles: NH_3-H_2O and H_2O-LiBr.

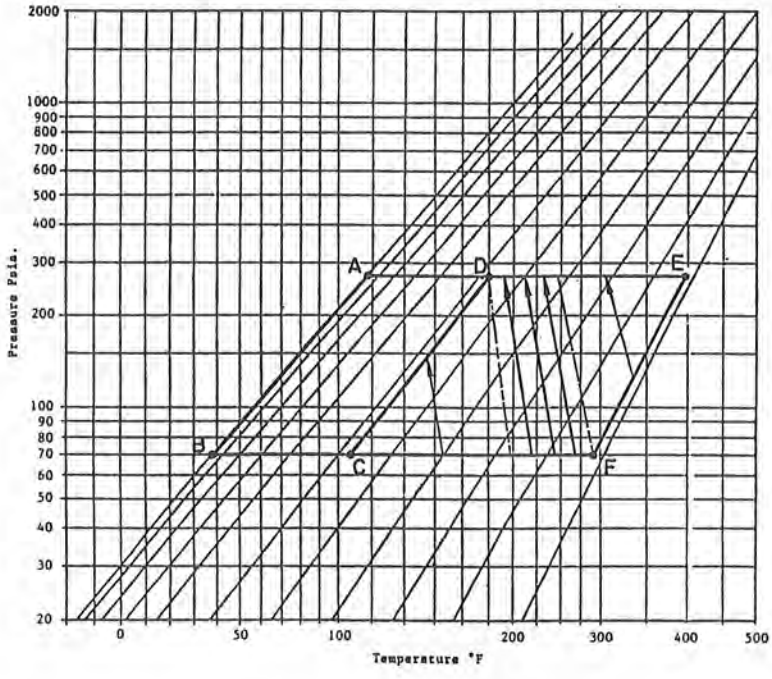

Fig. 3-2 GAX Cycle

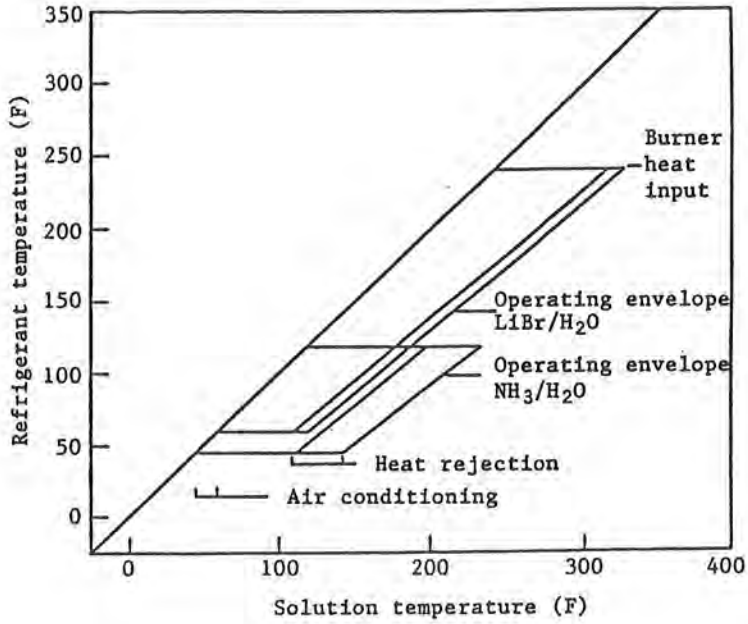

Fig. 3-3 Dual Cycle

4. Investigation for New Working Fluids

4.1 Proposed working fluids

A number of substances, natural or artificial, have prospects for use as refrigerants or absorbents, along with a limitless number of combinations of these substances. Since the basic concepts regarding absorption chiller and heat pump cycles were introduced, numerous working fluids have been investigated.

Based on more than 450 working-fluid related documents from throughout the world, including unpublished ones, Macriss et al. have recently classified, by type of fluids and their data range available, all the studies on working fluids that have been performed so far. They also analyzed the precision of existing data on physical properties of major working fluids.[1)2)] Most of the investigations, conducted primarily in Japan, the U.S.A., West Germany, the U.K., France, and the U.S.S.R., are recent and have coincided with the development of absorption chillers.

Macriss et al., presented the refrigerants that have been investigated so far. These are shown in Table 4-1. In general, refrigerants are largely classified into inorganic and organic matters. Inorganic refrigerants are mainly water and ammonia, whereas organic refrigerants are principally amines, alcohols, and Freons. Absorbents are also largely classified into inorganic and organic matters.

Inorganic absorbents are salts, whereas organic absorbents are alcohols, ethers, alcohol-ethers, amides, amines, amine-alcohols, esters, ketones, acids, aldehydes, and their mixtures.

Tables 4-2 to 4-10 show the numbers of studies proposed for particular absorbents and their physical properties, listed using the data by Macriss et. al.[1)2)] The figures in the tables stand for the numbers of studies and indicate how many documents deal with each particular working fluid or its physical properties. One document may cover more than one working fluid or more than one physical property. Therefore, the numbers of the studies in the tables do not necessarily match the total number of documents. They reveal trends in research on working fluids and indicate what physical properties are considered most critical in such investigations. Note that absorbents which are covered by only one document are listed at the bottom of a table.

Table 4-1 Investigated Refrigerants

No.	Classification		Name	Chemical Formula	Molecular Weight	Boiling Point (°C)
1	Inorganic matters		Water	H_2O	18.0	100.0
2			Ammonia	NH_3	17.0	-33.3
3			Sulfur dioxide	SO_2	64.1	-10.0
4	Organic matters	Amines	Methylamine	CH_3NH_2	31.1	-6.1
5			Dimethylamine	$(CH_3)_2NH_2$	45.1	7.2
6			Trimethylamine	$(CH_3)_3NH_2$	59.1	2.8
7			Ethylamine	$C_2H_5NH_2$	45.1	16.6
8		Alcohols	Methanol	CH_3OH	32.0	65
9			Ethanol	C_2H_5OH	46.1	78.3
10			n-Propanol	C_2H_7OH	60.0	97.2
11			TFE	CF_3CH_2OH	100.0	73.6
12			HFIP	$(CF_3)_2CHOH$	168.0	59.0
13		Freons	R11	CCl_3F	137.4	23.9
14			R12	CCl_2F_2	120.9	-29.4
15			R21	$CHFCl_2$	102.9	8.9
16			R22	CHF_2Cl	86.5	-40.6
17			R30	CH_2Cl_2	84.9	40.0
18			R31	CH_2ClF	68.5	-8.9
19			R123	CHF_2CFCl_2	152.9	20.0
20			R123a	$CHClFCClF_2$	152.9	29.4
21			R123b	CF_3CHCl_2	152.9	27.8
22			R124	$CHClFCF_3$	136.5	-12.1
23			R124a	CHF_2CClF_2	136.5	-9.4
24			R131a	$CHCl_2CHClF$	151.4	85.0
25			R133a	CHF_2CHClF	118.5	5.6
26			R134	CHF_2CHF_2	102.0	94
27			R140a	CCl_2HCCH_2	133.4	112.8
28			R143a	CH_3CF_3	84.0	-47
29			R152	CH_2FCH_2F	66.0	30
30			R1130	$CHClCHCl$	96.9	58.9
31			R1112a	$CClFCClF$	132.4	18.9
32			R1120	CCl_2CClH	131.4	82.2
33		Hydrocarbon	Hexane	$CH_3(CH_2)_4CH_3$	86.0	68

Table 4-2 Absorbents Using Water as Refrigerant and Numbers of Studies Thereof

Absorbent	Vapor Pressure	Crystallization Temperature	Other Physical Properties	Mass and Heat Transfer	Corrosion	Stability, Toxicity, Flammability
LiBr	4/16 (11)	4/7 (7)	6/46 (37)	3/6 (3)	3/15 (15)	
LiCl	0/9 (9)	0/2 (2)	0/28 (28)		0/7 (7)	
LiI	1/3 (3)	0/1 (1)	0/9 (9)			
LiSCN	1/0	1/0				
CsF	1/0	1/0				
H_2SO_4	0/1 (0)		0/1 (0)			
CH_3CH_2COOH	0/2 (0)					
TEG		0/1 (0)	0/1 (0)			
LiBr+LiCl	1/3 (3)		0/1 (1)			
LiBr+LiSCN	2/4 (3)	2/3 (2)	0/12 (12)		0/10 (10)	
LiBr+CsBr	2/0	1/0				
LiBr+$ZnBr_2$	1/2 (2)	2/6 (6)	0/6 (6)			
LiBr+$ZnCl_2$	0/3 (3)	0/3 (3)	0/11 (11)		0/5 (5)	
LiBr+n-Octanol			0/3 (3)			
LiBr+EG	1/3 (3)	0/2 (2)	3/5 (5)	1/0	1/0	
LiBr+BLN	0/5 (5)	0/3 (3)	0/19 (19)		0/7 (7)	
LiCl+CsCl	2/0					
LiCl+$ZnBr_2$		1/2 (2)				
LiCl+$ZnCl_2$	1/0	1/0				
LiI+EG	0/1 (1)	1/1 (1)				
RbF+CsF	1/0	1/0				
LiBr+$ZnBr_2$+$CaBr_2$	1/0	6/0				
LiBr+$ZnBr_2$+EG	0/1 (1)	0/1 (1)	0/6 (6)		0/1 (1)	
LiBr+$ZnBr_2$+DEG	0/1 (1)	0/1 (1)				
LiBr+$ZnBr_2$+PD		1/0	1/0	1/0		
LiBr+LiI+EG	0/1 (1)	0/1 (1)				

Other absorbents

$ZnCl_2$, $ZnBr_2$, CsBr, KF, Cs Acetate, $ZnNO_3$, $LiClO_3$, $LiNO_3$, $LiBF_4$, $LiCF_3CO_2$, $LiCCl_3CO_2$, NaOH, NH_4SCN, DMETEG, Li Benzenesulfonate, Li H_2 phosphite, LiBr+Baysilone, LiBr+CH_3OH, LiBr+$LiClO_3$, LiCl+Li Acetate, LiNO2+$LiClO_3$, LiSCN+LiCl, LiCl+$CaCl_2$, LiBr+ethanolamine, LiBr+$ZnBr_2$+DMEDEG, LiBr+ethanol, LiBr+$ZnBr_2$+MBEDEG

Table 4-3 Absorbents Using Ammonia as Refrigerant and Numbers of Studies Thereof

Absorbent	Vapor Pressure	Crystallization Temperature	Other Physical Properties	Mass and Heat Transfer	Corrosion	Stability, Toxicity, Flammability
H2O	10/28(0)	1/1(0)	3/31(5)	1/0		
NaSCN	2/0	1/0	5/0			1/0
LiSCN	2/0		3/0			
NH4I	2/0					
N_2O+LiBr	0/3(0)		0/7(0)			
N_2O+$LiNO_3$	0/4(0)		0/5(0)			
Other absorbents LiNO3, NaBr, NH_4Br, NaI, H_2O+CrO_2, NaSCN+NaI, DMETEG, DMETrEG, 1,4-Butanediol, 2,3-Butanediol, TEG, Polydimethylsiloxane, Nitrobenzene, Octylamine, DMA, Aniline, 1,4-Butanediol+NaSCN, 1,4-Butanediol+NaI, 1,4-Butanediol+NH4I, TEG+NaSCN, 1,4-Butanediol+NaI+NaSCN						

Table 4-4 Absorbents Using Sulfur Dioxide as Refrigerant and Numbers of Studies Thereof

Absorbent	Vapor Pressure	Crystallization Temperature	Heat of Mixing	Mass and Heat Transfer	Corrosion	Stability, Toxicity, Flammability
DMETEG	1/0		1/0			
DMF	1/0		1/0			
DMA	1/0		1/0			
2-Octanone	1/0					
Ethyl laurate	1/0					
Nitrobenzene	2/0					
n-Heptyl alcohol	1/0					

Table 4-5 Absorbents Using Amine as Refrigerant and Numbers of Studies Thereof

Refrigerant	Absorbent	Vapor Pressure	Crystallization Temperature	Other Physical Properties	Mass and Heat Transfer	Corrosion	Stability, Toxicity, Flammability
Methylamine CH_3NH_2	H_2O	0/1(1)		0/15(15)			
	H_2O+LiBr	0/3(0)		0/7(0)			
	NaSCN	2/0	1/0				
	LiSCN	2/1(0)		3/0			
	$LiNO_3$	0/1(0)					
	$Zn(SCN)_2$	1/0					
	Ni(SCN)x	1/0					
	$Co(SCN)_2$	1/0					
	CuSCN	1/0					
	$Cu(SCN)_2$	1/0					
	NaSCN+LiSCN	2/0					
	EG	1/3(0)					
	TEG	1/1(0)					
	MEDEG	1/0					
	BDL	0/1(0)					
	Glycerol	0/1(0)					
	1,4-Butanediol	1/0					
	DMETEG	1/0					
	LiSCN+DMETEG	2/0					
	LiSCN+EG	1/0					
	LiSCN+Butanediol	1/0					
	LiSCN+Ethanolamine	1/0					
	LiSCN+DMF	1/0					
Dimethylamine $(CH_3)_2NH_2$	TEG	1/0					
Trimethylamine $(CH_3)_3NH_2$	TEG	1/0					
Ethylamine $C_2H_5NH_2$	H_2O	0/5(5)		0/14(14)			

Table 4-6 Absorbents Using Alcohol as Refrigerant and Numbers of Studies Thereof

Refrigerant	Absorbent	Vapor Pressure	Crystallization Temperature	Other Physical Properties	Mass and Heat Transfer	Corrosion	Stability, Toxicity, Flammability
Methanol CH_3OH	H_2O	0/1(0)					
	LiBr	3/8(1)	0/3(2)	0/13(9)			0/1(0)
	LiCl	2/0	0/1(1)				
	LiI		0/1(0)	0/4(0)			
	LiSCN	0/2(0)	0/1(0)	0/4(0)			
	$ZnBr_2$	2/3(1)	0/1(1)	0/1(7)			
	$ZnCl_2$	1/0					
	H_2O+LiBr	0/2(0)	0/1(0)		0/1(0)		
	LiBr+LiCl	1/0					
	LiBr+$ZnBr_2$	4/8(3)	0/2(1)	0/13(9)			0/1(0)
	LiCl+$ZnBr_2$	1/0					
	LiI+$ZnBr_2$	0/4(4)	0/2(2)	0/10(10)			
Ethanol C_2H_5OH	H_2O	0/1(0)		0/4(0)			
	LiBr	2/1(1)	0/1(1)	0/5(5)			
	LiCl	1/0					
	LiI	0/2(2)	0/1(1)	0/3(3)			
	$ZnBr_2$	1/0					
	$ZnCl_2$	1/0					
	LiBr+$ZnBr_2$	1/0					
n-Propanol C_3H_7OH	LiBr		0/1(1)				
	LiCl	1/0					
	$ZnBr_2$	1/0					
	$ZnCl_2$	1/0					
Trifluoro-ethanol TFE	DMETEG	0/4(0)	0/1(0)	0/5(0)		0/1(0)	
	NMP	0/4(0)		0/4(0)			0/1(0)
	TEG		0/1(0)	0/1(0)			
	DWA		0/1(0)				
	BZL		0/1(0)				
	QUN		0/2(0)				
Hexafluoro-isopropanol HFIP	QUN		0/2(0)	0/1(0)			

Table 4-7 Absorbents Using Freon as Refrigerant and Numbers of Studies Thereof (No. 1)

Refrigerant	Absorbent	Vapor Pressure	Crystallization Temperature	Other Physical Properties	Mass and Heat Transfer	Corrosion	Stability, Toxicity, Flammability
R11	DMETEG	1/0					
	2-Octanone	1/0					
	Linoleic Acid	1/0					
	Diethyl Malonate	1/0					
	n-Heptyl Alcohol	1/0					
R12	DMETEG	1/0					
	DMA	1/0					
	DMETEG +Benzyl Alcohol	1/0					
	R22+DMETEG	1/0					
	R22+DMA	1/0					
	R22+DMETEG +Benzyl Alcohol	1/0					
R21	DMETEG	4/2(0)		1/2(0)		1/0	1/0
	DMETrEG	1/0					
	DMEDEG	1/0		2/0			
	DMF	3/3(2)		0/11(9)			
	DMA	1/0		2/0			
	DMH	2/0		2/0			
	DEO	2/0					
	DEAP	2/0					
	Other absorbents NMP, DEM, EB, n-BB, TAN, n-HA, Z-(OCN), PON, OA, LLA, VA, APN, BAD, ETL, NB, AN, DMAN, MCAN, OC, MM, OCA, DMETEG+DMF						

Table 4-8 Absorbents Using Freon as Refrigerant and Numbers of Studies Thereof (No. 2)

Refrigerant	Absorbent	Vapor Pressure	Crystallization Temperature	Other Physical Properties	Mass and Heat Transfer	Corrosion	Stability, Toxicity, Flammability
R22	DMETEG	5/6(3)	0/1(1)	4/7(5)	0/1(1)	1/2(2)	1/1(1)
	DMETrEG	0/4(0)		0/5(0)			
	DMEDEG	1/6(6)		2/8(8)			0/1(1)
	DMF	3/4(4)	0/1(0)	0/13(12)			0/1(1)
	DMA	2/0		1/0			0/1(1)
	DMH	2/0		1/0			
	DBP	0/1(0)		0/2(0)		0/1(0)	
	DMMP	0/2(0)		0/2(0)			
	DMSO	0/2(0)					
	DOS	1/0	0/1(0)	0/1(0)			
	DDP		0/1(0)	0/1(0)			
	DCP		0/1(0)	0/1(0)			
	IBA	0/3(2)		0/10(10)			
	TAN	1/0	0/1(0)	0/1(0)			
	Other absorbents TMM, TMS, PON, APN, BAD, VA, LLA, DEO, DEM, EB, DBC, MMETrPG, NMP, DMETEG+BA						
R30	DMETEG	1/0					
R31	DMETEG	1/0					

Table 4-9 Absorbents Using Freon as Refrigerant and Numbers of Studies Thereof (No. 3)

Refrig-erant	Absorbent	Vapor Pressure	Crystal-lization Tempera-ture	Other Physical Properties	Mass and Heat Transfer	Corro-sion	Stability, Toxicity, Flammability
R123	DMETrEG						0/1(0)
R123a	ETFE	2/0		3/1(1)			1/0
	DMETEG	0/3(0)		0/3(0)		0/1(1)	0/1(0)
R123b	DMH	1/0					
	NMP	1/0					
R124	DMF						0/1(1)
	DMA						0/1(1)
	DMEDEG						0/1(1)
	DMETEG						0/1(1)
	NMP						0/1(1)
	DMA+phosphite						0/1(1)
R124a	DMETEG	1/0					
R131a	DMH	1/0					
R133a	ETFE	1/0		3/0			3/0
	NMP	0/2(0)		0/6(0)			0/1(0)
	DMETrEG						0/1(0)
R134	DMETEG	1/0					
	NMP						0/1(0)
R140a	DMD	1/0					
R143a	NMP						0/1(0)
R152	DMF	0/4(1)		0/13(6)			
R1130	DMH	1/0					
	DMD	1/0					
R1112a	DMH	1/0					
R1120	DMD	1/0					

Table 4-10 Absorbents Using Hydrocarbon as Refrigerant and Numbers of Studies Thereof

Refrig-erant	Absorbent	Vapor Pressure	Crystal-lization Temper-ature	Other Physical Properties	Mass and Heat Transfer	Corro-sion	Stability, Toxicity, Flamma-bility
Hexane	TDK		0/1(0)				

Note 1) Other physical properties
Density, Viscosity, Specific heat, Heat of mixing, Enthalpy, Entropy, Heat conductivity, Refractive index

Note 2) Figures in the tables mean A/F(J)
A: No. of studies in U.S.A.
F: No. of studies in foreign nations other than U.S.A.
J: No. of studies in Japan

Note 3) Abbreviations of absorbents

Abbreviation	Chemical Name
BDL	1, 4 - Butanediol
BDL	2, 3 - Butanediol
4, BLN	4 - Butyrolactone
BZL	Benzothiazol
DBP	Dibutyl phthalate
DCP	Dicapryl phthalate
DDP	Didecyl phthalate
DEG	Diethylene glycol
DMA	N, N - Dimethyl acetamide
DMEDEG	Dimethylether diethylene glycol
DMETEG	Dimethylether tetraethylene glycol
DMETrEG	Dimethylether triethylene glycol
DMF	N, N - Dimethyl formamide
DMMP	Dimethyl methyl phosphonate
DMSO	Dimethyl sulfoxide
DOP	Dioctyl phthalate
DOS	Dioctyl sebacate
DWA	Dowtherm A
EG	Ethylene glycol
ETFE	Ethyl tetrahydro furfuryl ether
GYL	Glycerol
HFIP	Hexafluoroisopropanol
IBA	Isobutyl acetate
MBEDEG	Monobutylether diethylene glycol
NMP	N - Methyl - 2 - pyrrolidone
PD	Pentanediol
PPA	Propionic acid
QUN	Quinoline
TAN	Triacetin
TDK	Tetradecane
TEG	Tetraethylene glycol
TFE	Trifluoroethanol

Abbreviation	Chemical Name
AN	Aniline
APN	Acetophenone
BA	Benzyl alcohol
BAD	Benzaldehyde
BDL	1, 4 - Butanediol
BDL	2, 3 - Butanediol
DBC	Dibutyl Carbitol
DEAP	Diethyl adipate
DEF	N, N - Diethyl formamide
DEM	Diethyl malonate
DEO	Diethyl oxalate
DMA	N, N - Dimethyl acetamide
DMAN	N, N - Dimethyl aniline
DMD	N, N - Dimethyl dodecanamide
DMEDEG	Dimethylether diethylene glycol
DMETEG	Dimethylether tetraethylene glycol
DMETrEG	Dimethylether triethylene glycol
DMF	N, N - Dimethyl formamide
DMH	N, N - Dimethyl hexanamide
DOPL	Dioctyl phthalate
DOS	Dioctyl sebacate
EB	Ethyl benzoate
EG	Ethylene glycol
ETFE	Ethyl tetrahydro furfuryl ether
ETL	Ethyl laurate
LBS	Lithium benzenesulfonate
LLA	Linoleic acid
MCAN	M-Chloro aniline
MEA	Ethanolamine
MEDEG	Monoethylether diethylene glycol
METrPG	Monomethylether of tripropylene glyco
MM	N - Methylmorpholine
n-BB	n-Butyl benzoate
n-HA	n-Heptyl alcohol
NB	Nitrobenzene
NMP	N - Methyl - 2 - pyrrolidone
OA	Oleic acid
OC	Octyl cyanide
OCA	Octylamine
PDS	Polydimethylsiloxane
TAN	Triacetin
TEG	Tetraethylene glycol
TMM	N, N, N, N - Tetramethylmalonamide
TMS	N, N, N, N - Tetramethylsuccinamide
VA	Valeric acid
2-(OCN)	2 - Octanone
2,4 PON	2 - 4 pentanedione
4, BLN	4 - Butyrolactone

4.2 Working fluid investigation procedure

It takes a tremendous amount of time and labor to pick, out of a virtually limitless number of combinations of refrigerants and absorbents, a working fluid that meets the target requirements. Major physical properties of pure substances can be determined by conventional studies or estimated by their chemical structures. The physical properties of working fluid, a mixed fluid, including the behavior of dissolution of absorbent into the refrigerant and the fluid stability in solution, must be measured, unless data thereof are available. This is the principal cause that has delayed discovery of a new working fluid to replace the H_2O-LiBr and NH_3-H_2O types.

Table 4-11 shows the physical properties to be considered in a final evaluation of the applicability of a working fluid to absorption chillers or heat pumps.

Table 4-11 Physical Properties of Working Fluid

1) Vapor pressure	8) Thermal conductivity
2) Crystallization temperature	9) Heat transfer characteristics
3) Density	10) Mass transfer characteristics
4) Viscosity	11) Corrosion
5) Specific heat	12) Chemical and thermal stability
6) Heat of mixing	13) Toxicity
7) Enthalpy	14) Flammability

If all the physical properties shown in Table 4-11 are to be measured, an enormous amount of time and labor is required to evaluate only one working fluid. Therefore, the following stepwise screening method is generally adopted: First, some prospective refrigerants, absorbents, or working fluids are selected based on past literatures or chemical structures. Next, more essential characteristics, such as the most fundamental physical properties, to the other are measured to narrow down the prospective working fluids. Fig. 4-1 shows the flow chart of the primary screening adopted by Bokelmann et al. as an example.

4.3 Investigation of major working fluid

4.3.1 Working fluid using inorganic matter as refrigerant

4.3.1.1 Working fluid using H_2O as refrigerant

H_2O-LiBr working fluid, which is the only one in practical use that utilizes H_2O as a refrigerant, has limited applications, as mentioned in 3.1 above. Absorbents such as those shown in Table 4-2 are being

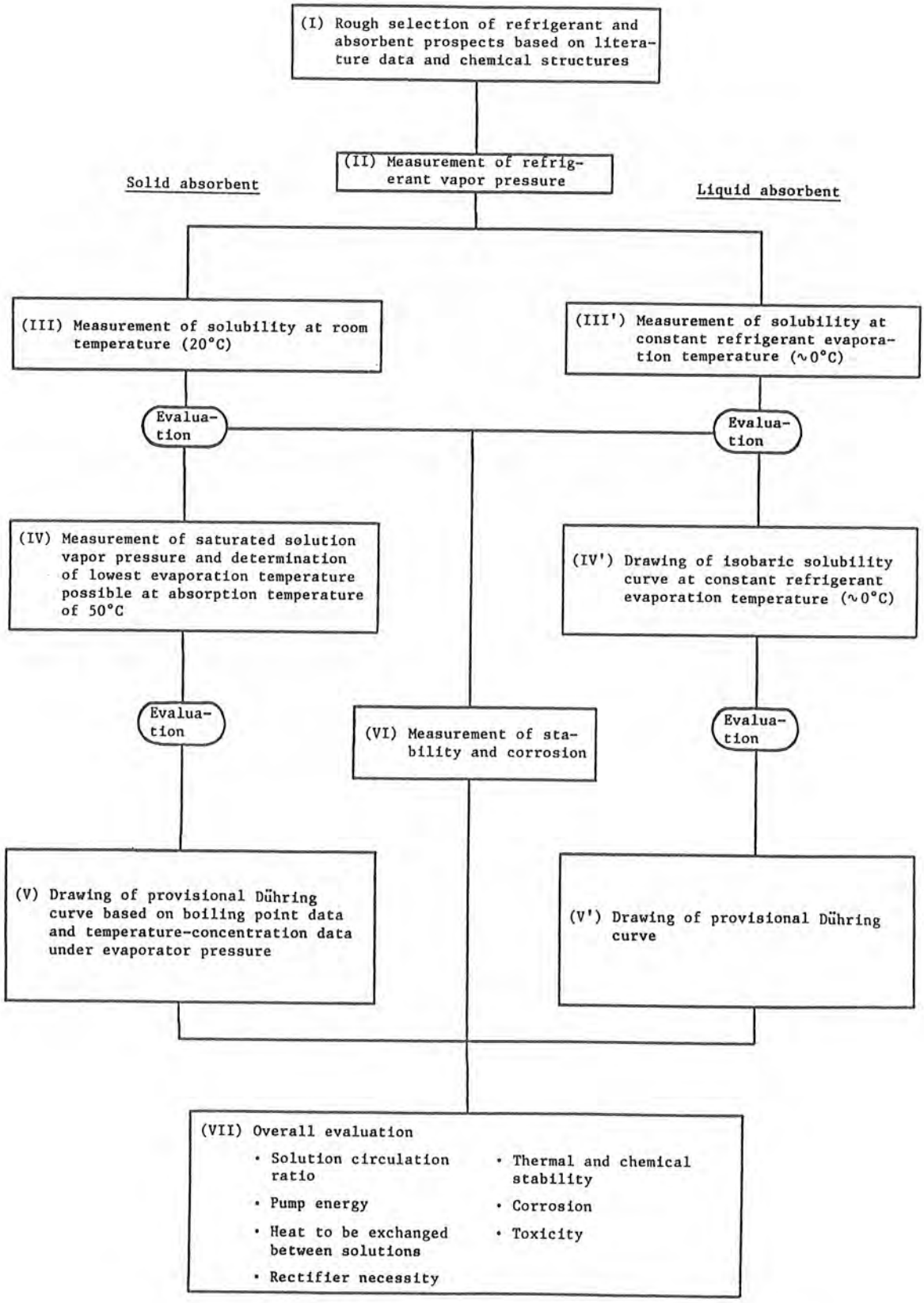

Fig. 4-1 Primary Investigation Procedure of Working Fluid

investigated to replace LiBr. Another approach is to determine two- or three-component absorbents by adding inorganic and organic matters to LiBr. The primary purpose of these investigations is to improve the solubility of the H_2O-LiBr mixture and to equip absorption chillers with air-cooled cooling and heat pump capabilities.

According to Table 4-2, the main absorbents which have drawn attention are Licl and LiI as single-component types, LiBr-LiCl, LiBr-LiSCN, LiBr-$ZnBr_2$, LiBr-$ZnCl_2$, LiBr-ethylene glycol ($C_2H_6O_2$), and LiBr-butyrolactone ($C_4H_6O_2$) as two-component types, and LiBr-$ZnBr_2$-$CaBr_2$, and LiBr-$ZnBr_2$-ethylene glycol as three-component types. The major physical properties of working fluids using these absorbents have been measured.[3)]

We also tried to determine the most suitable absorbent of this type for the same purpose as described above.[9)10)] According to almost the same procedure as shown in Fig. 4-1, we selected LiBr-$ZnCl_2$ (1:1 by weight) from halogenides and their combinations. Fig. 4-2 shows boiling points and crystallization temperatures of major absorbents; Fig. 4-3 shows the vapor pressure curves of LiBr-$ZnCl_2$ (1:1 by weight) aqueous solution.

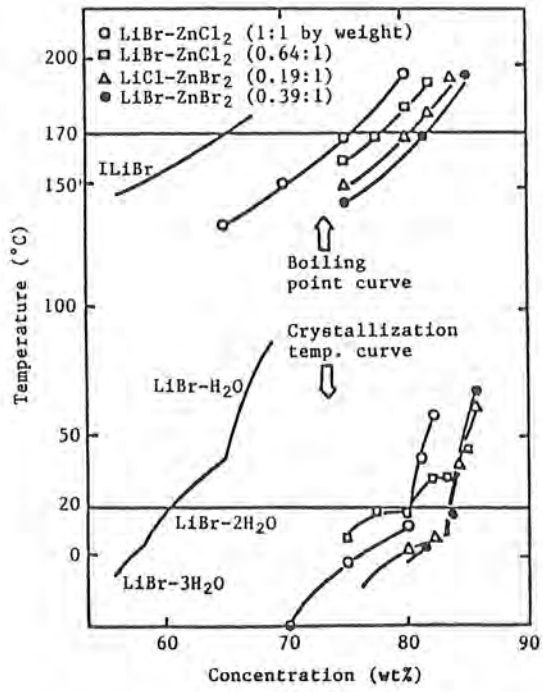

Fig. 4-2 Boiling Points and Crystallization Temperatures of Major Absorbent Solution

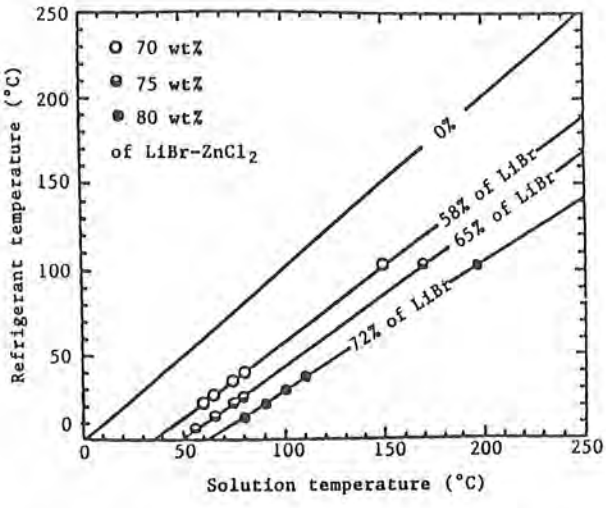

Fig. 4-3 Vapor Pressure of LiBr-$ZnCl_2$ Aqueous Solution

At 20°C, the maximum concentrations of H_2O-LiBr and H_2O-LiBr-$ZnCl_2$ (1:1 by weight) solutions are 60.6 wt% and 80.0 wt%, respectively. When these aqueous solutions are kept at a temperature of 50°C, the saturation temperatures, or minimum vaporization temperatures, of the refrigerant H_2O are +9°C and -9°C, respectively, as shown in Figs. 3-1 and 4-3. Therefore, H_2O-LiBr-$ZnCl_2$ (1:1 by weight) was judged capable of heat pump operation using 0°C or less outdoor air as the heat source (Step IV in Fig. 4-1). All the types except the H_2O-LiBr mixture in Fig. 4-2 are subject to this possibility.

Instead of drawing provisional Dühring curves in Step V, we made Step VII evaluation based on Fig. 4-2, on the assumption that the Dühring curves of the halogenide aqueous solutions have the same slope as that of the LiBr aqueous solution. At an evaporation temperature of 0°C and an absorption temperature of 50°C, the boiling point of LiBr aqueous solution is 170°C; in our investigation, therefore, a solution whose boiling point was 170°C was regarded as dilute solution and a solution whose solubility was highest at 20°C was regarded as concentrated solution. Table 4-12 shows the concentrations and solution circulation ratios of the concentrated and dilute solutions of all the absorbents in Fig. 4-2. The LiBr-$ZnCl_2$ (1:1 by weight) solution, whose solution circulation ratio was the smallest, was judged to be the most suitable. Refer to relevant literature for the physical properties, heat and mass transfer characteristics of this system.[10)11)]

Table 4-12 Solution Circulation Ratios of Selected Absorbent Prospects

Absorbent (weight ratio)	Concentration		Solution Circulation Ratio
	Dilute Solution	Concentrated Solution	
LiBr-$ZnCl_2$ (1:1)	75.0 wt%	80 wt%	16.0
LiBr-$ZnCl_2$ (0.64:1)	77.5	80	32.0
LiCl-$ZnBr_2$ (0.19:1)	80.0	83	27.7
LiBr-$ZnBr_2$ (0.39:1)	81.5	83	55.3

Corrosiveness is one of the most important factors in evaluating a working fluid using H_2O as refrigerant. In general, corrosion causes hydrogen gas to be generated with this system. At the maximum allowable pressure rise of 1 mmHg, the hydrogen gas generation rate is 0.24 cc/m^2/day for cooling and 0.48 cc/m^2/day for heating in terms of the entire inner area of the absorption chiller and 11.1 cc/m^2/day and 22.2 cc/m^2/day in terms of the generator inner area.[12)]

4.3.1.2 Working fluid using NH_3 as refrigerant

NH_3-H_2O working fluid, which is in practical use among working fluid types using NH_3 as a refrigerant, has been the longest history of use as an absorption chiller working fluid. However, it is also subject to the limitations described in 3.2 above. As shown in Table 4-3, in Japan no investigation has been made on this system because of the toxicity of NH_3, despite the active involvement of Western nations in absorbent investigation on this system and cycle improvement thereof.

Bokelmann et al. selected $LiNO_3$-H_2O rather than $LiBr_3$-H_2O in view of solubility; furthermore, they selected $LiNO_3$-H_2O (25 wt%) as the most suitable absorbent in view of solubility, crystalization temperature, and viscosity.[5)6)] Fig. 4-4 shows isobaric solubility curves, which can be found by completing Step IV' in Fig. 4-1. The results gained through evaluation in Step VII are shown in Table 4-13. The $LiNO_3$-H_2O solution has smaller specific heat than NH_3-H_2O solution; therefore, the specific heat of exchange becomes smaller. Another advantage of this system is that the water content in the gas phase is small and no rectifier is necessary.

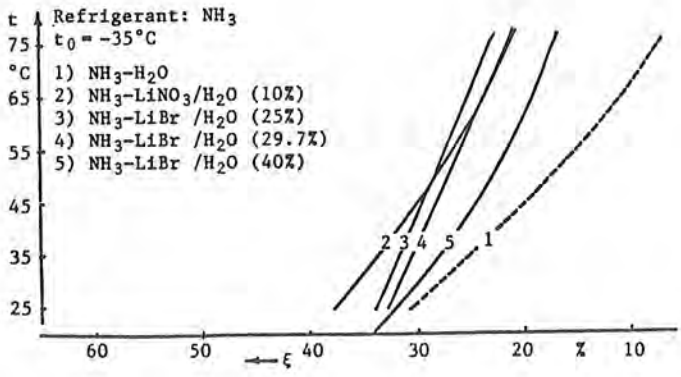

Fig. 4-4 Isobaric Salubility Curve of NH_3 System

Table 4-13 Comparative Evaluations of Promising Working Fluids

Working Fluid	Refrigerant r_0	Refrigerant P_{50}	ξ_a	ξ_r	f	$10^3 n_p$	n_L	Rectification	Toxicity
TFE-MNP	449	0.358	0.15	0.43	3.04	0.205	0.86	Yes	Yes
R123a-DTG	183	1.97	0.13	0.28	5.80	4.91	4.98	No	No
Methylamin-EGL	859	7.76	0.15	0.28	6.37	5.15	1.72	(Yes)	Yes
R22-DTrG	205	19.3	0.24	0.38	5.59	36.89	4.28	No	No
NH_3-$LiNO_3$/H_2O	1261	20.3	0.27	0.41	5.25	6.49	0.98	(No)	Yes
NH_3-H_2O	1261	20.3	0.23	0.41	4.28	6.56	1.15	Yes	Yes
R22-DTG	205	19.3	0.22	0.35	5.89	38.76	4.58	No	No
R123a-ETFE	183	1.97	0.10	0.31	(4.29)	(4.14)	(3.66)	Yes	No

Evaporation temperature : 0°C
Condensation temperature: 50°C
Absorption end temperature: 50°C
Generation temperature : 150°C

4.3.2 Working fluid using organic matter as refrigerant

4.3.2.1 Working fluid using amines as refrigerant

The most representative of this type refrigerant is methyl amine, as shown in Table 4-5. Remarkably, methyl amine has lower pressure than ammonia. For absorbents, various kinds of inorganic and organic matters and mixtures thereof have been investigated. Fig. 4-5 shows the isobaric solubility curves of representative absorbents.[5)]

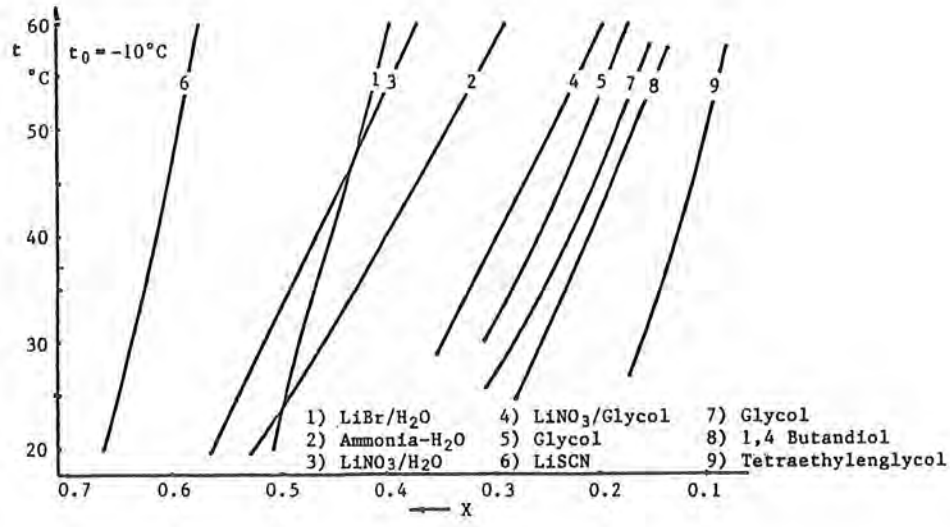

Fig. 4-5 Isobaric Solubility Curve of CH_3-NH_3 System

Organic absorbent systems are less subject to problems regarding crystallization than inorganic absorbent systems. On the other hand, organic absorbent systems have a small refrigerant concentration, which increases the solution circulation ratio. Among the organic matters, ethylene glycol is considered the most suitable.

Despite its large refrigerant concentration, the LiSCN system has a large slope of the solubility curve; it is difficult to separate the refrigerant from the absorbent LiSCN. It also has fear of decomposition at high temperatures. LiBr-H_2O and $LiNO_3$-H_2O systems decompose at 150°C and 160°C, respectively. The $LiNO_3$-Glycol system crystallizes at a refrigerant concentration of 35 wt% or less.

Accordingly, Bokelmann et al. checked for thermal stability at 160°C and 190°C and selected methyl amine-ethylene glycol as the most promising working fluid of amine systems. The evaluation results of working fluids other than that type are shown in Table 4-13.

Methyl amine has toxicity, although it is less toxic than ammonia. Therefore, much thought must be given to practical use of a working fluid using methyl amine as the refrigerant.

4.3.2.2 Working fluid using alcohols are refrigerant

Working fluids using alcohols as the refrigerant allow the evaporator temperature to be reduced to 0°C or below and are thus expected to be applicable to refrigerators as well as heat pumps.

Representative alcohols for use as the refrigerant are methanol, ethanol, and trifluoroethanol (TFE). Investigations have been made on LiBr, LiI, LiSCN, LiBr-$ZnBr_2$, and LiI-$ZnBr_2$ as major absorbents for methanol and LiBr, LiI, and LiBr-$ZnBr_2$ as major absorbents for ethanol. The major physical properties of these working fluids have been measured.[1)2)3)]

Bokelmann et al. reviewed existing literature and made a preliminary investigation to select the most suitable absorbent for methanol refrigerant; they selected 25 types of inorganic and organic absorbents selected as candidates and investigated them according to the procedure shown in Fig. 4-1.[6)] The results gained through Step IV are shown in Table 4-14. Although LiBr-$ZnBr_2$ (1 mol/ 1 mol) was considered the best prospect, it turned out to have no thermal stability at 130°C or higher. It was also discovered that methanol decomposition was promoted in the presence of $ZnBr_2$.

Table 4-14 Absorbent Prospects for Methanol Refrigerants

Absorbent	ξ_s	$\frac{Ps_{50}}{mbar}$	$\frac{ts_{50}}{°C}$
$CaBr_2$	0.63	348	39
$Ca(NO_3)_2$	0.369	148	28
CdJ_2	0.334	406	42
KSCN	0.795	—	—
$LiNO_3$	0.649	279	34
LiOH	0.941	—	—
NaBr	0.856	—	—
NaJ	0.579	305	36
NaSCN	0.719	374	41
$SrBr_2$	0.435	260	32
SrJ_2	0.412	230	31
$ZnCl_2$	0.404	—	—
ZnJ_2	0.232	61	6
LiBr/NaJ (1:1)	0.777	458	45
LiBr/$SrBr_2$ (1:3)	0.555	165	23
Nat	0.304	336	38
Thy	0.153	219	30
LiBr/Nat (1:1)	0.405	89	12
LiBr/Thy (1:1)	0.288	41	0
LiBr/HMPT (1:1)	0.329	138	21
LiBr	0.415	21	-11
LiSCH	0.43	10	-21
$ZnBr_2$	0.29	85	12
LiBr/$ZnBr_2$ (1:1)	0.176	2	-30
LiBr/$ZnBr_2$ (2:1)	0.279	7	-25

Lately, trifluoroethanol (TFE) has drawn attention as a refrigerant for absorption heat pumps. The latent heat for vaporization of trifluoroethanol is lower than that of water, ammonia, or methanol but higher than that of Freons. In addition, trifluoroethanol, whose vapor pressure is low, is potentially capable of producing a double effect cycle. In terms of molecular structure, trifluoroethanol is highly soluble into organic solvent. It is reported to be thermally stable up to 300°C. However, it is flammable and a question of toxicity still remains.

TFE-n methyl 2 pyrrolidone (NMP) has been applied to a low-temperature absorption chiller experimental model, which uses, as the drive heat source, solar heat, operated by the New Energy Development Organization, Japan. In addition, TFE-DMETEG and TFE-TEG systems have been proposed as prospects.

As candidates for an absorbent for use with TFE, Bokelmann et al. selected 43 kinds of organic matters which have high boiling points and are expected to be stable in terms of their chemical structure, and then evaluated them according to the procedure shown in Fig. 4-1. Finally, they selected NMP as the most promising absorbent.[6] Fig. 4-6 shows the solubility curves obtained in Step IV' with regard to the absorbent types selected through Step III'. Fig. 4-7 shows the solubility curves at a evaporation temperature of 50°C, and Fig. 4-8 shows the provisional Dühring curves drawn in Step V'.

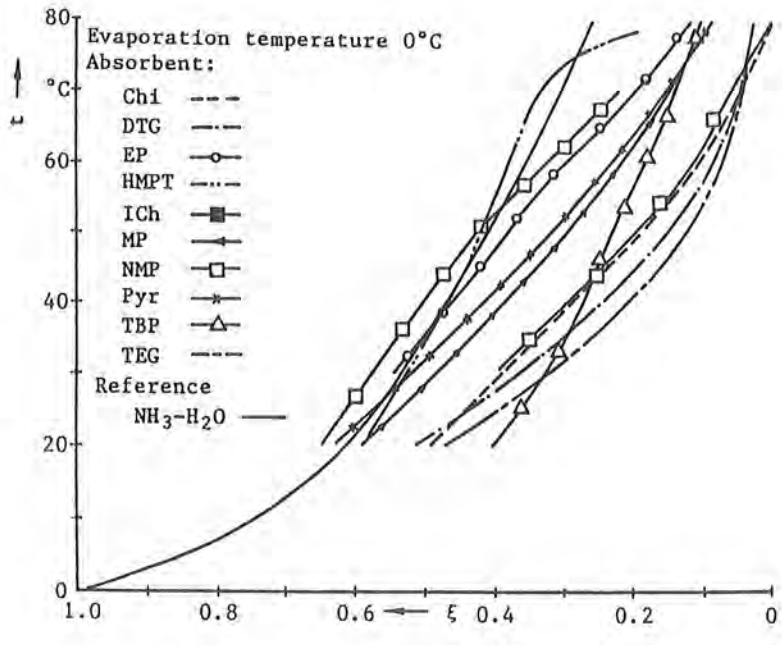

Fig. 4-6 Isobaric Solubility Curve of TFE Type System (Evaporator temperature: 0°C)

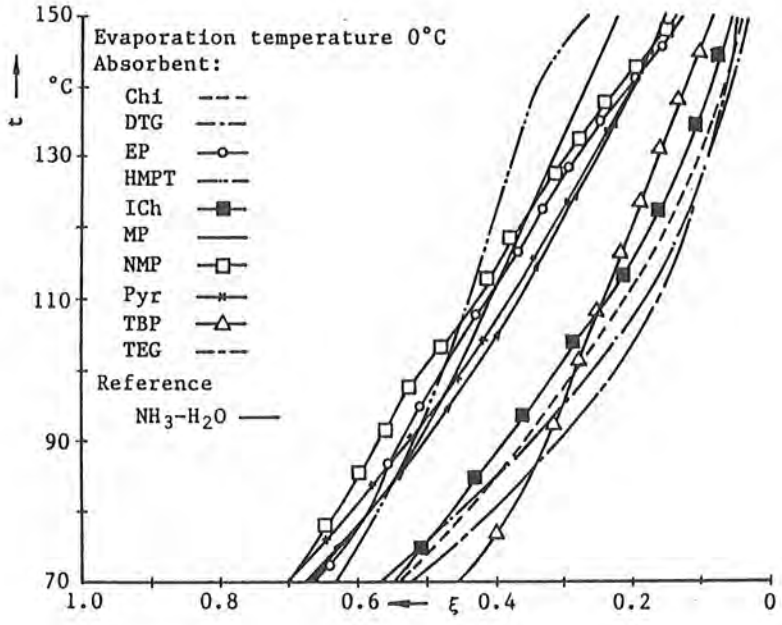

Fig. 4-7 Isobaric Solubility Curve of TFE System (Evaporation temperature: 50°C)

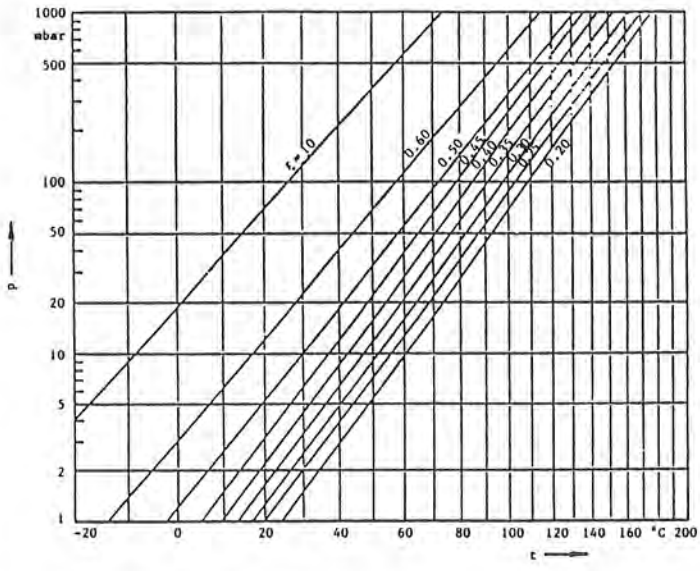

Fig. 4-8 Dühring Curve of TFE-NMP System

The experimetnal results concerning stability tested in Step VI are shown in Table 4-15. Overall results gained through Step VII are shown in Table 4-16. The TFE-NMP type was selected, since it is small in pump energy Ap and heat to be exchanged between solutions Al and is thermally stable, although it requires rectification because of a boiling-point difference of 200°C or less between the refrigerant and absorbent.

Table 4-15 Thermal Stability Test Results of TFE System

Working Fluid	Concentration	Vessel Material	Pressure Rise after ( ) Days			Notes	Evaluation
			160°C	180°C	200°C		
TFE-EP	0.31	Polished steel alloy	0(42)	0(65)	0(26)	Decomposition not found	+
TFE-Iai	0.55	Steel alloy	0(20)	—	—	—	(+)
TFE-HMPT	0.4	Steel alloy	130°C: 40(41)	150°C: 100(46)	—	Extremely colored	-
HMPT	1.0	Steel alloy	130°C: 300(41)	—	—	Extremely colored	-
TFE-NMP	0.40	Steel alloy	0(21)	0(71)	0(14)	Decomposition not found	+
TFE-TBP	0.19	Steel alloy	0(15) 50(18) 230(25)	—	—	—	-
TFE-TBP	0.24	Polished steel alloy	160(6) 680(12)	—	—	—	-

Table 4-16 Overall Evaluations of TFE System

Working Fluid	ξa	ξr	f	$\frac{\Delta t_s}{K}$	$\frac{\rho_L}{kg/m^3}$	$\frac{C_L}{J/kg\,K}$	$10^{-3}Ap$	$\frac{10^{-3}A_L}{1/K}$	Thermal Stability	Evaluation
TFE-Chi	0.107	0.197	9.9	161	1152	1990	0.65	39.4	(+)	+
TFE-DTG	0.091	0.153	14.7	201	1026	1990	1.08	60.7	(+)	+-
TFE-EP	0.301	0.385	8.3	144	1149	1970	0.55	32.0	+	++
TFE-HMPT	0.380	0.420	15.5	161	1178	1960	0.99	63.3	-	-
TFE-ICh	0.109	0.198	10.0	169	1104	1990	0.68	39.9	(+)	+
TFE-MP	0.216	0.298	9.6	170	1140	1980	0.64	37.9	(+)	-
TFE-NMP	0.328	0.423	7.1	129	1184	1890	0.45	25.7	+	++
TFE-Pyr	0.236	0.323	8.8	171	1202	1980	0.55	34.4	(+)	++
TFE-TBP	0.183	0.229	17.8	215	1071	1980	1.26	74.1	0	-
TFE-TEG	0.073	0.122	18.9	240	1157	1990	1.23	79.3	(+)	-

Operating conditions:
Evaporation temperature: 0°C
Condensation temperature: 50°C
Absorption temperature : 50 ∿ 60°C

4.3.2.3 Working fluid using Freons as refrigerant

According to Table 4-7, major Freon refrigerants which have so far drawn attention are R21, R22, R123a, and R133a. R21 is chemically unstable and R133a is toxic. Major absorbents for a Freon refrigerant are DMEDEG, DMETrEG, DMETEG, and ETFE, as ethers, and DMF and DMA, as amides.

Working fluids using Freon as the refrigerant are considered the most promising for use in absorption heat pumps. In Japan as well as abroad, some of these have been developed to the phase of prototype operation or field testing. R22-DMEDEG (E141)[13] and R22-DMETEG (E181)[14] systems have been investigated in Japan; a R123a-ETFE[15] system has been investigated in the U.S.A.

With a large difference in boiling point (315°C) between the refrigerant and the absorbent, the R22-DMETEG system is excellent in thermal stability. Because of its small latent heat for vaporization of R22, however, the R22-DMETEG system has a large solution circulation ratio and cannot be expected to have a large C.O.P. (coefficient of performance). The R22-DMEDEG type is thermally stable and has a slightly higher C.O.P. than the R22-DMETEG type. Although R123a-ETFE type is also thermally stable, R123a is lower in latent heat for vaporization than R22; with the small difference in boiling point (127°C) between the refrigerant and the absorbent, the R123a-ETFE type requires a rectifier.

Bokelmann et al. selected R22, R30, R123a, and R133a as Freon refrigerants and evaluated numerous types of working fluids made by combining these Freon refrigerants with various absorbents according to the procedure shown in Fig. 4-1, in the same way as for TFE refrigerant systems.[5)6)] In the process of evaluation, R30 and R133a were eliminated due to chemical unstability and toxicity, respectively. R22-DMETrEG and R123a-DMETEG were selected as prospects. Through a series of evaluations, it was pointed out that NMP decomposes in the presence of chlorine compounds such as R123a and R133a. The evaluation results of the two working fluids selected are shown in Table 4-13.

R22-DMETrEG has the following advantages: R22-DMETrEG has a larger refrigerant concentration, smaller solution circulation ratio, and approximately 30% smaller viscosity, compared with R22-DMETEG. With a large difference in boiling point of 260°C between the refrigerant and the absorbent, R22-DMETrEG requires no rectifier.

R123a-DMETEG has the following merits: R123a-DMETEG, whose vapor pressure is comparatively low for a possible double effect cycle, has a large difference in boiling point 247°C between the refrigerant and the absorbent and thus requires no rectifier. Also, it needs comparatively small pump energy. Note that R123a has low toxicity and low flammability, although it is slightly thermally unstable. In an aluminum autoclave at 160°C, R123a did not show any significant change in pressure even after 30 days. In an alloy steel autoclave at 160°C, however, it recorded a pressure rise.[6)]

5. Promising Working Fluid

5.1 Working fluid for absorption chiller and heat pump

The working fluids mentioned above have been investigated primarily to meet the requirements for heat pumps. The ones brought to the phase of prototype development, as well as the new working fluids proposed by Bokelmann et al., are shown as promising working fluids in Table 5-1.

Table 5-1 Promising Working Fluids for Absorption Chiller and Absorption Heat Pump

Refrigerant	Absorbent	Proposer	Remarks
H_2O	$LiBr/ZnCl_2$ (1/1 wt)	Manago et al.[9)10)]	Phase of prototype development Target: COPc = 1.0, COPh = 1.56
NH_3	$LiBr/H_2O$ (60/40 wt)	Phillips B. A.[7)]	Phase of 3RT breadboard Target: COPc = 0.7, COPh = 1.6
	NaSCN	Columbia Gas	Phase of 3RT prototype Target: COPc = 0.8, COPh = 1.6
	$LiNO_3/H_2O$ (75/25 wt)	Bokelmann et al.[5)6)]	
CH_3NH_2	EG	- ditto -	
TFE	NMP	Mashimo[16)]	Phase of low-temperature chiller experimental model development Refrigeration capacity: 45,000 kcal/hr
		Bokelmann et al.	
R22	DMEDEG (E141)	Wakamatsu et al.[13)]	1.3RT field test completion/interruption COPc = 0.55, COPh = 1.2
	DMETrEG	Bokelmann et al.	
	DMETEG (E181)	Ouchi et al.	
R123a	DMETEG	Bokelmann et al.	
	ETFE	Murphy et al.[15)]	3RT field test completion/interruption COPc = 0.65, COPh = 1.50
R133a	NMP	Gaz de France etc.	
	ETFE	Allied Chemical	

5.2 Working fluid for heat transformer

The working fluid practically used for heat transformers is H_2O-LiBr system. In Europe, and especially in West Germany, new working fluids have been recently studied with a focus on greater temperature rise and higher efficiency.

The requirements for heat transformer working fluids are basically similar to the requirements for absorption chiller and heat pump working fluids. The major requirements thereof are shown in Table 2-1.

Through a series of investigations on working fluids for heat pumps, Bokelmann suggested the five working fluids in the upper portion of Table 5-2 as prospects for use in heat transformers.[17] In the lower portion of the table, all the working fluids are compared in performance, based on a generator temperature of 100°C and a concentration difference between the cocnentrated and dilute solution of 5 wt%.

Table 5-2 Promising Working Fluids for Heat Transformer

	General									
	Working Fluid	r_o kJ/kg	$t_{critical}$ °C	P_{20} bar	P_{100} bar	Price DM/kg sol	Toxicity	Corrosion	Δtm	Rect.	Data
1	TFE-OTG	449	250	0.07	2.3	28	Yes	No	201	No	--
2	TFE-NMP	449	250	0.07	2.3	27	Yes	No	129	(Yes)	--
3	TFE-Pyr	449	250	0.07	2.3	25	Yes	No	171	(No)	--
4	MFIP-NMP	428	195	0.16	5.5	(2500)	less (as spt)	(No)	145	(Yes)	--
5	PFPA-OTG	(255)	?	0.03	ca. 1	295	less (as spt)	Yes Inhibitor	179	(No)	--
6	NH_3-H_2O	1260	132	8.6	63	2	Yes	Partly	133	Yes	--
7	H_2O-LiBr	2500	374	0.02	1	25	No	Yes Inhibitor	--	No	--

	Comparison at different Working Conditions											
	t_E = 100°C t_c = 20°C				t_E = 100°C t_c = 50°C				t_E = 50°C t_c = 20°C			
	ξa	ta	Δta	f	ξa	ta	Δta	f	ξa	ta	Δta	f
1	0.05	185	20	19	0.18	155	8	16	0.05	128	15	19
2	0.20	ca. 210	ca. 12	16	0.52	160	10	10	0.20	1.38	5	16
3	0.15	ca. 225	ca. 20	17	0.45	165	15	11	0.15	140	10	17
4	(0.65)	(220)	(10)	(7)	0.82	160	8	4	(0.65)	130	12	7
5	(0.57)	(185)	(10)	(8.5)	(0.72)	(150)	(10)	(6)	(0.57)	(125)	(70)	(8.5)
6	--	--	--	--	--	--	--	--	0.28	125	10	14
7	--	--	--	--	0.38	146	14	12	--	--	--	--

Notes) r_0 : latent heat for vaporization of refrigerant at 0°C (kS/kg)
P_{20}, P_{100}: vapor pressure at 20°C, 100°C (bar)
Δtm : boiling point difference between refrigerant and absorbent (°C)
Rect. : rectifier necessary or not
Data : data available or not
ξa : refrigerant concentration of concentrated (weak) solution (wt%)
ta : absorber temperature (°C)
Δta : absorber temperature difference (°C)
f : solution circulation ratio
t_E : evaporation temperature (°C)
tc : condenser temperature (°C)

Spaces in the table mean that no cycle is established under the corresponding temperatures due to high pressure for NH_3-H_2O and due to crystallization for H_2O-LiBr. As an example, a cycle using a TFE-Pyr system is given in Fig. 5-1.

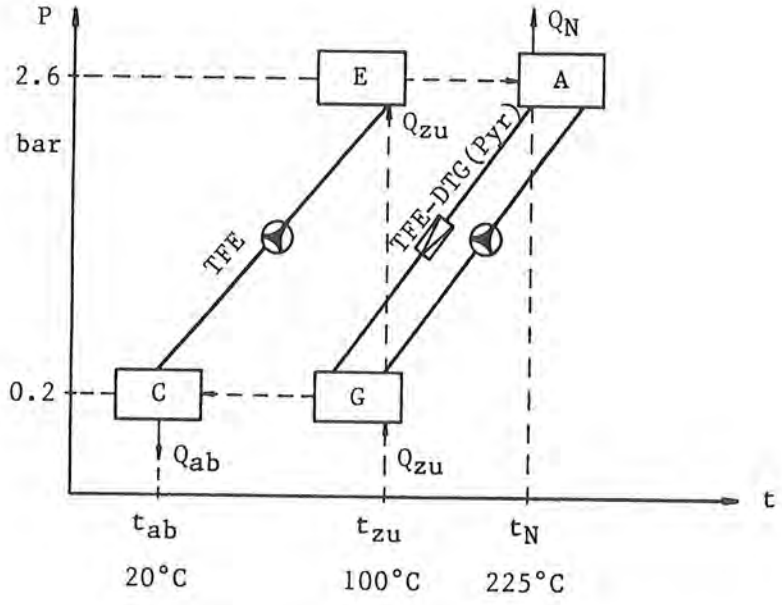

Fig. 5-1 Heat Transformer Cycle of TFE-pyr System

6. Conclusion

The working fluids investigated for use in absorption chillers and heat pumps have been described above. Despite a wide range of investigaitons on a tremendous number of working fluids, only the NH_3-H_2O and H_2O-LiBr systems, both of which were developed at the early stage of absorption chiller development, have reached the phase of practical use.

There are presently strong needs for new working fluids. I hope for further progress in this field and for the prompt discovery of new working fluids.

References

1) Macriss R.A., Zawacki T.S., "Absorption Fluids Data Survey: Final Report on USA Data", U.S. DOE, ORNL/Sub/84-47989/1, 1986

2) Macriss R.A. et al., "Absorption Fluids Data Survey: Final Report on Foreign Data", U.S. DOE, ORNL/Sub/84-47989/2, 1987

3) Uemura and Iyoki, Refrigeration, Japan, 62 (711), 38, 1987.

4) Takada, "Absorption Chiller", Japanese Association of refrigeration, 14, 1982

5) Bokelmann H. et al., "Presentation of New Working Fluids for Absorption Heat Pumps", Proceedings of Absorption Heat Pumps Congress, Paris, March 20-22, 1985

6) Bokelmann H., "Auswahl, Messung Thermophysikalischer Eigenshaften und Beurteilung der Eignung von Niederdruck-Stoffsystemen fur Absorptions-Warmepumpen", Genehmigte Dissertation zur Erlangung des Grades Doktor-Ingenieur, Universitat Essen, 1984

7) Phillips B.A., " A new future for absorption?", ASHRAE JOURNAL, Nov., 38, 1986

8) Ball D.A., "High Performance Heat Exchangers for the Battelle Dual Cycle Absorption Concept", U.S.-Japan Absorption Workshop, Nov. 9, 1987, Tokyo

9) Oouchi et al., Proceedings of the 1982 Conference of the Japanese Association of Refrigeration, 13, 1982

10) Manago et al., Energy and Resources, Japan, 8 (3), 77, 1987

11) Manago et al., The 20th Autumn Convention Abstracts of the Society of Chemical Engineers, Japan, 114, 1987

12) Hurd R.M. et al., "Summary Report on the corrosion of Mild Steel in Concentrated Lithium Bromide Solutions at Elevated Temperatures", AGA, TRACOR 64-129-U, 1964

13) Wakamatsu et al., Proceedings of the 17th Conference of Air-conditioning and Refrigeration, Japan, 136, 1983

14) Oouchi et al., ibid, 144, 1983

15) Murphy et al., "Development of a Residential Gas Absorption Heat Pump", Proceedings of International Gas Research Conference, 482, 1983, London

16) Mashimo K., "Development of Absorption Systems with a New Working Pair TFE/NMP", U.S.0Japan Absorption Workshop, Nov. 9, 1987, Tokyo

17) Bokelmann H., "Industrial Heat Recovery with Heat Transformers - Practical Applications and Development of Advanced Systems, Proceedings of the 1987 IEA Heat Pump Conference, 287, 1987

RESEARCH AND DEVELOPMENT ON WORKING FLUIDS FOR ABSORPTION HEAT PUMPS

ABSORPTION SYSTEMS COMMERCIALLY AVAILABLE IN JAPAN

	Chiller	Chiller/ Heater	Heat Pump	Heat Transformer
Output	• Chilled water (4–15°C)	• Chilled water (4–15°C) • Hot water (40–80°C)	• Hot water • Low-press. Steam (60–95°C)	• Hot water • Steam (100–155°C)
Driving Heat	• Hot water • Steam	• Town gas • Waste heat	• Town gas • Steam	• Waste heat (60–100°C)
Heat Source	None	None	• Waste heat (20–60°C)	None
Application	• Cooling • Industrial cooling	• Cooling & Heating	• Industrial heating	• Industrial heating

DEVELOPMENT OF ABSORPTION HEAT PUMPS IN JAPAN

- Ammonia — Water
- R22 – DMETEG (E181)
- R22 – DMEDEG (E141)
- TFE – NMP
- Water – LiBr – $ZnCl_2$

EVALUATION CRITERIA FOR ABSORPTION HEAT PUMPS

- Possibility to introduce a double-effect cycle
- Temperature range:
  - Lower heat source temperature than 0°C
  - Higher output temperature than 50°C
- Cycle performance:
  - Larger heating and cooling capacity
  - Higher coefficient of performance
  - Moderate operating pressure
  - Smaller auxiliary power

MAJOR REQUIREMENTS FOR WORKING FLUIDS

	Requirements
Refrigerant	• Lower freezing point than 0°C • Large latent heat of vaporization • Low operating pressure
Absorbent	• High degree of solubility • Large b.P. difference between absorbent and refrigerant
Refrigerant-Absorbent Mixture	• Small solution circulation ratio • Small pump energy • Small amount of heat exchanged between solutions • Thermal and chemical stability • Non-toxicity

LIMITATIONS OF WATER-LiBr AND AMMONIA — WATER MIXTURE

- Water-LiBr:
  - Higher evaporator temperature than 0°C
  - Low degree of solubility
  - Corrosiveness
- Ammonia-water:
  - Toxicity
  - Flammability
  - High operating pressure
  - Small boiling point difference between refrigerant and absorbent

REFRIGERANTS

- Inorganic
  - Water
  - Ammonia
- Organic
  - Amines
  - Alcohols
  - Halogenated carbon

ABSORBENTS

- Inorganic
  - Salts
- Organic
  - Alcohols
  - Ethers
  - Alcohol-ethers
  - Amides
  - Amines
  - Amine-alcohols
  - Esters
  - Ketones
  - Acids
  - Aldehydes

PHYSICAL PROPERTIES OF WORKING FLUID

1. Vapor pressure
2. Crystallization temperature
3. Density
4. Viscosity
5. Specific heat
6. Heat of mixing
7. Enthalpy
8. Thermal conductivity
9. Heat transfer characteristics
10. Mass transfer characteristics
11. Corrosion
12. Chemical and thermal stability
13. Toxicity
14. Flammability

PRIMARY SCREENING PROCEDURE OF SOLID ABSORBENT FLUIDS

I. Coarse selection of candidate fluids
II. Meas. of refrigerant vapor press.
III. Meas. of solubility at room temp.
IV. Det. of lowest possible evaporator temp. at absorber temp. of 50°C
V. Drawing of provisional Dühring curve
VI. Meas. of stability and corrosion
VII. Overall evaluation

LOWEST POSSIBLE EVAPORATOR TEMP. & PROVISIONAL DÜHRING CURVE

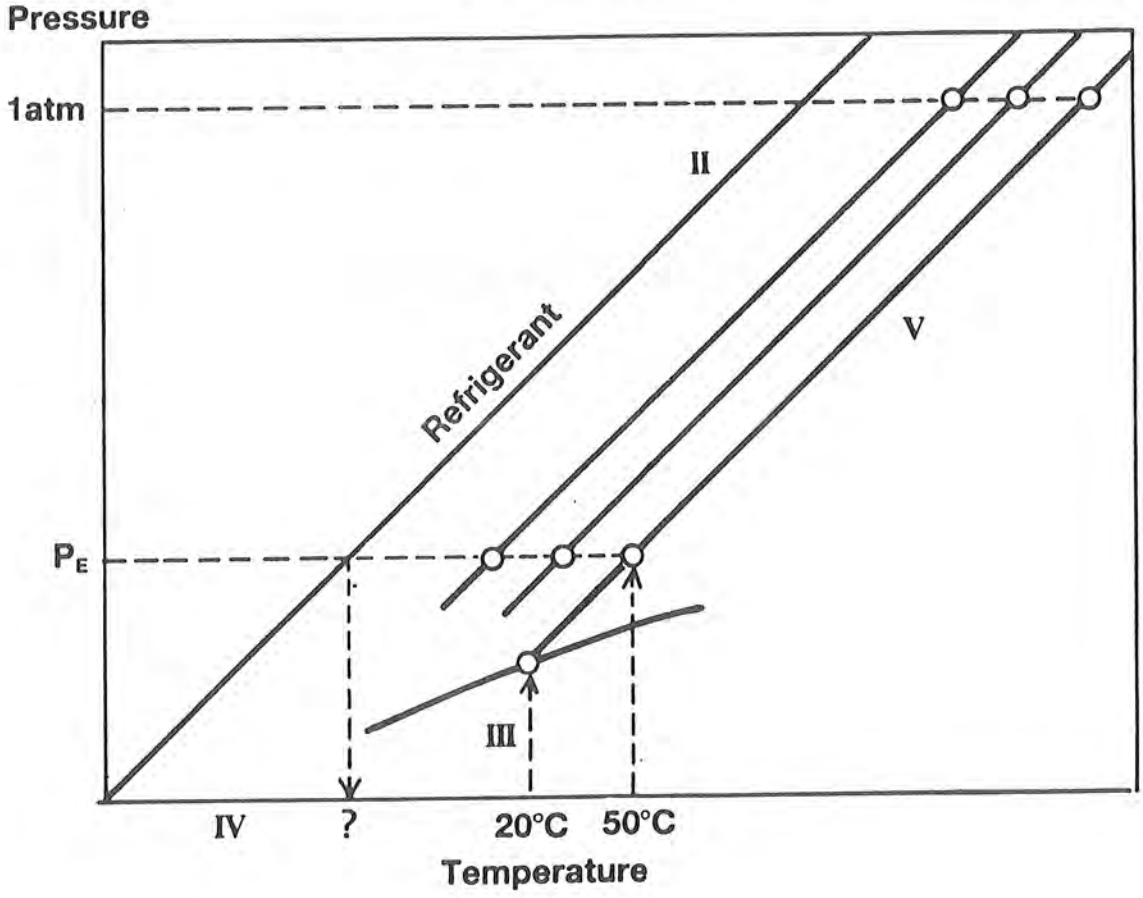

PRIMARY SCREENING PROCEDURE OF LIQUID ABSORBENT FLUIDS

I. Coarse selection of candidate fluids
II. Meas. of refrigerant vapor press.
III. Meas. of solubility at evaporator temp.
IV. Drawing of isobaric solubility curve
V. Drawing of provisional Dühring curve
VI. Meas. of stability and corrosion
VII. Overall evaluation

SOLUBILITY AT EVAPORATOR TEMP.

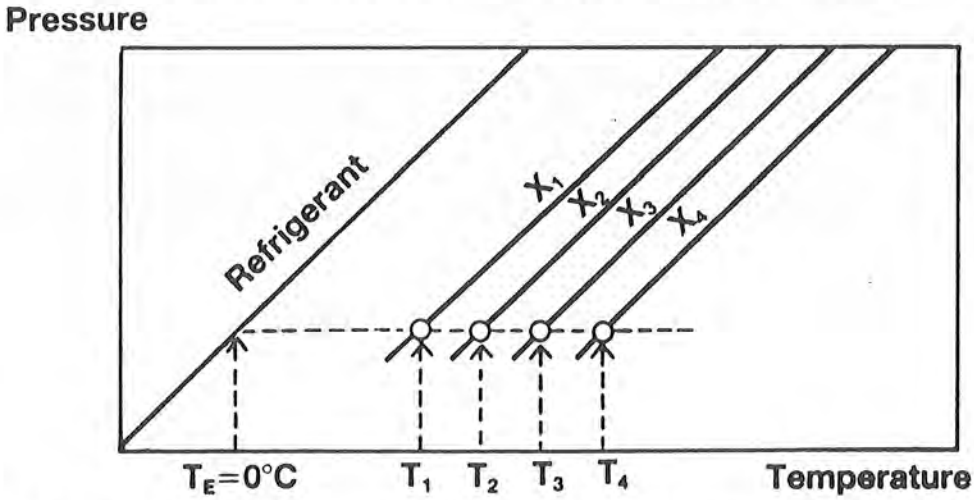

ISOBARIC SOLUBILITY CURVE

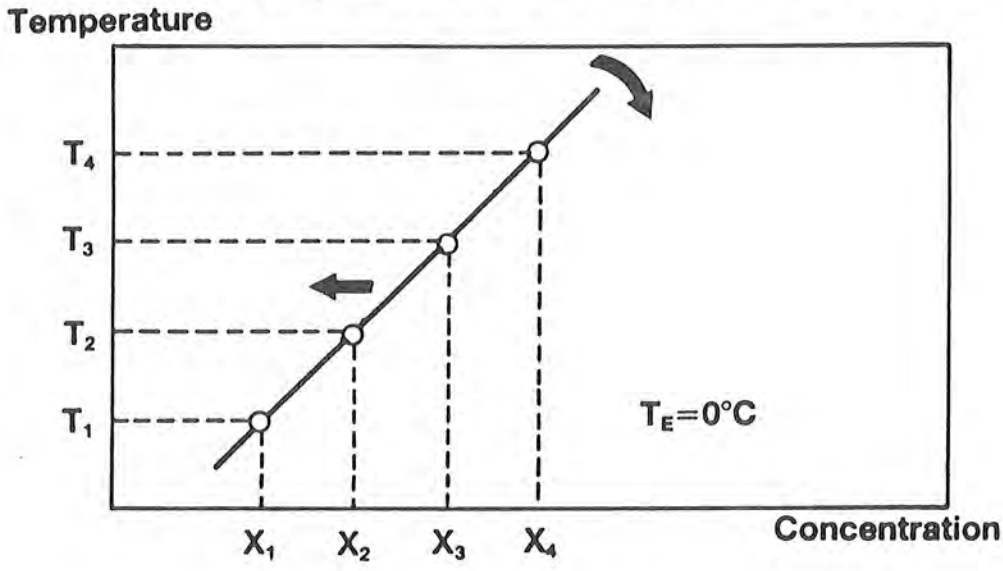

ABSORBENTS USING WATER AS REFRIGERANT

Absorbents	Property data	Corrosion data
LiCl	Available	Available
Li I		
LiBr-LiCl		
LiBr-LiSCN		Available
LiBr-$ZnBr_2$		
LiBr-$ZnCl_2$		Available
LiBr-EG		Available
LiBr-BLN		Available

BOILING POINT & CRYSTALLIZATION TEMPERATURE OF LiBr-LiCl SOLUTION

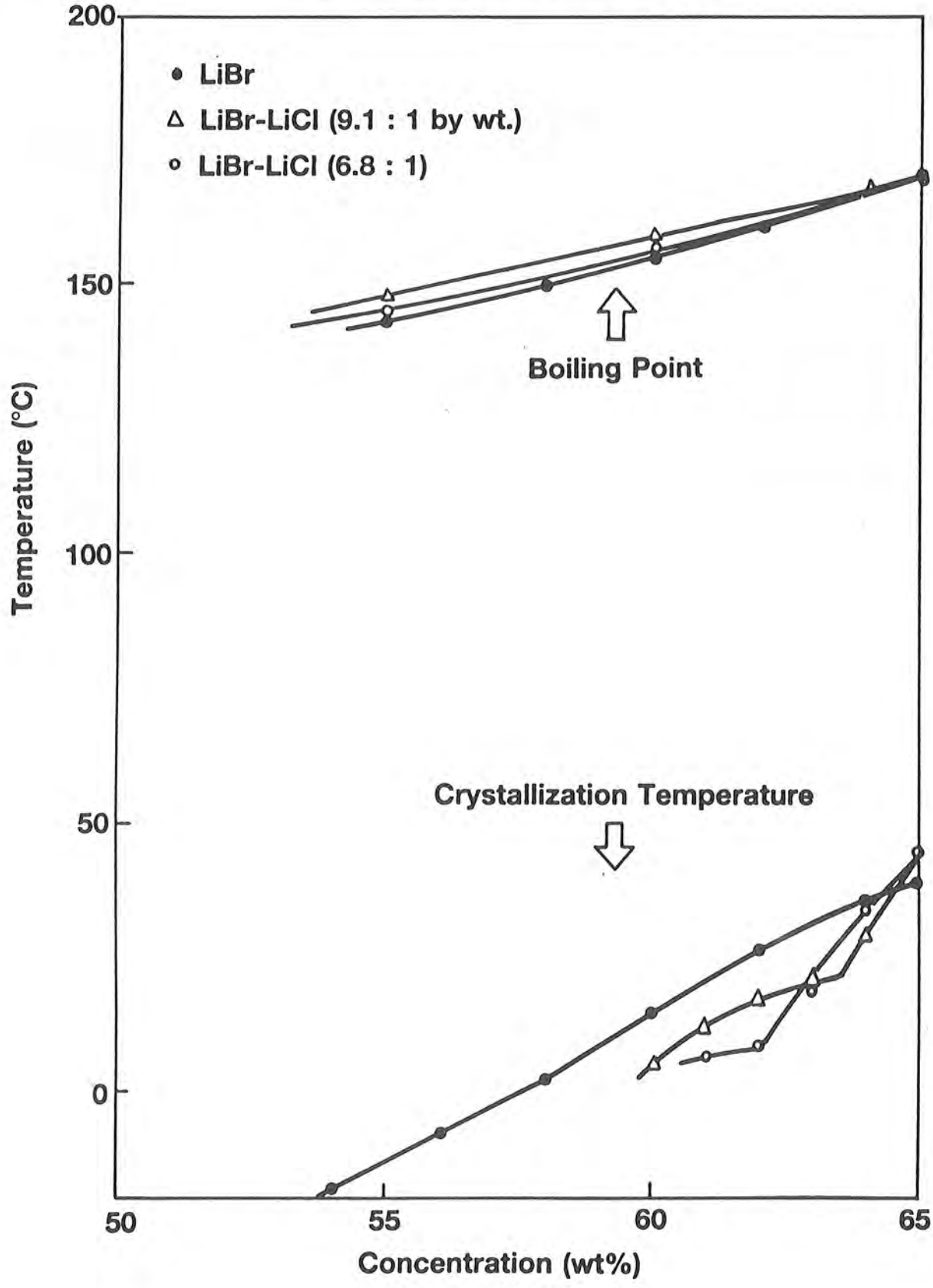

BOILING POINT & CRYSTALLIZATION TEMPERATURE OF $LiBr-ZnCl_2$ SOLUTION

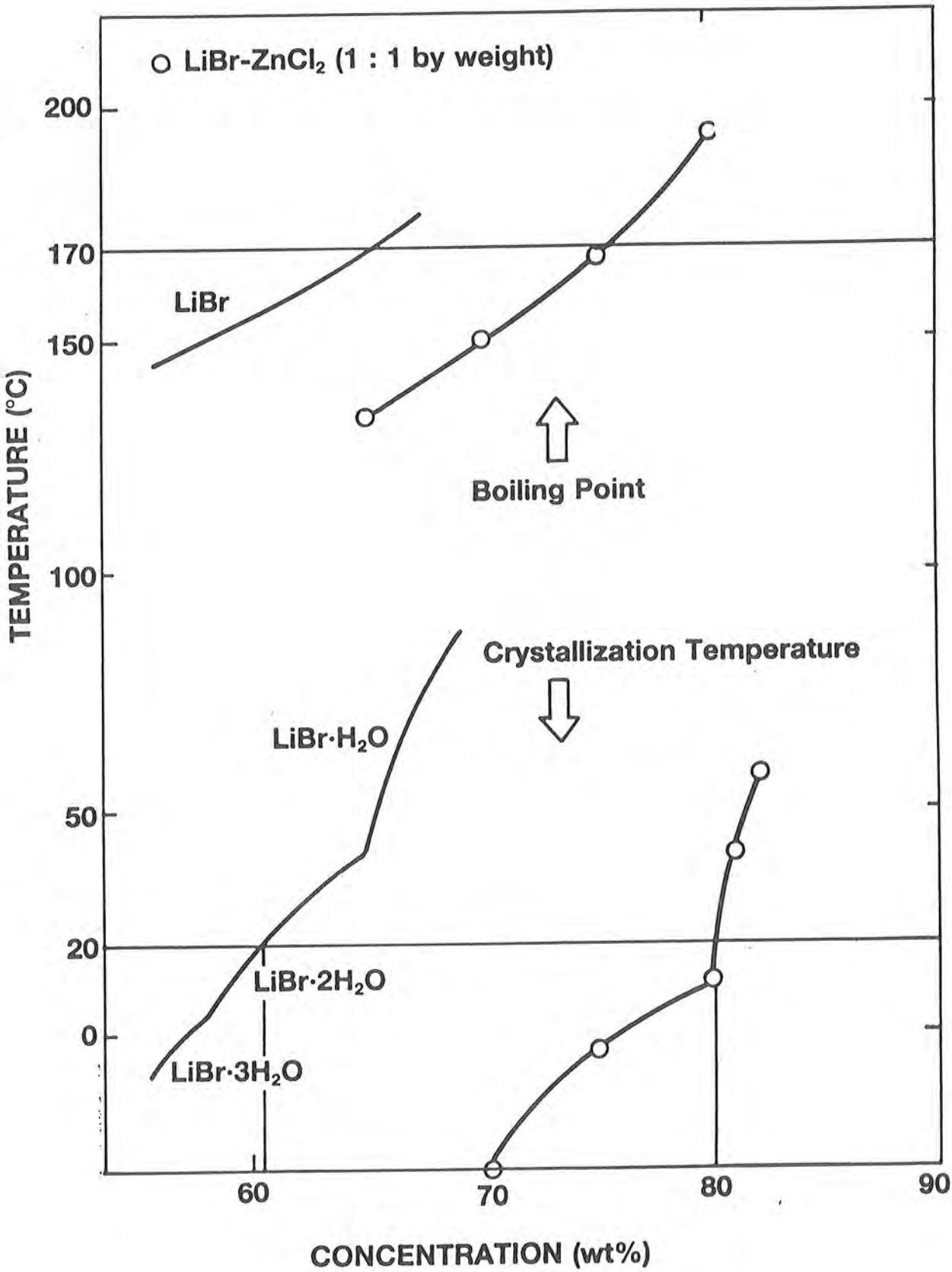

DÜHRING CURVE OF WATER-LiBr & WATER-LiBr-ZnCl AND LOWEST POSSIBLE EVAPORATOR TEMP.

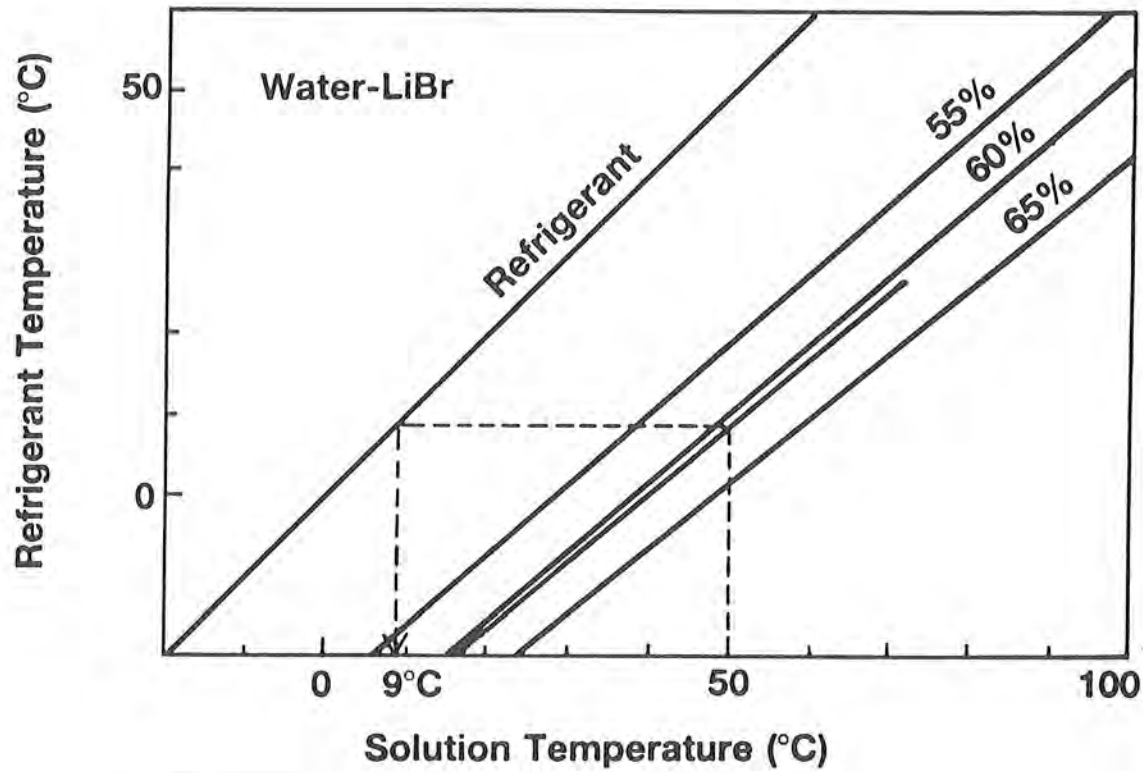

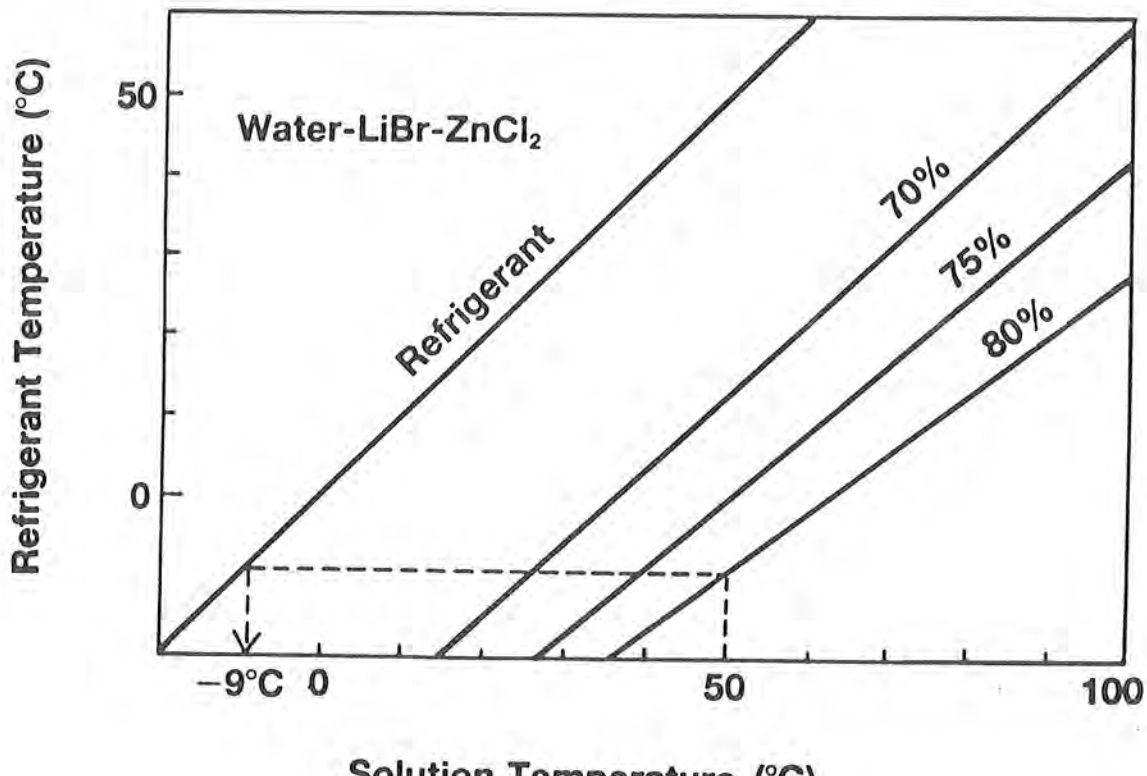

ABSORBENTS USING AMMONIA AS REFRIGERANT

ISOBARIC SOLUBILITY CURVE

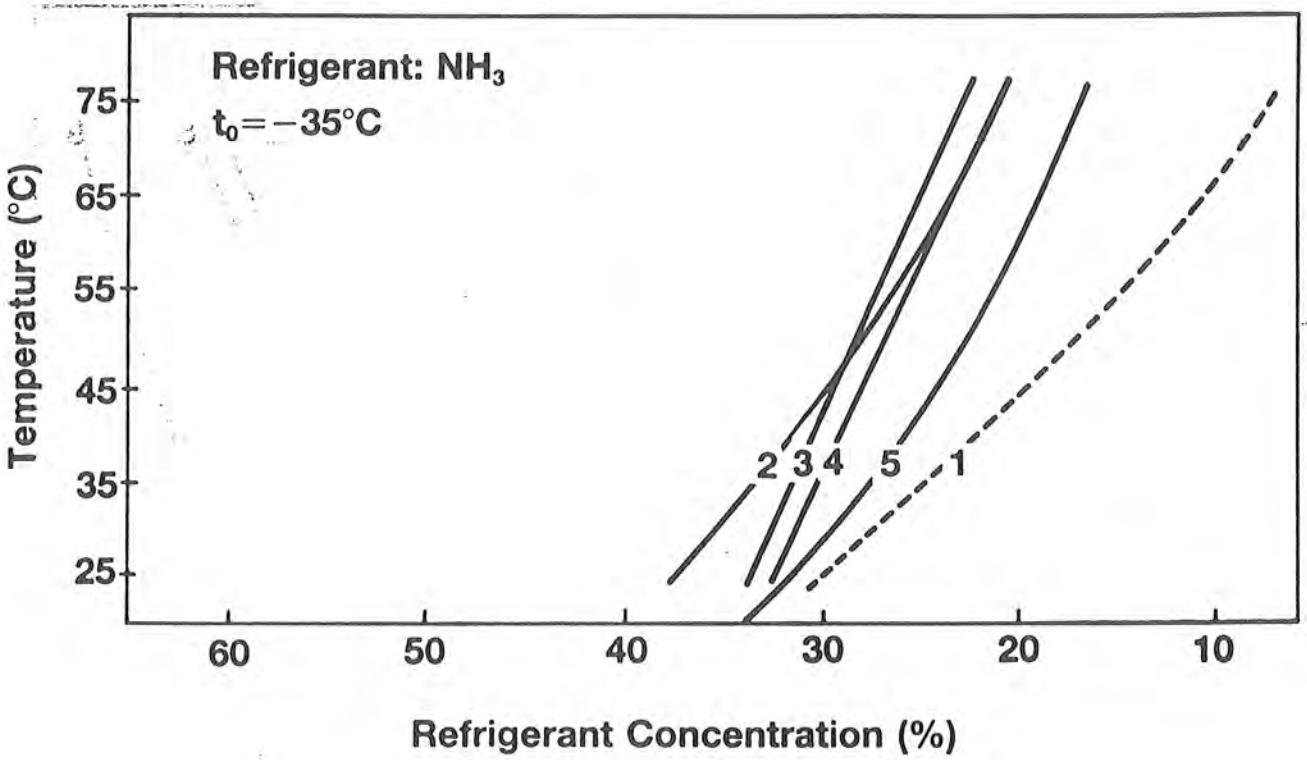

1) NH_3-H_2O
2) NH_3-$LiNO_3$/H_2O (10%)
3) NH_3-LiBr/H_2O (25%)
4) NH_3-LiBr/H_2O (29.7%)
5) NH_3-LiBr/H_2O (40%)

ABSORBENTS USING AMINES AS REFRIGERANT

ISOBARIC SOLUBILITY CURVE OF METYLAMINE

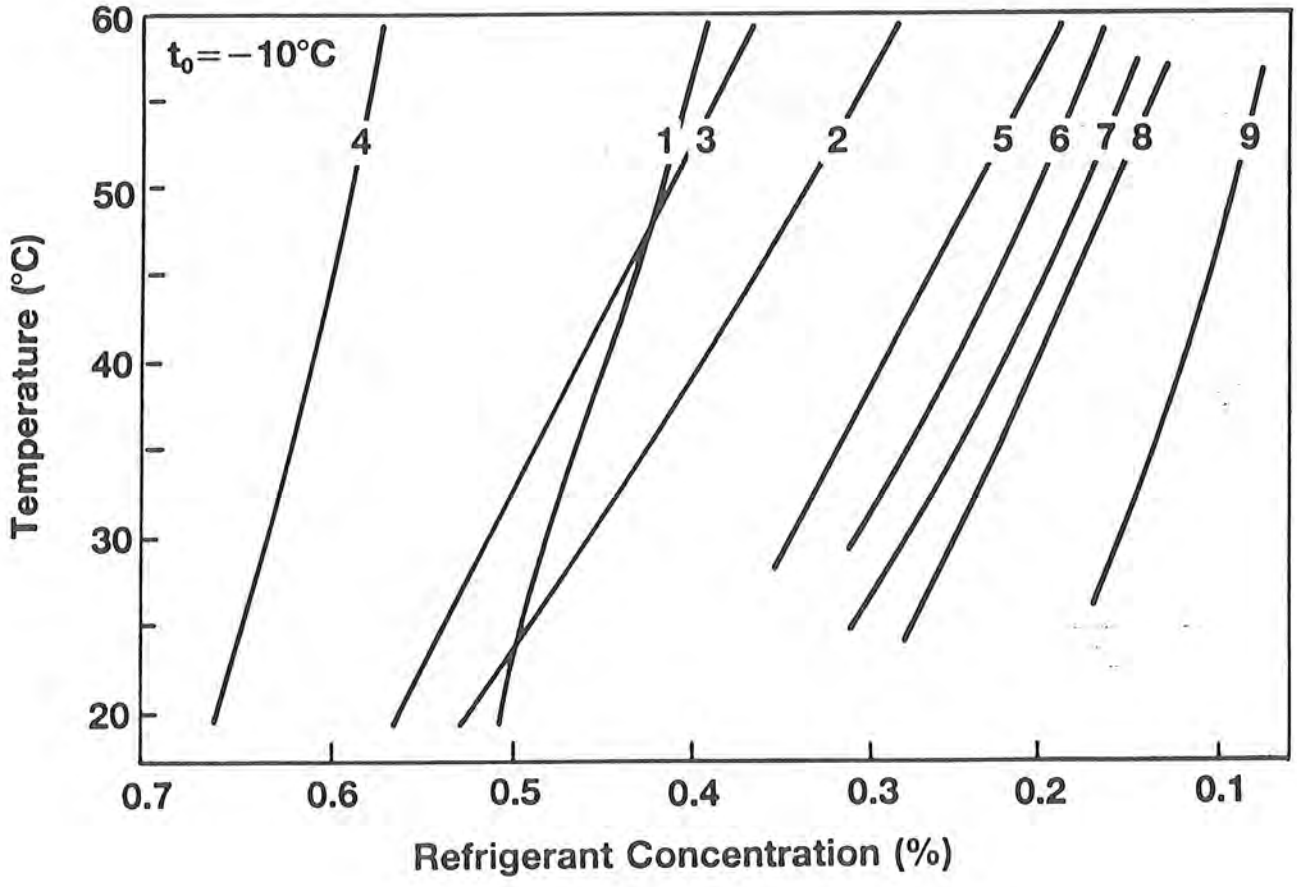

1) $LiBr/H_2O$
2) Ammonia-H_2O
3) $LiNO_3/H_2O$
4) LiSCN
5) $LiNO_3$/Glycol
6) Glycol
7) Glycerol
8) 1,4 Butandiol
9) Tetraethylenglycol

ABSORBENTS USING ALCOHOLS AS REFRIGERANT

Refrigerant	Absorbent
Methanol	LiBr $ZnBr_2$ $LiBr\text{-}ZnBr_2$ $LiI\text{-}ZnBr_2$
Ethanol	LiBr LiI
Trifluoroethanol	NMP

PROPERTIES OF MAJOR REFRIGERANTS

Refrigerant	Heat of Vaporization (KJ/Kg)	Pressure @50°C (bar)
TFE	378	0.384
Water	2256	0.123
Ammonia	1368	20.3
Methanol	1105	0.540
R22	235	19.3
R123a	174	2.05

ISOBARIC SOLUBILITY CURVE OF TFE

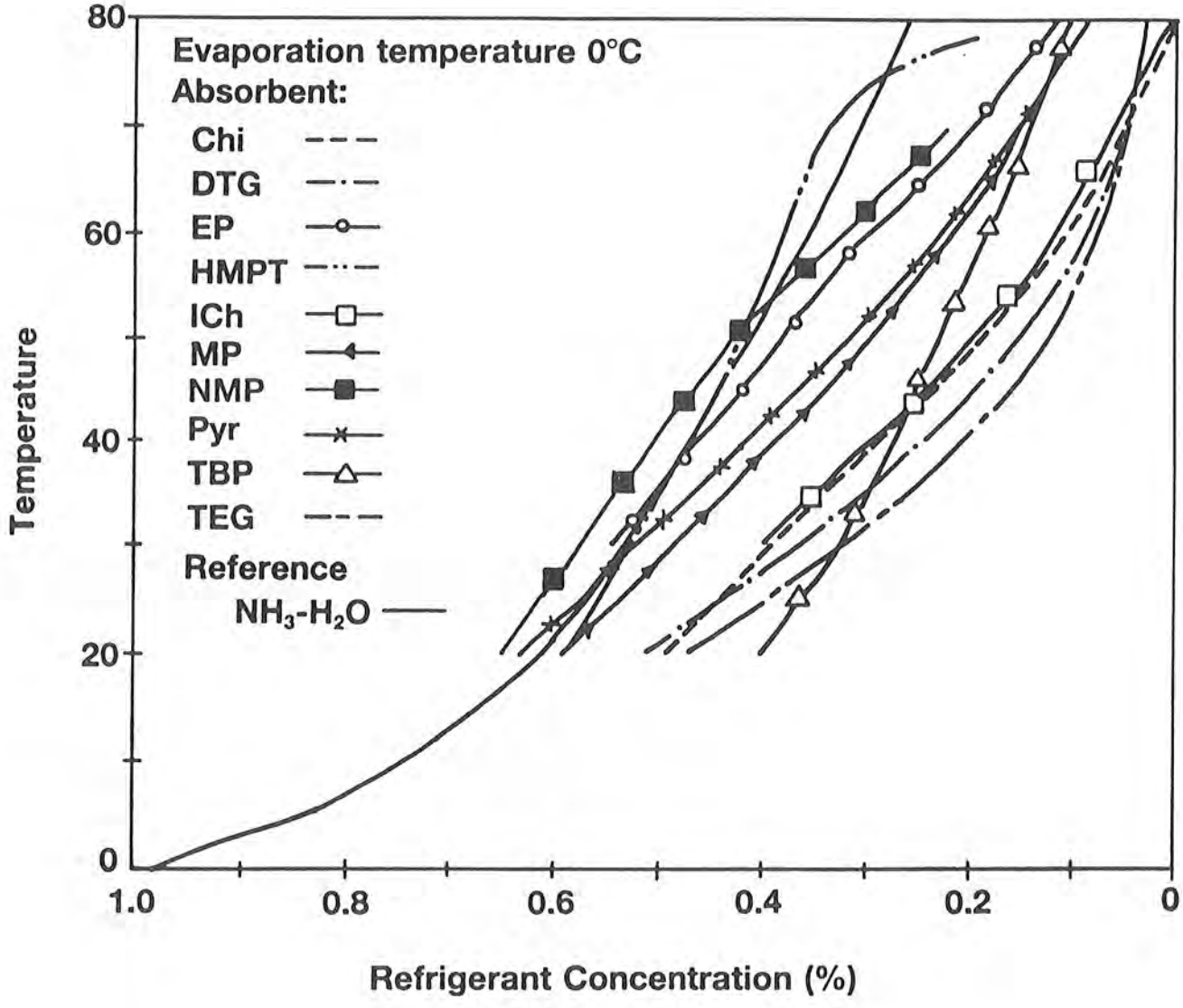

ABSORBENTS USING HALOGENATED CARBONS AS REFRIGERANT

Working Fluid	Organization	Application
R22-DMETEG (E181)	HITACHI	Residential AHP
R22-DMEDEG (E141)	MATSUSHITA	Residential AHP
R22-DMF	MATSUSHITA	Solar Refrigerator
R123a-ETFE	GRI	Residential AHP

Working Fluid	Toxicity	Rectification	Stability
R22-DMETEG (E181)	no	no	yes
R22-DMEDEG (E141)		yes	yes
R22-DMF		yes	no
R22-DMETrEG		no	yes
R123a-ETFE		yes	yes
R123a-DMETEG (E181)		no	(yes)

PROMISSING WORKING FLUIDS

Refrigerant	Absorbent	Proposer
Water	$LiBr/ZnCl_2$ (1/1 wt)	Manago et al.
NH_3	$LiBr/H_2O$ (60/40 wt)	Phillips B. A.
	NaSCN	Columbia Gas
	$LiNO_3/H_2O$ (75/25 wt)	Bokelmann et al.
CH_3NH_2	EG	— ditto —
TFE	NMP	Mashimo
		Bokelmann et al.
R22	DMEDEG (E141)	Wakamatsu et al.
	DMETrEG	Bokelmann et al.
	DMETEG (E181)	Ouchi et al.
R123a	DMETEG	Bokelmann et al.
	ETFE	Murphy et al.

5. PRACTICAL STUDIES ON ABSORBERS IN JAPAN

Naoyuki Inoue
Refrigeration Engineering Division
EBARA Corporation
Fujisawa, Japan

1. Introduction

As is well-known, an absorption refrigerator consists of many heat exchangers, such as an evaporator, an absorber, a condenser, a generator, a solution heat exchanger and so on, but its performance is well related, among other things, to the absorber characteristics. However, in the absorber, a mass transfer accompanied by heat generation takes place with the absorption of refrigerant vapor, and also heat transfer takes place with removal of the generated heat. Thus, since the phenomena are complicated, there are many analytical methods.

In this paper, some of the methods employed in Japan at the time of actual machine design or performance evaluation are introduced. Further, experimental research which has evaluated the high performance tubes is introduced in detail, since there seems to be very little research being carried out in foreign nations. In this research, a simultaneous heat and mass transfer model has been used.

2. Evaluation of absorber performance

When it is attempted to design proportionally or improve the absorption machine based on experimental data, it is usual to put together the experimental characteristics of each heat exchanger in the form of transfer coefficients, and calculate cycles based on those coefficients. As for the absorber, too, its transfer phenomena are expressed in terms of transfer coefficients. And depending on the driving forces which are used for the transfer expressions, the following models have been proposed:

A: Heat transfer model using temperature difference as the driving force[1)]
B: Mass transfer model using temperature difference as the driving force[2)]
C: Mass transfer model using pressure difference as the driving force[3)]
D: Mass transfer model using other types of driving forces[4)]
E: Simultaneous heat and mass transfer model[5)-12)]

Depending on the driving force measuring position, average driving force seeking method, etc., these models are further subclassified into more types. Some instances of definitions of driving forces are shown in Table 1.

Among them, those which are often referred to in various reports on absorption refrigerators, are heat transfer models using temperature difference as the driving force. These are described

below at some length.

3. Evaluation by heat transfer model

Let's assume an absorber as shown in Fig. 1. Fig. 2 shows an example of temperature distribution in the absorber, calculated by a simultaneous heat and mass transfer model[10]. Fig. 2a represents a case in which the absorber inlet solution temperature is high and the vapor pressure of the solution is higher than the absorber's pressure. In the absorber, solution temperature drops sharply due to vaporization of the refrigerant from the solution, and then ordinary absorption and cooling occur. Fig. 2b represents a case in which solution enters the absorber at an equilibrium temperature. Fig. 2c represents a case in which the absorber inlet solution temperature is low, so a high rate of absorption occurs at the absorber inlet. The solution temperature rises temporarily, then the solution temperature drops gradually due to ordinary absorption and cooling.

In the case of a heat transfer model using temperature difference, log-mean temperature differences based on the inlet/outlet temperatures are usually used as the driving force. That is, temperatures from the solution equilibrium temperature at the inlet to that at the outlet are approximated on the assumption that they show a logarithmic distribution (Fig. 3).

Table 1. Various driving forces for absorber evaluation

A. Heat transfer model using temperature difference

$$Q = KA\Delta T \qquad \Delta T = \frac{(T_{s1} - T_{w2}) - (T_{s2} - T_{w1})}{\ln((T_{s1} - T_{w2})/(T_{s2} - T_{w1}))}$$

- Q : Rate of heat transfer [kW]
- A : Area of absorber tube surface [m^2]
- K : Overall heat transfer coefficient [$kW/m^2{}^\circ C$]
- T_{s1} : Solution equilibrium temperature at absorber inlet [°C]
- T_{s2} : Solution equilibrium temperature at absorber outlet [°C]
- T_{w1} : Cooling water temperature at absorber inlet [°C]
- T_{w2} : Cooling water temperature at absorber outlet [°C]

B. Mass transfer model using temperature difference

$$G_R = \beta A \Delta C \qquad \Delta C = \frac{(C_{s1} - C_{w2}) - (C_{s2} - C_{w1})}{\ln((C_{s1} - C_{w2})/(C_{s2} - C_{w1}))}$$

- G_R : Rate of refrigerant mass transfer [kg/s]
- A : Area of absorber tube surface [m^2]
- β : Mass transfer coefficient [m/s]
- C_{s1} : Solution concentration at absorber inlet [$kg(H_2O)/m^3$]
- C_{s2} : Solution concentration at absorber outlet [$kg(H_2O)/m^3$]
- C_{w1} : Equilibrium concentration at absorber tube surface temperature (absorber inlet)
- C_{w2} : Equilibrium concentration at absorber tube surface temperature (absorber outlet)

Various models are derived depending on the unit of concentration and treatment of equilibrium concentration

C. Mass transfer model using pressure difference

$$G_R = KA\Delta P \qquad \Delta P = \frac{\Delta P_{s1} - \Delta P_{s2}}{\ln(\Delta P_{s1} - \Delta P_{s2})}$$

- G_R : Rate of refrigerant mass transfer [kg/s]
- A : Area of absorber tube surface [m^2]
- K : Mass transfer coefficient [$kg/(m^2 \cdot Pa \cdot s)$]
- ΔP_{s1} : Difference between refrigerant vapor pressure and solution vapor pressure at absorber inlet [Pa]
- ΔP_{s2} : Difference between refrigerant vapor pressure and solution vapor pressure at absorber outlet [Pa]

D. Mass transfer model using other types of driving force

E. Simultaneous heat and mass transfer model

$$Q = K\int_0^A (T_S - T_W)\,dA$$

$$G_R = \beta\int_0^A (C_S^* - C_S)\,dA$$

- Q : Rate of heat transfer [kW]
- G_R : Rate of refrigerant mass transfer [kg/s]
- A : Area of absorber tube surface [m^2]
- K : Overall heat transfer coefficient [$kW/m^2{}^\circ C$]
- T_S : Solution temperature [°C]
- T_W : Cooling water temperature [°C]
- β : Mass transfer coefficient [m/s]
- C_S : Solution concentration [$kg(H_2O)/m^3$]
- C_S^* : Equilibrium concentration at solution temperature [$kg(H_2O)/m^3$]

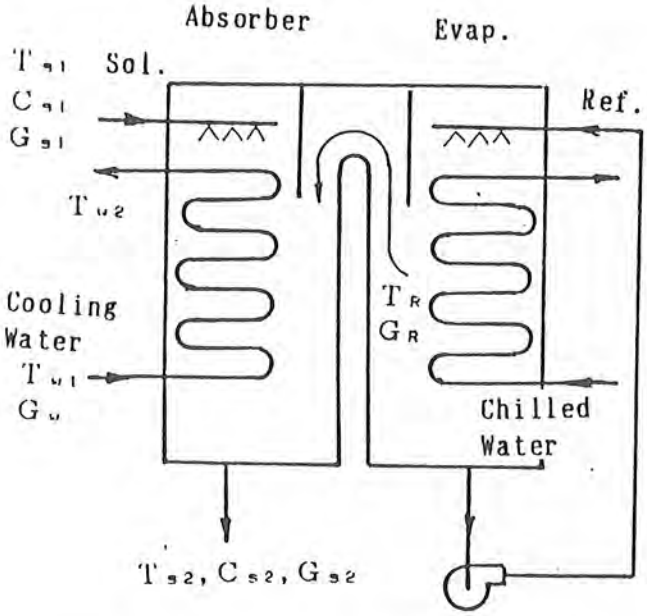

Fig. 1 Model of Absorber

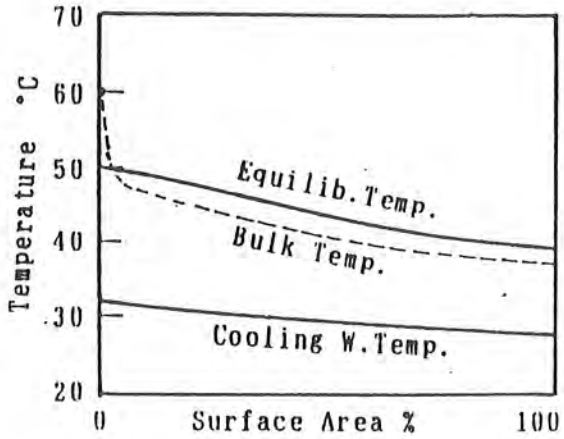

Fig. 2a

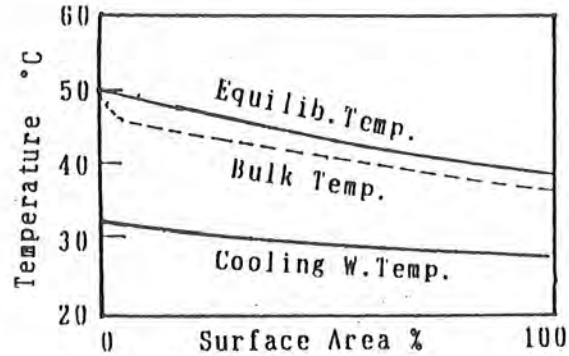

Fig. 2b

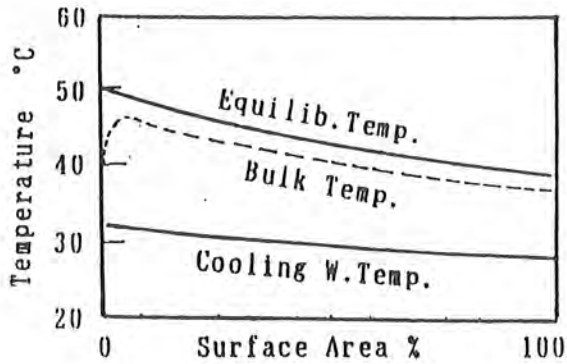

Fig. 2c

Fig. 2 Distribution of temperature

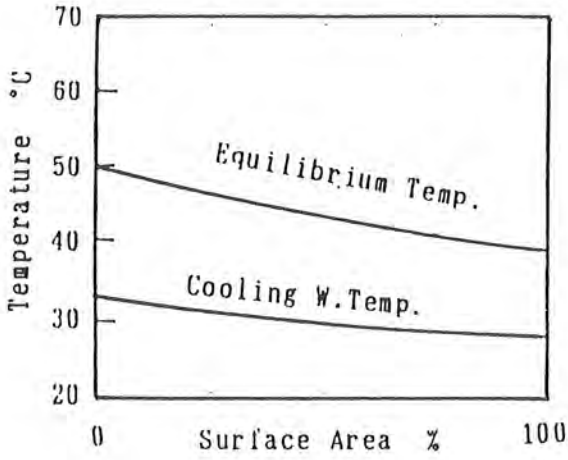

Fig. 3 Logarithmic Temp. Distribution

Table 2 Mean Temperature difference between sol. equi. and cooling W.
(A = 0.75㎡, Solution = 35g/s, Cooling water = 625g/s)

Temperature Distribution Heat Transfer Rate to Cooling Water kW			Fig.2a 10.06	Fig.2b 10.46	Fig.2c 10.84
Integrating temp. difference		℃	13.94	14.30	14.66
Assuming logarithmic temp. distribution	Inlet Equi. T. based on inlet conc.	℃	14.36	14.44	14.51
	Inlet Equi. T. based on adiabatic change	℃	14.02	14.44	14.85

$$Q = KA\Delta T$$

$$\Delta T = \frac{(T_{s1}^{*} - T_{w2}) - (T_{s2}^{*} - T_{w1})}{\ln((T_{s1}^{*} - T_{w2})/(T_{s2}^{*} - T_{w1}))}$$

Q : Rate of heat transfer [kW]
A : Area of absorber tube surface [㎡]
K : Overall heat transfer coefficient [kW/㎡℃]
T_s^{*} : Solution equilibrium temperature at the bulk concentration [℃]
T_w : Bulk temperature of cooling water [℃]
Suffix 1 : Absorber inlet
Suffix 2 : Absorber outlet

This approximation by log-mean is a method that has been employed empirically. Table 2 shows how mean temperature differences differ from the integration of a simultaneous heat and mass transfer model. When calculating the inlet equilibrium temperature, there are two cases as shown in Table 2. One case is seeking it with the inlet concentration unchanged, and other case is seeking it with adiabatic change (e.g. taking account of inlet concentration and temperature changes until reaching an equilibrium). In an ordinary absorption refrigerator, there is not a very large extent of superheating or subcooling at the absorber inlet (less than several ℃), thus showing that there is no conspicuous difference between a log-mean temperature method by a heat transfer model and an integrated mean temperature method by a simultaneous heat and mass transfer model. However, as shown in literature (10), when NTU (number of transfer unit which means a nondimensional area) is small, or when the inlet conditions of the solution deviate a great deal from the gas-liquid equilibrium, the possibility for error arises.

Incidentally, many of cycle calculation programs (simulation programs) published so far employ a heat transfer model using temperature difference as the driving force. Although the absorber

outlet temperature used in the driving force is an equilibrium temperature, the actual temperature passing from the absorber is a bulk temperature which is subcooled. That is, when calculating the cycle, the subcooling must be taken into account. However, many programs seem to have omitted or neglected this subcooling.

A heat transfer model using temperature difference inadvertently evaluates the heat and mass transfer as one transfer without separating the respective transfer speeds. Described below is a simultaneous heat and mass transfer model, evaluates them separately.

4. Simultaneous heat and mass transfer model
(temperature distribution and concentration distribution taken into account)

The overall heat transfer coefficient and mass transfer coefficient are defined as follows:

$$Q = K \int_0^A (T_s - T_w)\,dA$$

$$G_R = B \int_0^A (C_s^* - C_s^*)\,dA$$

Q : Rate of heat transfer [kW]

G_R : Rate of refrigerant mass transfer [kg/s]

A : Area of absorber tube surface [m^2]

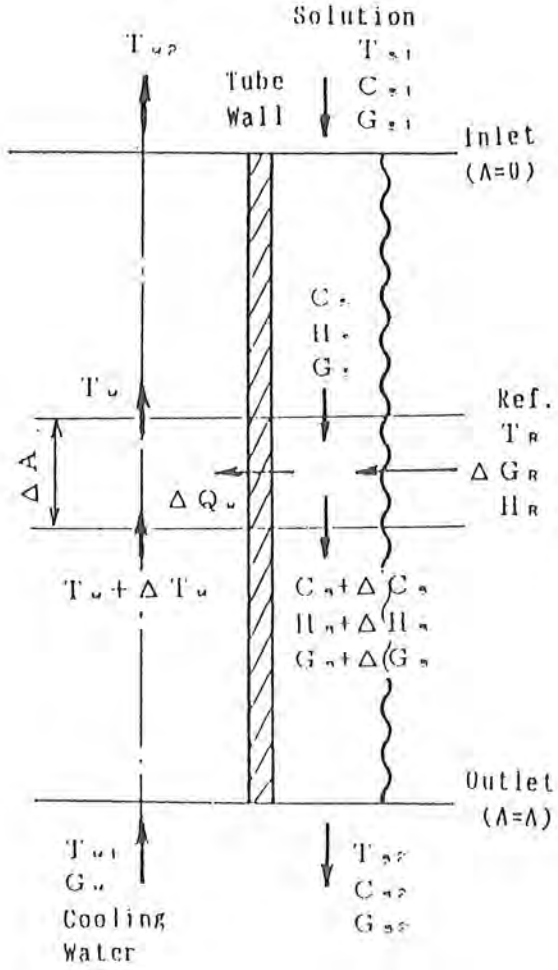

Fig. 4 Analytical model of absorber

K : Overall heat transfer coefficient [kW/m²℃]

Ts : Bulk solution temperature [℃]

Tw : Bulk cooling water temperature[℃]

β : Mass transfer coefficient [m/s]

Cs : Bulk solution concentration [kg(H_2O)/m³]

Cs *: Equilibrium concentration at bulk solution temperature [kg(H_2O)/m³]

The temperature distribution and concentration distribution are obtained by positing a model as shown in Fig. 4; and heat balance and mass balance of the solution, and also heat balance of the cooling water are considered at minutes sections.

Heat balance of solution

$$H_R \Delta G_R + G_S H_S - (C_S + \Delta G_S)(H_S + \Delta H_S) = K(T_S - T_W)\Delta A$$

Mass balance of solution (solute)

$$G_S C_S / \gamma_S + \Delta G_R = (G_S + \Delta G_S)(C_S + \Delta C_S)/\gamma_S - \Delta \gamma_S)$$

Heat balance of cooling water

$$G_W \Delta T_W = K(T_S - T_W)\Delta A$$

Mass balance of solution, refrigerant

$$\Delta G_R = \Delta G_S = \beta (C_S^* - C_S)\Delta A$$

ΔG_R : Rate of refrigerant vapor transfer [kg(H_2O)/s]

H_R : Refrigerant vapor enthalpy [kJ/kg]

H_S : Solution enthalpy [kJ/kg]

γ_S : Specific gravity of solution [kg/m^3]

G_S : Flow rate of solution [kg/s]

G_W : Flow rate of cooling water [kg/s]

The experimental K and β must be obtained by solving the equations above so that the boundary conditions below may be satisfied. The heat transfer coefficient of the solution is obtained by deducting the cooling water side heat transfer coefficient (resistance) and metal resistance from the overall heat transfer coefficient.

At the inlet (A = 0):

$$C_S = C_{S1},\ T_S = T_{S1},\ T_W = T_{W2}$$

At the outlet ($A = A_O$)

$$C_S = C_{S2},\ T_S = T_{S2},\ T_W = T_{W1}$$

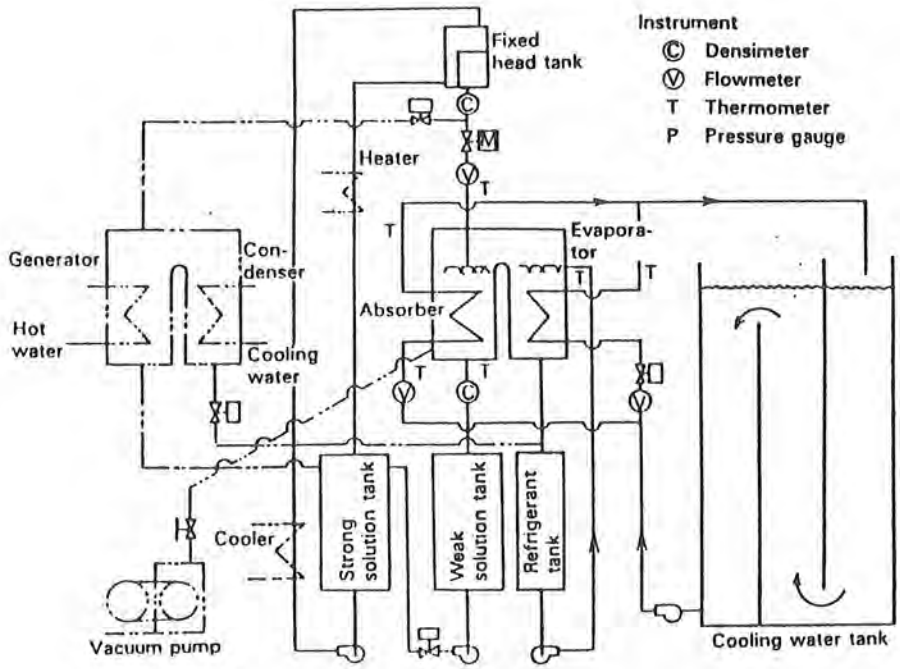

Fig. 5 Test apparatus flow sheet

5. Evaluation experiments with various heat transfer tubes

5.1 Test apparatus and test method

The test apparatus flow sheet is shown in Fig. 5. The solid lines denote units and pipings which are directly related to the measurement of the absorber performance. The two-dotted lines denote sections used when absorption solution is regenerated, etc.

In order to stabilize the operation, each test apparatus is batch-operated. Before starting the test, temperature and concentration of solution, and temperature and flow rate of cooling water must be adjusted to the test conditions. Just when the test has started, set the solution feed valve to a specified degree of opening, and feed strong solution from the constant head tank to the absorber in a state free from flow rate fluctuations. During the test, the solution getting out of the constant head tank is stored in the weak solution tank beneath the absorber. Refrigerant vapor to the absorber is supplied from the evaporator.

Saturated temperature of the evaporater refrigerant is detected so that evaporating temperature may reach the target value, and based on the temperature, the flow rate of chilled water to the evaporator is controlled, and then the quantity of refrigerant generated is adjusted. Several minutes after feeding the solution, a steady state is reached, making it possible to carry out performance measurement.

The main points of measurement are marked symbolically. The temperature of each section was measured by a thermocouple, while the flow rates of cooling water and chilled water were measured by a rotary volumetric flow meter, and the flow rate of solution was

measured by an electromagnetic flow meter. The concentration of solution was measured by an oscillating densitymeter and converted into the concentration in consideration of temperature-specific gravity relations. All of the measurements above were taken in the computer by a data logger, and based on these data, adjustive operation and steady state confirmation were carried out, followed by performance measurement, etc. Data at the time of performance measurement were employed after confirming heat balance.

The absorber itself consisted of a horizontal tube bundle, using tubes 250 mm in effective length and 19 mm in outside diameter, each in 6 rows and 8 tiers. 6 rows of spray tubes were arranged on the highest tier with spray ports provided at 20 mm pitches in the longitudinal spray direction. The solution was sprayed from the spray tubes mentioned above almost evenly over the 6 rows of tubes, dropping naturally from the upper to lower tiers. Meanwhile, the cooling water was run from the lowest tier tubes in a set of 3 tubes, through 16 passes in total. Looked at from the absorber as a whole, the solution and cooling water flow counter to each other.

Test tubes were mounted to the absorber tube sheets by means of the expanding tubes. The tube was replaced by extraction, with the next test tubes expanded again. The vacuum tightness of the test apparatus as a whole was ascertained by a mass spectrometer test on helium gas that it is less than 1×10^{-6} [cc/sec]. However, after replacing the tubes, it was ascertained by a soap test on the expanding tube sections, and also ascertained by a vacuum standing test.

5.2 Contents of experiment

5.2.1 Effect of surfactant

The experiment used water as the refrigerant, and LiBr solution as the absorption solution. Most absorption refrigerating machines use plain (bare) tubes for the absorber, and also use 2-ethyl-1-hexanol (isomer of octyl alcohol) added to an absorption solution.

In this experiment, too, a plain tube was employed to evaluate the effect of surfactant 2-ethyl-1-hexanol. The surfactant, amounting to about 250 ppm to the solution by weight fraction, was mixed into the strong solution tank. The surfactant entering the absorber amounts to about 60 to 80 ppm to the solution, which represents the quantity dissolved in the absorption solution. From the fact that liquid drops of the surfactant were not found in the solution at the absorber outlet, it may be thought that all of the surfactant was supplied in a dissolved state.

In order to cover the practical service range, the sprayed quantity was tested at a considerably small flow rate. When expressed in Reynold's number, it stood at about Re = 4 to 25. ($Re = 4\Gamma / \nu\gamma$, Γ : solution flow rate per wetted length [kg/ms]; ν : kinematic viscocity [m^2/s]; γ : specific weight [kg/m^3])

5.2.2 Effect of surface configuration

As test tubes, in addition to a plain tube, a tube featuring improved performance due to surface configuration was also used. The specifications and configurations of the representative test tubes measured at this experiment are shown in Table 3. All effects of

surface configuration were tested by using an absorption solution containing the surfactant.

Table 3 Specification of tested tube (Copper)

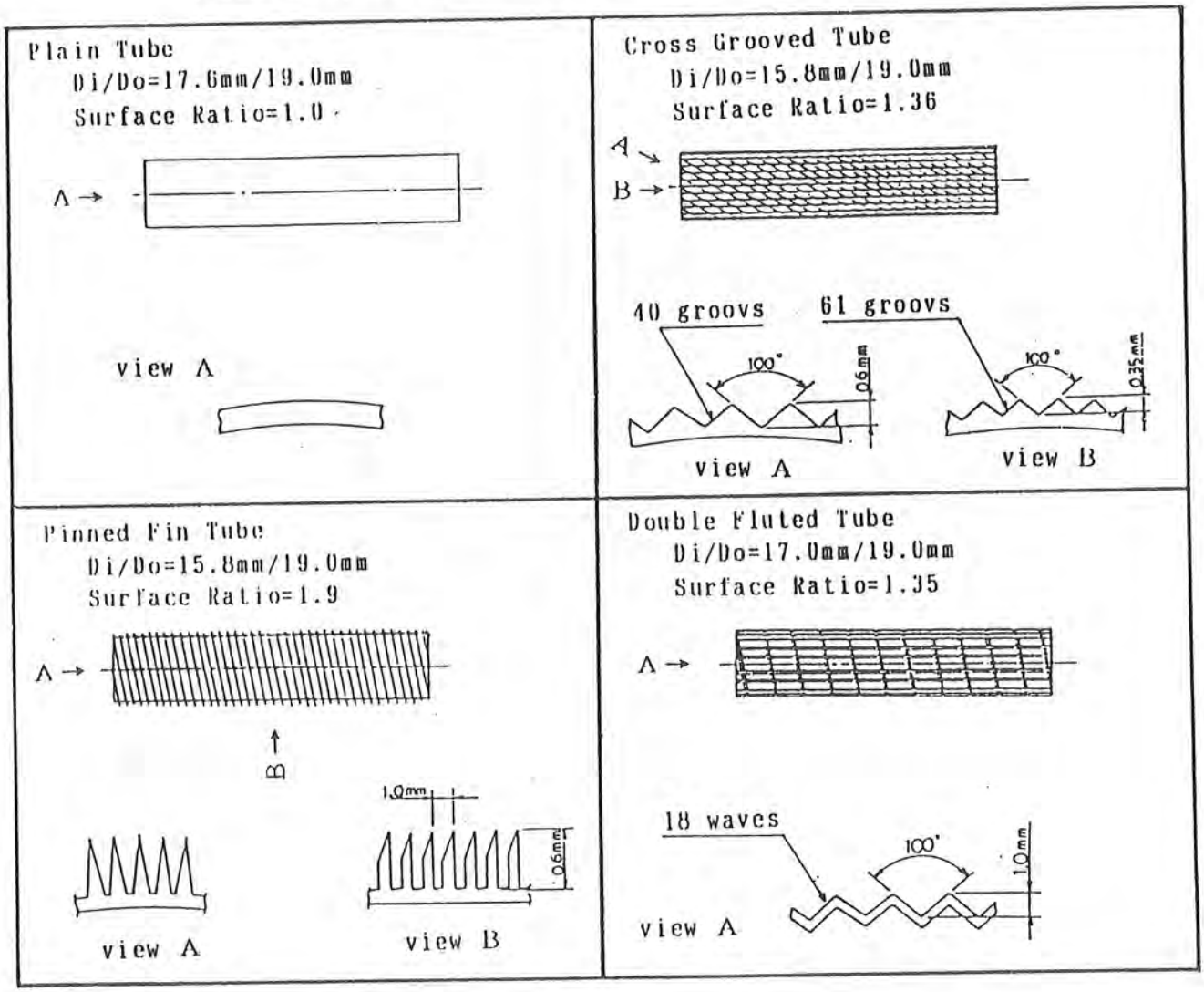

Refrigerant Saturated Temp.		T_R = 10 °C
LiBr Solution	Inlet Concentration Inlet Temperature Flow Rate	ξ_L = 60 wt(LiBr)% Ts_1 = 40 °C Gs_1 = 30～150 kg/H
Cooling Water	Inlet Temperature Flow Rate	Tw_1 = 28 °C Gw = 2250 kg/H

Table 4 Test conditions (H_2O-LiBr)

5.3 Results of experiment and consideration

5.3.1 Absorbed quantity of vapor

Shown in Fig. 6 is a comparison of an absorbed quantity of vapor. On longitudinal-axis is taken the quantity of absorbed refrigerant per tube length, and on lateral-axis is taken the quantity of solution sprayed per wetted length. The absorption performance is affected more by the addition of surfactant than by the difference in tube configuration. Although the pinned fin tube and cross grooving tube completely differ in configuration, they remain almost the same in absorption quantity.

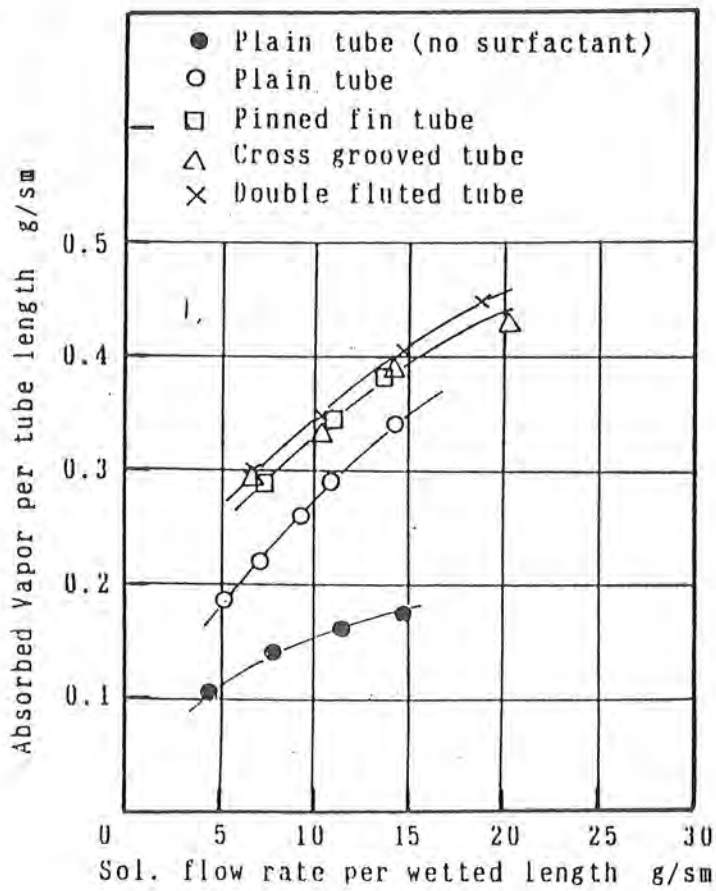

Fig. 6 Comparison of absorbed vapor

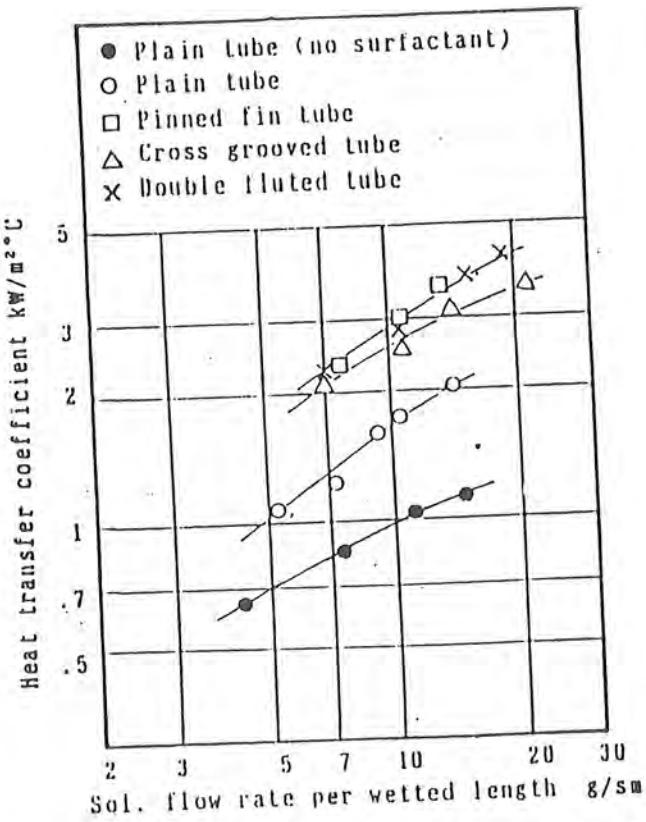

Fig. 7 Heat transfer coefficient (Plain tube reference)

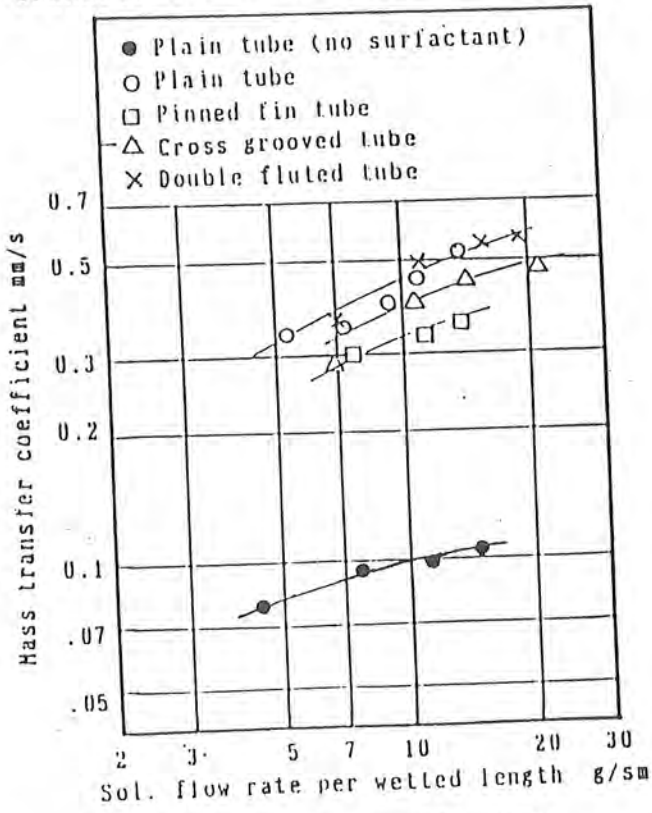

Fig. 8 Mass transfer coefficient

5.3.2 Heat and mass transfer coefficients

Heat transfer and mass transfer coefficients are shown in Fig. 7 and Fig. 8. As a reference area for transfer coefficients, the external surface area for plain tubes with the same outside diameter was employed.

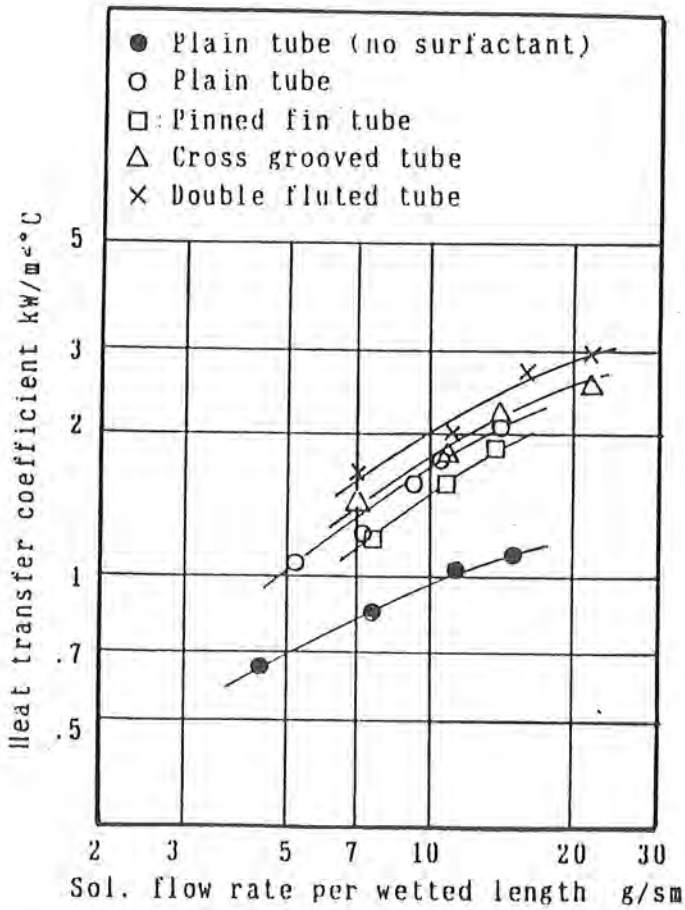

Fig. 9 Heat transfer coefficient (External surface area reference)

By the addition of surfactant, the transfer coefficients have improved conspicuously. A comparison of heat transfer coefficients by configuration shows that the pinned fin tube having a large surface area presents the largest value. Fig. 9 shows transfer coefficients based on the actual external surface area. It is seen that the increase of transfer coefficients is mainly due to the increased area.

As for mass transfer, since the vapor absorbing area hardly increases even when the external surface area is enlarged, a mass transfer coefficient increases mainly due to the effect of surfactant. As described later, the fluid state of liquid film differs with tube configurations, and this fluidity seems to govern the transfer coefficients. That is, in cases where Marangoni convection develops even into macro movement, a large value is shown.

Earlier, reference was made to the fact that, although the pinned fin tube differs completely in configuration from the cross grooving tube, they remain almost the same in absorption quantity. Let's approach it from the aspect of transfer coefficients. It may

be said that, with an increased heat transfer area, the pinned fin tube secures an improved heat transfer, and thereby lowers the solution temperature, affects the gas/liquid equilibrium concentration, increases the mass transfer driving force (concentration difference), and thereby increases the rate of mass transfer. Meanwhile, it may be said that, by utilizing Marangoni convection and also macro movement, the cross grooving tube effectively utilizes an increased heat transfer area. Fig. 10 shows an example of temperature and concentration distributions in the absorber. These data show differences in the driving force between the pinned fin tube and cross grooving tube. Though they were improved in different ways, they were completed with almost the same rate of absorption (refrigerant mass transfer). The double fluted tube was improved in similar ways to the cross grooving tube, but features higher transfer coefficients due to more active Marangoni convection and macro movement.

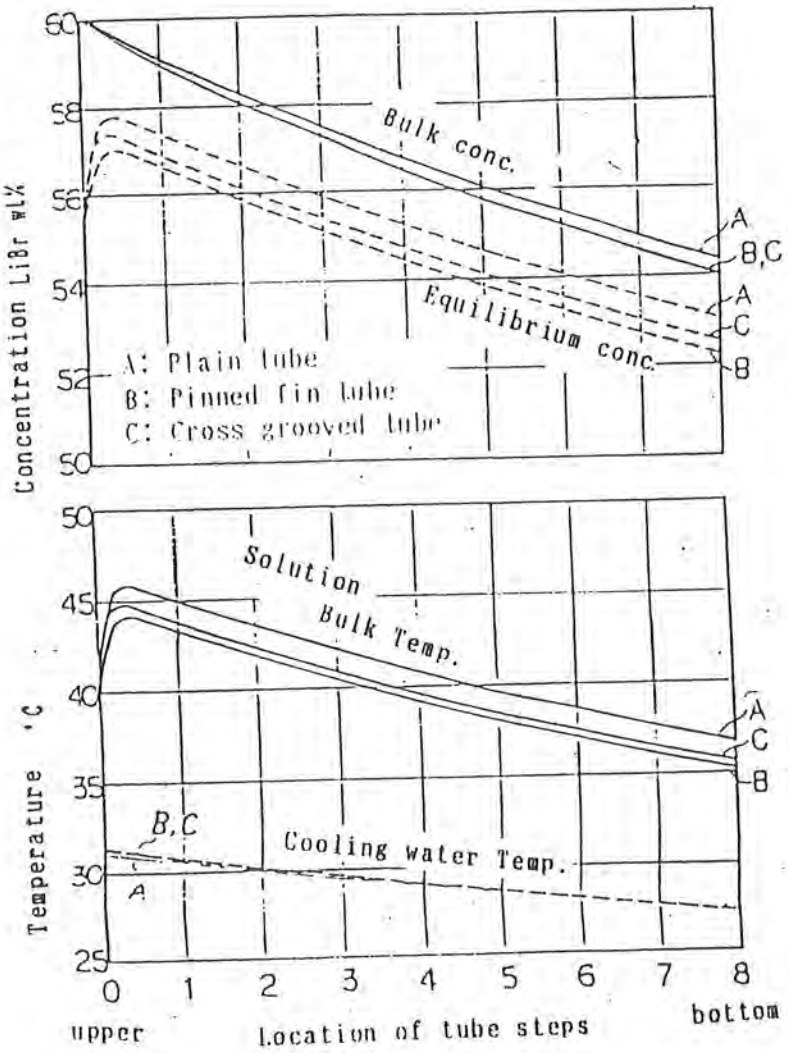

Fig. 10 Distribution of Temp. and Conc.

5.3.3 Role and effect of surfactant

The addition of surfactant led to dramatic improvements in

transfer coefficient values. This may be explained by agitation due to Marangoni convection as observed in literature (13), or by a macro movement developed from Marangoni convection as described in literature (14). In fact, depending on the tube configuration, further development is visible as more macro movement, even with the naked eye. A tube causing the macro movement has a higher rate of absorption (higher mass transfer). Fig. 11 shows simplified models of solution film fluidity, as obtained from video-taped records and expanded observations.

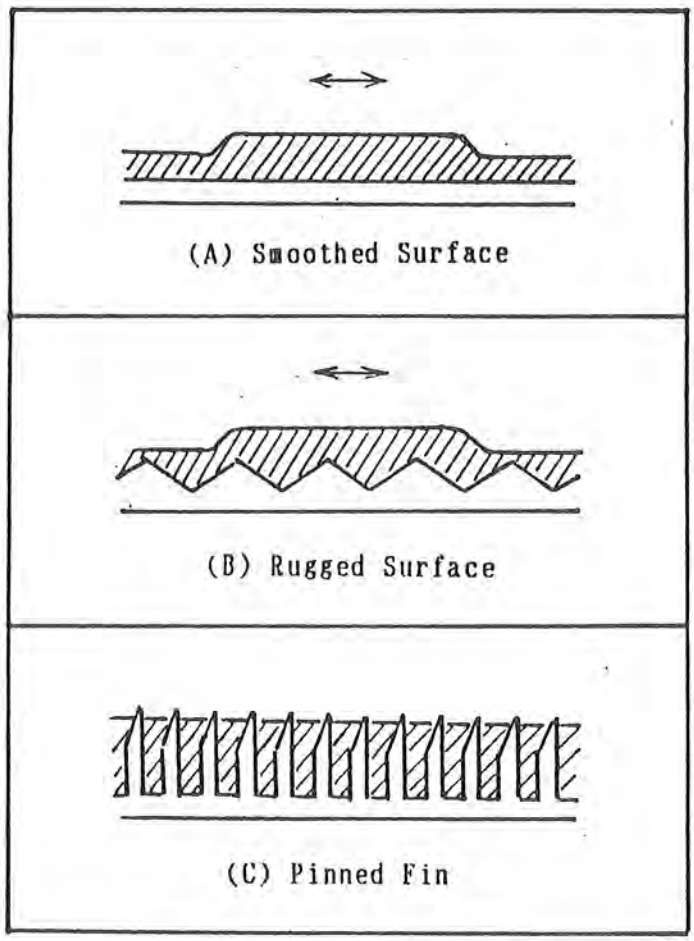

Fig. 11 Solution film state

A : In case of a plain tube which is smooth on the surface, or in the case of a double fluted tube which is smooth in the longitudinal direction, a violent motion (macro movement) of the solution film is seen. In the case of the double fluted tube, among others, a violent motion (vibration) in the tube longitudinal direction is seen.

B : In the case of a cross grooving tube, the rugged surface resists to fluidity, somewhat checking the macro movement, though the macro movement is clearly visible with the naked eye.

C : In the case of a pinned fin tube, though the solution film tries to fluidize, it is observed that the pins check the fluidity, so that the solution film does not develop into a

macro movement.

Marangoni convection is generated when a difference in surface tension occurs due to the surfactant concentration distribution over the solution film surface. The concentration distribution may be caused:

(a) by absorption of refrigerant;
(b) by relations between absorption speed of the surfactant dissolved in the solution and fluidity;
(c) by other reasons.

At present, (a) is thought to be the main cause, since a macro movement disappears when absorption rate becomes small by a noncondensable gas to be added to the absorber or by refrigerant to be put into the solution.

5.2.3 High performance heat transfer tube

Shown in Fig. 12 is an example of relations between a mass transfer coefficient and the rate of absorption, with the overall heat transfer coefficient as a parameter. The tested tube positions were shwon by dots.

From Fig. 12 it is known that, with the addition of surfactant, the mass transfer coefficient already reaches a considerably favorable level, and that, in order to produce a heat transfer tube for an absorber higher in performance, it is more effective to improve the overall heat transfer coefficient, rather than to improve the mass transfer coefficient.

Accordingly, as a possible high performance heat transfer tube, we may devise one whose outside shape does not check development from Marangoni convection to macro movement, and which may have as large a surface area as possible to provide an increased rate of heat transfer, while featuring an improved heat transfer performance inside the tube.

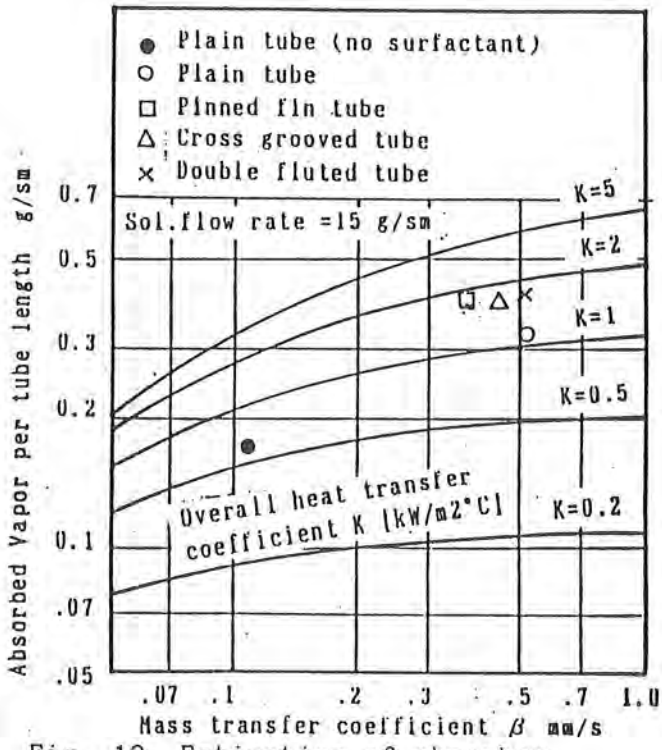

Fig. 12 Estimation of absorber

6. Conclusion

Enumerated above are some of the methods for evaluating the absorbers which have so far be published and are used currently in Japan. Among them, those using temperature difference as the driving force have been explained with examples.

Furthermore, a method for evaluation, that takes account of simultaneous heat and mass transfer, has been introduced. And, by using this method, the effect of surfactant, performance of high performance tubes, etc. were measured. From these evaluation results, it may be said that the performance of absorber heat transfer tubes is greatly affected by surfactant, and that one of the methods for improving the heat transfer tube performance is to secure as large a surface area as possible, without checking development from Marangoni convection to macro movement.

Reference (Japanese Texts)

1. K. Sekoguti et al. "Evaluating Method for Absorber's Performance in Absorption Ref. Machine" Paper for Conference of JSME (日本機械学会講演論文集) No.788-1, 124 (1978)

2. Y. Kunigi et al. "Heat Transfer Performance of Absorber Absorption Refrigerating Machine" (神戸商船大学紀要) Trans. JAR Vol.2 No.3

3. T. Ozono et al. "A Study of Absorption Refrigerator Bulletin of Kobe Mercantile Marine University Class 2, No.27, P23-30 (1979)

4. S. Takada "Absorption Refrigerating Machine" JAR P69, 70 (1982)

5. N. Inoue "Study on Absorption in an Absorption Chiller"

Paper for 7th Conference of Air Conditioning and Refrig.
(第7回空気調和・冷凍連合講演会　講演論文集) P39 (1973)

6. N. Inoue et al. "Study on Absorber for an Absorption Chiller 1st Rep." Paper for Conference of Air Conditioning and Refrig.
(空気調和・冷凍連合講演会　講演論文集) P1-4 (1986)

7. N. Inoue et al. "Study on Absorber for an Absorption Chiller 2nd Ref." Paper for Conference of Air Conditioning and Refrig.
(空気調和・衛生工学会　講演論文集) P141-144 (1986)

8. N. Inoue et al. "Study on Absorber for an Absorption Chiller 3rd Ref." Paper for Conference of Air Conditioning and Refrig.
(空気調和・冷凍連合講演会　講演論文集) P85-88 (1987)

9. K.Nakao et al. "Study on Vertical Heat Exchanger for Absorption Heat Transformer"
23th National Heat Transfer Symposium of Japan
(第23回日本伝熱シンポジウム講演論文集) P367-369 (1986)

10. N. Inoue "Performance of Absorber for Absorption Ref. Machine" 24th National Heat Transfer Symposium of Japan
(第24回日本伝熱シンポジウム講演論文集) P498-500 (1987)

11. Nagaoka et al. "Study on Heat Transfer Tube for an Absorber 1st. Rep." 24th National Heat Transfer Symposium of Japan
(第24回日本伝熱シンポジウム講演論文集) P504-506 (1987)

12. Nagaoka et al. "Study on Heat Transfer Tube for an Absorber 2nd. Rep." 24th National Heat Transfer Symposium of Japan
(第24回日本伝熱シンポジウム講演論文集) P507-509 (1987)

13. T. Kasiwagi "The Activity of Surfactant in High-Performance Absorber and Absorption Enhancement"
Refrig. Vol.60 No.687 P72-79 (1985)

14. K. Fujinawa "Turbulence Phenomena at Fluid-Fluid Interface"
J. JSME Vol.87 No.792 P74-80 (1984)

6. DEVELOPMENT OF HIGH SOLUBILITY WORKING PAIR FOR ABSORPTION MACHINE

Sankichi Takahashi, Yasuo Koseki
Hitachi Research Laboratory
Hitachi, Ltd.
Japan

1. General

In order to achieve a higher performance, more compactness and simplified system for an absorption machine, it is necessary to develop a working pair having high solubility.

Along with the steady progress of city redevelopment which is actively underway in major Japanese cities, including Tokyo, there are growing needs for such technologies.

By mixing $CaCl_2$ into LiBr, the authors have developed a working pair having high solubility and steam absorbability. By using this working pair as test sample, the authors have conducted a corrosion test for materials and a single stage absorption refrigerator (4 RT) performance test, having a bright outlook on its commercialization.

2. Development Trends of Working Pairs

Although development of various working fluids has been conducted, only H_2O/LiBr and H_2O/NH_3 have so far been commercialized. In Japan, for reasons that 1) there is legal control on working pairs, 2) because of the mild climate, demand for cooling is in the main and 3) it is necessary to facilitate development of heat pumps for cold districts, efforts have been mainly made to develop a) LiBr mixed working pairs and b) TFE working pairs. As for a), Hitachi and Osaka Gas, and as for b), Daikin and Mitsubishi Electric Corp. are, respectively, at the stage of pilot plant.

3. Effect of High Solubility

Due to the increasing solubility of working pair, the crystallization line moves to the high temperature side, so that the operation cycle can be set in the high temperature side. As a consequence, the concentration of working pair and absorption temperature (steam absorbability) in the abosrber increase. Since this increases the temperature difference from the cooling temperature, it makes more compact machine design and air cooling possible. When applied to a heat pump, higher temperature heat can be recovered from the heat source having the same temperature.

4. New Mechanism of Solubility Increase

As shown in Fig. 1, in the strong aqueous solution, such as LiBr solution, much water molecules are hydrated around ions. As a result, the steam vapor pressure drops below a level evaluated by Raoult's Law,

and the steam absorbability increases. However, since free water molecules decrease, the solubility drops.

Therefore, in order to increase the solubility without causing the steam absorbability to drop, it is necessary to add hetero (+) ion (Ca^{2+}), large in hydration number, to weaken the hydrating power of Li ion, and thereby cause water molecules common to both ions (Li^{+}, Ca^{2+}) (co-hydration model), so that free water molecules may increase in the aqueous solution.

The validity of this model has been ascertained by measuring the compressibility (volumetric shrinkage effect due to co-hydration) of aqueous solution.

5. Measurement of Solubility

Usually, the solid-liquid equilibrium method is used to measure the solubility. However, since the mixing (constituent) ratio changes between the solid and liquid phases in the case of mixed solution, the crystalization temperature method was employed. After heating the sample, which has been adjusted to a specified concentration and mixing ratio, to 60°C, it was cooled down at a constant speed and the crystalization temperature was measured from temperature changes at the time of crystalization (heat generation).

The steam vapor pressure characteristics were measured by the gas-liquid equilibrium (evaporation, condensation) method.

6. Properties of Working Pair

Fig. 2 shows the relations between the $LiBr/CaCl_2$ mixing ratio and solubility. The solubility becomes highest when the mixing ratio is 0.33. The solid line denotes theoretical calculation values based on the co-hydration model, coinciding well with the experimental results.

The steam characteristics of this working pair are almost similar to those of LiBr, having a high steam absorbability like LiBr.

7. Corrosion Tests

When $CaCl_2$ is added to the working pair developed, it presents acidity. Since corrosiveness stronger than that of LiBr is expected, test pieces and elementary part models were subjected to careful corrosion tests. As a result, an organic inhibitor effective to prevention of corrosion has been discovered and a basis for commercialization of this working pair has been established.

8. Performance of 4 RT Pilot Refrigerator

Fig. 3 shows the results of performance tests on the working pair whose mixing ratio is 0.33. Since the pilot refrigerator can be used even when the concentration is higher than 65%, it can generate low 7°C even when the cooling temperature is about 45°C.

9. Application to Heat Storage

The working pair developed can be used at various mixing ratios. The authors are using the working fluid whose mixing ratio is 0.67, for

heat storage by concentration difference. In this case, due to the mixture of $CaCl_2$, the working pair cost is characteristically is low.

10. Summary

By adding a salt solution containing a hetero (+) ion large in hydration number to LiBr solution, a co-hydrated state of water molecules has been formed, leading to an increased solubility of working pair. As a result, the authors have obtained a bright outlook on commercialization of an air-cooled absorption refrigerator and increases in output heat temperature from heat pumps.

11. Literature

Omitted.

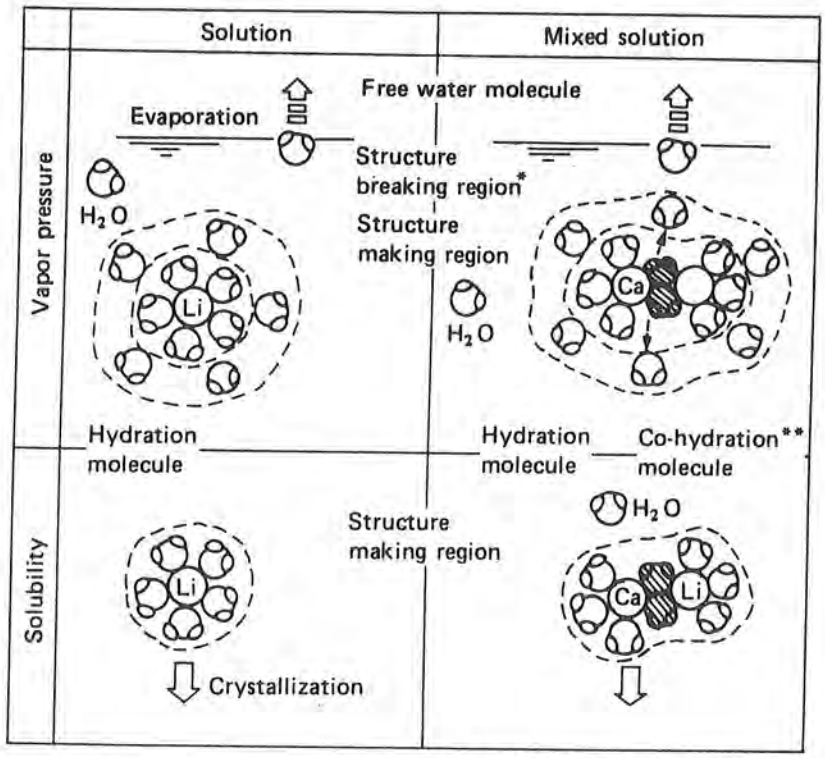

Fig. 1 New mechanism of solubility increasing with "co-hydration model"

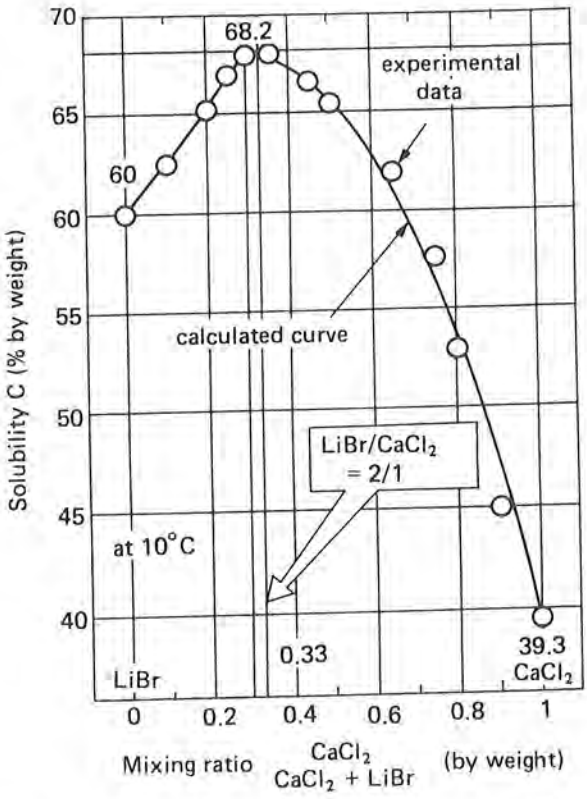

Fig. 2 Solubility vs. mixing ratio

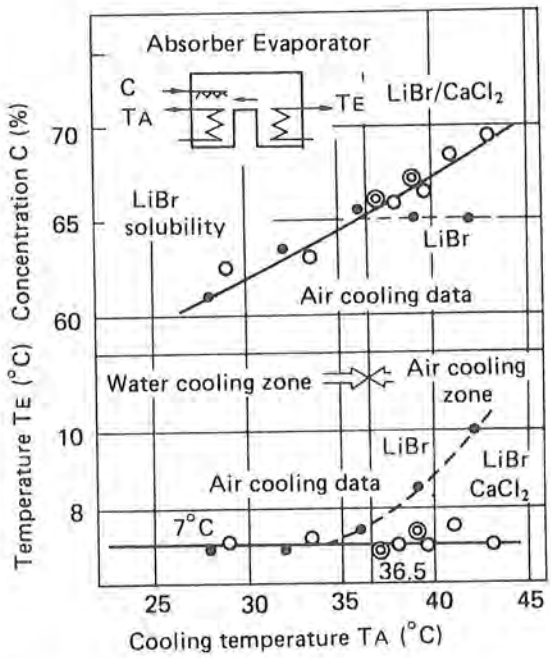

Fig. 3 Performance of absorption refrigerator using $LiBr/CaCl_2$

7. STUDIES ON CYCLES OF ADVANCED ABSORPTION HEAT PUMP SYSTEMS

Yoshikazu Nagaoka Kikutaro Fujikura
Noriyuki Nishiyama Masahiro Oka
Research & Development Institute
Tokyo Gas Co., Ltd.
Tokyo, Japan

1. Introduction

At the previous workshop we reported the first step of cycle evaluation. This method is such that, by referring to Grossmanx's literature, 72 cycles surveyed were classified by system type, cycle type, temperature level, pressure level and concentration level, and evaluated in terms of five evaluation items.

Table 1. Evaluation coefficients

Coefficient	Definition
NM	(Number of main components) Number of component evaporator, condenser, absorber and generator
NA	(Number of auxiliary components) Number of component solution heat exchanger and pump
COP	(Coefficient of performance) Theoretical COP in the cooling/heating modes $COP_c = \Sigma Q_E / \Sigma Q_G$ $COP_h = \Sigma (Q_A + Q_C) / \Sigma Q_G$
TSC	(Transfer surface coefficient) Ratio of heat quantity effectively utilized for cooling/heating, to total quantity of heat utilized $TSC_c = \Sigma Q_E / \Sigma Q$ $TSC_h = \Sigma (Q_A + Q_C) / \Sigma Q$
TF	(Temperature factor) Indicator of the heating temperature $TF = (T_3 - T_2)/(T_2 - T_1)$

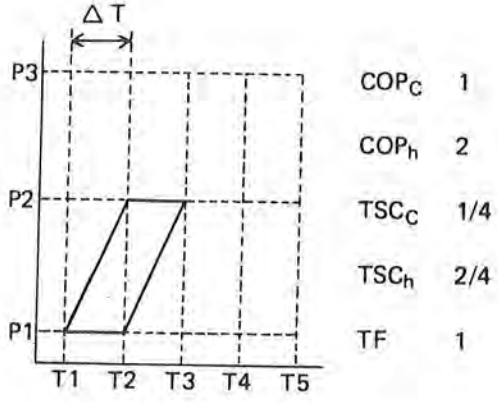

(1) No. 1

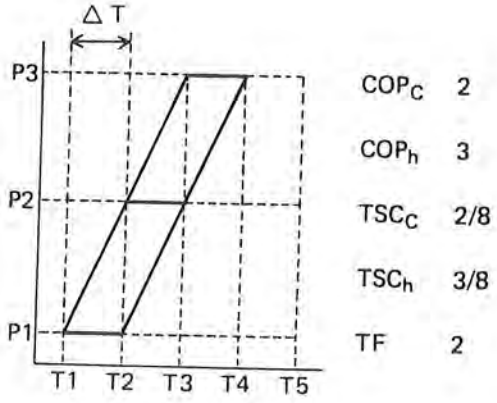

(2) No. 2

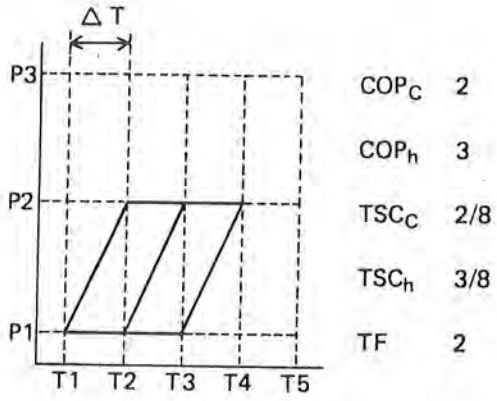

(3) No. 3

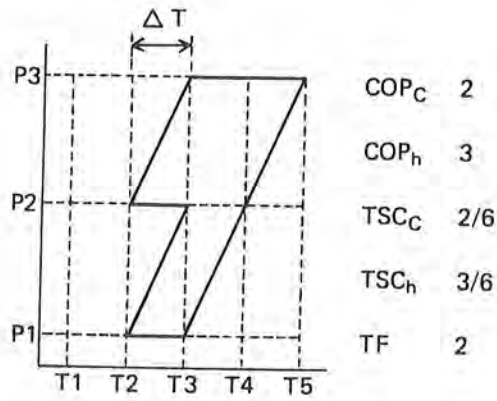

(4) No. 4

Fig. 1 Best cycles based on the primary evaluation

At the current workshop, we report the results of the second step of cycle evaluation carried out on 4 cycles selected as a result of the first step of evaluation by applying Dühring diagram for working fluids to examine the cycle working range if those cycles can be realized, and part of the third step of evaluation for calculating the COP of cycles.

2. First Step of Cycle Evaluation

2.1 Evaluation method and results of evaluation

The cycles were carried out in terms of evaluation items shown in Table 1, and the best 4 cycles, shown in Fig. 1, were selected.

2.2 Problems

(1) There are cycles hard to classify/evaluate.
(2) There is no concept of evaluation width, since the concentration is expressed by a straight line.

2.3 Cycles hard to classify/evaluate

(1) Cycles as a combination of absorption type and compression type.
(2) Cycles, such as GAX, that have heat exchangers.
(3) Heat pump transformers.
(4) Cycles having more than 2 types of chilled/hot water temperature level.

3. Second Step of Cycle Evaluation

3.1 Evaluation method

By applying Dühring diagram for working fluids to the 4 cycles, examine the cycle working range (temperature, pressure, concentration). In this case, the concentration width of absorbent is assumed to be 0.

3.2 Temperature conditions

Table 2. Temperature conditions

Operation	Evaluation temperature of refrigerant T_e	Condensation temperature of refrigerant T_c
Cooling	5 ℃	35 ℃
Heating	− 5 ℃	50 ℃

3.3 Types of working fluids to be examined

Working fluids to be examined are shown in Table 3. 1 to 3 types of working fluids have been selected for each of the four representative refrigerant groups.

Table 3. Working fluids

Type of refrigerant	Working fluids
Water group	① Water + LiBr
Ammonia group	② Ammonia + water ③ Ammonia + $LiNO_3$/water ④ Methylamine + etylene glycol
Alcohol group	⑤ Methanol + LiBr ⑥ Methanol + LiBr/water ⑦ TFE + NMP
CFC group	⑧ R22 + DTrG ⑨ R123a + DTG

3.4 Evaluation results

The evaluation results are shown in Table 4.

In the table, ○ denotes that commercial operation of cycle is possible, △ denotes that commercial operation is difficult to realize commercial operation, since max. temperature is over 160℃, or max. pressure is over 20 kg/cm², and × denotes that operation is impossible.

Table 4. Results of second step of cycle evaluation

Type of cycle			No. 1		No. 2		No. 3		No. 4	
Operation mode			Cooling	Heating	Cooling	Heating	Cooling	Heating	Cooling	Heating
Working fluids	Water	Water + LiBr	○	×	○	×	×	×	×	×
	Ammonia	Ammonia + water	○	○	○	△	○	△	○	△
		Ammonia + $LiNO_3$/water	○	○	○	△	○	△	○	△
		Metylamine + EG	○	○	○	△	○	△	○	△
	Alcohol	Methanol + LiBr	○	×	○	△	△	×	×	×
		Methanol + LiBr/water	○	△	○	△	△	×	△	×
		TFE + NMP	○	○	○	△	○	×	○	×
	Flon	R22 + DTrG	○	○	△	△	○	△	○	△
		R123a + DTG	○	○	○	△	○	△	○	△

3.5 Problems

(1) Treatment of concentration width remains yet be determined.

(2) The evaluation method for cycles, such as GAX, whose heat exchange is performed internally, remains yet to be determined.

(3) Only single-effect cycles are capable of heat pump operation in the heating mode, and it is difficult to exceed the target value with the same cycle in the cooling and heating modes. Thus, it is necessary to devise a new cycle for heating and also examine the possibility of change-over between cooling and heating modes.

4. Third Step of Cycle Evaluation

4.1 Evaluation method

COP of cycles, which were found operable by the second step of evaluation, is calculated under the third step of evaluation, and the values obtained are compared with the target values.

(1) Take account of the concentration width.

(2) Evaluate such cycles as GAX that exchange heat internally.

(3) As a heat pump cycle in the heating mode to be evaluated, newly include a two-cascade cycle that is a combination of 2 single-effect cycles and uses 2 types of working fluids. As a cycle in the cooling mode to be evaluated, also include a triple-effect two-cascade refrigeratrion cycle.
(4) The cycle's COP shall be over 1.2 in both the cooling and heating modes. The temperature conditions at this time shall be same as in Table 2.

4.2 Definition of single-effect cycle's COP

The assumption when obtaining the COP is shown below.

(1) A refrigerant heat exchanger shall be neglected.
(2) The temperature efficiency of heat exchangers shall be assumed to be 100%.

The cooling COP η_C and the heating COP η_H are defined by the following equations.

$$\eta_C = Q_E / Q_G \quad (1)$$

$$\eta_H = (Q_A + Q_C) / Q_G = 1 + \eta_C \quad (2)$$

$$Q_E = G_R (H_{R1} - H_{RL5}) \quad (3)$$

where Q_E : Heat quantity of evaporator
Q_G : Heat quantity of generator
Q_A : Heat quantity of absorber
Q_C : Heat quantity of condenser
G_R : Mass flow rate of refrigerant
H_{R1} : Gas phase enthalpy of refrigerant in evaporator
H_{RL5} : Liquid phase enthalpy of refrigerant in condenser

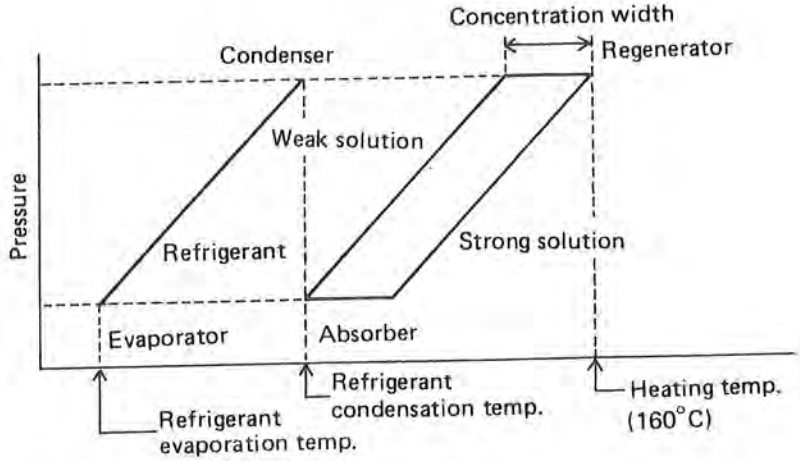

Fig. 2 Definition of concentration

4.3 How to seek the concentration for single-effect cycle (see Fig. 2)

(1) The concentration of strong solution shall be either smaller of concentration at 160℃ of heating temperature or concentration of crystallization.
(2) The concentration of weak solution shall be concentration equilibratory with evaporator/absorber temperatures.

4.4 How to seek COP single-effect cycle

Since the quantity of heat exchanged internally differs according to the concentration width, the quantity of heat recovered by the heat exchanger Q_{EX}, the quantity of heat applied with the regenerator Q_G and the quantity of heat discharged by the absorber have been examined in three cases.

4.4.1 Case of small concentatin width (see Fig. 3)

For heat exchange in the cycle, only the solution heat exchanger is considered.

- Heat quantity exchanged by solution heat exchanger Q_{EX1}

$$Q_{EX1} = G_{S2}(H_{S4} - H_{S5}) = G_{S1}(H_{S7} - H_{S6}) \quad (4)$$

where G_{S1} : Dilute solution mass flow rate
G_{S2} : Conc. solution mass flow rate
H_{S4} : Enthalpy of absorbent at the point ④

- Heat quantity of the generator Q_G

$$Q_G = G_R (H_{R3} + H_{R4})/2 + G_{S2} H_{S4} - G_{S1} H_{S7} \quad (5)$$

- Heat quantity of absorber Q_A

$$Q_A = G_R H_R 1 + G_{S2} H_{S5} - G_{S1} H_{S6} \quad (6)$$

$$G_R = G_{S1} - G_{S2} \quad (7)$$

where G_R : Total mass flow rate of refrigerant vapor
H_{R3} : Enthalpy of refrigerant vapor at the point ③

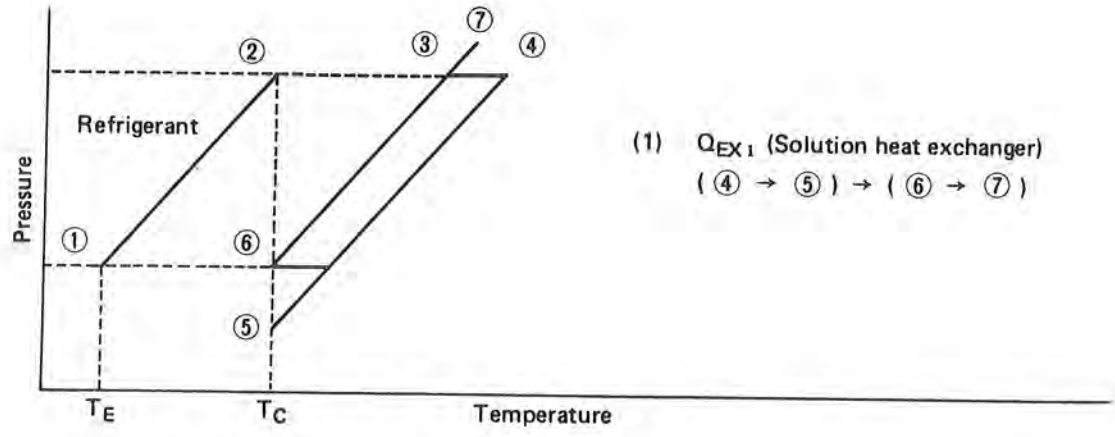

Fig. 3 Dühring diagram

4.4.2 Case of middle concentration width (see Fig. 4)

For heat exchange in the cycle, AX (heat exchange between absorber and weak solution), GX (heat exchange between generator and strong solution), and liquid heat exchanger are considiered.

- Heat quantity exchanged by solution heat exchanger Q_{EX1}

$$Q_{EX1} = G_{S2}(H_{S8} - H_{S5}) = G_{S1}(H_{S11} - H_{S7}) \quad (8)$$

- Heat quantity exchanged by AX (heat exchange between absorber and weak solution) Q_{EX2}

$$Q_{EX2} = G_{S1}(H_{S7} - H_{S6})$$

$$= G_{R2} H_{R1} + G_{S2} H_{S5} - (G_{S2} + G_{R2}) H_{S9} \quad (9)$$

- Heat quantity exchanged by GX (heat exchange between generator and strong solution) Q_{EX3}

$$Q_{EX3} = G_{S2}(H_{S4} - H_{S8})$$
$$= G_{R3}(H_{R3} + H_{R10})/2 + (G_{S1} - G_{R3}) H_{S10} - G_{S1} H_{S11} \quad (10)$$

where G_{R2} = Mass flow rate of refrigerant in absorber whose heat is exchanged by AX

G_{R3} = Mass flow rate of refrigerant in generator whose heat is exchanged by GX

- Heat quantity of generator Q_G

$$Q_G = (G_R - G_{R3})(H_{R10} + H_{R4})/2 + G_{S2} H_{S4} - (G_{S1} - G_{R3}) H_{S10} \quad (11)$$

- Heat quantity absorbed by absorber Q_A

$$Q_A = (G_R - G_{R2}) H_{R1} + (G_{S2} + G_{R2}) H_{S9} - G_{S1} H_{S6} \quad (12)$$

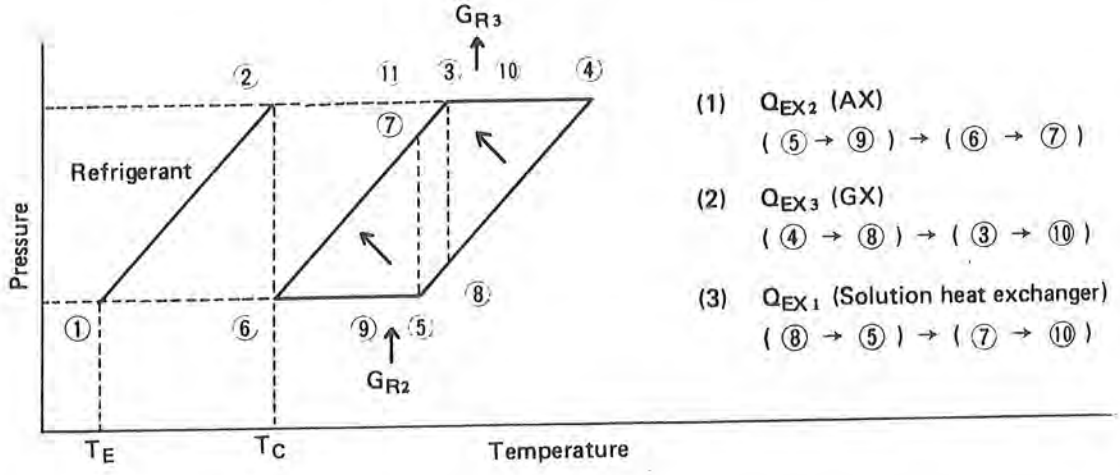

Fig. 4 Dühring diagram

4.4.3 Case of large concentration width (see Fig. 5)

For heat exchange in the cycle, GAX (heat exchange between generator and absorber) are considered.

- Heat quantity exchanged by AX Q_{EX2}

$$Q_{EX2} = G_{S1}(H_{S3} - H_{S6})$$
$$= G_{R2} H_{R1} + (G_{S2} + G_{R4}) H_{S8} - (G_{S2} + G_{R2} + G_{R4}) H_{S9} \quad (13)$$

- Heat quantity exchanged by GX Q_{EX3}

$$Q_{EX3} = G_{S2}(H_{S4} - H_{S5})$$
$$= G_{R3}(H_{R7} + H_{R10})/2 + (G_{S1} - G_{R3} - G_{R5}) H_{S10} \quad (14)$$

- Heat quantity exchanged by GAX (heat exchange between generator and absorber) Q_{EX4}

$$Q_{EX4} = G_{R4} H_{R1} + G_{S2} H_{S5} - (G_{S2} + G_{R4}) H_{S8}$$
$$= G_{R5}(H_{R3} + H_{R7})/2 + (G_{S1} - G_{R5}) H_{S7} - G_{S1} H_{S3} \quad (15)$$

where G_{R4} = Mass flow rate of refrigerant in absorber whose heat is exchanged by GAX

G_{R5} = Mass flow rate of refrigerant in regenerator whose heat is exchanged by GAX

- Heat quantity of regenerator Q_G

$$Q_G = (G_R - G_{R3} - G_{R5})(H_{R10} + H_{R4})/2 + G_{S2} H_{S4} \quad (16)$$

- Heat quantity of absorber Q_A

$$Q_A = (G_R - G_{R2} - G_{R4})H_{R1} + (G_{S2} + G_{R2} + G_{R4})H_{S9} - G_{S1} H_{S6} \quad (17)$$

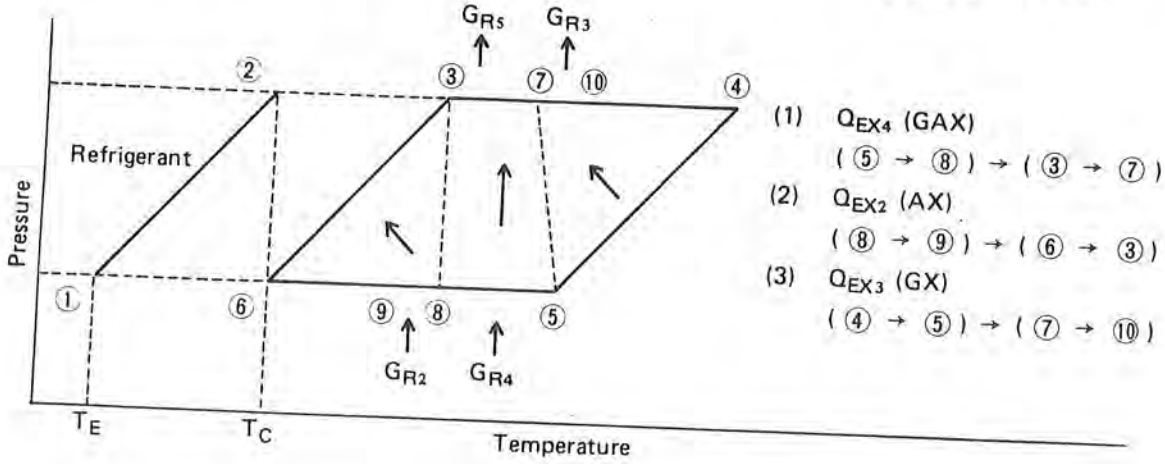

Fig. 5 Dühring diagram

4.5 How to seek COP of combined single-effect cycles

In the preceding section, we described the procedures for calculating COP of single-effect cycles. In this section, the procedures for calculating COP of combined single-effect cycles. The overall cycle COP is expressed by a function of COP of each single-effect cycle.

4.5.1 Two-cascade heat pump cycle (see Fig. 6)

This cycle is used for heating. Assuming that the cooling COP and heating COP in the high temperature side are η_{C1} and η_{H1}, and the cooling COP and heating COP in the low temperature side are η_{C2} and η_{H2}, the overall cycle efficiency in the heating mode is given by the equation (22).

$$Q_{G1} + Q_{E1} = Q_{A1} + Q_{C1}, \quad Q_{G2} + Q_{E2} = Q_{A2} + Q_{C2} \quad (18)$$

$$Q_{E1} = Q_{A2} + Q_{C2} = Q_{G2} + Q_{E2} \quad (19)$$

$$\eta_{C1} = Q_{E1}/Q_{G1}, \quad \eta_{H1} = 1 + \eta_{C1} \quad (20)$$

$$\eta_{C2} = Q_{E2}/Q_{G2}, \quad \eta_{H2} = 1 + \eta_{C2} \quad (21)$$

$$\eta_{HT} = (Q_{A1} + /Q_{C1})/(Q_{G1} + Q_{G2}) = \eta_{H1}\eta_{H2}/(\eta_{H1} + \eta_{H2} - 1) \quad (22)$$

4.5.2 Triple-effect two-cascade refrigeration cycle (Fig. 7)

This cycle is used for cooling. Assuming that the cooling COP and heating COP in the high temperature side are η_{C1} and η_{H1}, and the cooling COP and heating COP in the low temperature side are η_{C2} and η_{H2}, the overall cycle efficiency in the cooling mode is given by the equation (23).

$$Q_{G1} + Q_{E1} = Q_{A1} + Q_{C1}, \quad Q_{G2} + Q_{E2} = Q_{A2} + Q_{C2} \tag{23}$$

$$Q_{G2} = Q_{A1} + Q_{C1} = Q_{G1} + Q_{E1} \tag{24}$$

$$\eta_{C1} = Q_{E1}/Q_{G1}, \quad \eta_{H1} = 1 + \eta_{C1} \tag{25}$$

$$\eta_{C2} = Q_{E2}/Q_{G2}, \quad \eta_{H2} = 1 + \eta_{C2} \tag{26}$$

$$\eta_{CT} = (Q_{E1} + /Q_{E2})/Q_{G1} = \eta_{C1} + \eta_{C2} + \eta_{C1}\eta_{C2} \tag{27}$$

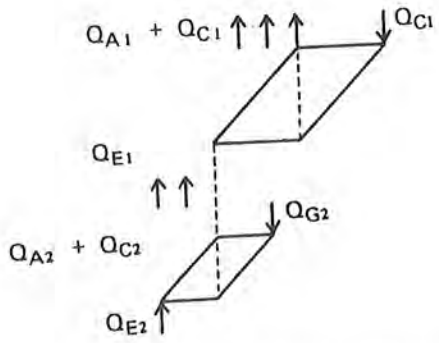

Fig. 6 Two-cascade heat pump

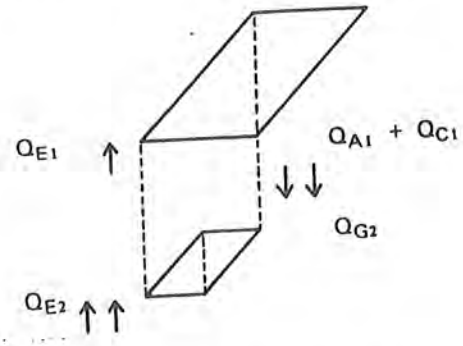

Fig. 7 Triple-effect two-cascade refrigerator

4.6 Cycles evaluated

Cycles covered by the third step of evaluation are shown below. We selected combined single-effect cycles which were highly rated under the second step of evaluation. Other cycles will be examined from now on.

(1) Single-effect heat pump cycle (heating)
(2) Two-cascade heat pump cycle (heating, combined single-effect cycles)
(3) Triple-effect two-cascade refrigeration cycle (cooling, combined single-effect cycles)

The working fluids are shown below. Those selected were working fluids for which Dühring diagram and concentration enthalpy diagram are fully provided.

(1) Water + LiBr (2) Ammonia + water
(3) TFE + NMP (4) R22 + DTG

Table 5. Results of single-effect heat pump

Working fluids	Ammonia + water	TFE + NMP	R22 + DTG
Heating COP	1.54 ①	1.51 ②	1.2 ①
Evaluation results	○	○	○

Table 6. Results of two-cascade heat pump

Working fluids	High temperature side	Water + LiBr	Water + LiBr	Water + LiBr
	Low temperature side	Ammonia+water	TFE+NMP	R22+DTG
Heating COP	High temperature side	1.80 ①	1.80 ①	1.8 ①
	Low temperature side	1.63 ①	1.74 ①	1.4 ①
	Overall	1.21	1.23	1.2
Evaluation results		○	○	○

Table 7. Results of triple-effect two-cascade refrigerator

Working fluids	High temperature side	Ammonia+water	TFE+NMP	R22+DTG
	Low temperature side	Ammonia+water	Water + LiBr	Water + LiBr
Heating COP	High temperature side		0.45 ①	0.1 ①
	Low temperature side		0.84 ①	0.9 ①
	Overall		1.69	1.0
Evaluation results		×	○	×

○ : COP over the target value (1.2 for cooling/heating)
× : COP below the target value (1.2 for cooling/heating)

4.7 Evaluation results (see Tables 5 to 7)

①, ② and ③ in the tables denote, respectively, the values calculated according to the cases of ① small concentration width, ② medium concentration width and ③ large concentration width for heat exchange.

5. Definition of Terms Concerning Cycles

At present, we are continuing to evaluate cycles. Given below are terms defined concerning cycles.

5.1 Terms related to classification of cycles

(1) [effect]: value of theoretical performance for cycle in the cooling mode
(2) [stage]: number of evaporator(s)– absorber(s) or condenser(s) not affecting the theoretical performance
(3) [cascade]: type of working fluids
(4) [refrigerator]: refrigeration cycle
(5) [heat pump]: heat pump type 1
(6) [heat transformer]: heat pump type 2
(7) [heat pump transformer]: combined heat pump and heat transformer

5.2 Terms of cycles having heat exchangers

(1) AX (absorber heat exchange) cycle: a cycle having heat exchanger between absorber and solution
(2) GX (generator heat exchange) cycle: a cycle having heat exchanger between generator and solution
(3) GAX (generator absorber heat exchange) cycle: a cycle having heat exchanger between generator and absorber

The cycles named as per the definition above are given in Table 8.

6. Conclusion

At the current workshop we have reported on the second and third steps of cycle evaluation. However, since the third step of evaluation remains yet to be completed, we intend to continue it. Furthermore, we have a plan to make a more detailed arithmetic model presupposing trial manufacture of a prototype machine to conduct a sensitivity analysis of cycles.

Table 8. Comparison of cycle names

cycle	G. Alefeld	Phillips	Trane	This work
	single-effect	single-effect	single-effect	single-effect
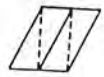	double-effect	two-stage GAX	double-effect generator/common condenser	double-effect
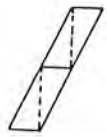	double-effect	double-effect		double-effect
	double-effect	resorber augmented	double-effect evaporation employing resorption/ desorption	double-effect
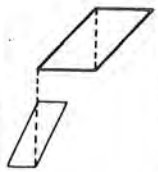				two-cascade heat pump
	double-effect			double-effect two-cascade heat pump
	triple-effect refrigerator			triple-effect refrigerator

CONTENTS

FIRST STEP OF EVALUATION (1)

OBJECTS

72 cycles surveyed in literature.

METHOD

Evaluation in terms of 5 evaluation items.

Table 1. Evaluation coefficients

Coefficient	Definition
NM	(Number of main components) Number of component evaporator, condenser, absorber and generator
NA	(Number of auxiliary components) Number of component solution heat exchanger and pump
COP	(Coefficient of performance) Theoretical COP in the cooling/heating modes $COP_c = \Sigma Q_E / \Sigma Q_G$ $COP_h = \Sigma (Q_A + Q_C) / \Sigma Q_G$
TSC	(Transfer surface coefficient) Ratio of heat quantity effectively utilized for cooling/heating, to total quantity of heat utilized $TSC_c = \Sigma Q_E / \Sigma Q$ $TSC_h = \Sigma (Q_A + Q_C) / \Sigma Q$
TF	(Temperature factor) Indicator of the heating temperature $TF = (T_3 - T_2)/(T_2 - T_1)$

CONDITIONS

(1) $NM \leqq 5$
(2) $NA \leqq 2$
(3) $COP_C \geqq 2$, $COP_H \geqq 2$
(4) $TSC_C \geqq 1/4$, $TSC_H \geqq 1/2$
(5) $TF \geqq 2$

FIRST STEP OF EVALUATION (2)

RESULTS

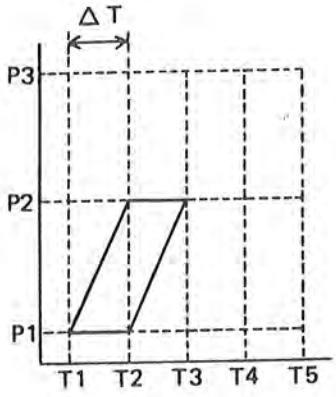

COP_C 1
COP_h 2
TSC_C 1/4
TSC_h 2/4
TF 1

(1) No. 1

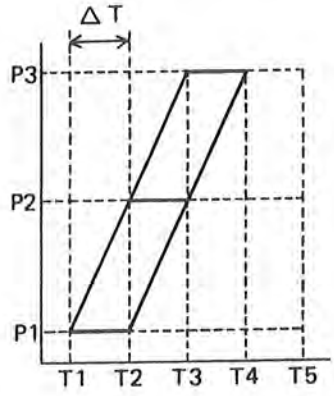

COP_C 2
COP_h 3
TSC_C 2/8
TSC_h 3/8
TF 2

(2) No. 2

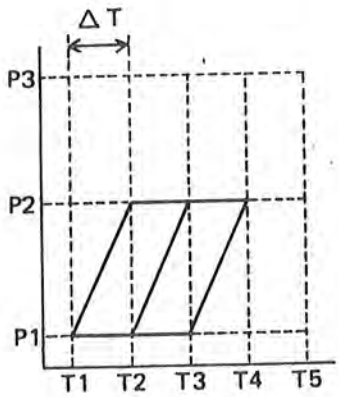

COP_C 2
COP_h 3
TSC_C 2/8
TSC_h 3/8
TF 2

(3) No. 3

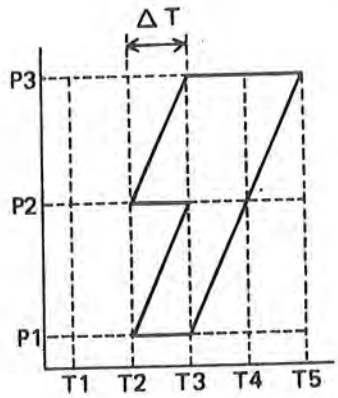

COP_C 2
COP_h 3
TSC_C 2/6
TSC_h 3/6
TF 2

(4) No. 4

Fig. 1 Best cycles based on the primary evaluation

PROBLEMS

(1) There is no concept of concentration width.
(2) There are cycles hard to classify/evaluate.
- Cycles as combination of absorption type and compression type
- Cycles, such as GAX, that have heat exchangers.
- Heat pump transformers.
- Cycles having more than 2 types of chilled/hot water temperature level.

SECOND STEP OF EVALUATION (1)

OBJECTS

4 cycles selected under first step of evaluation.

METHOD

By applying Dühring diagram for working fluids to the 4 cycles, examine the cycle working range (temperature, pressure, concentration).

Table 2. Temperature conditions

Operation	Evaluation temperature of refrigerant T_e	Condensation temperature of refrigerant T_c
Cooling	5 ℃	35 ℃
Heating	− 5 ℃	50 ℃

Table 3. Working fluids

Type of refrigerant	Working fluids
Water group	① Water + LiBr
Ammonia group	② Ammonia + water ③ Ammonia + $LiNO_3$/water ④ Methylamine + etylene glycol
Alcohol group	⑤ Methanol + LiBr ⑥ Methanol + LiBr/water ⑦ TFE + NMP
CFC group	⑧ R22 + DTrG ⑨ R123a + DTG

CONDITIONS

(1) Maximum temperature $T_{MAX} \leqq 160℃$
(2) Maximum pressure $P_{MAX} \leqq 20\ kg/cm^2$
(3) Maximum concentration no crystallization

SECOND STEP OF EVALUATION (2)

RESULTS

○ : Commercial operation is possible.
△ : Problems involved in temperature/pressure
(max. temperature: 160℃, max. pressure: over 20 kg/cm²)
× : Operation is impossible.

Table 4. Results of second step of cycle evaluation

Type of cycle			No. 1		No. 2		No. 3		No. 4	
Operation mode			Cooling	Heating	Cooling	Heating	Cooling	Heating	Cooling	Heating
Working fluids	Water	Water + LiBr	○	×	○	×	×	×	×	×
	Ammonia	Ammonia + water	○	○	○	△	○	△	○	△
		Ammonia + $LiNO_3$/water	○	○	○	△	○	△	○	△
		Metylamine + EG	○	○	○	△	○	△	○	△
	Alcohol	Methanol + LiBr	○	×	○	△	△	×	×	×
		Methanol + LiBr/water	○	△	○	△	△	×	△	×
		TFE + NMP	○	○	○	△	○	×	○	×
	Flon	R22 + DTrG	○	○	△	△	○	△	○	△
		R123a + DTG	○	○	○	△	○	△	○	△

PROBLEMS

(1) Treatment of concentration width remains yet be determined.
(2) The evaluation method for cycles, such as GAX, remains yet to be determined.
(3) Only single-effect cycles are capable of heat pump operation in the heating mode.

THIRD STEP OF EVALUATION (1)

OBJECTS

(1) Single-effect cycle
(2) Combined single-effect cycle

METHOD (1)

Evaluation of COP for cycles.

1. ASSUMPTION
   (1) A refrigerant heat exchanger shall be neglected.
   (2) The temperature efficiency of heat exchangers shall be assumed to be 100%.

2. DEFINITION OF COP OF SINGLE-EFFECT CYCLE
   (1) COOLING COP

$$\eta_C = Q_E / Q_G \quad (1)$$

   (2) HEATING COP

$$\eta_H = (Q_A + Q_C)/Q_G = 1 + \eta_C \quad (2)$$

$$Q_E = G_R (H_{R1} - H_{RL3}) \quad (3)$$

where Q_E : Heat quantity of evaporator
Q_G : Heat quantity of generator
Q_A : Heat quantity of absorber
Q_C : Heat quantity of condenser
G_R : Mass flow rate of refrigerant
H_{R1} : Gas phase enthalpy of refrigerant in evaporator
H_{RL3} : Liquid phase enthalpy of refrigerant in condenser

THIRD STEP OF EVALUATION (2)

METHOD (2)

3. CONCENTRATION
   (1) The concentration of strong solution shall be either smaller of concentration at 160℃ of heating temperature or concentration of crystallization.
   (2) The concentration of weak solution shall be concentration equilibratory with evaporator/absorber temperatures.

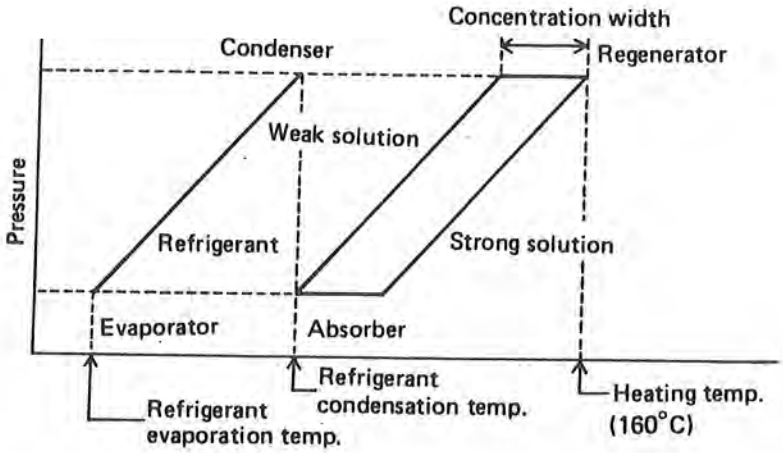

Fig. 2 Definition of concentration

THIRD STEP OF EVALUATION (3)

METHOD (3)

4. COP OF SINGLE-EFFECT CYCLE

(1) CASE OF SMALL CONCENTRATION WIDTH

- Heat quantity exchanged by solution heat exchanger Q_{EX1}

$$Q_{EX1} = G_{S2}(H_{S4} - H_{S5}) = G_{S1}(H_{S7} - H_{S6}) \quad (4)$$

where G_{S1} : Dilute solution mass flow rate
G_{S2} : Conc. solution mass flow rate
H_{S4} : Enthalpy of absorbent at the point ④

- Heat quantity of the generator Q_G

$$Q_G = G_R (H_{R3} + H_{R4})/2 + G_{S2} H_{S4} - G_{S1} H_{S7} \quad (5)$$

- Heat quantity of absorber Q_A

$$Q_A = G_R H_R 1 + G_{S2} H_{S5} - G_{S1} H_{S6} \quad (6)$$

$$G_R = G_{S1} - G_{S2} \quad (7)$$

where G_R : Total mass flow rate of refrigerant vapor
H_{R3} : Enthalpy of refrigerant vapor at the point ③

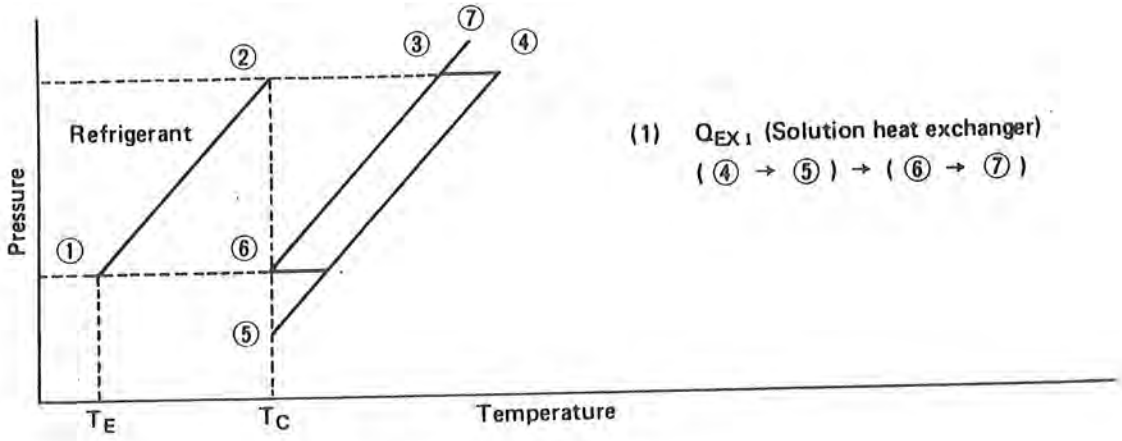

Fig. 3 Dühring diagram

THIRD STEP OF EVALUATION (4)

METHOD (4)

(2) CASE OF MIDDLE CONCENTRATION WIDTH

- Heat quantity exchanged by solution heat exchanger Q_{EX1}

$$Q_{EX1} = G_{S2}(H_{S8} - H_{S5}) = G_{S1}(H_{S11} - H_{S7}) \quad (8)$$

- Heat quantity exchanged by AX (heat exchange between absorber and weak solution) Q_{EX2}

$$Q_{EX2} = G_{S1}(H_{S7} - H_{S6}) = G_{R2}H_{R1} + G_{S2}H_{S5} - (G_{S2} + G_{R2})H_{S9} \quad (9)$$

- Heat quantity exchanged by GX (heat exchange between generator and strong solution) Q_{EX3}

$$Q_{EX3} = G_{S2}(H_{S4} - H_{S8}) = G_{R3}(H_{R3} + H_{R10})/2 + (G_{S1} - G_{R3})H_{S10} - G_{S1}H_{S11} \quad (10)$$

where G_{R2} = Mass flow rate of refrigerant in absorber whose heat is exchanged by AX

G_{R3} = Mass flow rate of refrigerant in generator whose heat is exchanged by GX

- Heat quantity of generator Q_G

$$Q_G = (G_R - G_{R3})(H_{R10} + H_{R4})/2 + G_{S2}H_{S4} - (G_{S1} - G_{R3})H_{S10} \quad (11)$$

- Heat quantity absorbed by absorber Q_A

$$Q_A = (G_R - G_{R2})H_{R1} + (G_{S2} + G_{R2})H_{S9} - G_{S1}H_{S6} \quad (12)$$

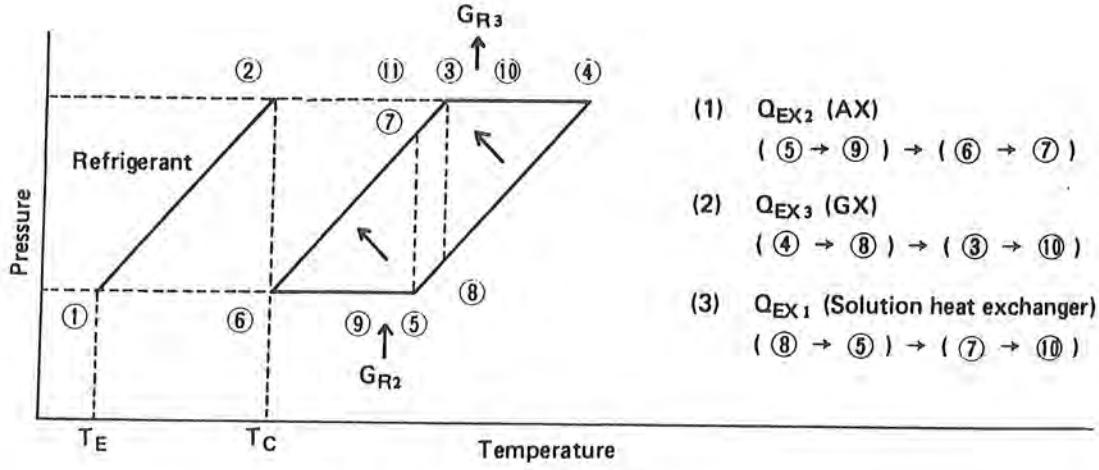

Fig. 4 Dühring diagram

THIRD STEP OF EVALUATION (5)

METHOD (5)

(3) CASE OF LARGE CONCENTRATION WIDTH

- Heat quantity exchanged by AX Q_{EX2}

$$Q_{EX2} = G_{S1}(H_{S3} - H_{S6}) = G_{R2}H_{R1} + (G_{S2} + G_{R1})H_{S8} - (G_{S2} + G_{R2} + G_{R1})H_{S9} \quad (13)$$

- Heat quantity exchanged by GX Q_{EX3}

$$Q_{EX3} = G_{S2}(H_{S1} - H_{S5}) = G_{R3}(H_{R2} + H_{R10})/2 + (G_{S1} - G_{R3} - G_{R5})H_{S10} \quad (14)$$

- Heat quantity exchanged by GAX (heat exchange between generator and absorber) Q_{EX1}

$$Q_{EX1} = G_{R1}H_{R1} + G_{S2}H_{S7} - (G_{S2} + G_{R1})H_{S8} = G_{R5}(H_{R4} + H_{R7})/2 + (G_{S1} - G_{R5})H_{S7} - G_{S1}H_{S9} \quad (15)$$

where G_{R1} = Mass flow rate of refrigerant in absorber whose heat is exchanged by GAX

G_{R5} = Mass flow rate of refrigerant in regenerator whose heat is exchanged by GAX

- Heat quantity of regenerator Q_G

$$Q_G = (G_R - G_{R4} - G_{R5})(H_{R10} + H_{R1})/2 + G_{S2}H_{S1} \quad (16)$$

- Heat quantity of absorber Q_A

$$Q_A = (G_R - G_{R2} - G_{R1})H_{R1} + (G_{S2} + G_{R2} + G_{R1})H_{S9} - G_{S1}H_{S5} \quad (17)$$

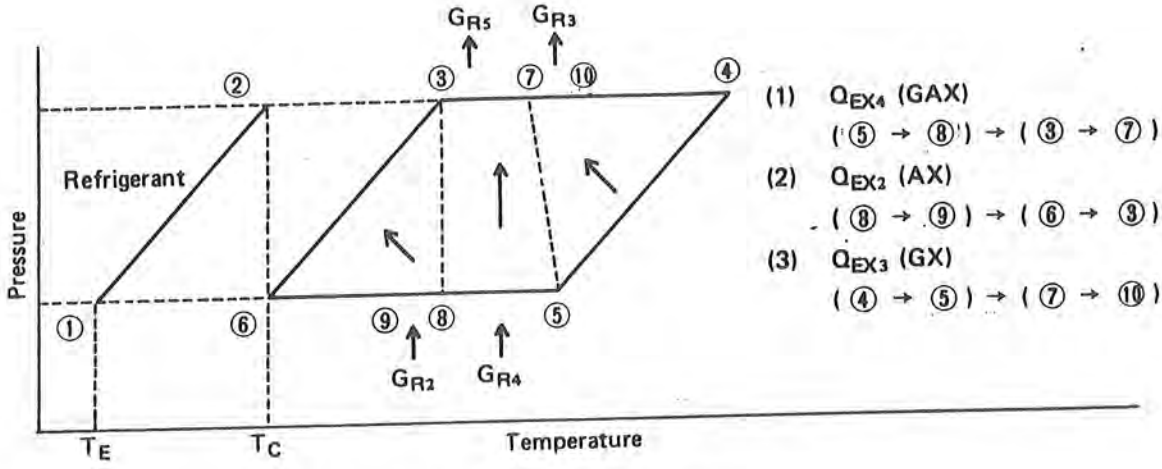

Fig. 5 Dühring diagram

THIRD STEP OF EVALUATION (6)

METHOD (6)

5. COP OF COMBINED SINGLE-EFFECT CYCLES

(1) TWO-CASCADE HEAT PUMP

$$Q_{G1} + Q_{E1} = Q_{A1} + Q_{C1}\ ,\quad Q_{G2} + Q_{E2} = Q_{A2} + Q_{C2} \tag{18}$$

$$Q_{E1} = Q_{A2} + Q_{C2} = Q_{G2} + Q_{E2} \tag{19}$$

$$\eta_{C1} = Q_{E1}/Q_{G1}\ ,\quad \eta_{H1} = 1 + \eta_{C1} \tag{20}$$

$$\eta_{C2} = Q_{E2}/Q_{G2}\ ,\quad \eta_{H2} = 1 + \eta_{C2} \tag{21}$$

$$\eta_{HT} = (Q_{A1} + /Q_{C1})/(Q_{G1} + Q_{G2}) = \eta_{H1}\eta_{H2}/(\eta_{H1} + \eta_{H2} - 1) \tag{22}$$

(2) TRIPLE-EFFECT TWO-CASCADE REFRIGERATOR

$$Q_{G1} + Q_{E1} = Q_{A1} + Q_{C1}\ ,\quad Q_{G2} + Q_{E2} = Q_{A2} + Q_{C2} \tag{23}$$

$$Q_{G2} = Q_{A1} + Q_{C1} = Q_{G1} + Q_{E1} \tag{24}$$

$$\eta_{C1} = Q_{E1}/Q_{G1}\ ,\quad \eta_{H1} = 1 + \eta_{C1} \tag{25}$$

$$\eta_{C2} = Q_{E2}/Q_{G2}\ ,\quad \eta_{H2} = 1 + \eta_{C2} \tag{26}$$

$$\eta_{CT} = (Q_{E1} + /Q_{E2})/\ Q_{G1} = \eta_{C1} + \eta_{C2} + \eta_{C1}\eta_{C2} \tag{27}$$

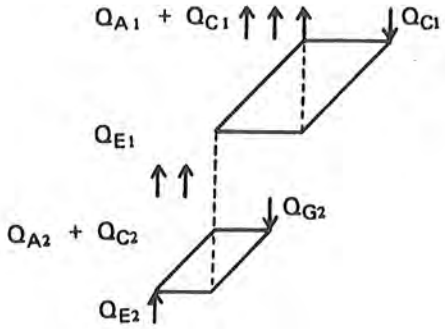

Fig. 6 Two-cascade heat pump

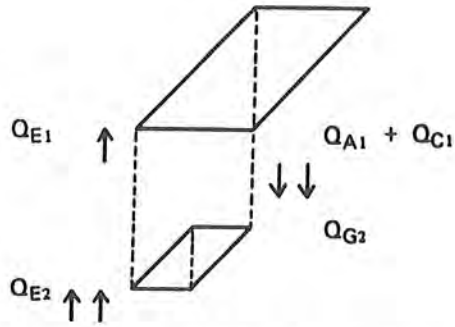

Fig. 7 Triple-effect two-cascade refrigerator

THIRD STEP OF EVALUATION (7)

RESULTS

○ : COP over the target value (1.2 for cooling/heating)
× : COP below the target value (1.2 for cooling/heating)

Table 5. Results of single-effect heat pump

Working fluids	Ammonia + water	TFE + NMP	R22 + DTG
Heating COP	1.54 ①	1.51 ②	1.2 ①
Results	○	○	○

Table 6. Results of two-cascade heat pump

Working fluids	High temperature side	Water + LiBr	Water + LiBr	Water + LiBr
	Low temperature side	Ammonia+water	TFE+NMP	R22+DTG
Heating COP	High temperature side	1.80 ①	1.80 ①	1.8 ①
	Low temperature side	1.63 ①	1.74 ③	1.4 ③
	Overall	1.21	1.23	1.2
Results		○	○	○

Table 7. Results of triple-effect two-cascade refrigerator

Working fluids	High temperature side	Ammonia+water	TFE+NMP	R22+DTG
	Low temperature side	Ammonia+water	Water + LiBr	Water + LiBr
Cooling COP	High temperature side		0.45 ①	0.1 ①
	Low temperature side		0.84 ①	0.9 ①
	Overall		1.69	1.0
Evaluation results		×	○	×

where ① : Case of small concentration width
② : Case of middle concentration width
③ : Case of large concentration width

DEFINITION OF TERMS (1)

1. TERMS RELATED TO CLASSIFICATION OF CYCLES
   (1) [effect]: value of theoretical performance for cycle in the cooling mode
   (2) [stage]: number of evaporator(s) — absorber(s) or condenser (s) not affecting the theoretical performance
   (3) [cascade]: type of working fluids
   (4) [refrigerator]: refrigeration cycle
   (5) [heat pump]: heat pump type 1
   (6) [heat transformer]: heat pump type 2
   (7) [heat pump transformer]: combined heat pump and heat transformer

2. TERMS OF CYCLES HAVING HEAT EXCHANGERS
   (1) AX (absorber heat exchange) cycle: a cycle having heat exchanger between absorber and solution
   (2) GX (generator heat exchange) cycle: a cycle having heat exchanger between generator and solution
   (3) GAX (generator absorber heat exchange) cycle: a cycle having heat exchanger between generator and absorber

DEFINITION OF TERMS (2)

3. COMPARISON OF TERMS

Table 8. Comparison of cycle names

cycle	G. Alefeld	Phillips	Trane	This work
	single-effect	single-effect	single-effect	single-effect
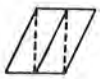	double-effect	two-stage GAX	double-effect generator/common condenser	double-effect
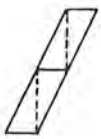	double-effect	double-effect		double-effect
	double-effect	resorber augmented	double-effect evaporation employing resorption/ desorption	double-effect
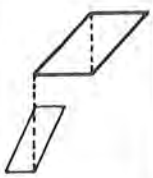				two-cascade heat pump
	double-effect			double-effect two-cascade heat pump
	triple-effect refrigerator			triple-effect refrigerator

8. DEMONSTRATION OF SOLAR POWERED ABSORPTION REFRIGERATING MACHINE USING TFE/NMP

Katsuyuki Mashimo
Sanyo Electric Co., Ltd.
Gunma, Japan

Introduction

An absorption refrigerating machine is a kind of heat engine that utilizes evaporation and absorption action caused by a saturated vapor pressure difference due to temperature differences between refrigerant and absorbent.

Since the absorption machine currently in commercial use utilizes water as refrigerant, and lithium bromide water solution as absorbent, it is difficult to lower evaporating temperature below 273 K due to freezing of the refrigerant and crystallization of the absorbent.

One of the working fluids for the absorption machine that allows to reach low temperature below 273 K, is an ammonia-water system. However, its use in Japan is prohibited due to toxicity, corrosiveness and explosiveness of ammonia. Thus, research has been conducted on working fluids using halocarbons as refrigerants for the air-cooled,air source heat pump rather than low temperature refrigeration, since halocarbons feature excellent low temperature characteristics. However, they have not been commercialized up to date.

Trifluoroethanol(TFE), refrigerant, and N-methyl 2-pyrrolidone(NMP), absorbent, have been developed as working fluids suitable for new working pairs, thanks to the intermolecular force that exists between refrigerant and absorbent.

Performance characteristics of the absorption process have been calculated for evaluation based on chemical, physical and thermodynamic analysis of experimental data. As a result, a prototype solar powered absorption refrigerating machine using TFE/NMP has been developed, and various data are being obtained at a demonstration plant.

The development of absorption machine in which the temperature in the warehouse is 268 to 273 K by solar heat collected at 393 to 413 K as the driving energy, is now being carried out in one of the "Sunshine Projects" under the sponsorship of New Energy Development Organization (NEDO).

This paper reports on the development of the new working fluids TFE/NMP and its use with the absorption refrigerating machine under demonstration.

Working fluids for absorption machines

Refrigerant-absorbents which seem to be promising as working fluids for absorption machines are shown in Table 1 as a result of research conducted in recent years [1],[2],[3],[4],[5],[6].

Table 1. Refrigerant-absorbent systems which are deemed promising

Absorbent \ Refrigerant	TFE CF_3CH_2OH	R123a $CHClFCClF_2$	R133a CHF_2CHClF
HMPT $OP[N(CH_3)_2]_3$ (Hexamethylphosphricacidtriamid)	○		○
Chi C_9H_7N (Chinolin)	○		
TEG $H(OC_2H_4)_4OH$ (Tetra-ethylene glycol)	○		
TEGDME $CH_3(OC_2H_4)_4OCH_3$ (Tetra-ethylene glycol dimethylether)	○	○	○
NMP C_5H_9NO (N-methyl pyrrolidone)	○	○	○
TrEGDME $CH_3(OC_2H_4)_3OCH_3$ (Tri-ethylene glycol dimethylether)	○	○	○
ETFE $(C_4H_7O)CH_2OC_2H_5$ (Ethyl-tetrahydrofurfurylether)		○	○
DMF $CHON(CH_3)_2$ (Dimethylformamid)			○
TBP $C_6H_4(CO_2C_4H_9)_2$ (Tri N-buthylphosphate)	○		○
Pyr C_4H_7NO (Pyrrolidone)	○		

Dissolution in the refrigerant-absorbent can be assumed from the viewpoint of intermolecular force. High solubility of the refrigerant-absorbent fluid pair means that the affinity between the refrigerant and the absorbent is strong, the vapor pressure of the solution presents more negative deviations from Raoult's Law, and depression of vapor pressure in the refrigerant-absorbenthat fluid system is high.

Gaz de France and Total Energie Development conducted research on R133a/NMP jointly, by using a test machine, while Allied Chemical conducted research on R133a/ETFE and R123a/ETFE.

In Japan, absorption machines of the R22/DEGDME system and the R22/TEGDME system were manufactured by way of trial by using R22 as refrigerant, and their results were announced.

Development of a new working pair TFE/NMP [7][8]

Refrigerant TFE

Research has been conducted on combinations of refrigerant and absorbent featuring large solubility and vapor pressure lowering of the solution with large negative deviations from Raoult's law. As a result, with regard to chemical stability, we made investigations on halogenated alcohols with large heats of vaporization and selected 2.2.2-trifluoroethanol (TFE) as refrigerant. TFE has $-CF_3$ electron withdrawing group and electrophilicity. Table 2 shows the properties of TFE.

Table 2. Properties of TFE

Refrigerant	Chemical formula	Molecular weight	Boiling point (K)	Freezing point (K)	Latent heat of evaporation (kJ/kg)	Specific heat (kJ/kg·K)	Viscosity (mPa·S)	Surface tension (N/m)	Density (kg/m³)	Flash point (K)	Ignition point (K)
2,2,2-trifluoro-ethanol	CF_3CH_2OH	100.04	348	228	356	1.72	1.56	1.89×10^{-2}	1372	313	none

* 348K ** 293K *** 303K

Absorbent NMP

Absorbents combined with the refrigerant 2.2.2-trifluoro ethanol are ethers, polyols, esters, amides, imides, ketones, aldehydes,nitrides and their mixtures. An overall evaluation of properties, heat characteristics and marketability resulted in the discovery of a superiority of N-alkyl-2-pyrrolidone, and the selection of N-methyl-2-pyrrolidone (NMP) as absorbent. NMP has $-CH_3$ electron releasing group and presents necleophilicity. Table 3 shows the properties of NMP.

Table 3. Properties of NMP

Absorbent	Chemical formula	Molecular weight	Boiling point (K)	Freezing point (K)	Latent heat of evaporation (kJ/kg) *	Specific heat (kJ/kg·K) **	Viscosity (mPa·S) ***	Surface tension (N/m) ***	Density (kg/m³) ***	Flash point (K)	Ignition point (K)
N-methyl-2-pyrrolydone	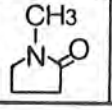	99.14	477	248	439	1.73	1.55	3.91×10^{-2}	1022	368	619

* 477K ** 293K *** 303K

Fig. 1 shows the dissolution of TFE and NMP from which it is assumed that the combination is caused by electrical attraction between the $H\delta^+$ of electrophilic TFE and the $O\delta^-$ of nucleophilic NMP.

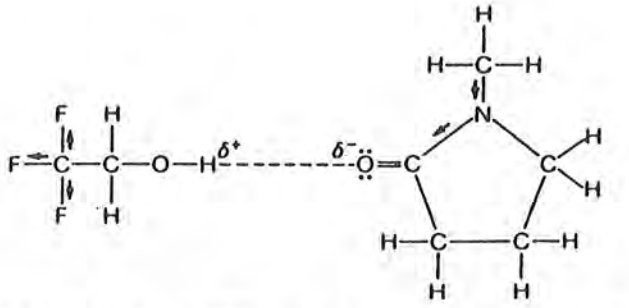

2,2,2-trifluoroethanol (TFE) N-methyl-2-pyrrolidone (NMP)

Fig. 1 Dissolution of the TFE-NMP system

Basic properties of TFE/NMP

Vapor pressure and thermal data on refrigerant, absorbent and solution are required in order to analyze both the thermodynamic properties of working fluids and the cycle characteristics of the absorption machine.

An enthalpy-concentration diagram is required for calculating heat exchanged and COP in absorption machines and for analyzing the cycle characteristics. Using the results measured for vapor pressure, specific heat and heat of mixing, an isobaric curve has been drawn from the vapor pressure, and an isothermal curve has been drawn from the specific heat and heat of mixing.

The enthalpy-concentration diagram is drawn with temperature and pressure as parameters for a refrigerant, absorbent and solution. In this case, it is based on 418.4 kJ/kg which is the enthalpy of a refrigerant and an absorbent at 273 K.

Fig. 2 shows the pressure-temperature diagram and Fig. 3 shows the enthalpy-concentration diagram of TFE/NMP.

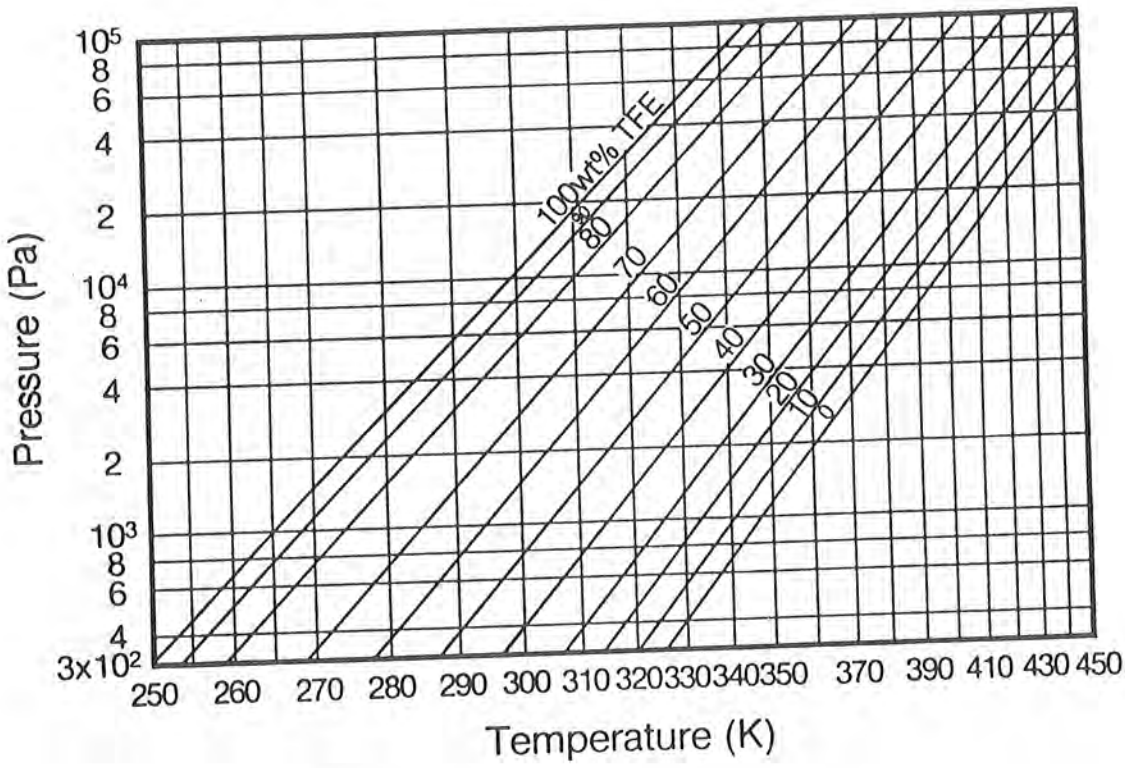

Fig. 2 Pressure-temperature diagram

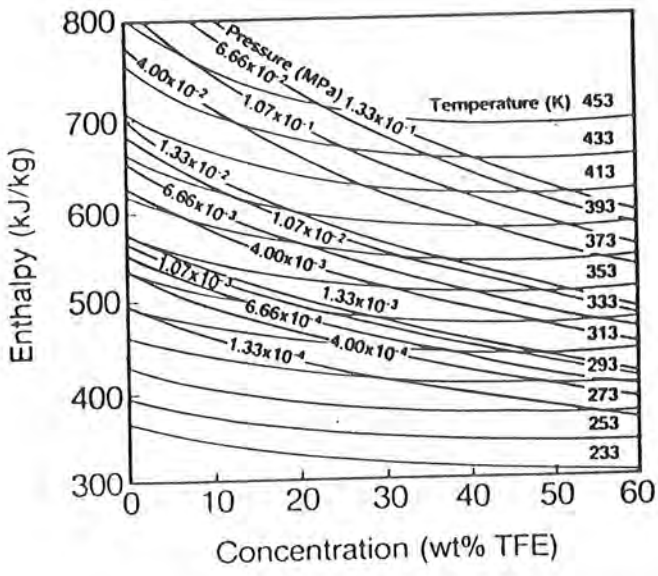

Fig. 3 Enthalpy-concentration diagram

A pressure-enthalpy diagram(Mollier diagram) as well as an enthalpy-concentration diagram are required for TFE/NMP in calculating heat exchanged and COP of an absorption machine. Enthalpy of liquid, vapor and their coexistence in TFE are presented.[9]

Solar-powered absorption refrigerating machine

The absorption machine comprises a generator (G), a rectifier (R), a partial condenser (PC), a condenser (C), an evaporator (E), an absorber (A), a liquid-liquid heat exchanger (HE) and a solution pump (P).

Fig. 4 shows the cycle flow for the absorption machine.

The heat exchanged (q) for each part can be obtained by heat balance with enthalpies (i), circulating ratio (f) and reflux ratio (f') of the refrigerant and solution.

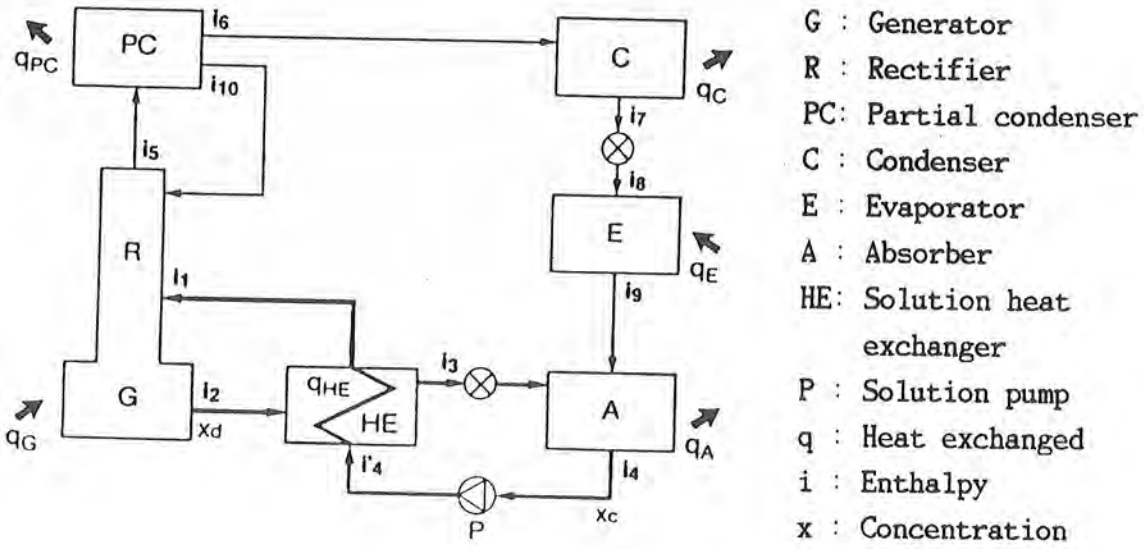

Fig. 4 Cycle flow

Based on experimentally determined solubility and thermodynamic data, an evaporator temperature of 258 K is obtained when the generator temperature stands at 393 K and the temperature of both the condenser and absorber, at 311 K. At this point, the operating pressures are 733 Pa at the evaporator and 18670 Pa at the condenser. With this working fluid, TFE/NMP, an absorption refrigeration machine lowers the temperature below the freezing zone easily.

Fig. 5 shows the prototype solar powered absorption refrigerating machine and table 4 shows experimental data at standard rating conditions in the demonstration plant.

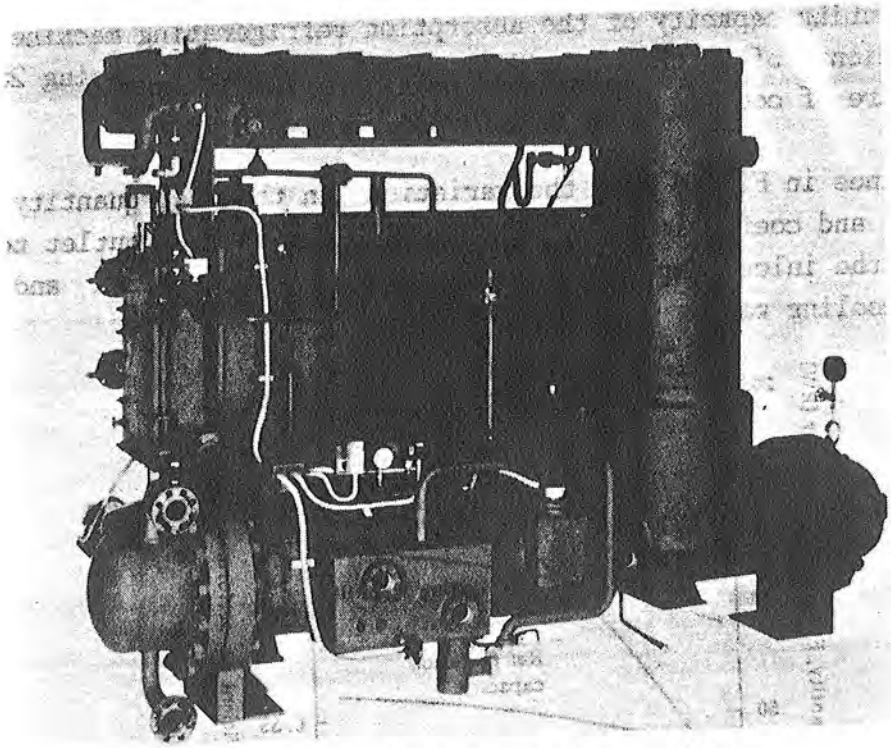

Fig. 5 Prototype absorption machine

Table 4. Experimental data at standard rating conditions

Item	Design specifications	Experimental data (July 23, 1987)
Refrigerant	TFE (trifluoroethanol)	
Absorbent	NMP (N-methl 2-pyrrolidone)	
Refrigerating capacity	52.0 kW	61.23 kW
Temp. of takeout brine	266.0 K	266.1 K
Temperature of heat source high temperature water	413.0 K	412.6 K
Cooling water temperature	302.0 K	302.2 K
Coefficient of performance	0.43 or more	0.476
	261k brine can be taken out.	
External dimensions	3280L × 2110W × 2294H	

The refrigerating capacity of the absorption refrigerating machine is 61.23 kW and coefficient of performance (COP) is 0.476 when obtaining 266 K brine (inlet temperature of cooling water : 302 K).

The solid lines in Fig. 6 show the variation in the heat quantity, refrigeration capacity and coefficient of performance if the brine outlet temperature is varied when the inlet temperature of heating water is 413 K and the inlet temperature of cooling water, 302 K.

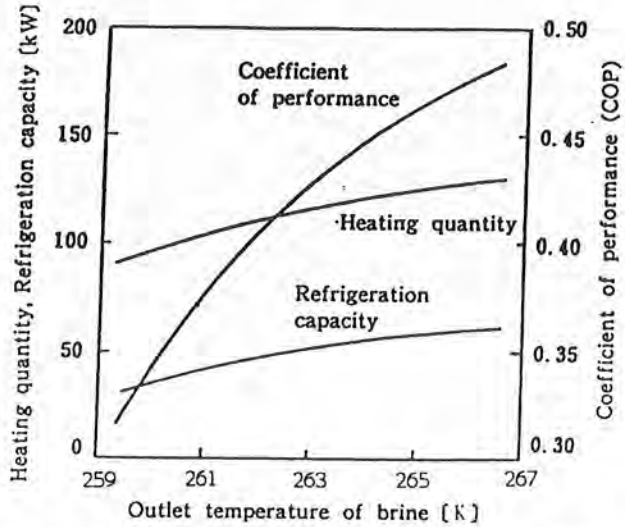

Fig. 6 Performance when the outlet temperature of brine is varied

Solar refrigeration warehouse system

The absorption refrigerating machine with TFE/NMP is now demonstrated for a solar refrigeration warehouse system.

Inner mirror vacuum glass tube type solar collectors (294 pieces) are used to produce high temperature water of 413k. The high temperature water is stored in the high temperature thermal storage tank, and is used as the heat source for the absorption refrigerating machine. The high temperature thermal storage tank contains 15m³ of high temperature water and 6m³ of N_2, and is adjusted to 1.21MPa at the maximum system working temperature of 438K.

The heat source of the absorption refrigerating machine is supplied at high temperature water of 413K in summer, 393K in winter, and 403K in the off-seasons in accordance with the cooling water temperature. Operation continues until the temperature of the takeout brine is decreased to 266K ~ 261K. Brine is first stored in the brine tank, then delivered to the refrigerated warehouse with the temperature held at 266K. If the temperature inside the brine tank reaches 261K or below, brine is supplied to the low temperature thermal storage tank to store the latent heat.

Normally, the daytime solar energy is stored to improve the solar energy dependency of the system. To minimize the heat loss of thermal storage, the cold heat source with the smallest possible temperature difference from the external environmental temperature is stored. The low temperature thermal storage storage tank contains 2,550 kg of latent heat storing agent.

The refrigerated warehouse is divided into three rooms A, B and C. Rooms A and B are maintained at 271±1K and Room C at 272±1K.

Fig. 7 shows a system flow.

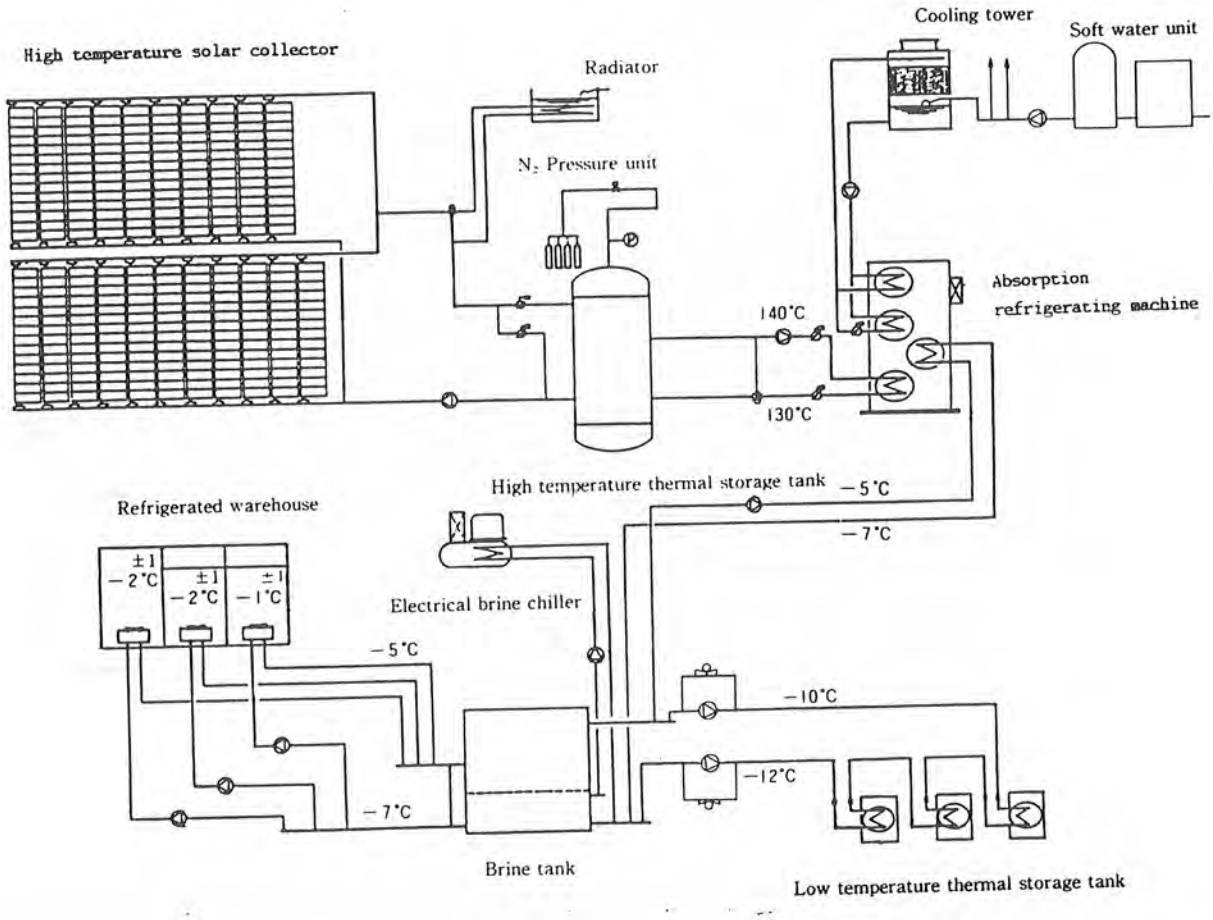

Fig. 7 System flow

After its completion on March 9, 1987, this plant has been operated continuously since April 1. The system's heat balance on the operation results over the past year from April 1, 1987 to March 31, 1988 has been compiled and given in Fig. 8.[10]

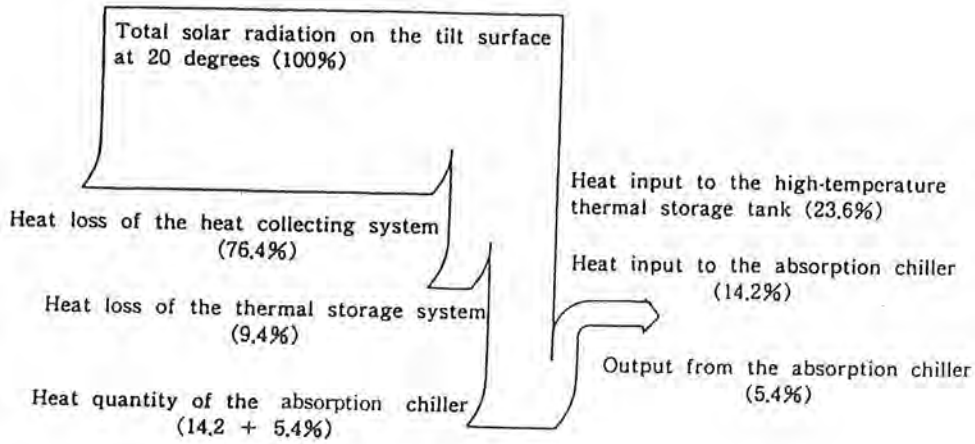

Fig. 8 System heat balance

The solar radiation on the tilt surface at 20 degrees is the solar radiation shone onto the total opening area (411.6 m²) of the reflector of the solar collector. The total solar radiation over the past year was 486,430 Mcal(2,033,280 MJ), 23.6% of which has been stored in the high-temperature thermal storage tank after subtracting the loss due to the solar collector and piping system. Of the heat quantity stored in the high-temperature thermal storage tank, the heat quantity actually used by the absorption machine was 69,000 Mcal(288,420 MJ) and the absorption machine provided an output of 26,500 Mcal (110,800 MJ) after being operated for a total of 995 hours. The year-round cop was 0.38 —— a favorable result as compared with the initial plan. When the entire system is taken into account, the ratio of the absorption machine output with respect to the solar radiation on the tilt surface at 20 degrees was 5.4 %, by far exceeding the planned value of 4.4 %.

Fig. 9 shows a pilot plant in operation and Table 5 shows an outline of the plant.

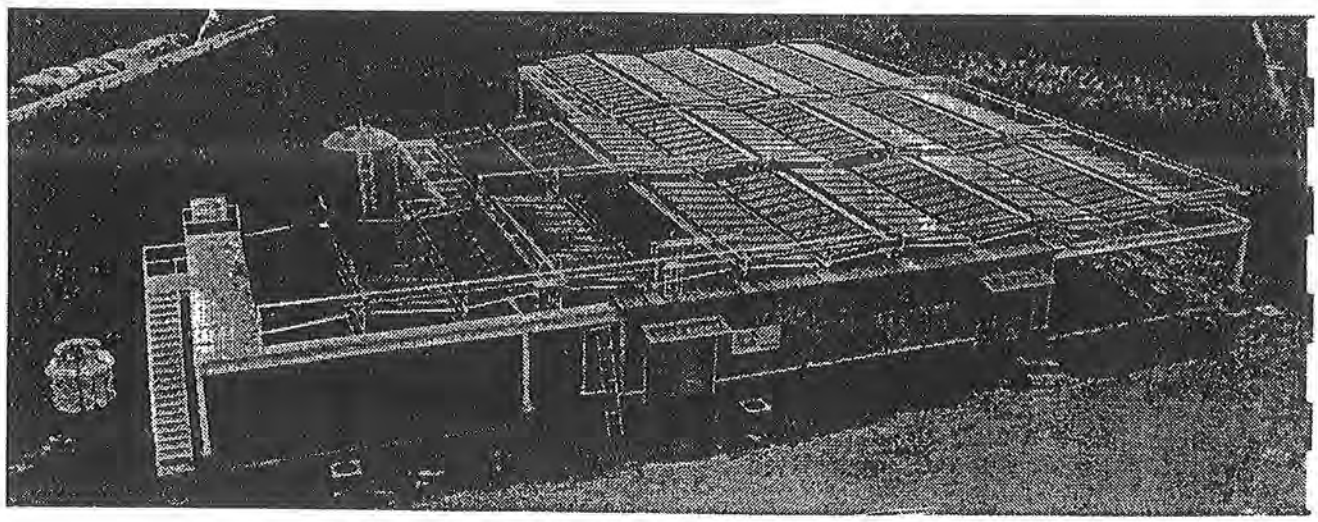

Fig. 9 Pilot plant in operation

Table 5. Outline of the plant

1. Site location	
Kitanakagusuku Village, Okinawa	
2. Size	
Site area	4,199 m²
Construction area	1,080 m²
Height to eaves	3.6m²
Major equipment	
High temperature solar collector	294pcs, 413k solar heat Collection
High temperature thermal storage tank	15m³
Absorption chiller	52kW
	266K takeout
Brine tank	8m³
Low temperature thermal storage tank	96MJ, 3 units
3. Size of refrigerated warehouse	
Structure	Prefabricated type
Floor area	167.67m² (incl. front room 37.26m²)
Warehouse capacity	402.5 m³
4. Conditions inside warehouse	273K to 268K
5. Storage items	Seaweed(hitoegusa, etc.) vegetables(celery, etc.), cut flowers(chrysanthemums, etc.)
6. Completion date	March 1987

Conclusions

Research is active concerning the availability of organic working fluids that will replace NH_3/H_2O. As for the TFE/NMP system, research has been conducted at Essen University and some data on the properties have been reported. Concerning the system, the patents of both working fluids and absorption refrigerating systems were registered in the U.S. and parts of Europe.[11][12] Test results of a solar powered absorption refrigerating machine in demonstrative operation satisfied the planned values.

Japan's $LiBr/H_2O$ absorption machines are widely known in Europe and the U.S., and there is increasing interest in research trends concerning new absorption systems[13].

It is hoped that the development of this system will fill the important role of solving future energy problems.

References

1. Steimle, F., "Arbeitsstoffsysteme für eine Absorptionswärmepumpe" , Universität Essen, (1984)
2. Giesberger, W., Trepp, Ch., Ki Extra 14 (1981) 37
3. Marphy, K. P., Phillips, B. A., ASHRAE Trans. Part 1 B (1983) 23
4. "Gas de France Research on Prototype Absorption Heat Pumps", Report of Gas de France (1985)
5. Pierson, J. L., "First Phase of Industrialization of an Absorption Heat Pump Project" , Report of Total Energy Development (1985)
6. Bokelmann, H., Renz, M., klima kälte Heizung 10 (1983) 403
7. Nakayama, T. et al. "Development of Refrigerant-Absorbent Fluid System for Absorption Cycles" XVII IIR Congress B.2.8, Wien (Austria), September 1987.
8. Mashimo, K. et al. "Development of Organic Working Fluids TFE/NMP and Application to absorption Refrigerating System (in Japanese)" 21th JAR Conference 109-112, Nagano (Japan), April 1987.
9. Halocarbon Products Co., FLUORINOLS, Fluorinol-100
10. Japan's Sunshine Project, 1987 Annual Summary of Solar Energy R & D Program, P. Ⅱ .21-25, July 1988, Published by Japan Industrial Technology Association
11. Nakayama, T. et al. United States Patent 4455247, (1984)
12. Mashimo, K. et al. United States Patent 4468934, (1984)
13. Mashimo, K. "6.4 Absorption Heat Pump" Proceedings of JAR International Symposium, Tokyo (Japan), March 1988

9. DEVELOPMENT OF AIR-COOLED GAS-FIRED ABSORPTION WATER CHILLER-HEATER

Shigekichi Kurosawa, Tokyo Gas Co., Ltd.
Yoshikazu Nagaoka, Tokyo Gas Co., Ltd.
Akio Yoshida, Osaka Gas Co., Ltd.
Masato Ogawa, Toho Gas Co., Ltd.
Yoshifumi Kunugi, Hitachi, Ltd.
Japan

1. Preface

Absorption chiller-heaters, which use gas as their fuel, have diffused so widely that they now represent the majority of air conditioners installed in large-size buildings whose floor space is not less than 3,000 ㎡. Meanwhile, they have not been so widely accepted in medium-size buildings between 700 and 3,000 ㎡ in floor space where packaged air conditioners — of air-cooled type in the main — are mainly installed.

The greatest cause that has prevented absorption chiller-heaters from becoming popular in medium-size buildings lies in the fact that the air-cooled type has not been developed. In order to popularize them, it is indispensable to make them available as the air-cooled type. If the existing water-cooled type could be replaced by the air-cooled type, the cooling tower, cooling water pump, cooling water piping, etc. would become unnecessary, bringing about great advantages in terms of construction and installation cost, operating cost, etc., while accompanying great merits, such as an increased ease of handling, enhanced level of reliability, etc. Duhring chart, as shown in Fig. 1.1. Principal working media (fluids) which can form an air-cooled absorption/refrigeration cycle are summarized in Table 1.1.

As mentioned above, it is extremely difficult to bring about an air-cooled chiller-heater with a high cooling COP. However, in order to meet the demand for the air-cooled type, we have set about technological development in order to overcome the difficulties in materializing the air-cooled type.

The points of technological development were set as follows:

1) The sole working medium available is the water-lithium bromide group.
2) The key technology consists in cooling the absorber, cooling the condenser, supply of refrigerant vapor to the absorber, etc.
3) The key component is the absorber whose only function is to absorb the liquid film flowing down inside the vertical tube and the air-cooled fin installed outside the tube.
4) The difference in equlibrium temperature between the absorber inlet and outlet is about 6 to 9K, so that it is effective to exchange heat of orthogonal counterflows of absorbent solution and cooling air.
5) It is indispensable to materialize the temperature and concentration of the absorber outlet solution comparable to those of the water-cooled machine.

This report will describe the absorbing performance, etc. of the cooled absorption/refrigeration cycle, have been developed or made commercially available, such as the ammonia group and R22 group. Among them, the ammonia-water group is extremely difficult to be put to practical use because of the defects inherent in ammonia, such as corrosiveness, explosiveness, toxicity, etc. Meanwhile, R22-tetraethylene glycol-dimethyl ether group, because of single-effect performance, is low in cooling COP (0.55)*and large in working pressure difference (1,2 MPa), so that this group has not yet been put to practical use. The three-component group, in which ethylene glycol is added to lithium bromide in order to improve the latter's crystallization, has been studied but has not yet been put to practical use, because of the low cooling COP and poor thermal stability.

On the other hand, if water-lithium bromide group — the only combination that has put the double-effect absorption/refrigeration cycle to practical use — is air-cooled in its entirely,lithium bromide will crystallize, and the working pressure will exceed atmospheric pressure. Mainly due to these reasons, it has been thought extremely difficult to realize air-cooling with this group. If the cooled air outlet temperature becomes higher than 40℃, the temperature and concentration of the solution at the absorber outlet will also become high, making the refrigeration cycle's working point shift to the high-temperature, high-concentration and high-pressure side so that the working pressure will become higher than atmospheric pressure and the lithium bromide will crystallize. Such difficulties in realizing an air-cooled absorbtion refrigeration cycle is pictorially represented in vertical absorber and the air-cooled absorber which use various types of heat transfer tubes.

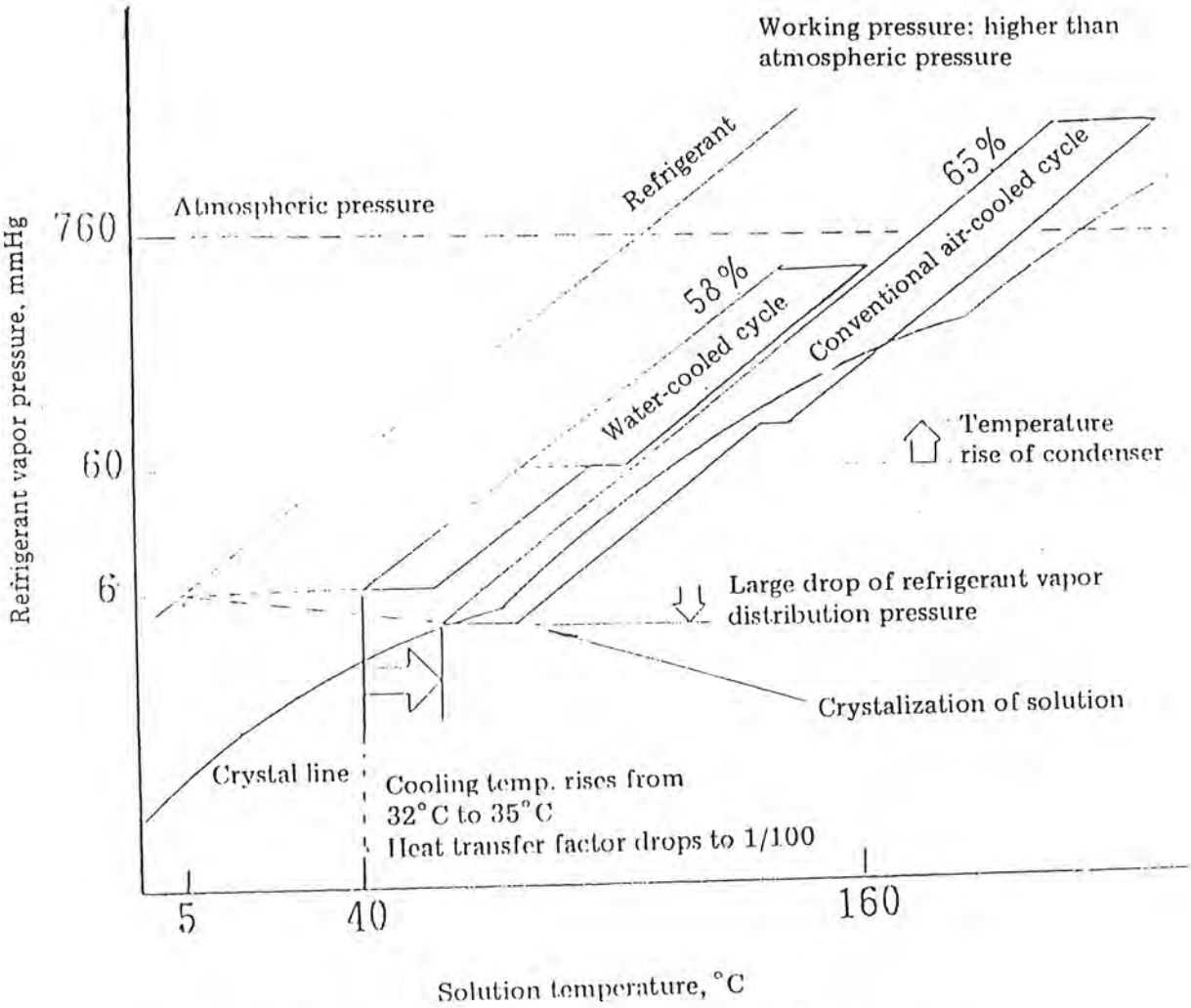

Fig. 1.1 Difficulties in realizing an air-cooled absorption/refrigeration cycle

Table 1.1 Evaluation of working media

Refrigerant absorbent	H_2O LiBr	H_2O LiBr+8G	NH_2 H_2O	R22 TEG • DMG	Remarks
Crystal of absorbent	Present	Head to crysta-lize	Nil	Nil	Crystal allowance
Working pressure	Vacuum	Vacuum	1.3MPa	1.2MPa	Pump power, Pressure vessel
Rectifier	Unnec-essary	Unnec-essary	Neces-sary	Unnec-essary	
Toxicity	Nil	Nil	Toxic	Nil	Toxicants, explo-sives, Class VI oils
Flammability	Nil	Class VI oils	Explo-sive	Class VI oils	
Thermal stability	Stable	Devel-oped at 140℃	Stable	Devel-oped at 200℃	Mainte-nance
Metal cor-rosiveness	Large	Large	Large	Small	
COP	0.9*	0.5	0.5	0.5	* Double effect
Regeneration temperature	90 ～ 170*	90～	150～	150～	
Direct expansion evaporator	Diffi-cult*	Diffi-cult*	Suitable for chiller	Easy	* Refrig-erant Frozen
Overall evaluation	○	△	×	△	

2. Absorbing performance of vertical absorbing tube[1]
(Report #1: Performance of smooth inner surface tube)

2.1 Symbols

Cp : specific heat, J/kg • K
ΔC : difference in refrigerant density, kg/m³
di : inside diameter of tube, m
do : outside diameter of tube, m
$G\ell$: average flow rate of solution of flowing-down liquid film, kg/s
Gs : quantity of refrigerant absorbed (rate of refrigerant mass transfer), kg/s
Gw : flow rate of cooling water, kg/s
L : length of heat transfer tube, m

Nu : Nusselt number
Pr : Prandtl number
Γ : flow rate of liquid film per unit width ($G\ell / \pi \cdot di$), kg/m・s
$4\Gamma / \mu$: film Reynolds number
μ : viscosity, kg/m・s
ξ : concentration of solution
ρ : density of solution, kg/m^3

2.2 Specimen heat transfer tube

Table 2.1 lists the type and dimensions of the specimen heat transfer tubes whose inner surface is smooth and whose length and inside diameter differ from one another, have been employed. The tube engineering material is copper.

Table 2.1 Specifications for specimen absorber

Type of absorber		Vertical tube absorption cross flow
Heat transfer tube	Type	Smooth inside surface tube
	Outside diameter	14.9 mm
	Inside diameter	13.7 mm
	Length	1.65 m
	Number of tubes	8 tubes × 1 row
Cross fin	Type	Slit fin
	Width	304 mm
	Depth	34 mm
	Length	0.18 mm
	Pitch	2.3 mm

2.3 Apparatus and method for experiment

Fig. 2.1 shows the system of apparatus for experiment. The apparatus for experiment are composed of a specimen heat transfer tube, an evaporator, a solution tank, circulating pump, etc., coming as a batch style. The specimen heat transfer tubes were constructed into double-tube heat exchangers whose outside was cooled with cooling water. The evaporator was heated with an electric heater so as to made constant the amount of vapor generated and also the evaporating temperature of water by agitating the refrigerant by means of the circulating pump.

Solution of lithium bromide, whose concentration had previously been adjusted to 55%, was sealed into the solution tank, agitated with the circulating pump, and thoroughly deaerated by means of a

vacuum pump. It was supplied to the inside of the heat transfer tube after having its flow rate adjusted by a needle valve. The solution, which had absorbed steam within the specimen heat transfer tube, was re-circulated to the solution tank until it became stabilized. When stabilized it was flowed into the flow meter which acted also as a solution collecting bottle (capacity: 1,000$m\ell$) via the change-over valve to measure its flow rate and concentration. Pressure of the upper and lower headers was measured by means of a digital manometer. The flow rate of cooling water was measured by means of a float-type flow meter and a measuring cylinder. Temperature of each section was measured by means of a 0.4-class sheathed thermocouple T 1 mm in diameter.

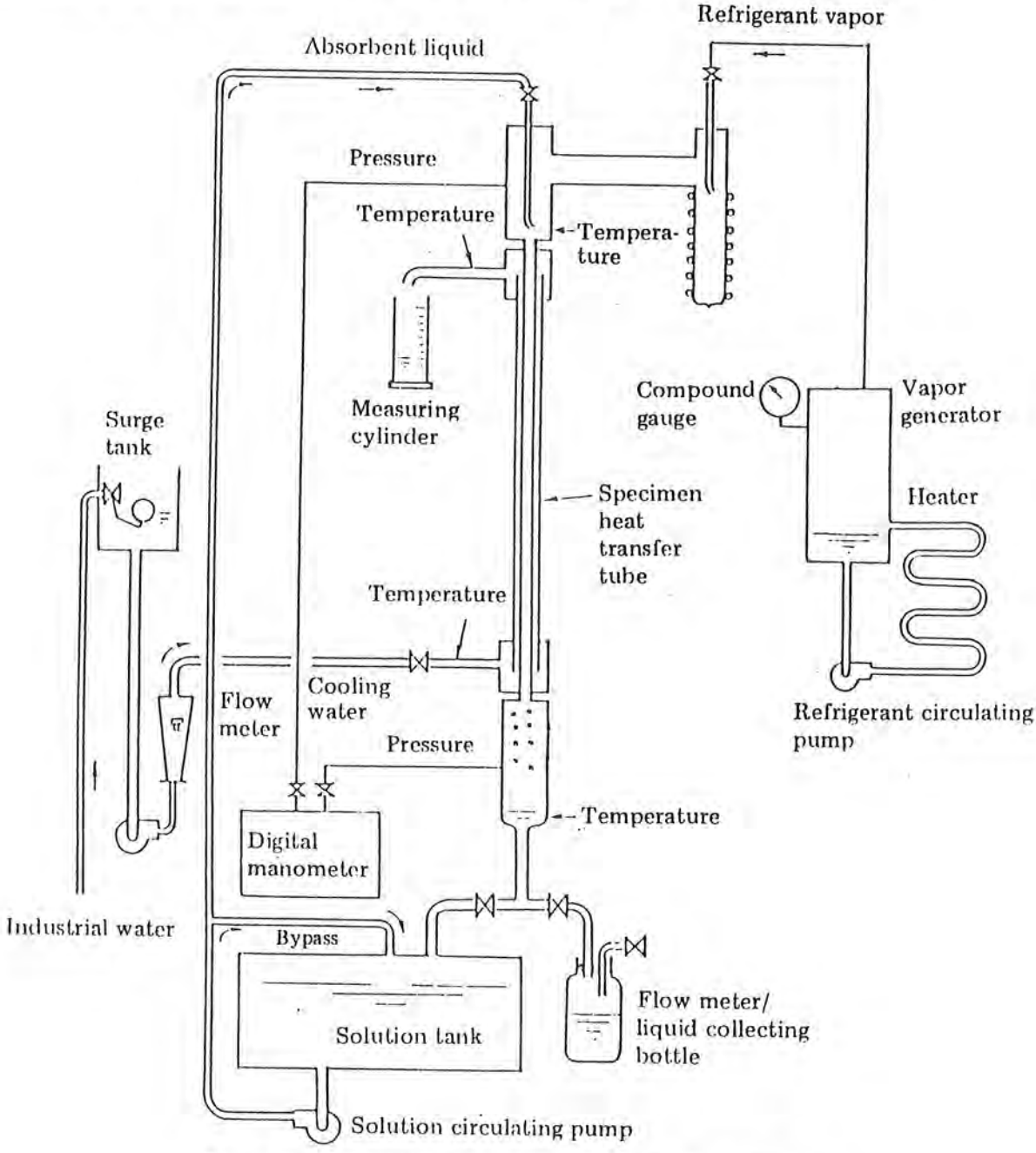

Fig. 2.1 Experimental apparatus system for single tube absorption

Fig. 2.2 illustrates the structure of the upper header of the vertical tube. Between the cooling-water header and the absorber header there was created a space about 5 mm in width for preventing the solution from being cooled by the cooling water within the absorber header. In like manner the lower header was also made adiabatic. Incidentally, the whole of the vertical tube was made adiabatic by winding a double layer of polyurethane foam around it. During the experiment, extraction of air by means of a vacuum pump was limited to the solution tank. It was ascertained that the air which leaked from the entire apparatus was less than 2×10^{-4} cc/s, as a result of leaving it in a vacuum.

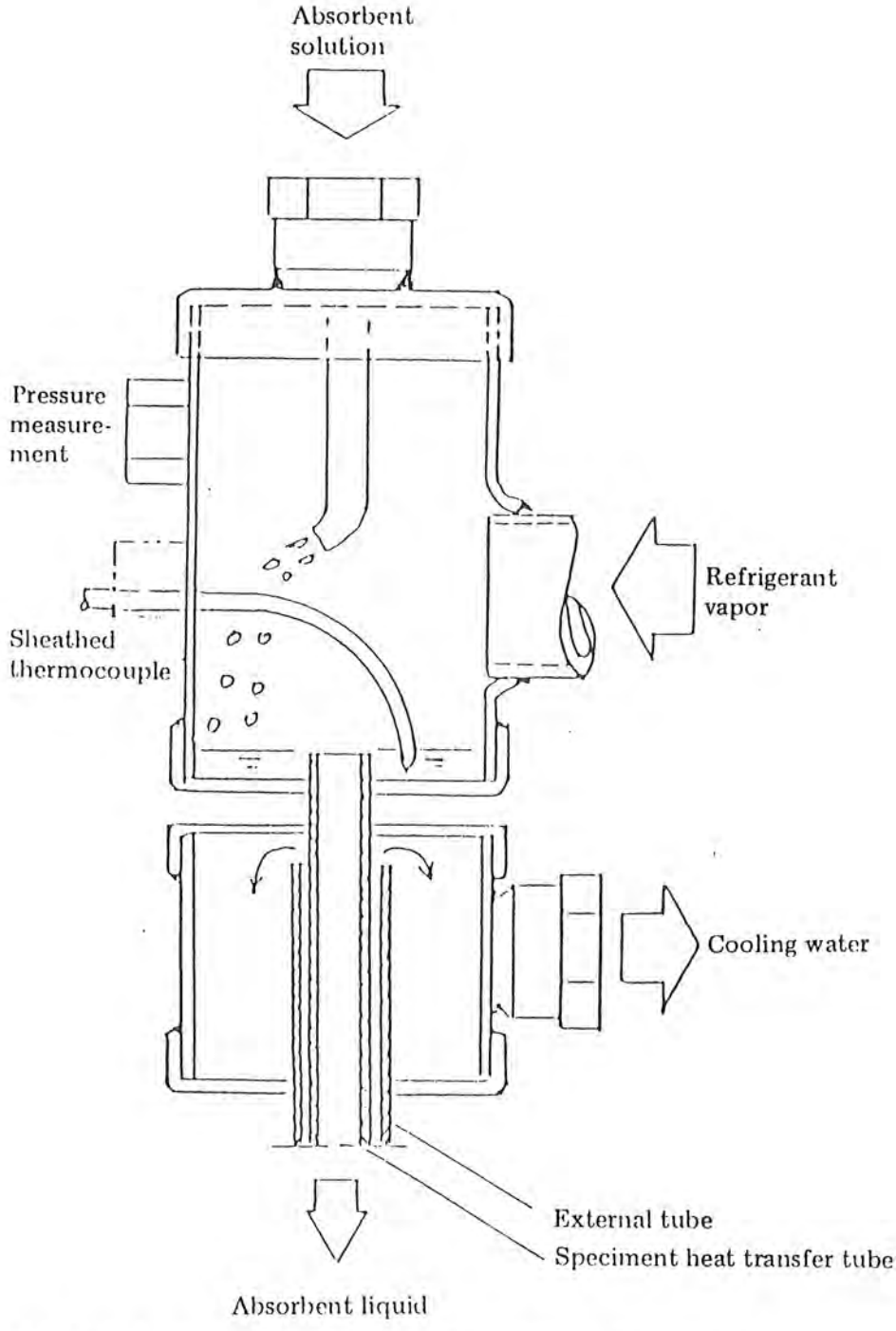

Fig. 2.2 Double tube heat exchanger inlet header

2.4 Method of putting results of experiment in order

Q[W], the quantity of heat exchanged, was found according to the formula (1) by using the cooling water inlet temperature, $T\ell i$ [℃], the outlet temperarure, Two[℃], quantity of cooling water, Gw[kg/s], and specific heat, Cp[J/kg・K], i.e.,

$$Q = Gw \cdot Cp(Two - Twi) \quad (1)$$

Heat exchange performed in the vertical tube is a counterflow heat exchange. By using the inlet temperature of solution, which was actually measured, $T\ell i$[℃], outlet temperature, $T\ell o$[℃], and inlet and outlet temperatures of cooling water, the log-mean temperature difference, $\Delta T\ell n$[K], was defined according to the formula (2) so as to find the overall heat transfer coefficient, K[W/㎡・K], according to the formula (3).

$$\Delta T\ell n = \{(Tli - Two) - (Tlo - Twi)\} / \ell n \{(Tli - Two)/(Tlo - Twi)\} \quad (2)$$

$$K = Q/\Delta T\ell n \cdot (\pi \cdot di \cdot L) \quad (3)$$

The water-side heat transfer factor of the outer surface of the tube, αo[W/㎡・K], was found by using the formula (4), which was often utilized for finding the turbulent flow heat.

$$Nu = 0.023 \cdot Re^{0.8} \cdot Pr^{0.4} \quad (4)$$

The factor of heat transfer which was absorbed inside the vertical tube, α[W/㎡・K], was found by applying the formula (5). Incidentally, heat resistance offered by the heat transfer tube wall was neglected.

$$\alpha = 1/\{(1/K) - (di/do \cdot \alpha o)\} \quad (5)$$

On the other hand, considering that the interface of β[m/s] gas and liquid of a flowing-down liquid film is in equilibrium with pressure inside the apparatus, and by using the diffirence in density of refrigerant, ΔC[kg/㎥], found from the equilibrium solution's concentration and the concentration of the solution of the flowing-down liquid film, the coefficient of mass transfer, β [m/s], was defined according to the formula (6).

$$\beta = Gs/\{\Delta C \cdot (\pi \cdot di \cdot L)\} \quad (6)$$

where Gs[kg/s] denotes the quantity of absorbed refrigerant.

According to the Duhring chart, when pressure is approximately constant, the grading of an increase or decrease in the solution tempreture to an increase or decrease in the equilibrium solution's concentration is constant. Therefore, the equilibrim solution temperature at the inlet and outlet was found from the measured solution's concentrartion and pressure inside the apparatus, while by using the formula (2) the log-mean temperature difference, $\Delta T\ell n$, was defiend. The difference, ΔT, between the log-mean temperature difference of this equilibrium temprature, $\Delta T\ell n$, and the log-mean temperature difference, $\Delta T\ell n$, is the difference in the non-equilibrium temperature which is necessary for the refrigerant to shift from the interface of gas and liquid to the inside of the flowing-down liquid film. If this ΔT is multiplied by the grading, $\Delta\xi/\Delta T$, found from the solution's concentration and the solution's temperature present in the vicinity of the pressure inside the apparatus, by making reference to the Duhring chart, the non-equilibrium concentration difference, $\Delta\xi$, between the equilibrium solution's concentration and the actually measured solution's concentration can be found by means of the formula (7).

$$\Delta\xi = (\Delta T\ell n^* - \Delta T\ell n) \cdot (\Delta\xi / \Delta T) \quad (7)$$

Since the difference in the solution's concentration, $\Delta\xi$ [−], was infinitesimal when compared with the concentration level of the solution, it was considered to be the same as the difference, ΔC, in the concentration of the solution. So the difference in the density of the refrigerant between the gas-liquid interface and the inside of the flowing-down liquid film was found according to the formula (8) by using the average solution's concentration, ξ [−], and the solution's density, ρ [kg/cm³].

$$\Delta C = \Delta\xi \cdot (1-\xi) \cdot \rho \quad (8)$$

where the pressure-balanced temperature of the solution was calculated by utilizing ASHRAE's data.

2.5 Results of experiment and their evaluation

The experiment was conducted by using an inlet solution's concentration of 55[LiBr%], inlet solution temperature of 45 to 55[℃], and cooling water temperature of 19 to 32[℃]. In Fig. 2.3 the film Reynold's number, $4\Gamma/\mu$, was shown along the bottom of the figure and the heat transfer factor, α [w/m² • K], along the left-hand side to indicate the results of the experiment on the absorption inside the vertical tube. For reference, the factor of heat transfer of absorption inside the vertical tube with a smooth inside surface was plotted by using a symbol mark X.

Salazar's data were concerned with the case where a water solution of LiBr was flowed down inside a vertical tube, 40 mm in diameter and 1.9 m in length, and was made to absorb refrigerant vapor and cooled by evaporating the refrigerant on the tube outside. The solution temperature was about 120 to 145℃ and it was devised to supply the solution by rotating the solution in the direction of the tangential line. It is seen from the figure that the results of Salazar's experiment agreed approximately with the results of the experiment conducted by the present authors and that the heat transfer factor was proportional to about 0.8th power of the film Reynolds number.

Fig. 2.4 shows that the film Reynolds number $4\Gamma/\mu$ was plotted along the horizontal axis and the coefficient of shifting of matter, β [m/s], along the vertical axis. The coefficient of mass transfer, β [m/s], along the horizontal axis and approximately proportional to the 0.5th power of the film Reynolds number. It was ascertained that the mass transfer factor had a tendency similar to the factor heat transfer factor.

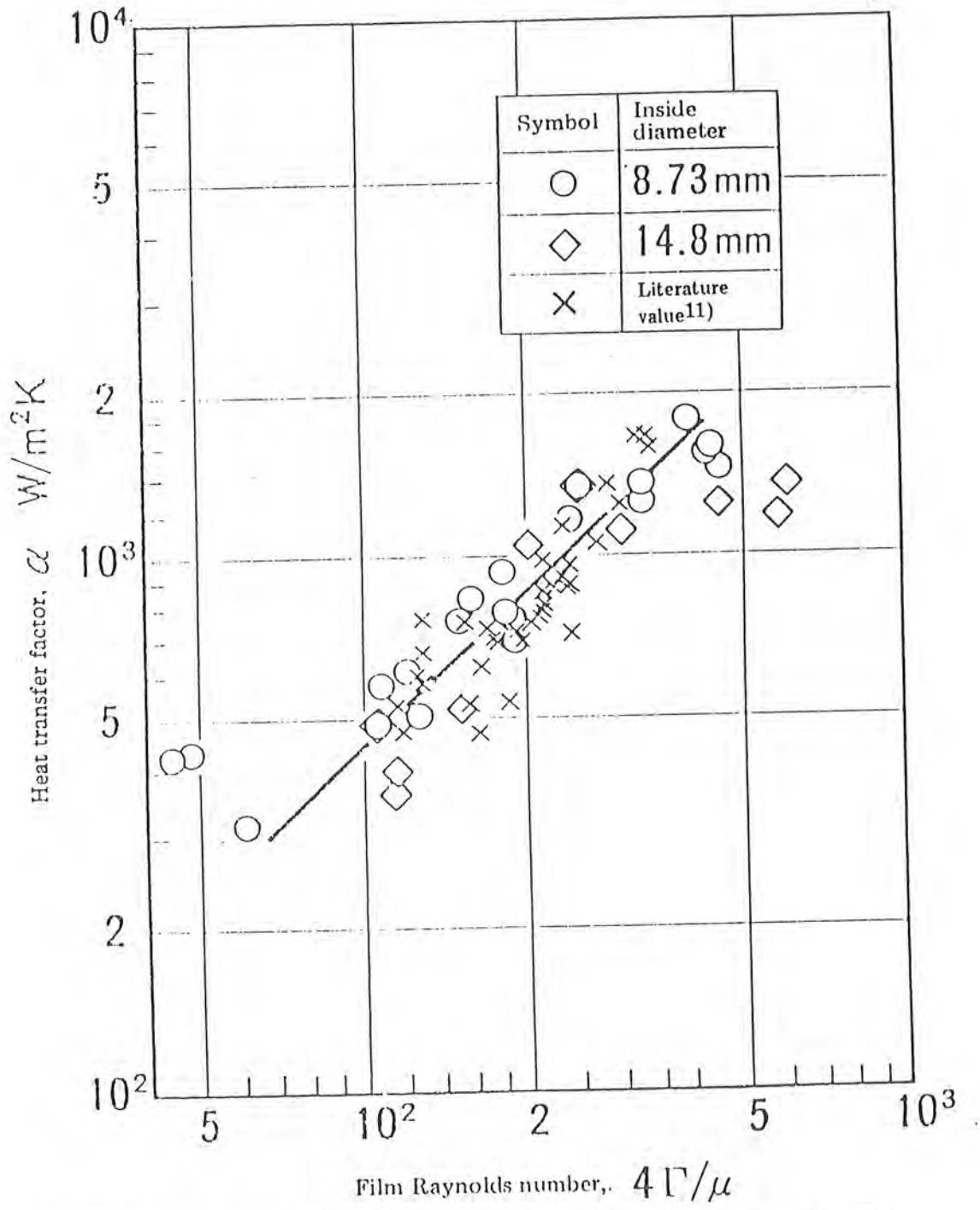

Fig. 2.3 Heat transfer factor of absorption in vertical tube with smooth inner surface

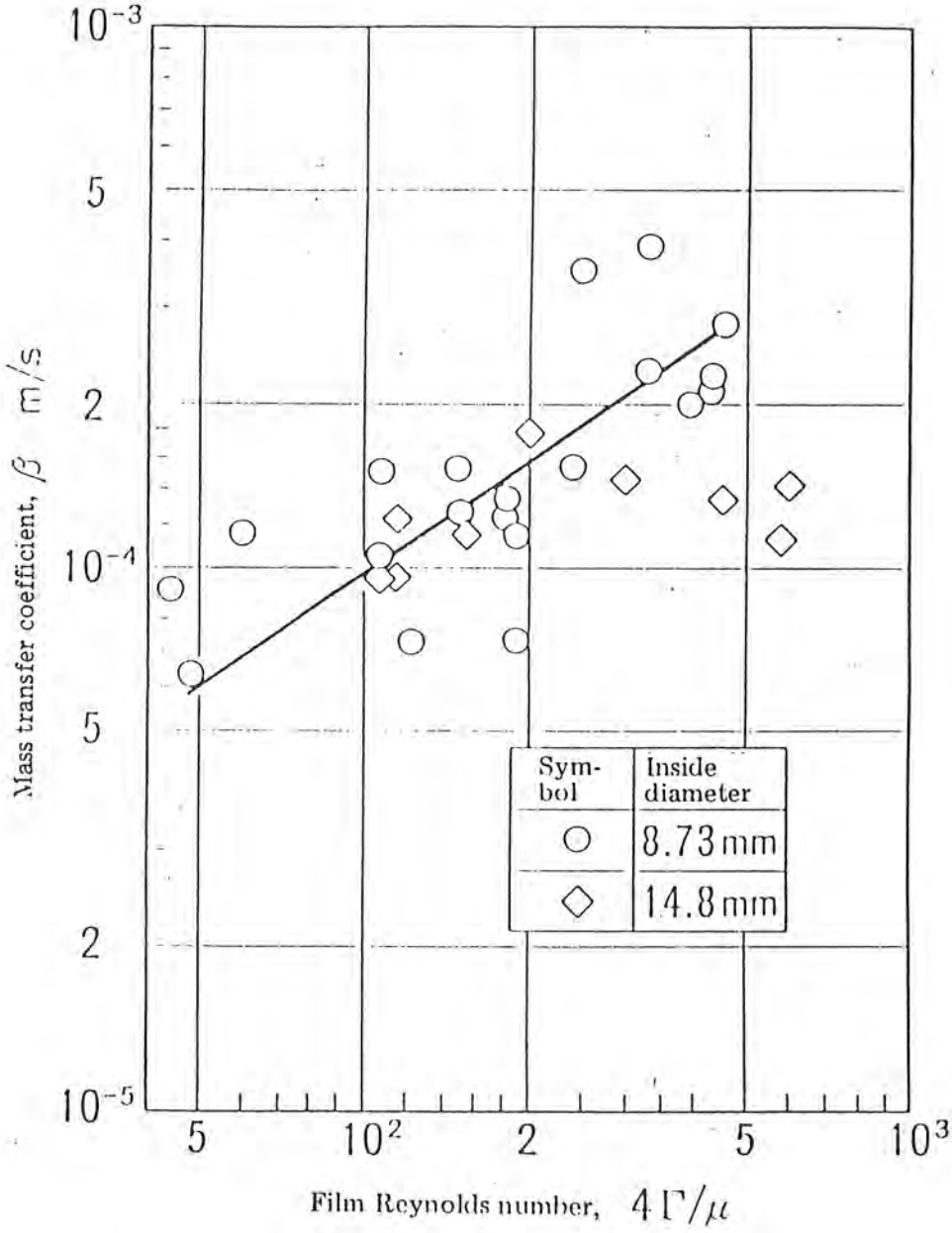

Fig. 2.4 Mass transfer coefficient of absorption in vertical tube with smooth inner surface

3. Absorption performace of vertical absorption tube[2] (Report #2: Performance of groups of tube with smooth inner surface)

3.1 Symbols

A : area of heat transfer, m^2

C : specific heat, kJ/kg

D : Quantity of vapor, kg/s
G : flow rate, kg/s
g : acceleration of gravity, m/s^2
h : enthalpy, kJ/kg
K : overall heat transfer coefficient, $kW/m^2 \cdot K$
Nu : Nusselt number
P : pressure, Pa
Q : quantity of heat exchanged, kW
T : absorbent liquid temperature, K
t : air temperature, K
α : heat conductivity, $kW/m^2 \cdot K$
β : mass transfer coefficient, m/h
Γ : flow rate per unit length, $kg/m \cdot s$
ν : coefficient of active viscosity, m^2/s
ξ : concentration of absorbent liquid, %
ρ : density, kg/m^3

Accompaniment letters
A : absorber
a : air
E : evaporator
ℓ : absorbent liquid
γ : refrigerant vapor
i : inlet, inside of heat transfer tube
o : outlet, outside of heat transfer tube

3.2 Calculation of absorption heat transfer and mass transfer coefficients

Fig. 3.1 shows a model of absorbent action by using it various methods of calculation will be described.

(1) Factor of absorption heat transfer

The quantity of heat exchanged by the absorber will be denoted from the refrigerant side and the absorbent liquid side, respectively, as:

$$Qa = Ca \cdot Ga \cdot (Ts - Ti) \quad (1)$$

$$Q\ell = G\ell \cdot (hi - hs) + D \cdot (hv - ho) \quad (2)$$

Theoretically speaking, Qa agrees with $Q\ell$. Therefore, by way of verification, an examination was made by referring to the quantity of heat exchanged for these two items. Hereinafter Qa and $Q\ell$ will be generally referred to as Q. Q, the quantity of heat exchanged will be denoted by the following formula by using the overall heat transfer coefficient, Ki, and the log-mean temperature difference, ΔTm, i.e.,

$$Q = Ki \cdot Ai \cdot \Delta Tm \quad (3)$$

where

$$\Delta Tm = \{(Ti - to) - (To - ti)\} / \ell n \{(Ti - to)/(To - ti)\} \quad (4)$$

On the other hand, the relationship between the overall heat transfer coefficient, Ki, and the factor of heat transfer inside the tube, αi, and the factor of heat transfer outside the tube, αo, is given by the following formula.

$$1/Ki = (1/\alpha i) + (Ai/\alpha o \cdot Ao) \quad (5)$$

By using the formulas (1) to (5), the factor of absorbed heat transfer, αi, was found.

(2) Coefficient of mass transfer

The quantity of refrigerant vapor absorbed consists of the quantity of vapor, D_1, which can be found from the heat balance of the vapor generator and of the quantity of vapor, D_2, which can be found from the balance of the quantity of discharged heat of the absorber.

The former is

$$D_1 = Q(hv - hr) \tag{6}$$

while the latter is

$$D_2 = \{Q - G\ell i(hi - ho)\} / (hv - ho) \tag{7}$$

Theoretically, D_1 and D_2 become equal to each other. Therefore, by way of verification, the coefficient of mass transfer was found by using the above two items according to the following method: Firstly, by using the concentration of absorbent liquid, the log-mean concentration difference was determined in the manner given in the formula (8).

$$\Delta \xi m = \{(\xi i - \xi s) - (\xi o - \xi s)\} / \ell n \{(\xi i - \xi s)/(\xi o - \xi s)\} \tag{8}$$

where ξi, ξo are actually measured values and ξs is a saturated concentration at solution temperature, To, and under pressure P.

Therefore, the coefficient of mass transfer, β, was found as:

$$\beta = D/(\rho \ell \cdot Ai \cdot \Delta \xi m) \tag{9}$$

3.3 Apparatus and method for experiment

Table 2.1 lists technical data about the specimen absorber. By using the above heat transfer tube and cross fin, an absorber featuring absorption inside the vertical tube and orthogonal type using air cooling has been manufactured. Fig.3.2 shows apparatus for experiments on specimen absorbers. The apparratus for experiment are composed of a specimen absorber, vapor generator, condenser, regenerator, heat exchanger, etc. which are designed for operating a refrigeration cycle. The items for measurement consist, as shown in Fig. 3.2, of temperature of the working liquid, its flow rate and pressure at each position shown in Fig. 3.2, in addition to the specific weight of the scattered liquid of the absorbent liquid in the absorber, specific weight of the liquid flowing down the heat transfer tube, running speed a temperature of cooling air.

For measuring these items, a Baume's hydrometer was employed for measuring the specific weight, a hot-wire anemoneter for the cooling air running speed, and a sheathed thermocouple T for the temperature. During measuring operation a high-speed dotting recorder was employed for monitoring the temperature within the cycle operation to ascertain that the temperature was steady-state satisfactorily.

3.4 Results of experiments and their assessment

Fig. 3.3 shows the relationship between the Nusselt number and the film Reynolds number. (The Nusselt number was calculated by determining its representative dimensions: $3\nu^2/g$). The heat transfer performance which was found from the data about the amount of heat radiated from the absorber into the mass of cooled air and the heat transfer performance found on the basis of the data about

the evaporator's capacity became approximatety equal in value to each other. It was found that the two values could be approximated to each other by using the Nusselt number, i.e., under the condition of $100 < Re < 1000$,

$$Nu = 0.85 \cdot Re^{0.639} \quad (10)$$

Secondly, in order to compare the heat absorbing and transferring performance measured along the internal surface of the vertical tube with that measured along its external surface, the heat absorbing and transferring performance, which had been disclosed formerly, was also entered in Fig. 3.3. According to this entry, it turned out that under the condition of $100 < Re < 400 \sim 600$, the heat transferring performance exhibited along the outer surface of the tube produced a better result than that along its outer surface. Moreover, it can be estimated that under the condition of $400 \sim 600 \leqq Re$, the situation of the heat transferring performance will be reversed. The reason for this reversal may be as follows: Since the liquid film is thin under the condition of $Re \leqq 400 \sim 600$, the effect of convection facilitation within the liquid film caused by vapor stream, which is conspicuous in the case of absorption inside the tube, does not become apparant but the film is broken partially by the vapor stream so that the heat transferring performance of absorption from the outer surface of the tube is better than that from its inner surface.

On the other hand, under the condition of $400 \sim 600 \leqq Re$, the liquid film is properly thick so that it is not broken and the effect of convection facilitation within the liquid film caused by vapor stream does not become apparent so that it can be considered that the absorption from the inner surface of the tube provides a better heat transferring performance than that from its outer surface.

Fig. 3.4 shows the relationship between the coefficient of mass transfer and the film Reynolds number. As in the case of the above-mentioned calculation of absorption heat transfer performance, on the basis of data about the quantity of heat discharged by the absorber into the mass of cooled air, the quantity of absorbed refrigerant was calculated so as to find the coefficient of mass transfer and also on the basis of the quantity of refrigerant vapor generated by the evaporator, the coefficient of mass transfer was found. The two coefficients have proved to approximate each other.

While under the condition of $100 < Re < 200 \sim 300$, the coefficient of mass transfer takes up an approximately fixed value, under the condition of $200 \sim 300 < Re$ the value becomes rapidly high, i.e.

$$\beta = 1.850 \times 10^{-8} Re^{2.78} \quad (11)$$

such a result may be due to the following reason: When Re is small, the liquid film was thin and the effect of convection facilitation is prevented from appearing so that the coefficient of mass transfer stays unchanged. On the other hand, when the Re value is high, the liquid film is comparatively thick, the convection is facilitated by the disturbed air-liquid interface, so that the coefficient of mass transfer may be rapidly improved.

Thirdly, the coefficient of mass transfer in the case of absorption from the outer surface of the vertical tube is compared

and examined. Fig. 3.4 shows the coefficient of mass transfer in the case of absorption from the tube outer surface, which was disclosed formerly. Under the condition of R ≒ 500, the value of the coefficient of mass transfer in the case of absorption from the outer surface is reversed to that in the case of absorption from the inner surface.

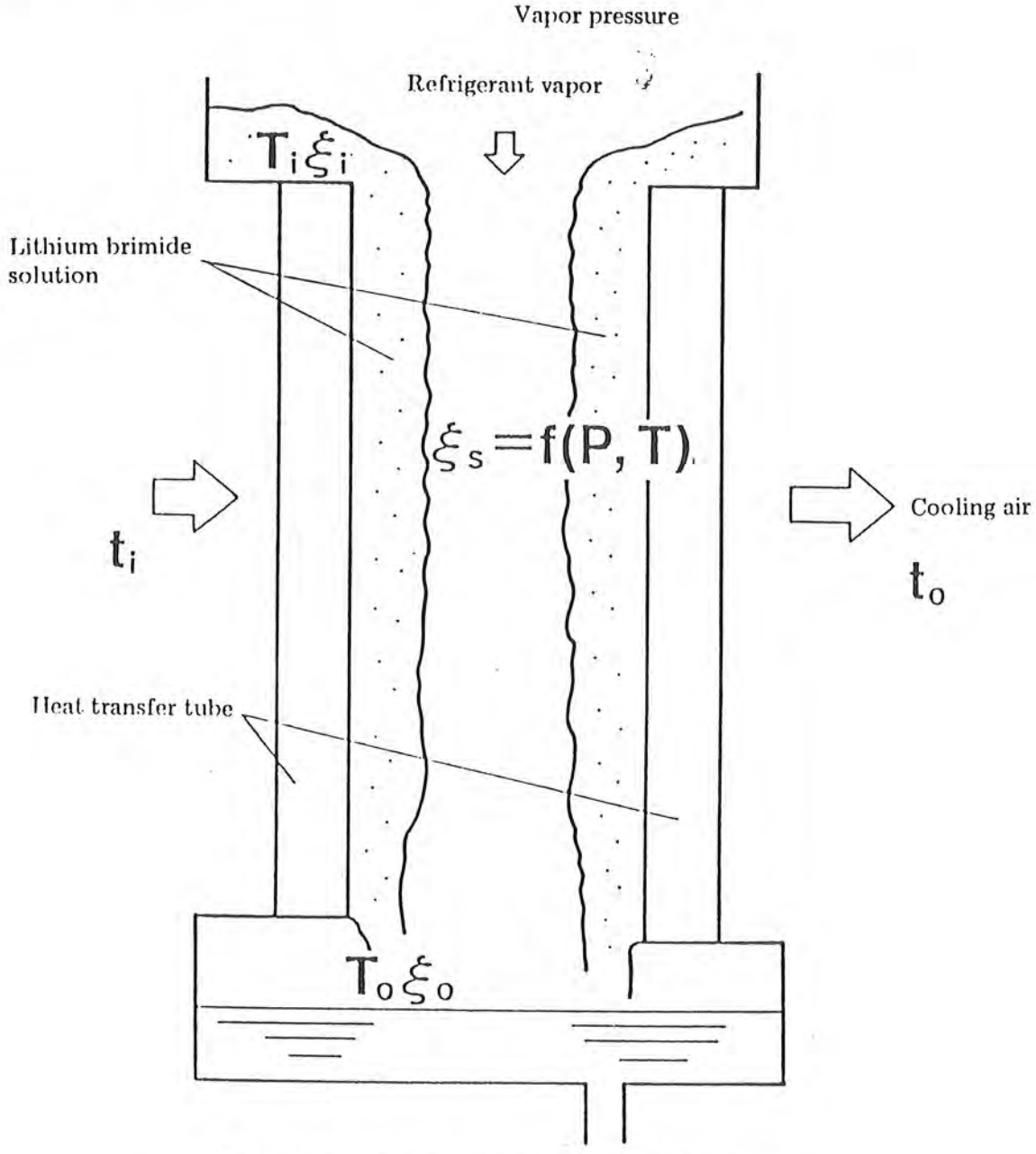

Fig. 3.1 Model of absorbent action

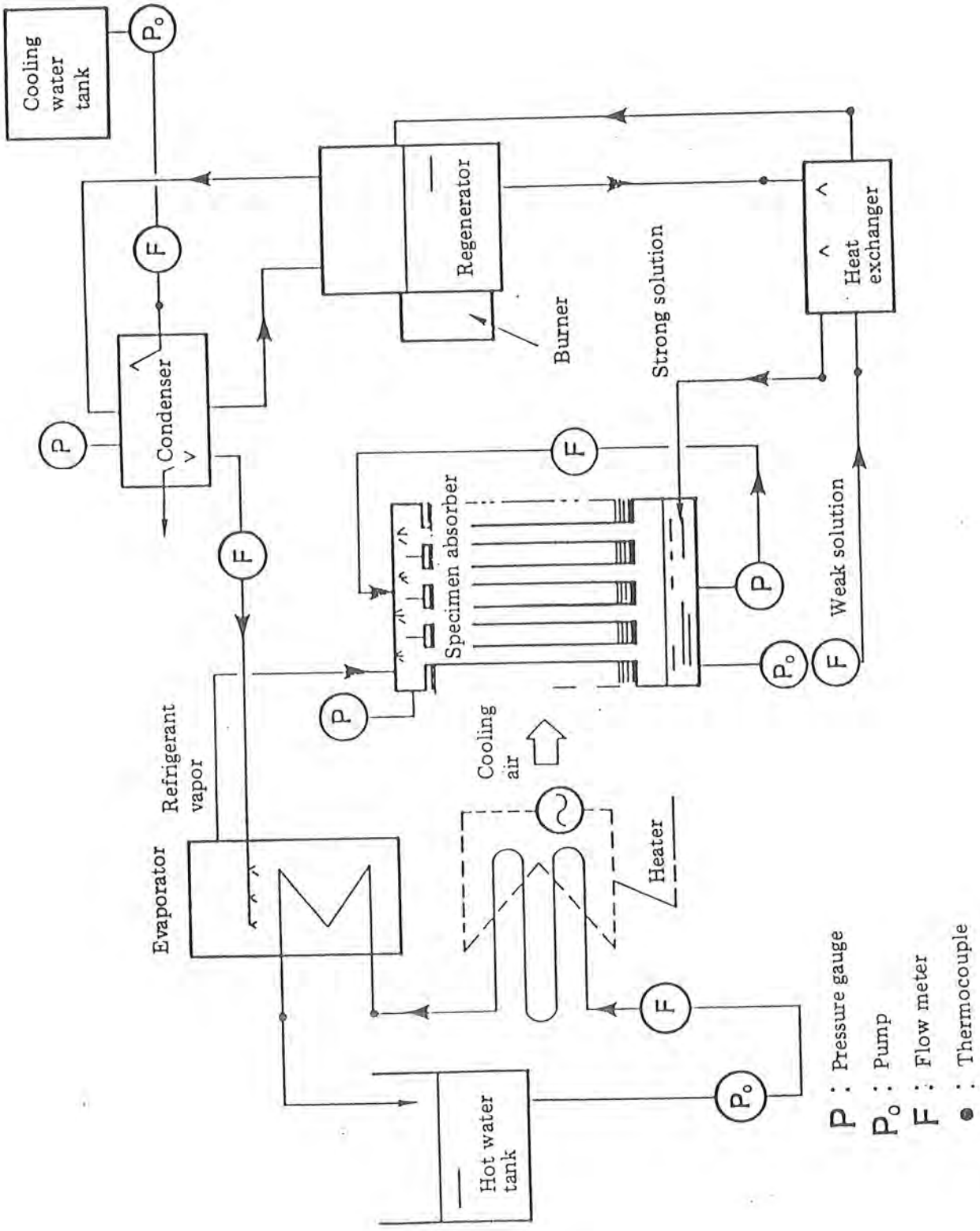

Fig. 3.2 Specimen absorber experimenting apparatus

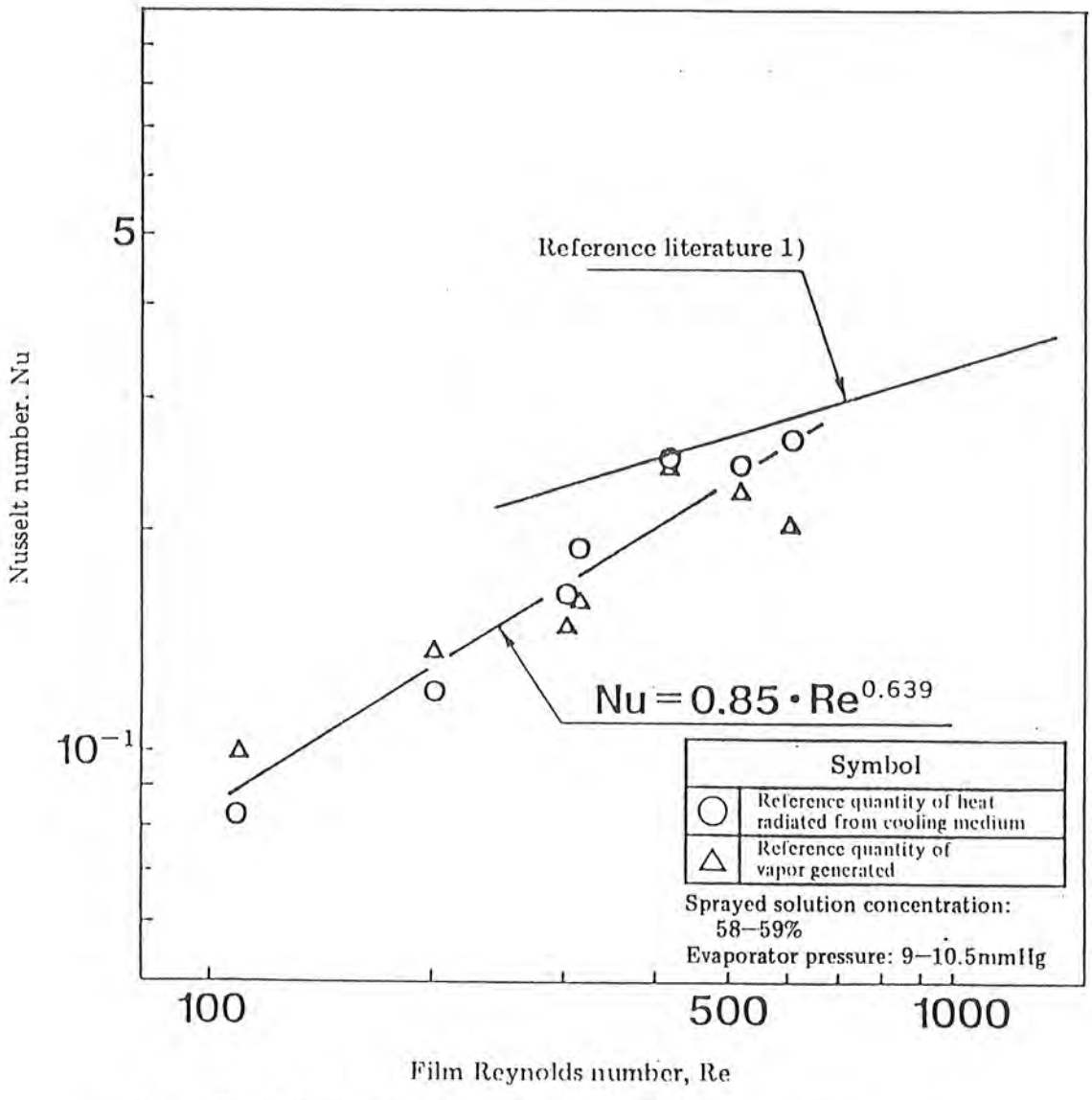

Fig. 3.3 Absorption heat transfer performance

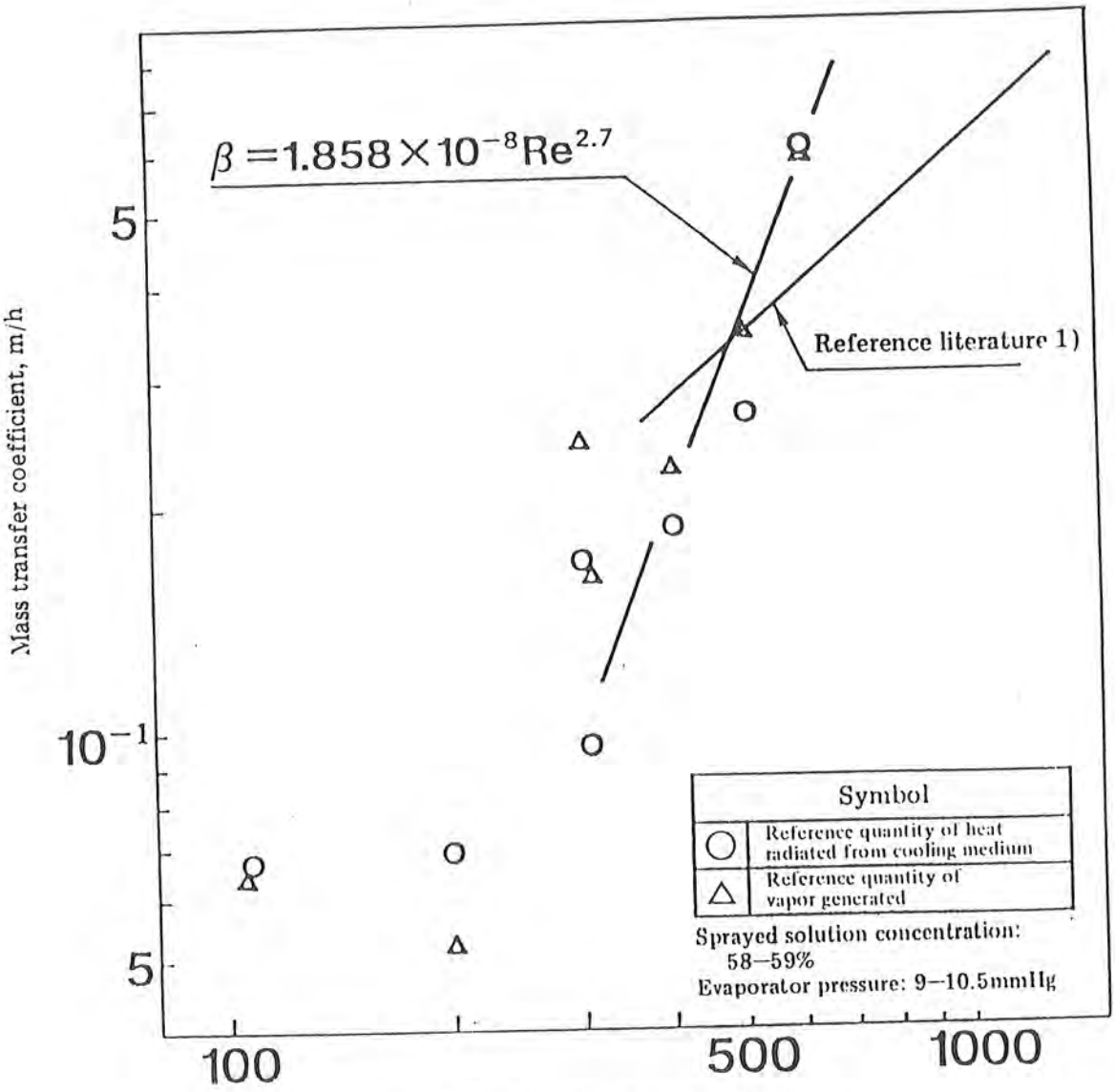

Fig. 3.4 Mass transfer coefficient

4. Absorbing performance of single tube absorber with grooved inner surface[3)]
(Report #2: Relations with film Reynolds number)

4.1 Symbols

Cp	:	specific heat, J/kg・K
ΔC	:	difference in refrigerant density, kg/m^3
di	:	inside diameter of tube, m
do	:	outside diameter of tube, m
$G\ell$	:	average flow rate of solution of flowing-down liquid film, kg/s
Gs	:	quantity of refrigerant absorbed (rate of refrigerant mass transfer), kg/s
Gw	:	flow rate of cooling water, kg/s
L	:	lengh of heat transfer tube, m
Nu	:	Nusselt number

Pr : Prandtl number
Γ : flow rate of liquid film per unit width($G\ell / \pi \cdot di$), kg/m・s
$4\Gamma / \mu$: film Reynolds number
μ : viscosity, kg/m・s
ξ : concentration of solution
ρ : density of solution, kg/m^3

4.2 Specimen heat transfer tube

Table 4.1 lists the specifications for the specimen heat transfer tubes whose inner surface groove shape, length and inside diameter differ from one another, have been employed. The tube engineering material is copper.

4.3 Apparatus and method for experiment

Fig. 4.1 shows the system of apparatus for experiment. The apparatus for experiment are composed of a specimen heat transfer tube, an evaporator, a solution tank, circulating pump, etc., coming as a batch style. The specimen heat transfer tubes were constructed into double-tube heat exchangers whose outside was cooled with cooling water. The evaporator was heated with an electric heater so as to made constant the amount of vapor generated and also the evaporating temperature of water by agitating the refrigerant by means of the circulating pump.

Solution of lithium bromide, whose concentration had previously been adjusted to 55%, was sealed into the solution tank, agitated with the circulating pump, and thoroughly decresed by means of a vacuum pump. It was supplied to the inside of the heat transfer tube after having its flow rate adjusted by a needle valve. The solution, which had absorbed steam within the specimen heat transfer tube, was re-circulated to the solution tank until it became stabilized. When stabilized it was flowed into the flow meter which acted also as a solution collecting bottle (capacity: 1,000$m\ell$) via the change-over valve to measure its flow rate and concentration. Pressure of the upper and lower headers was measured by means of a digital manometer. The flow rate of cooling water was measured by means of a float-type flow meter and a measuring cylinder. Temperature of each section was measured by means of a 0.4-class sheathed thermocouple T 1 mm in diameter.

4.4 Heat transfer performance of absorber

Q[W], the quantity of heat exchanged, was found according to the formula (1) by using the cooling water inlet temperature, Tℓ i[℃], the outlet temperarure, Two[℃], quantity of cooling water, Gw[kg/s], and specific heat, Cp[J/kg・K], i.e.,

$$Q = Gw \cdot Cp(Two - Twi) \quad (1)$$

Heat exchange performed in the vertical tube is a counterflow heat exchange. By using the inlet temperature of solution, which was actually measured, Tℓ i[℃], outlet temperature, Tℓ o[℃], and inlet and outlet temperatures of cooling water, the log-mean temperature difference, $\Delta T\ell n$[K], was defined according to the formula (2) so as to find the overall heat transfer coefficient,

K[W/m² • K], according to the formula (3).

$$\Delta T\ell n = \{(Tli - Two) - (Tlo - Twi)\} / \ell n \{(Tli - Two)/(Tlo - Twi)\} \quad (2)$$

$$K = Q/\Delta T\ell n \cdot (\pi \cdot di \cdot L) \quad (3)$$

The water-side heat transfer factor of the outer surface of the tube, αo[W/m² • K], was found by using the formula (4), which was often utilized for finding the turbulent flow heat.

$$Nu = 0.023 \cdot Re^{0.8} \cdot Pr^{0.4} \quad (4)$$

The factor of heat transfer which was absorbed inside the vertical tube, α [W/m² • K], was found by applying the formula (5). Incidentally, heat resistance offered by the heat transfer tube wall was neglected.

$$\alpha = 1/\{(1/K) - (di/do \cdot \alpha o)\} \quad (5)$$

On the other hand, considering that the interface of β [m/s] gas and liquid of a flowing-down liquid film is in equilibrium with pressure inside the apparatus, and by using the difference in density of refrigerant, ΔC[kg/m³], found from the equilibrium solution's concentration and the concentration of the solution of the flowing-down liquid film, the coefficient of mass transfer, β [m/s], was defined according to the formula (6).

$$\beta = Gs/\{\Delta C \cdot (\pi \cdot di \cdot L)\} \quad (6)$$

where Gs[kg/s] denotes the quantity of absorbed refrigerant, and ΔC denotes the difference of refrigerant density.

Incidentally, the difference of density, ΔC, between the gas-liquid interface and the inside of the flowing-down liquid film, can be found by the application of the formula (7) and by using the mean solution's concentration, ξ [−],and the solution's density, ρ [kg/m³].

$$\Delta C = \Delta \xi \cdot (1 - \xi) \cdot \rho \quad (7)$$

$\Delta \xi$ can be found by the application of the formula (8) and by using the difference in the non-equilibrium concentration between the equilibrium solution's concentration of the flowing-down liquid film and the measured solution.

$$\Delta \xi = (\Delta T\ell n^* - \Delta T\ell n) \cdot (\Delta \xi / \Delta T) \quad (8)$$

where $\Delta T\ell n^*$ denotes the log-mean temperature difference of the equilibrium temperature, and $\Delta T\ell n$ denotes the log-mean temperature difference. For calculating the pressure-equilibrium temperature, McNeely's data were employde.

4.5 Results of experiments and their evaluation

Firstly, Fig. 4.2 shows the relations between the quantity of vapor absorbed and the quantity of heat exchanged when a tube with grooved inner surface was employed. Since the amount of absorbed vapor was in proportion to the amount of exchanged heat, a phenomenon of absorption accompanying generation of heat could be affirmed. Accordingly, there was no difference in the relationship caused by the heat transfer tube Fig. 4.3 shows the film Reynolds number, $4\Gamma/\mu$, plotted along the horizontal axis and the factor of heat transfer, α [W/m² • K], along the vertical axis, in order to illustrate the results experiments on absorption performed inside the vertical tube. This figure shows also the results of experiments produce by the smooth inner surface tube described in

the preceeding-report. It is seen from Fig. 4.3 that the factor of heat transfer inside the tube was improved about 50% when the tube's inner surface was provided with grooves.

Fig. 4.4 is the graphical representation of a tube by means of two lines drawn at right angles on a piece of graph paper. Referring to the tube under consideration, the film Reynolds number, $4\Gamma/\mu$, is plotted along the X-axis (abscissas)and the coefficient of mass transfer, β [m/s], along the Y-axis (ordinates). This figure shows also the results of experiments conducted on a smooth inner surface tube. It is seen also from this figure that a grooved inner surface tube improves the coefficient of mass transfer about 50%. The correlation between the factor of heat transfer and the coefficient of mass transfer, which is the results of Figs. 4.3 and 4.4, is illustrated in Fig. 4.5. The factor and the coefficient may be said to be correlative to each tube of heat transfer. The elucidation of such absorption mechanisms is a problem to be solved in the future.

Table 4.1. Specifications for specimen inner grooved tube (mm)

No.	Number of grooves	Groove shape	Inside diameter	Outside diameter	Length	Inside diameter of double tube
1	60	Trapezoid	8.93	9.53	1025	13.84
2	90	Triangle	14.4	16.0	1625	22.61
Reference	Smooth inside surface tube		8.73 14.8	9.53 16.0	1025 1625	13.84 22.61

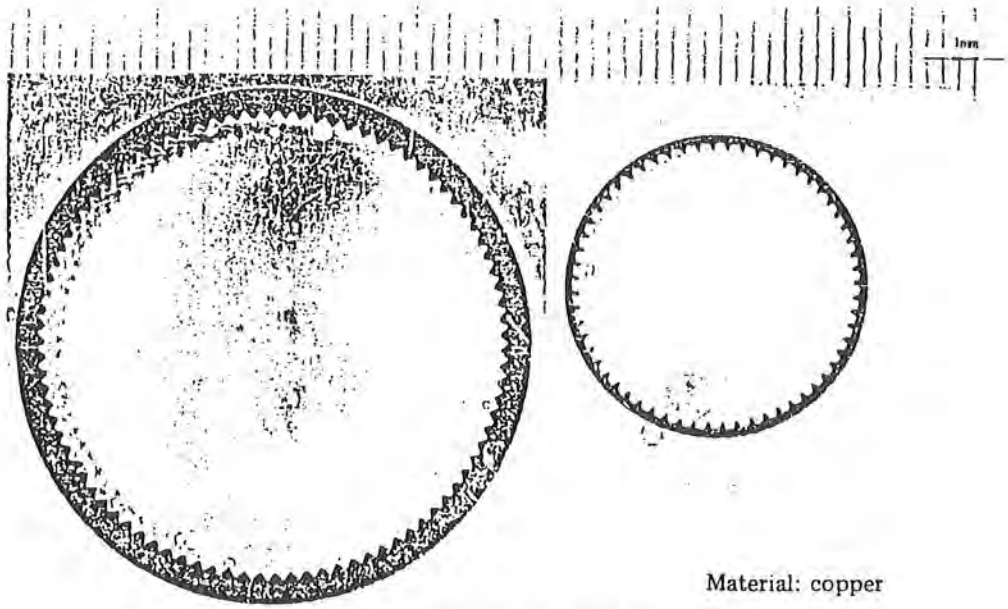

Reference drawing: Specimen inner grooved tube (cross-sectional view)

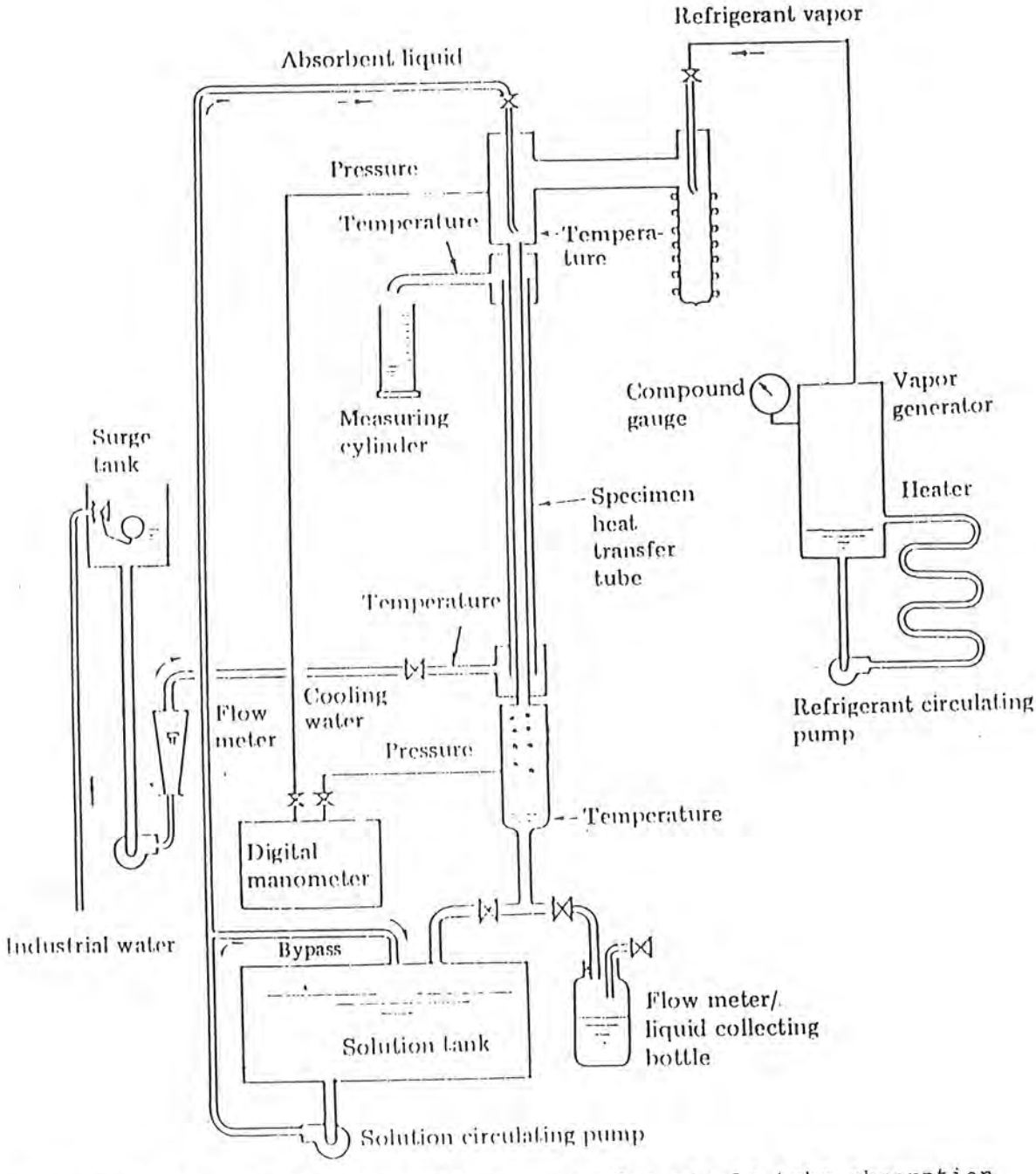

Fig. 4.1 Experimental apparatus system for single tube absorption

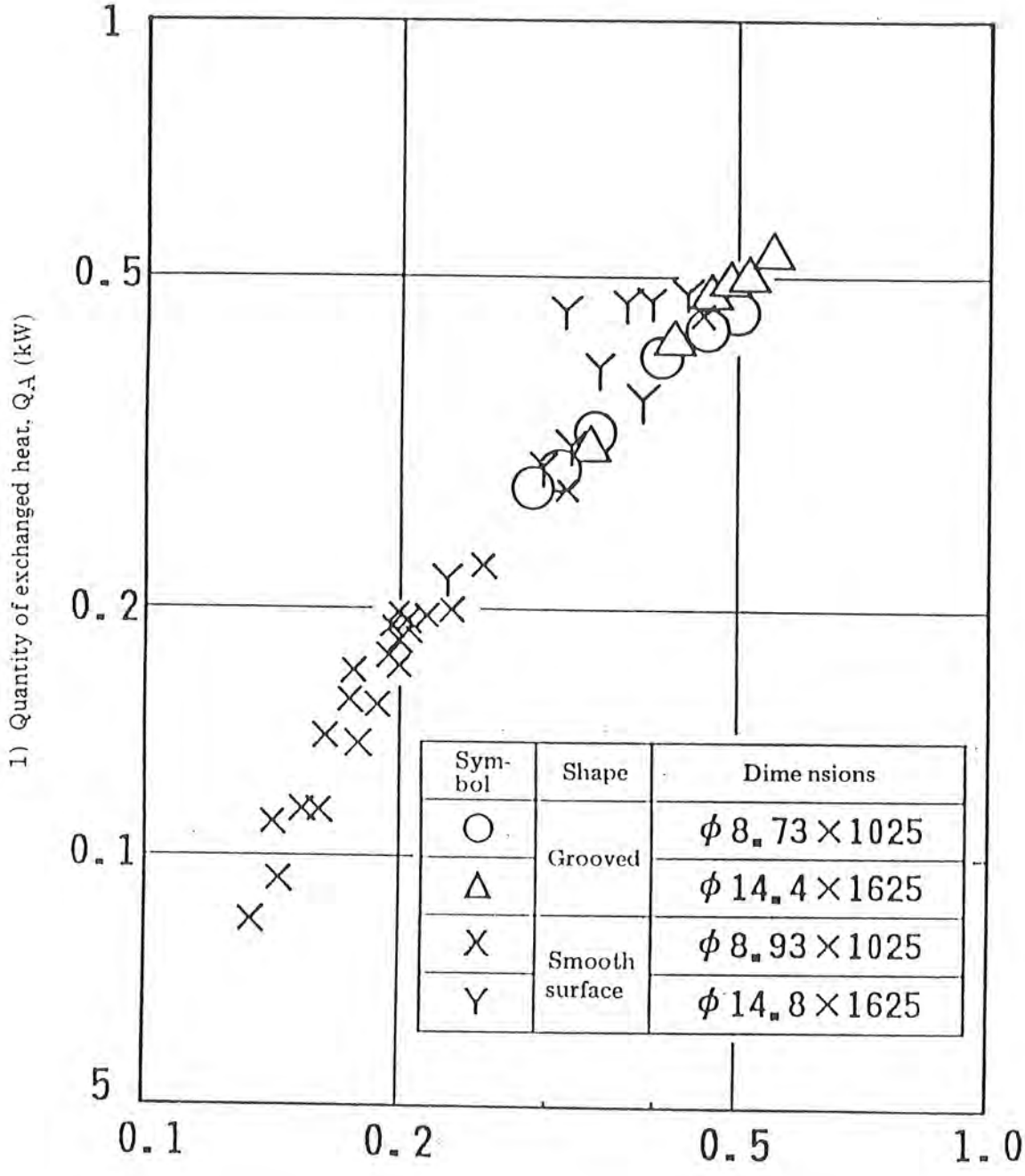

Fig. 4.2 Quantity of absorbed refrigerant and quantity of exchanged heat

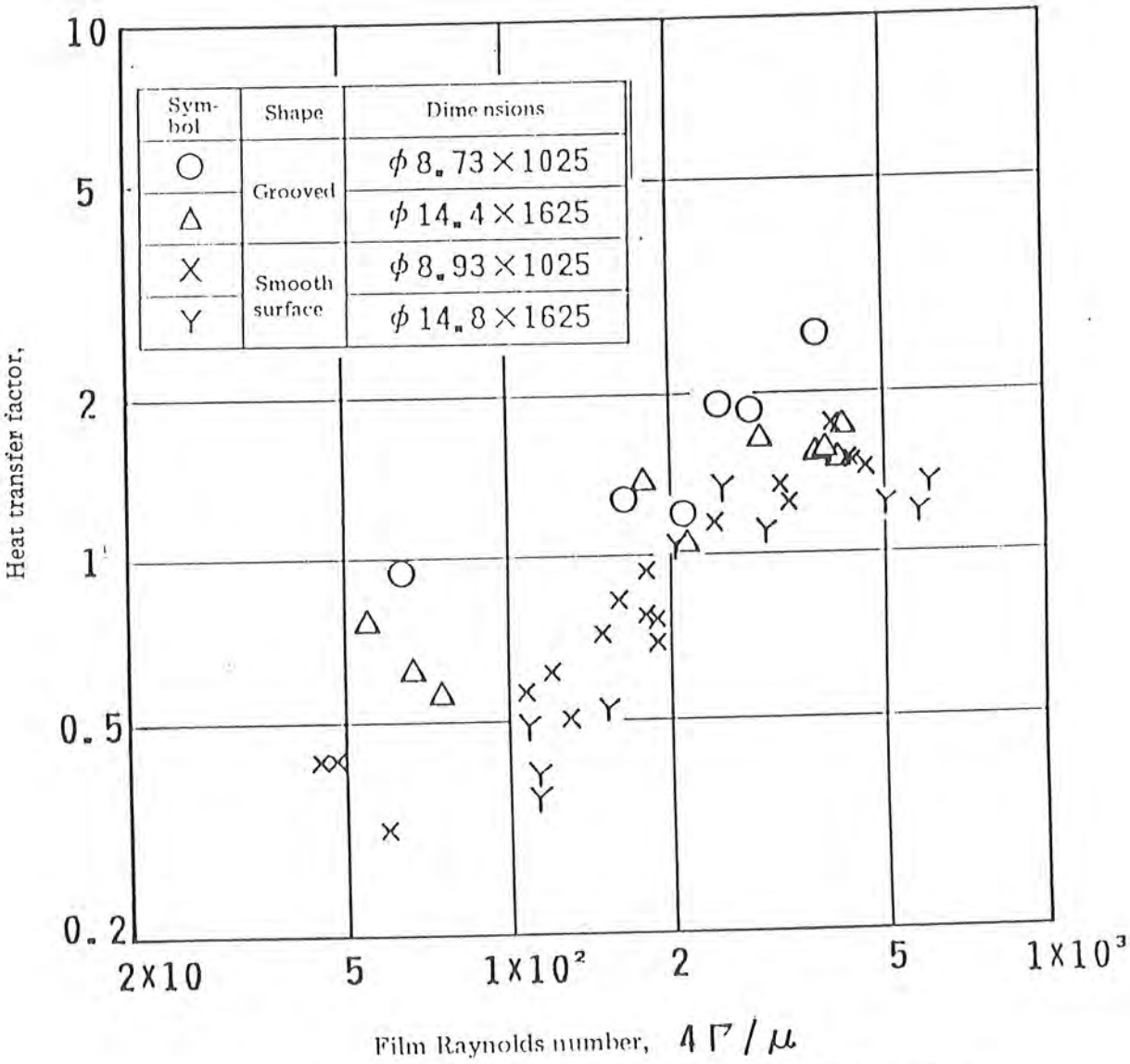

Fig. 4.3 Heat transfer factor of vertical absorbing tube

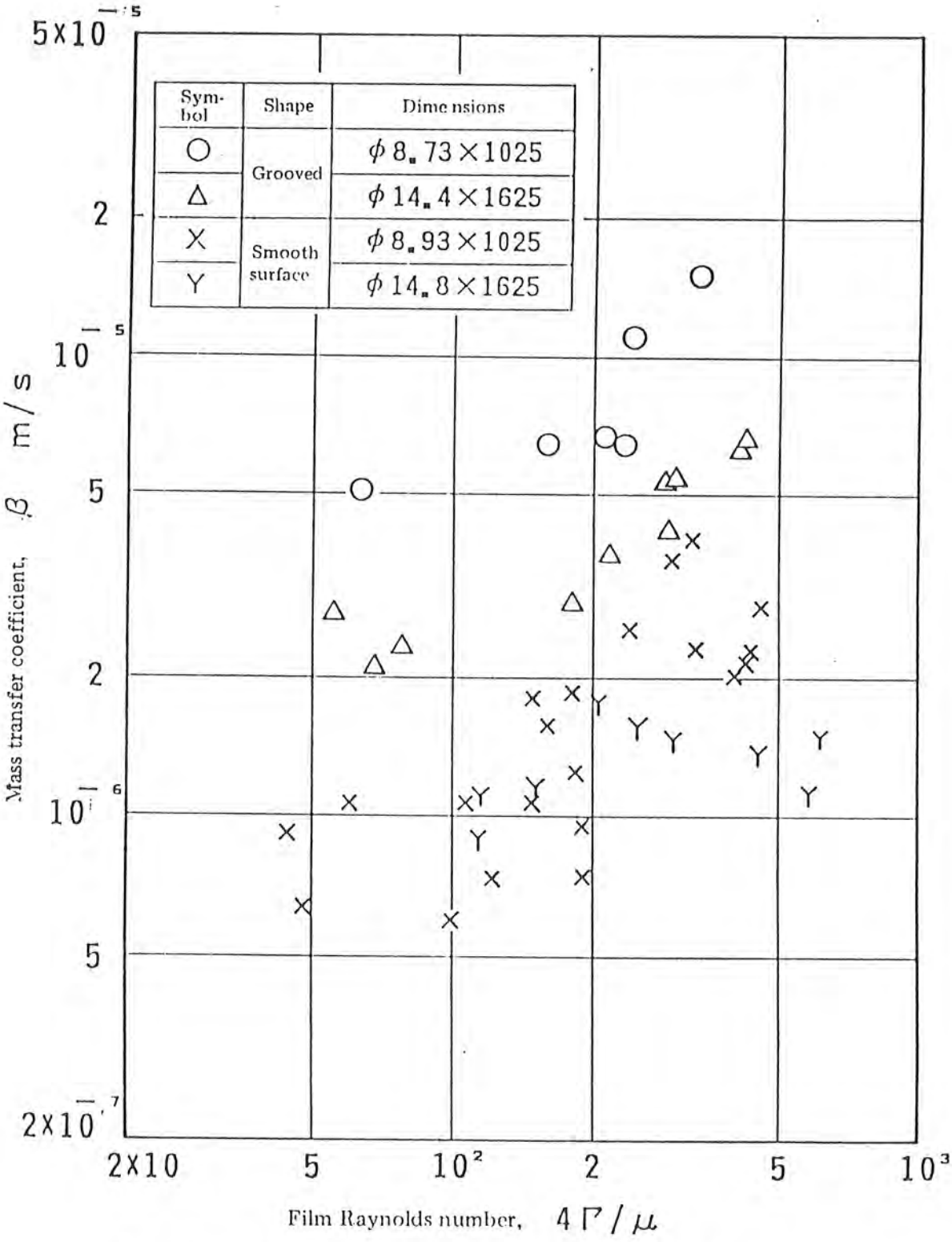

Fig. 4.4 Mass transfer coefficient of absorption in vertical tube

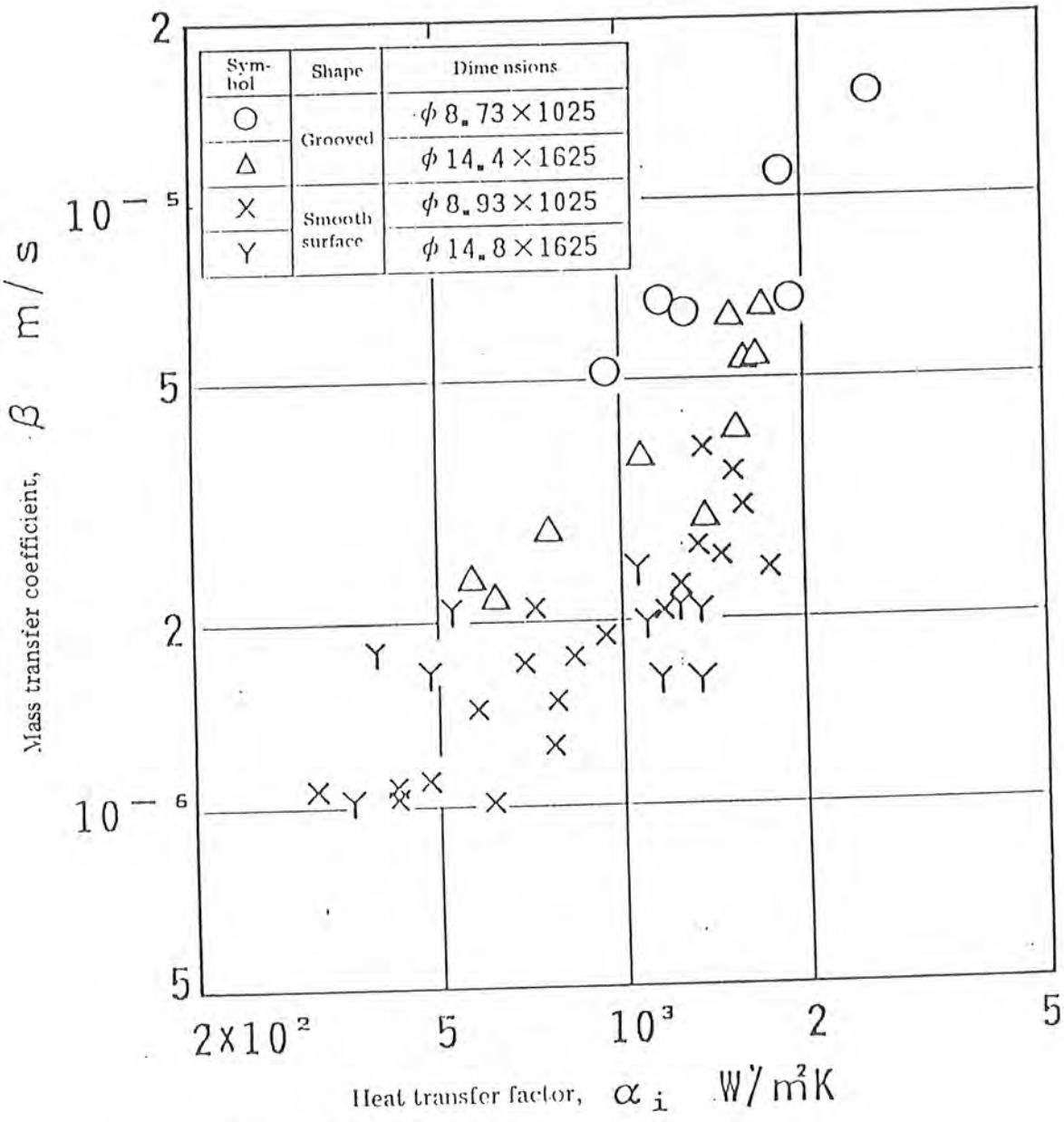

Fig. 4.5 Correlation between heat transfer factor and mass transfer coefficient

5. Absorbing performance of sigle tube absorber with grooved inner surface[1]
(Report #2: Relations with liquid film thickness)

5.1 Symbols

A : area of heat transfer, m^2
Cp : constant-pressure specific heat, kJ/kg
C : concentration of moisture, kg-H_2O/kg-sol.
C° : concentration of moisture in equilibrium with steam pressure, kg-H_2O/kg-sol.
ΔC : log-mean concentration difference, kg-H_2O/kg-sol.
d : tube diameter, m
g : acceleration of gravity, m/s^2
h : coefficient of heat transfer, kW/m^2K
K : liquid-phase-standard overall coefficient of mass transfer, m/s
k : thermal conductivity, kW/mK
L : tube length, m
N : speed of absorption per unit area, kg/m^2h
Nu : Nusselt number
P : partial steam pressure, Pa
Pr : Prandtl number
Q : quantity of heat transfer, kW
Re : Reynolds number
T : temperature of solution and steam, ℃
t : cooling water temperature, ℃
ΔT : log-mean temperature difference, K
U : overall coefficient of heat transfer, kW/m^2K
W : flow rate of solution and steam, kg/h
w : flow rate of cooling water, kg/h
Γ : flow rate of solution per unit immersed side length, kg/m • s
δ : liquid film thickness, mm
μ : viscosity, Pa • s
ρ : density, kg/m^3

Accompaniment letters

0 : state of equilibrium
1 : inlet, tube inside
2 : outlet, tube outside
10 : steam, water
20 : solution
30 : cooling water

5.2 Specimen absorbing tubes

Table 5.1 lists the specifications for the specimen absorbing tubes. The specimen consisted of two types of smooth inner surface absorbing tube and two types of grooved inner surface absorbing tubes, one of them having trapezoidal grooves and the other, triangular ones. The engineering material of all these types is copper.

Table 5.1 Specifications for specimen absorbing tube (mm)

Specimen absorbing tube	Groove shape	Number of grooves	Inside diameter	Length
Smooth inner surface tube	——	——	8.73	1025
	——	——	14.8	1625
Grooved inner surface tube	Trapezoid	60	8.93	1025
	Triangle	90	14.4	1625

5.3 Formula for calculation of absorbing performance

The heat transfer performance and heat absorbing performance are found as follows: Firstly, Q, which is the quantity of heat transfer, namely, the quantity of heat exchange is found from the cooling water's inlet temperature, t_{31}, outlet temperature, t_{32}, and flow rate, w.

$$Q = w \cdot Cp_{30} \cdot (t_{32} - t_{31}) \quad (1)$$

Here, the log-mean temperature, ΔT, is defined as follows.

$$\Delta T = \{(T_{21} - t_{32}) - (T_{22} - t_{31})\} / \ell n \{(T_{21} - t_{32})/(T_{22} - t_{31})\} \quad (2)$$

where T_{21} denotes solution's inlet temperature and T_{22}, solution's outlet temperature. Therefore, the overall coefficient of heat transfer, U, is found, i.e.,

$$U = Q/(\Delta T \cdot A) = Q/(\Delta T \cdot \pi \cdot d_1 \cdot L) \quad (3)$$

where A denotes the area of heat transfer. On the other hand, the coefficient of heat transfer of the water side on the outer surface of the tube, h_2, can be found from the formulas, (4) and (5), which are the formulas for turbulent heat transfer of circular tubes.

$$Nu = 0.023 \cdot Re^{0.8} \cdot Pr^{0.4} \quad (4)$$

$$h_2 = Nu \cdot k/d_2 \quad (5)$$

where k denotes thermal conductivity and if the heat resistance appeared by the absorbing tube wall is neglected, h_1, the coefficient of heat transfer inside the vertical tube is as given by the formula given below.

$$1/h_1 = 1/U - d_1/(d_2 \cdot h_2) \quad (6)$$

Secondly, K, which is the coefficient of liquid-phase-standard overall mass transfer, is found. Firstly, ΔC, which is the concentration difference, is defined.

$$\Delta C = \{(C^\circ_{21} - C_{21}) - (C^\circ_{22} - C_{22})\} / \ell n \{(C^\circ_{21} - C_{21})/(C^\circ_{22} - C_{22})\} \quad (7)$$

where C° denotes the moisture concentration which is in equilibrium with steam pressure, P_{10}. It is related to steam pressure, P_{10}, and solution temperature T_{20}, as shown by the formula (8).

$$C^\circ = C^\circ (P_{10} \cdot T_{20}) \quad (8)$$

In addition, the flow rate of steam, W_{10}, is found from formula (9), and the absorbing speed per unit area, N_{10}, is found by the formula (10), the coefficient of liquid-phase overall mass transfer, K, is obtained from the formula (11).

$$W_{10} = [(C_{22} - C_{21})/(1 - C_{21})]\ W_{22} \quad (9)$$

$$N_{10} = W_{10}/A \quad (10)$$

$$K = N_{10}/(\Delta C \cdot \rho) \quad (11)$$

Here, the thickness of liquid film, δ, is obtained from the formula (12), and the flow rate of solution per unit immersed side, Γ, can be obtained from the formula (13).

$$\delta = [3\mu\Gamma/(\rho^2 \cdot g)]^{1/3} \quad (12)$$

$$\Gamma = W_{20}/(\pi \cdot d_1) \quad (13)$$

5.4 Appartus and method for experiment

Fig. 5.1 shows the system of apparatus for experiment. The apparatus are composed of a specimen absorbing tube, a steam generator, a solution tank, circulating pumps for solution and refrigerant, etc. The specimen tube was designed as of double structure to have its outer surface cooled with cooling water. The steam generator was designed so to make the amount of steam generated and the evaporating temperature constant by having the liquid refrigerant agitated with the circulating pump, heated and adjusted with an electric heater.

The solution of lithium bromide was sealed into the solution tank, after having its moisture content adjusted to 0.45 previously and thoroughly deaerated by agitation with the circulating pump, and was supplied to the specimen absorbing tube while having its flow rate adjusted with a needle valve. The solution, which had absorbed steam in the specimen absorbing tube, was flowed out into the solution tank until its stabilization. When its stabilization was completed, the solution tank was changed over to a flow meter, which worked also as a collecting bottle, and was sampled to have its flow rate and concentration measured.

The pressure of the upper and lower headers of the specimen was measured with a digital manometer, the flow rate of cooling water, with a rotor meter and a measuring cylinder. In addition, the temperature of various sections was measured with a 0.4-class sheathed thermocouple T 1 mm diameter. The locations measured were shown in Fig. 5.1. Table 5.2 lists conditions of experiment.

5.5 Results of experiments and their evaluation

Fig. 5.2 shows the relations between the liquid film thickness of solution, δ, and the coefficient of heat transfer, h_1, and Fig. 5.3, the relations between the liquid film thickness, δ, and the coefficient of liquid-phase-standard overall heat transfer, K. It is seen from these figures:

1) Regardless of tube's inner surface which is either smooth or grooved, the coefficient of heat transfer increases as the liquid film thickness increases, and
2) If the inner surface is grooved, both the coefficient of heat transfer and the coefficient of overall mass transfer are improved. This is considered to be due to the fact that the effect of grooves consists in the improvement of heat and mass transfer within a liquid as a result of an increase in the area of heat transfer, facilitation of turbulent liquid flow showing that the groove helps materialize the high performance.

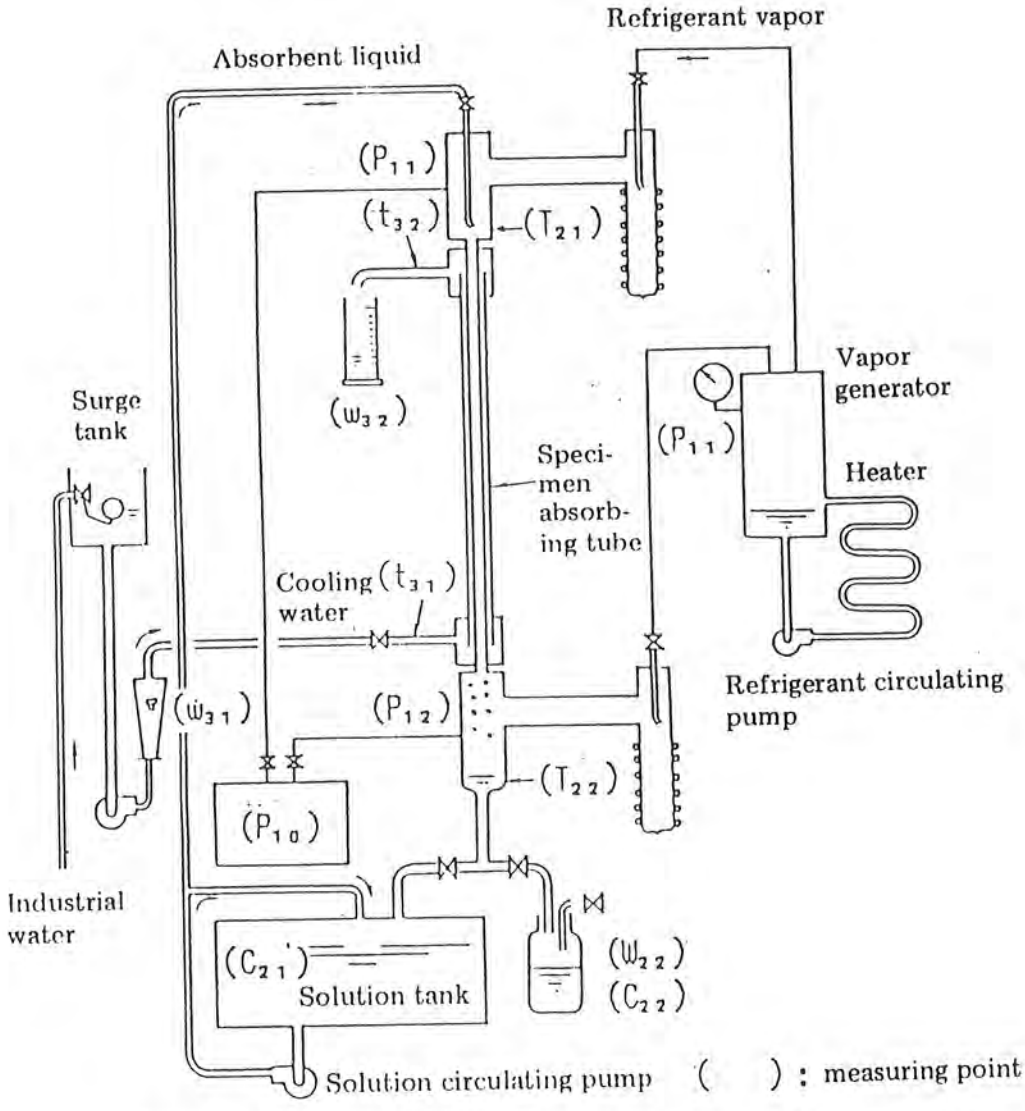

Fig. 5.1 Experimental apparatus for vertical absorbing tube

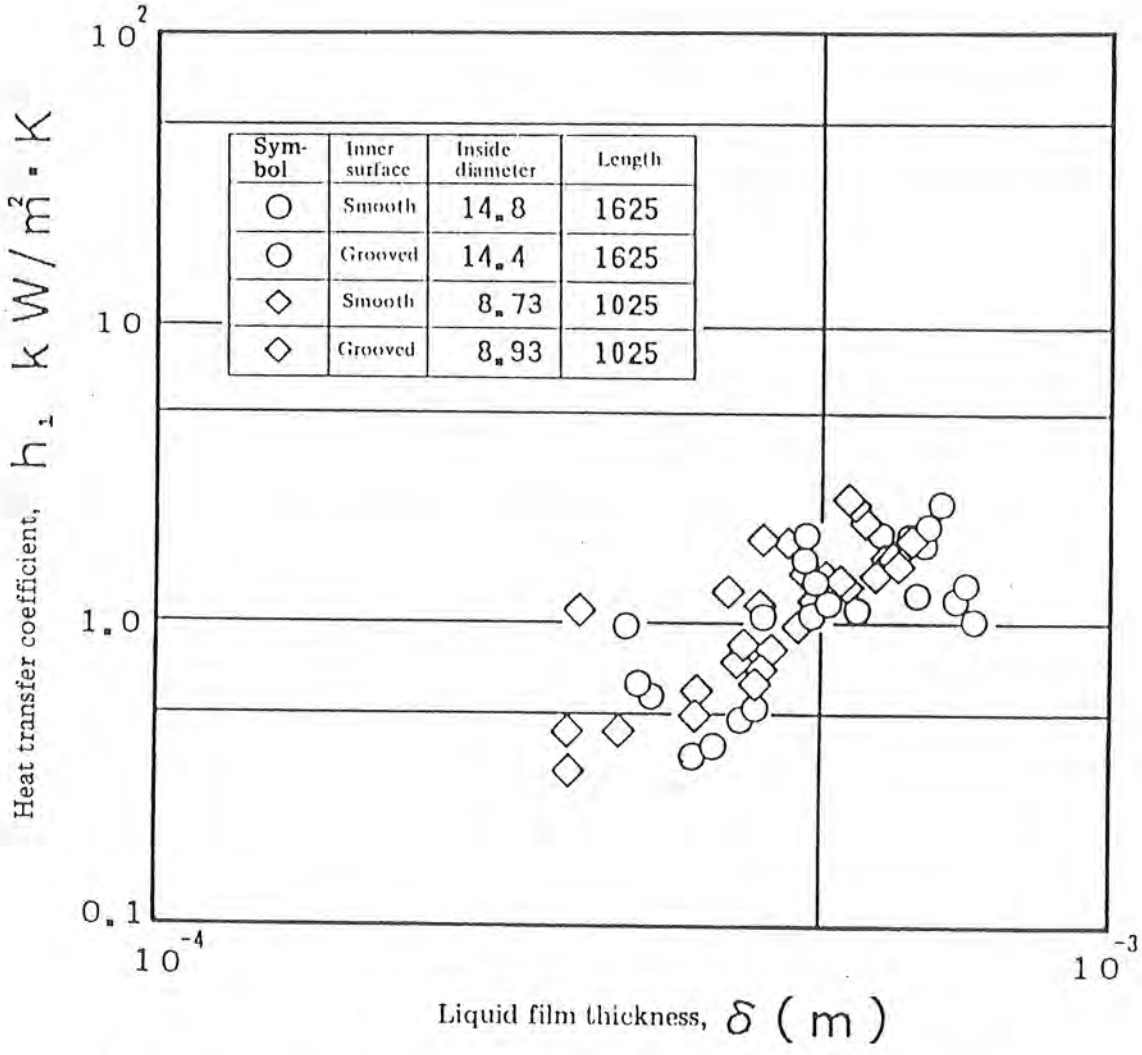

Fig. 5.2 Heat transfer coefficient of absorbing tube in vertical tube

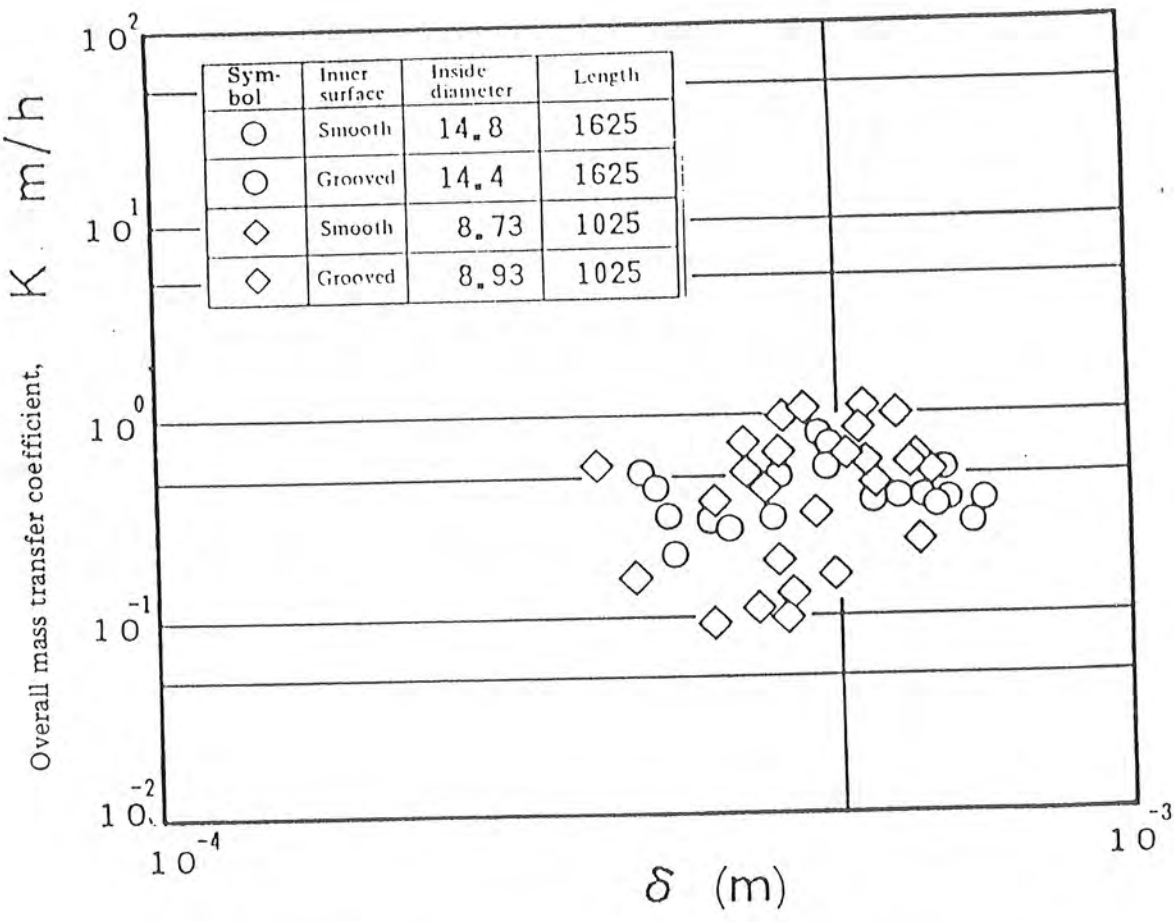

Fig. 5.3 Overall mass transfer coefficient of absorbing tube in vertical tube

6. Performance of air-cooled absorber[5)]

6.1 Completion of air-cooled absorber

The method for air-cooling the absorber of a water-lithium bromide group absorption refrigerating machine is broadly divided into the following two types.

i) Indirect cooling system: A heat carrier is circulated between an air-cooled heat exchanger (dry cooling tower) and absorber. It is easy to secure the flowpath of refrigerant vapor having a large volume flow rate between the evaporator and the absorber. But it has a defect that the heat exchange temperature difference resulting from the heat exchange between the absorber and the heat carrier tends to increase the absorber's outlet temperature.

ii) Direct cooling system: This system causes the absorption liquid and the cooled air to exchange heat with each other through the heat transfer surface. It is conceivable that this system absorbs the liquid film,flowing down the tube inside and specifies and air-cooled fin system on the outside of the tube. It is also conceivable to circulate quantities of absorption liquid whose sensible heat is utilized in the cooling tower to absorb the heat.

If the exchange of heat can be accomplished to obtain an absorption temperature lower than the outlet temperature, any cooling system will be able to sharply reduce the quantity of cooling air and at the same time the front area of an air-cooled heat exchange will be reduced. So, it is considered that a practical air-cooled absorption chiller-heater will be materialized.

The equilibrium temperature of an absorption liquid will differ according to its concentration even when it is placed under a fixed steam pressure. The higher the concentration, the higher becomes the equilibrium tempreture, and it indicates the boiling point rise of about 1.8K/%. In an ordinary absorption refrigeranting cycle there is a difference in concentration of about 3 to 5% between the inlet and outlet of the absorber and a difference of about 6 to 9K in the equilibrium temperature between the inlet and outlet. If, by taking note of the difference in the equilibrium temperature between the inlet and outlet, countercurrent heat exchange - is an ideal form of heat exchange - can be materialized, a liquid, whose temperature is lower than that of the cooled air outlet, will be obtained.

6.2 Apparatus and method for experiment

Fig. 6.1 shows an outlined structure of specimen air-cooled absorber and Table 6.1 lists technical data about this absorber. The air-cooled absorber consists of a smooth-inner-surface vertical absorption tube and an aluminum fin installed at right angles to the smooth inner surface and forms a cross-fin type heat exchanger. The higher header which supplies refrigerant vapor and absorbent liquid and the lower header having the liquid storing section provided with the vertical absorbing tube and spray pump which are connected to the upper header make up a mechanism unit to comprise the air-cooled absorber and four units are arranged in the direction

of flow of the cooling air. The concentrated solution from the regenerator flows first into the unit on the cooled air outlet side, flows down inside the vertical absorbing tube to exchange heat with the cooled air and is diluted by absorbing refrigerant vapor and is sent to the unit on the cooled air inlet side. The absorbing liquid, which is sent successively to the units on the cooled air inlet side to be diluted, is finally sent by the solution circulating pump to the regenerator. As mentioned above, the specimen air-cooled absorber makes up a 4-stage scattering type absorber. When taking note of the relations between the cooled air and absorption temperature, the specimen air-cooled absorber may be considered as performing 4-pass orthogonal counter flow heat exchange.

The dimensions of the front area up the specimen air-cooled absorber is 305 x 1650 mm. In order to prevent the spray pump from producing cavitation, the liquid storing section of each unit is provided with a float valve so as to control quantity of solution sent to the succeeding unit.

Fig. 6.2 shows the system of apparatus for experiment on the air-cooled absorber. The experiment was conducted by incorporating the specimen air-cooled absorber into a single-effect absorprion/refrigeration cycle. Table 6.2 lists the measuring method and the equipment employed. By placing the specimen air-cooled absorber in a testing wind tunnel, the quantity of cooling wind was found from wind velocity. The quantity of scatterd solution was found by means of a float-type flow meter corrected for density. For measuring the temperature, a sheathed thermocouple T was employed.

6.3 Results of experiments and thier evaluation

Fig. 6.3 shows an example of the flow of the cooled air set against the change in the absorption solution. On the graph, each unit (pass) number is plotted on the X-axis and on the Y-axis is plotted the concentration of the solution at each unit (pass) outlet. The conditions for experiment consisted of the cooled air inlet temperature of 35℃, room cooling capacity of 6.7 kW, refrigerant evaporating pressure of 930 Pa and the liquid film flow rate per unit width inside vertical absorbing tube as 0.33 kg/m・s. The testing conditions approximate the room cooling conditions of general type air-cooled machines. It is seen from Fig. 6.3 that the solution's temperature becomes lower and lower starting from the unit (pass) on the outlet side of the cooled air toward the units on its inlet side, namely, from about 55℃ of the first unit to about 44℃ of the fourth unit.

The cooled air is heated by exchanging its heat with the absorber so that its inlet temperature has risen from its inlet temperature of 35℃ to its outlet temperature of about 43.5℃. It has possible to confirm that the cooled air and absorption liquid had done orthogonal counter flow heat exchange.

Incidentally, the solution's temperature difference between the inlet and outlet of each unit (pass) was due to the drop of equilibrium temperature accompanied with the dilution of solution caused by the absorption of refrigerant within the vertical absorbing tube, the drop of equilibrium temperature caused by the drop of the fluidizing pressure of refrigerant vapor within the

vertical absorbing tube, subcooling of solution caused by the finitude of the co-efficient of mass transfer, and so on. In addition, the problem peculiar to this apparatus for experiment is as follows: Since the efficiency of the spray pump is extremely low, the solution is heated by the solution so that the inlet temperature of each unit (pass) is 3 to 4K higher than the equilibrium temperature of the solution in the machine.

The outlet solution temperature of the specimen air-cooled absorber is about 44℃, as shown in Fig. 6.4, approximates that of a water-cooled absorber.

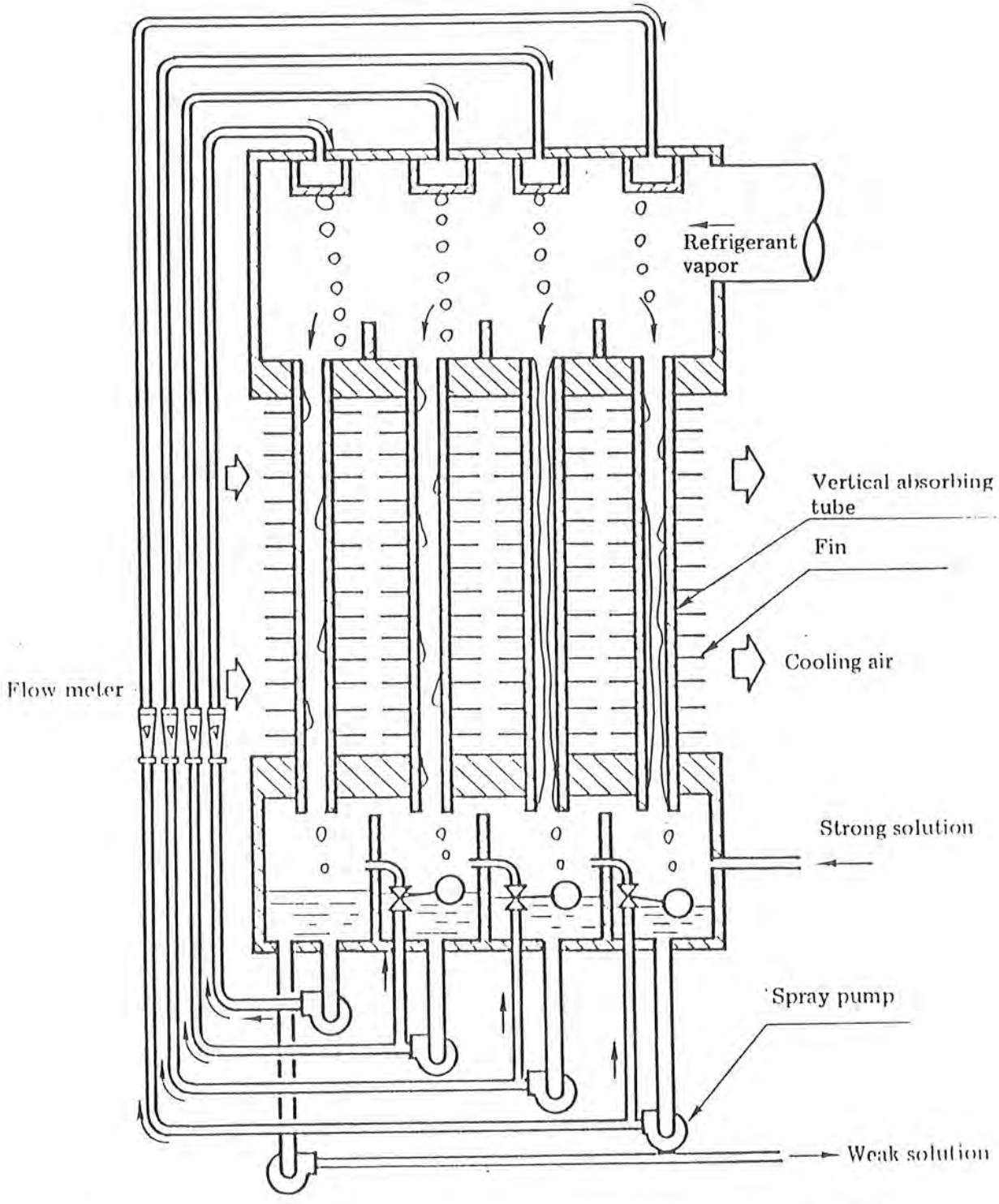

Fig. 6.1 Outlined structure of specimen air-cooled absorber

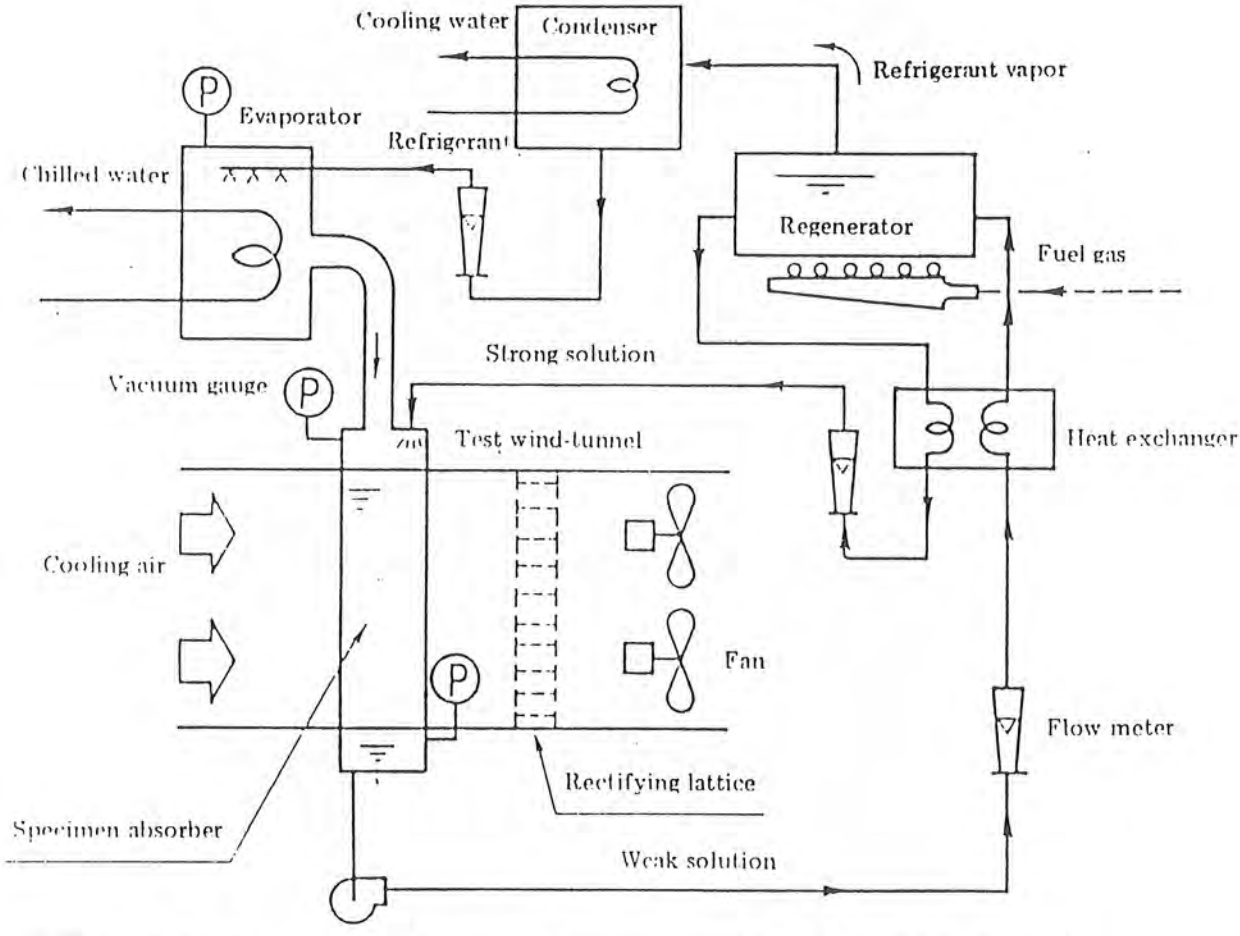

Fig. 6.2 Experimental apparatus system for air-cooled absorber

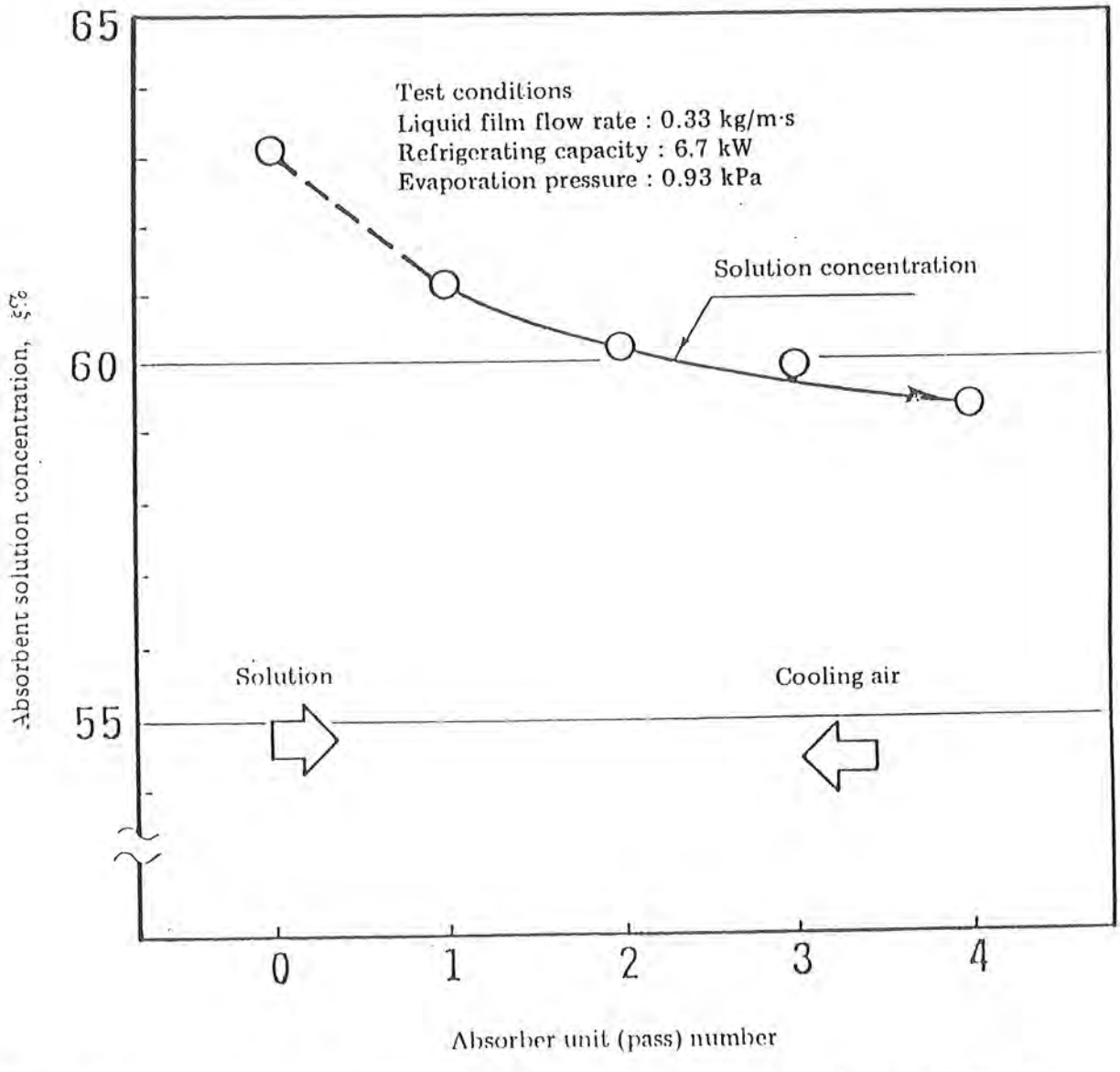

Fig. 6.3 Changes in concentration of specimen air-cooled absorber

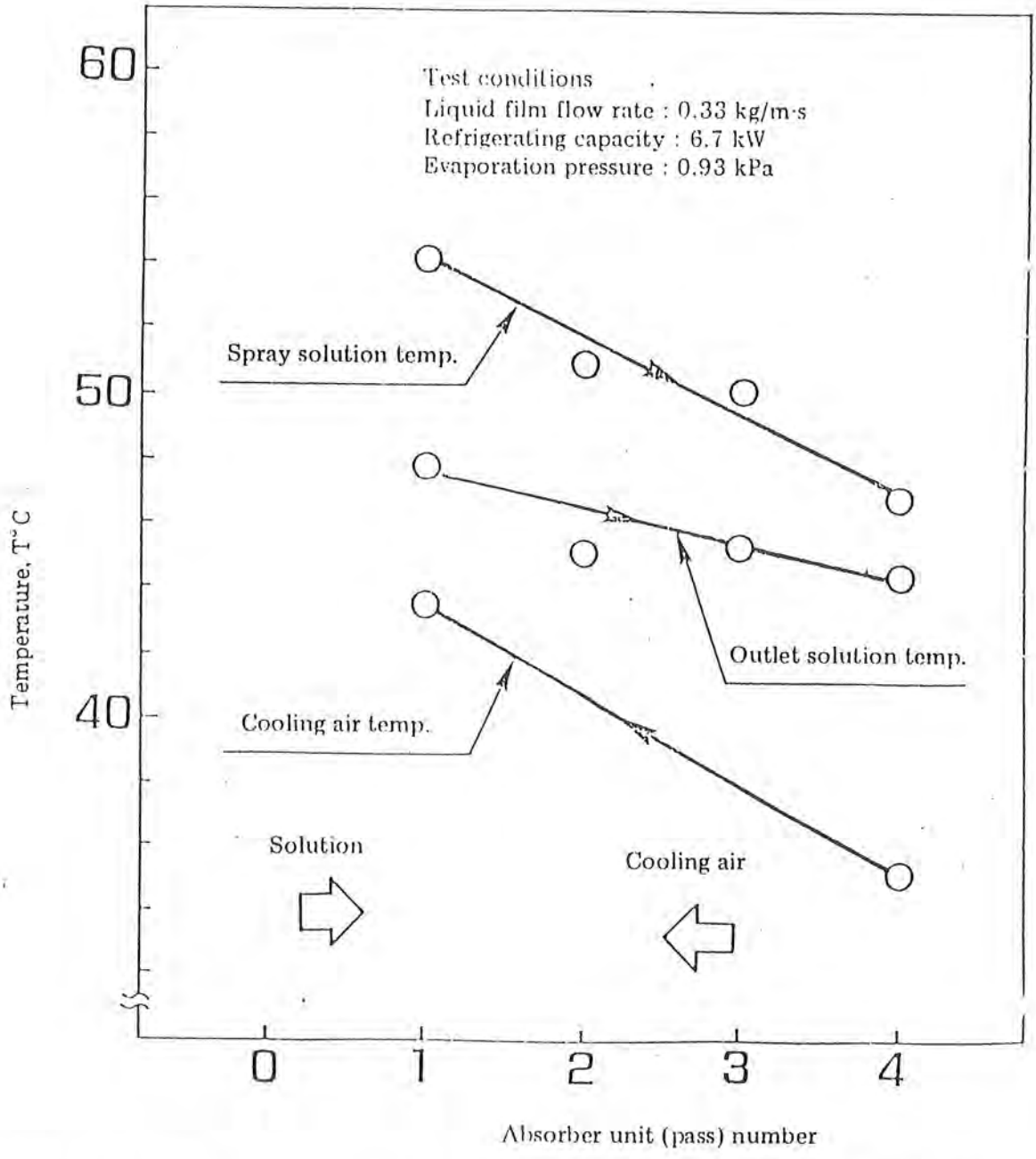

Fig. 6.4 Changes in temperature of specimen air-cooled absorber

7. Conclusion

As a result, detailed studies made on the absorbent performance of a unitary tube of the vertical absorbent tube unit whose inner surface is smooth, we have arrived at the following conclusions:

1) The factor of heat transfer of a vertical absorbent tube, which absorbs heat on its smooth inner surface, is proportional to about 0.8th power of the film Reynold's number and is approximately equal to the result of Salazar's experiment.
2) The mass transfer coefficient of a vertical absorbent tube, which absorbs heat on its smooth inner surface, is proportional to about 0.5th power of the film Reynold's number, showing the same inclination as the factor of heat transfer.

7.2 As a result of detailed studies made on the absorbent performance of a group of vertical absorbent tubes whose inner surface is smooth, we have arrived at the following conclusions:

1) The heat transfer performance of an orthogonal counterflow type absorber is given by the following formula:
$$Nu = 0.85 \cdot Re^{0.639}$$
2) The mass transfer coefficient of a tube, which makes absorption on its inner surface, is approximately fixed or 0.025 m/h under the condition of $Re < 200 \sim 300$ and under the condition of $Re > 200 \sim 300$, it is given by the following formula:
$$\beta = 1.858 \times 10^{-8} \cdot Re^{2.78}$$

7.3 As a result of detailed studies made on the absorbent performance, in relation to the film Reynold's number, of a unitary tube of the vertical absorbent tube unit, whose inner surface is grooved, we have drawn the following conclusions:

1) As a result of grooving its inner surface, the factor of heat transfer of the inside absorption type tube has been improved about 50% as compared with smooth-inner-surface type tube.
2) The mass transfer coefficient of the grooved-inner-surface type tube has also been improved 50% as compared with the smooth-inner-surface type tube.

7.4 As a result of detailed studies made on the absorbent performance, in relation to the thickness of the liquid film, of a unitary tube of the vertical absorbent tube unit whose inner surface is grooved, we have drawn the following conclusions:

1) If the inner surface of the vertical absorbent tube is grooved, both the heat transfer coefficient and the overall mass transfer coefficient will improve, when the liquid film thickness ranges from 0.3 to 0.7 mm, as compared with those of the smooth-inner-surface tube, making it possible to enhance the level of performance of the grooved-inner-surface type tube.
2) It will be necessary in the future to evaluate the grooved-inner-surface type tube, including the steam supply.

7.5 As a result of detailed studies made on the performance of the air-cooled absorber, we have drawn the following conclusions:

1) As a result of designing a 4-stage scattering type air-cooled absorber constructed of a vertical absorbent tube and air-cooled

fin into a single-effect absorbing/refrigerating cycle, the absorbent liquid temperature and concentration dropped successively from the cooled air outlet side toward its inlet side and it was confirmed that the cooled air and the absorbent liquid were performing orthogonal countercurrent type heat

2) It was possible to bring the absorber outlet liquid near the temperature and concentration of the water-cooled absorber under the condition of keeping the cooled air inlet temperature at about 35℃.

3) From the above results a bright prospect was obtained for materializing a double-effect absorbing/refrigeranting cycle of water-lithium bromide group products by cooling the absorber with air.